Laudatio

This volume is dedicated to Dr. Wolf-Dieter Deckwer on the occasion of his 60th birthday. He is Professor of Biochemical Engineering at the Technical University Braunschweig, Head of the Biochemical Engineering Division of the German Research Centre for Biotechnology, Braunschweig and member of the Advisory Boards of several international periodicals.

Wolf-Dieter Deckwer is recognised for his important contributions to biochemical engineering, especially for the evaluation of the interrelation between reactor engineering (fluid dynamics and transport processes in reactors) including scale up effects and the biology of the micro-organisms and cells. He has always stressed the engineering aspects of cultivation, the evaluation of quantitative engineering data for construction of bioreactors and of quantitative biological parameters for process development. In integrated process approaches he has taken into account the recovery and purification of the products beside the product formation.

His professional development is similar to several other typical biochemical engineers; they have a basic chemical engineering education, first focussing on chemical reaction engineering and later gradually shifted to biochemical engineering.

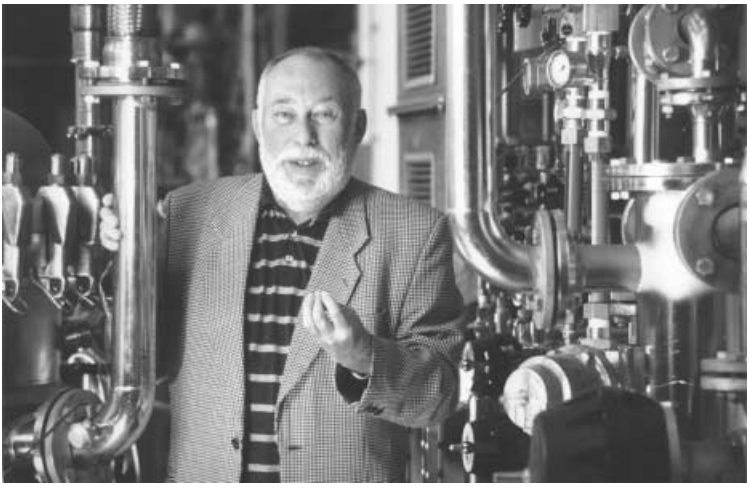

Prof. Dr. Wolf-Dieter Deckwer

Wolf-Dieter Deckwer studied chemistry and chemical engineering at the Technical University Berlin and in 1973 obtained his PhD degree in the Institute of Technical Chemistry at the same University. After his promotion he stayed in this institute and received the permission of teaching (Habilitation) in 1975.

He was dealing in the frame of his dissertation with chemical reaction engineering, especially with modelling of complex reactions in axial dispersed tubular reactors.

The director of this Institute, Dr. Herbert Kölbel, Professor of Technical Chemistry, has been involved during the second World War II in the development of upgrading coal to other hydrocarbons according to the Fischer-Tropsch synthesis in bubble column reactors with suspended catalysts. He was interested in gaining more knowledge's on of transport processes and chemical reactions in these reactors.

Wolf-Dieter Deckwer was working along this line and performed experimental investigations to characterise bubble column reactors without and with suspended catalysts, modelled transport processes and chemical reactions in them.

In 1976 he was appointed to Associate Professor for Technical Chemistry at the University Hannover. His research group experimentally investigated the interrelation of adsorption, transfer processes and chemical reaction in bubble columns by means of various model reactions: a) the formation of tertiary-butanol from isobutene in the presence of sulphuric acid as a catalyst; b) the absorption and interphase mass transfer of CO_2 in the presence and absence of the enzyme carboanhydrase; c) chlorination of toluene; d) Fischer-Tropsch synthesis. Based on these data, the processes were mathematically modelled. Fluid dynamic properties in Fischer-Tropsch Slurry Reactors were evaluated and mass transfer limitation of the process was proved. In addition, the solubilities of oxygen and CO_2 in various aqueous solutions and those of chlorine in benzene and toluene were determined. Within the framework of development of a process for reconditioning of nuclear fuel wastes the kinetics of the denitration of effluents with formic acid was investigated.

In 1980/81 he was visiting professor at the University of Pittsburgh, where he was dealing with fluid dynamics and transport processes in bubble column slurry reactors.

In the Institute für Technical Chemistry at the University Hannover, other research groups were dealing with the development of biotechnological processes in stirred tank and bubble column reactors in cooperation with the industry and performed basic investigations on the field of bioprocess engineering. By contact with these groups, Dr. Deckwer became interested in bioprocess engineering and his group started to investigate gas solubilities and transport processes in slightly and highly viscous model solutions and cultivation media. Influence of medium components on the fluid dynamics of bubble column reactors was evaluated as well. Model calculations were performed for non-limited and substrate-limited growth in tower loop bioreactors.

In 1981, he was appointed to be Professor and Head of the Institute of Technical Chemistry at the University of Oldenburg. Here, his group concerned itself with a) the evaluation of adsorption and reaction kinetics of the oxidation of

glucose with suspended Pt/C catalysts; b) the investigation of Fischer-Tropsch Synthesis with Fe/Mn-, Fe/Cu- and Fe/K-catalysts, respectively, in suspension phase. Hereby the CO_2 inhibition of the reaction was proved; c) the methanol synthesis from CO_2 and H_2 in a bubble column slurry reactor. In addition, investigations were carried out to determine fluid dynamic properties of aerated liquid hydrocarbons. Mass transfer rates were determined in gas-liquid solid fluidised beds and in stirred tank slurry reactors.

He is author of the book "Blasensäulen", which was published by Salle + Sauerländer, Frankfurt a. M. in 1985 and the english version "Bubble Column Reactors", which was published by John Wiley & Sons, Chichester in 1992.

In 1986, Dr. Deckwer was appointed to be Professor of Biochemical Engineering at the Technical University Braunschweig and to be the Head of the Biochemical Engineering Division of the National Research Center for Biotechnology. In this Division several topics have been investigated under his guidance. These investigations can be subdivided into the following groups: a) cultivation of micro-organisms and cells for product formation; b) optimisation of product formation by improved process monitoring and control and investigation of the scale up in pilot plant level; c) evaluation of relationships for mass transfer in various bioreactors and comparison of their performances; d) product recovery and purification by various techniques; e) pathway and energetic analysis of several micro-organisms; f) enzyme recovery and purification by affinity partitioning and Free-Flow Zone Electrophoresis.; g) development of methods for endotoxin removal from pharmaceutical intermediates with chemically modified membrane adsorbers; h) biodegradation of polymers; i) microbial degradation of toxic substances from waste streams; j) microbial retention of heavy metals; k) freeze drying of micro-organisms.

In following, some examples for process development are mentioned.

One of the main interests of his research group was the characterisation of processes with highly viscous cultivation medium. Xanthan production was used as a model system. The rates of growth of *Xanthomonas campestris,* xanthan formation and oxygen transfer were determined in stirred tank, bubble column and plunging jet bioreactors of different size partly (up to 1500 litres) as a function of the most important process parameters. The quality of the products was evaluated and controlled. Relationships were developed for the calculation of the oxygen transfer rate in these reactors during the cultivation. These relationships were confirmed by other research groups.

The formation of 1,3-propanediol from glycerol by *Klebsiella pneumoniae, Citrobacter* and *Clostridium butyricum*, respectively as well as 2,3-butanediol by *Enterobacter aerogenes* and their recovery and purification were central issues as well. The production was partly performed in a 2000 litre reactor. Glycerol metabolism in these microorganisms was established. In addition the application of the diols was investigated.

Mammalian cells were cultivated in high cell density perfusion operation mode for the production of therapeutically important proteins. Material and energy balances were determined and cell regulation was investigated. Methods were developed for the recovery and purification of the products with chromatography and expanded bed chromatography.

Several other processes were investigated and developed as well, e.g., a) Ambruticin S production in airlift and stirred tank reactor; b) high-cell density cultivation of *E. coli* and production of rDNA products; c) production of thermostable xylanase by *Thermomyces lanuginosus*; d) cultivation of *Tetrahymena thermophila* in 1.5 m^3 bioreactors. e) alginate production by *Azotobacter vinelandii.*

Most of the variables of these processes were monitored, material and energy balances were determined, pathway analysis was performed, regulation of growth and product formation was investigated, recovery and purification of the products were established and the systems were modelled.

He developed the biochemical engineering part of the biotechnology curriculum at the Technical University Braunschweig and is responsible for the engineering education of its students.

His former and present students and his colleagues thank him for his continuous support in biotechnology. By dedicating this volume of *Advances in Biochemical Engineering/Biotechnology* to Professor Deckwer, the authors of this volume and many other colleagues want to honour his outstanding achievements in the broad field of biochemical engineering.

Hannover, Spring 2001 Karl Schügerl

Preface

This special volume "Tools and Applications of Biochemical Engineering Science" is dedicated to Professor Wolf-Dieter Deckwer on the occasion of his 60th birthday. It was a great pleasure for me to act together with Professor Karl Schügerl as volume editor and to present here a collection of 11 outstanding review articles written mainly by former students, associates, colleagues and friends of Wolf-Dieter Deckwer.

The title of this special volume well reflects the research interests and scientific pursuit of Wolf-Dieter Deckwer during his more than 20 years' work in the area of biochemical engineering, particularly during the last 15 years when he was the head of the Biochemical Engineering Division of GBF (German National Research Center for Biotechnology). He has decisively pushed the development not only of "software tools" ranging from analytical means and mathematical models for monitoring and understanding cellular processes to gene expression systems for designing microorganisms, but also of "hardware tools" such as computer control systems, bioreaction and separation devices for effectively producing a variety of bioproducts on semi-production scale. New developments in some of these important tools in biochemical engineering are reviewed in articles included in this volume. Wolf-Dieter Deckwer was among the leading biochemical engineers who timely pointed out the necessity of applying these tools in an integrated manner for bioprocess development. By establishing "Integrated Bioprocess Development" as one of the GBF main research topics as early as 1990 he also actively promoted this idea. Such an integrated approach for bioprocess optimization and development is exemplified in several articles in this volume as well.

Wolf-Dieter Deckwer is not only a leader and organizer in biochemical engineering research. First of all, he is a successful scientist and has made significant contributions to many areas of chemical and biochemical engineering. He is well-known as a "(bio)reactor man". In fact, many of his works on transport phenomena and reaction kinetics in bubble columns have become classics in this field. Over the years, part of his interests has shifted to the fascinating kinetic and dynamic phenomena in the smallest bioreactor, the microorganism. He is also a "downstream man". He and his associates have made contributions to protein purification and hydrocyclone cell separation in recent years. He is also a "biodegradation man". The beauty of microorganisms to produce nothing but CO_2 and water, as he once said, fascinates him. Among others, he and his coworkers, in particular Rolf-Joachim Müller, have successfully de-

signed biodegradable plastics to help the organisms to realize this beauty and, of course, also to help our environment to keep its beauty. Here, I have mentioned only a few of the scientific achievements of Wolf-Dieter Deckwer. Prof. Karl Schügerl has listed more in his laudation for this special volume. The scientific work of Wolf-Dieter Deckwer is also well documented in his more than 370 scientific publications.

Perhaps less well documented are the achievements of Wolf-Dieter Deckwer as a very respected teacher during his 25- years' career as a professor at the University of Hannover, the University of Oldenburg and the Technical University of Braunschweig. More than one hundred PhD students from all around the world and perhaps even more diploma students have worked under his supervision. I had the good fortune to be one of his first PhD students at GBF and have benefited a great deal from his broad experience, sharp scientific instinct, clear judgment, challenging questions and at times also his criticism. His demand and enthusiasm for understanding and interpreting biological phenomena in meaningful physical models and by numbers may not be always comfortable for the students but are always helpful and fruitful, according to my experience. To achieve this goal or perhaps to reach a compromise he often spent the whole morning or afternoon in very detailed discussions with his students and coworkers. Such discussions were sometimes disrupted or postponed due to many inevitable commission sessions or other administration duties, more frequently as his Division of Biochemical Engineering at the GBF expanded (temporarily more than one hundred people). He is now been freed of many of these duties and has more time for his students and his research. I believe it will be an excellent time for his students and associates.

As a close and long-year coworker of Wolf-Dieter Deckwer, I know that he is enthusiatic about many research opportunities of biochemical engineering in the post-genome era. He has set out to join the efforts for developing new tools and methods to dig into the huge amount of biological information and to explore its use in biochemical engineering. I wish him every success in this new endeavor. I also hope that the reader of this special volume will get some impression of the tools and applications of biochemical engineering already achieved or presently under active development. For this, I would like to thank all the authors and reviewers of the articles. Thanks are also to Professor Thomas Scheper who has supported the idea of this special volume from the very beginning and given much help throughout the whole process. Last but not least, I thank Dr. Marion Hertel and Mrs. Ulrike Kreusel from the Springer-Verlag who have made this special volume a reality.

Braunschweig, May 2001 An-Ping Zeng

Methods for Biocatalyst Screening

Andreas Tholey, Elmar Heinzle

Technische Biochemie, Universität des Saarlandes, Im Stadtwald, Geb. 2, 66123 Saarbrücken, Germany
E-mail: e.heinzle@mx.uni-saarland.de

Dedicated to Prof. Dr. Wolf-Dieter Deckwer on the occasion of his 60th birthday

Biocatalysts are now widely accepted as useful alternative tools to classic organic synthetic techniques for the regio- and enantioselective synthesis under mild reaction conditions in many fields of chemistry. The development of techniques for the rational or evolutionary design of novel or modified enzymes has increased the need for fast and reliable methods for the identification of the most powerful catalysts. We present a short overview on screening techniques in this area. Beside classical methods such as spectrophotometry and fluorimetry, a number of new approaches like methods based on the measurement of pH changes or IR-thermography have been recently developed. Additionally the use of electrospray and matrix-assisted laser desorption/ionization mass spectrometry has gained increasing influence in this field of biotechnology.

Keywords. Enzymes, Mass spectrometry, IR-thermography, Optical detection, Fluorescence spectroscopy

Advances in Biochemical Engineering/
Biotechnology, Vol. 74
Managing Editor: Th. Scheper

List of Abbreviations

B. subtilis	*Bacillus subtilis*
C	concentration
CD	circular dichroism
CE	capillary electrophoresis
CID	collision induced decomposition
CLEC	crosslinked enzyme crystal
GC	gas chromatography
E. coli	*Escherichia coli*
ee	enantiomeric excess
epPCR	error prone polymerase chain reaction
ESI	electrospray ionization
FRET	fluorescence resonance energy transfer
HPLC	high performance/pressure liquid chromatography
HTRF	homogenous time resolved fluorescence
HTS	high-throughput-screening
IR	infrared
K_M	Michaelis-Menten constant
LC-MS	coupled liquid chromatography-mass spectrometry
MALDI	matrix assisted laser desorption/ionization
MS	mass spectrometry
NMR	nuclear magnetic resonance
PSD	post source decay
r	reaction rate
rac	racemic
t	time
UV/Vis	ultraviolet/visible
v_{max}	maximal velocity

1 Introduction

Biocatalysts, especially enzymes, possess a number of unique properties which make them useful for the synthesis of fine and commodity chemicals, therapeutics, and for use as biosensors [1–5]. During evolution living organisms developed enzymes for a great variety of classes of chemical reactions. The reaction conditions of enzyme catalyzed reactions are generally softer than those in classical chemistry thus exhibiting an enormous potential for environmentally friendly biocatalytic processes. Enzymes are highly selective and both regio- and enantiospecific biocatalysts. The regiospecificity offers the opportunity to shorten classical chemical synthesis paths which often require laborious protection and deprotection steps for other functional groups in the substrate [3, 6–8]. One of the most outstanding properties of enzymes is their enantiospecificity [9, 10]. Enzymes can catalyze reactions leading directly to chiral compounds, which are essential for many applications in pharmaceutical chem-

istry and agrochemistry. A further advantage of the use of biocatalysts resulting from the properties mentioned above is that generally much lower amounts of byproducts are formed, leading to both economic and ecological advantages compared to classical chemical methods.

In nature enzymes are selected to work in a defined aqueous environment, e.g., the cytosol of cells. Their activities in complex biological networks are controlled by various mechanisms that meet the requirements of the living organism. Usually, enzymes are not selected for high stability, particularly not in the harsh reaction conditions used in technological processes. Thus enzymes often have to be optimized concerning their resistance to high temperature, high pressure, use of organic solvents, for reactions in liquid substrates without additional solvents, or for contact with non-natural surfaces [11]. Often non-natural substrates are used requiring modified enzymes for industrial operation.

Modern approaches for the creation of diversity using recombinant DNA-methods are highly developed. The bottleneck in the development of a new catalyst is the screening for the most powerful candidates. This bottleneck mainly determines competitivity with chemical synthesis methods. Fast screening procedures reduce both development time and risk. The goals of screening may be the selection of enzymes for a distinct class of reactions (catalyst screening), or the screening of different substrates which can be converted by a particular enzyme (substrate screening), whereby stability, selectivity, and reactivity are the most important criteria. In both cases it is highly desirable that the reaction conditions during screening are as similar as possible to those in the future applications. This avoids time consuming optimization in wrong directions. Such screening conditions are presently very difficult to establish. New miniaturized reactors, both in flow-through and batch modes, are increasingly available and promise progress in this type of scale-down experiments [12–14]. Generally there is a need for methods for high-throughput screening.

2
Development of Biocatalysts

The experimental design for the finding of new enzymes strongly influences the screening procedure. The process for new biocatalyst development can be divided into three main steps: the design of the catalyst, the creation of diversity, and the screening process (Fig. 1). This procedure is iterative: the results of the screening process itself have a strong impact on the strategy for further design of a new generation of catalysts.

2.1
Biocatalyst Design

A reaction catalyzed by an enzyme is usually one step in a sequence of synthesis steps. In the very early phases of development of production processes, potential routes are identified and have to be tested for their feasibility. If a bioconversion step is included in a reaction sequence it is desirable that minimal workup is required for the application of the products of the preceding step.

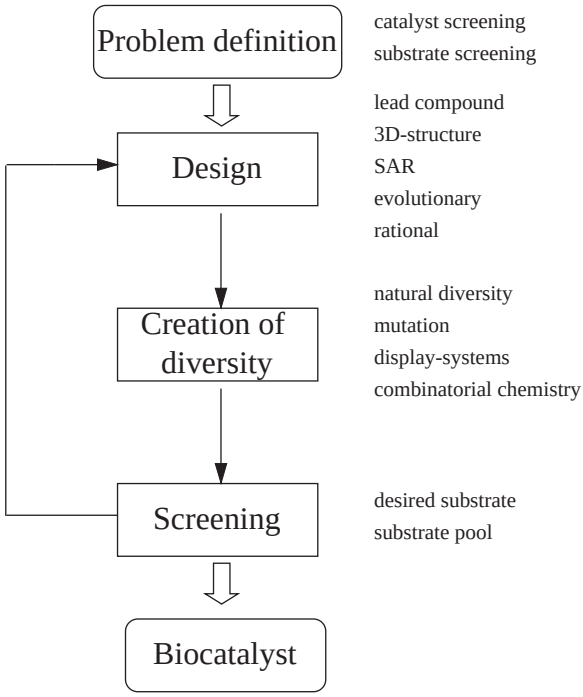

Fig. 1. Steps in the development of new biocatalysts

Ideally the same solvent is used and impurities and byproducts do not disturb the bioconversion. It is therefore useful to consider this both in the design of the catalyst and in the screening procedure.

Biocatalyst design can be done by using rational or evolutionary methods. Here one has to ask about the desired function and properties of the new catalyst and the conditions it should resist. The best basis for this work is the knowledge of the three-dimensional structure and the reaction mechanism of an enzyme. The knowledge of the structure, at least of the primary structure, is a prerequisite for targeted mutational creation of diversity. If structure and mechanism of catalysis of an enzyme are not known, only random mutagenesis and screening are possible, typically leading to a prolonged development time. If selection can be introduced, e.g., by biocatalytic conversion of a substance into an essential substrate for the host cell, this method may be very efficient. Structure activity relationships (SAR) in combination with bioinformatics can also be very helpful in this step of the development process.

2.2 Creation of Diversity

Starting from a lead biocatalyst defined in the first step one has to create a bank of catalysts with different properties. Resources for new catalysts are natural

pools like natural waste products or microbial sources for example [15]. Modern methods for the mutational creation of diversity start with sequencing of the gene of the desirable enzyme. For many bacterial genes complete sequences are already available in data bases. Isolation and sequencing of genes of eucaryotes, e.g., fungi, may be much more difficult. Most enzymes can be expressed in heterologous well characterized hosts like *E. coli*, *B. subtilis*, or yeast. For testing of the enzyme activity it is highly desirable to have the enzyme secreted or displayed on the surface of the host. Another possible display system uses phages [16]. If prosthetic groups or other posttranslational modifications are required for proper enzyme function, the selection of a suitable host is more difficult. After establishing a heterologous expression system, various methods may be used for creation of diversity by mutagenesis [15], directed evolution [17–19], or by combinatorial methods [20]. Most popular are presently error prone polymerase chain reaction (epPCR) [21] and DNA-shuffling [22, 23]. These methods may be used for any type of improvement of enzymes. Additionally, biocatalysts may be stabilized by different methods of chemical modification like the lipid coating technique [24], formation of cross-linked-enzyme crystals (CLEC) [25, 26], or immobilization [27]. In case of substrate screening, libraries of substances can be synthesized by methods of combinatorial chemistry [28].

2.3 Screening Procedure

The third step in the development of biocatalysts is the screening procedure. The screening process itself can be divided into three levels [29]. In the first stage, a fast and basic qualitative identification of potential transformations is made, eliminating the majority of negative candidates. In a second stage, a semiquantitative approach is chosen, whereas in the third stage a full quantitative analysis is necessary. Due to reasons of effectivity, the aim of every strategy of screening is to gain quantitative results as early as possible. There are two possible targets of a screening procedure. The first is a screening of a bank of catalysts with a desired substrate. The second is the screening of a class of potential catalysts with a substrate pool, e.g., a library of organic compounds. The knowledge of the potential substrates which can be converted by a catalyst delivers new insights into its function and into the catalytic mechanisms behind this, e.g., by structure-activity relationships. Starting with the results from a first screening, a new generation of enzymes can be designed in an iterative process. Often not only substrates but also inhibitors for enzymes are the subject of interest [30, 31]. Usually the source of potential inhibitors are synthetic libraries, which can be screened by the different methods described below [28].

The optimization of enzymes strongly depends on the field of application. For industrial applications, high reaction rates, stability under process conditions, and regio- and enantioselectivity are the most important properties of a catalyst, whereas affinity or substrate selectivity are of second order interest for a distinct process to be catalyzed. On the other hand, enzymes with a wide range of activity can be used for the production of several products reducing

costs. The identification of the optimal method of screening to answer the specific question is crucial. Another very important point is the matrix surrounding the catalysts to be screened. Enzymes in cell lysates or even in whole cells need other screening procedures than purified enzymes. Screening systems differ depending on the kind of analysis. A parallel approach for batch systems can be performed in microtiter plates whereas highly parallelized experiments can also be performed in continuously operating microchannel devices. Another question is whether all substrates and products have to be analyzed or whether the analysis of one compound in the reaction is enough. For quantitative measurements a parallel estimation of several parameters (decrease of substrate and increase of product for example) gives additionally information about selectivity and reliability of the data. Analytical methods used for screening purposes should be easy to handle, sensitive, specific, and fast, but usually not all of these requirements can be fulfilled.

3
Experimental Design of Screening Procedure

3.1
Differential or Integral Estimation of Kinetic Parameters?

There are basically two possibilities for quantifying biochemical reactions, the differential and the integral approach (Fig. 2).

In a batch reactor the material balance is

$$\frac{dC}{dt} = r = f(C) \tag{1}$$

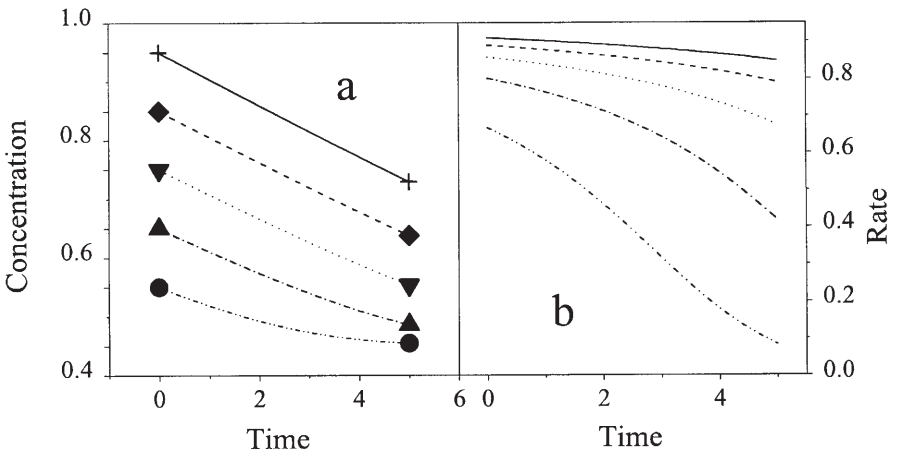

Fig. 2a, b. Principle of integral and differential measurement of reaction kinetics: **a** concentration-time course; **b** rate-time course. *Symbols* indicate initial and final concentrations in parallel integral measurements. Corresponding curves use *same dashes*

In the differential approach, Eq. (1) or algebraic modifications are used to estimate kinetic parameters. Most popular are rearrangements to give linear relationships, e.g., Lineweaver-Burk, Eadie-Hofstee, or Hanes-plot for Michaelis-Menten kinetics. To get a good estimate of the slope (Fig. 2b), concentration or a related signal is ideally measured continuously along one or more of the curves shown in Fig. 2a. After plotting, parameters are then derived by linear regression. Alternatively, Eq. (1) can be integrated numerically. Resulting concentration values are then compared with the experimental ones [32]. This is particularly useful for more complex kinetics. In the integral experimental approach measurements are only made after a certain period of time as indicated by the symbols in Fig. 2a. Usually a series of experiments is required. To estimate parameters based on such experiments, Eq. (1) must be integrated:

$$\int_{C(t=0)}^{C(t=t1)} \frac{dC}{f(C)} = \int_{0}^{t1} dt = t_1 \tag{2}$$

In most biological cases $f(C)$ is nonlinear and analytical integration is difficult or impossible. Numerical integration again allows calculation of concentration at the end of each experiment. Differences between simulated and experimental data are then minimized using, e.g., the least squares criterion. Both experimental approaches are compared in Table 1, especially with respect to their suitability for kinetic screening.

An important disadvantage of the differential approach is the need for measurement during reaction, which occupies measurement equipment during the whole experiment. Therefore, this approach is time consuming and only well suited for reactions which run at medium rates (less than 1 h). The integral approach is much better suited when sampling is required for the analysis. The integral approach is also superior, when only few data points are available.

Table 1. Comparison of differential and integral experimental approaches for estimating kinetic parameters in a screening environment

	Differential approach	Integral approach
Information content of single experiment	High	Low
Range of reaction time constants	Milliseconds to seconds in stopped flow apparatus Minutes to hours in microtiter plates	Seconds to minutes in tubular flow system Minutes to hours in microtiter plates
Suitability for microtiter-plate environment	Uses measurement instrument throughout experiment	Uses measurement instrument only once per well
Applicability of analytical methods available	Photometric measurement ideal for this type of experiment, frequent sampling required for other methods	Well suited for any type of analytical method
Potential for parallelization	Low	High

Differentiation of the experimental concentration-time curve would then need interpolation or smoothing, e. g., by using splines. Parallelization in a typical robotic environment is easy when using the integral method with a few or even only one single well for characterization of one enzyme variant.

3.2
Estimation of Enantioselectivity

The ability to catalyze reactions leading to enantiomerically pure products is one of the most important features of enzymes. Therefore there is a special need for the analysis of optical activity of substrates or products of biocatalytic conversions. The methods for the estimation of enantioselectivity of bioconversions can be divided into five general classes:

1. Comparison of the rates of conversion of the pure enantiomers. This approach is possible with all analytical methods described below. The main disadvantage is the need for the enantiomerically pure products.
2. Conversion of racemic mixtures with one of the enantiomers carrying a labeling group. This approach is well suited for screening by mass spectrometry (Sect. 4.2).
3. Separation of the enantiomeric products of a bioconversion by chromatographic or electrophoretic methods. These methods are well suited for enantiomeric synthesis.
4. Formation of diastereomers (NMR).
5. Direct measurement of the optical rotation. This is mainly coupled to preceding separation steps (Sect. 4.3).
   The different possibilities will be described in the corresponding sections.

4
Analytical Methods

Analytical methods to characterize the reaction process are strongly linked to the reactor system. In very early phases, plate-based methods like agarose plates or filter paper assays without distinct reaction compartments but very high throughput are used. Here diffusion plays an important role in the quantification. Microtiter plate systems are characterized by distinct mixed compartments, which is superior for quantification. Analytical methods for the screening of biocatalysts can be discriminated into three main classes: non-invasive, direct-invasive, and separation methods. Non-invasive methods do not interfere with the analytes except by some kind of electromagnetic radiation. Optical methods like UV- or IR spectroscopy, all kinds of fluorescence spectroscopy, and NMR belong to this class. Invasive methods like mass spectrometric methods directly influence the analyte. Chromatographic or electrophoretic methods need a coupling to one of the non-invasive or invasive methods for detection.

4.1 Non-Invasive Methods

4.1.1 *Optical Methods*

UV/Vis-spectroscopy is the classical method of analysis of enzyme activity. The principle is the change in absorption behavior of a substrate during the reaction process, for example by modification or liberation of a chromophoric function. A number of enzymes from different classes can be assayed spectrophotometrically using their natural substrates or cofactors. In this way, activity of acetyltransferases can be estimated by measurement of absorption of acetyl coenzyme A at 232 nm [33]. Oxidoreductases which require a cofactor, e.g., NAD/NADH, to carry out the transfer of hydrogen can be characterized by measuring the absorption of this cofactor depending on its oxidation stage [33].

A great advantage of spectrophotometric assays is that they can be carried out in microtiter plates or as filter paper assays, thus allowing a high sample throughput coupled with small sample volumes. Such systems were used for example for the screening of epoxide hydrolases [34]. A classical example of activity tests is for amylolytic enzymes where starch agar plates are stained with iodine after a certain reaction time. The radius of clear spots is a measure of the reaction rate [35].

Optical methods are easy to use, but unfortunately their application is often limited. The first limitation is caused by possible interference with the matrix, for example by light scattering. Therefore such tests usually can only be used in relatively pure solutions. The second problem is caused by the lack of chromophoric changes during reaction. When the desired reaction is not accompanied by a useful absorbance change it is common to use a synthetic substrate or a substrate analogue carrying a chromophoric group. When such artificial substrates are used to measure the enzyme, there is a real risk of measuring data entirely irrelevant to the actual reaction of interest. The reasons for this may be steric hindrance or hydrophobic/hydrophilic or charge-based interactions for example. A number of synthetic substrates have been used for different classes of enzymes [29]. The classical substrates for esterases are *p*-nitrophenolic esters. The esterase function can be monitored by the liberation of *p*-nitrophenol absorbing light at 400 nm [29].

When an enzyme catalyzed reaction creates a product with reactive groups not present in the substrate, it is possible that this group reacts with chemicals carrying chromophoric groups. For example, acetylcholinesterase is conveniently assayed by replacing the real substrate with acetylthiocholine. After enzymatic cleavage the liberated thiol group reacts with dithio-bis(2-nitrobenzoic acid) (DTNB, Ellmans reagent [36]) resulting in a yellow 4-nitrothiolate anion. Another classical example for coupled reactions is the analysis of hydrogen peroxide produced by oxidase catalyzed reactions. Hydrogen peroxide reacts with ABTS (2,2′-azino-bis(3-ethylbenzthiazoline)sulfonic acid) forming an intensive dye absorbing at 405 nm [37]. For kinetic studies these reactions should be fast and quantitative. The influence of such coupled reactions on enzyme ki-

netics has to be considered carefully, particularly when studying reversible reactions.

Spectrophotometric assays can be used for the estimation of the enantioselectivity of enzymatic reactions. Reetz and coworkers tested 48 mutants of a lipase produced by epPCR on a standard 96-well microtiter plate by incubating them in parallel with the pure *R*- and *S*-configured enantiomers of the substrate (*R*/*S*-4-nitrophenol esters) [10]. The proceeding of the enzyme catalyzed cleavage of the ester substrate was followed by UV absorption at 410 nm. Both reaction rates are then compared to estimate the enantiomeric excess (ee-value). They tested 1000 mutants in a first run, selecting 12 of them for development of a second generation. In this way they were able to increase the enantiomeric excess from 2% for the first mutants to 88% after four rounds of evolutive optimization.

The use of fluorescence-based assays is one of the key technologies in screening. The main advantage of these methods is their high sensitivity. Fluorogenic detection is about a thousand times more sensitive than detection of absorption. Thus much lower concentrations of substrates can be used, minimizing problems such as low solubility. However, several disadvantages are associated with these systems. Primarily, substrates have to be designed which carry fluorogenic groups, thus altering the properties of the substrates leading to the same problems of modified reactivity as mentioned above. Furthermore, the presence of quenching substances can inhibit signal generation. Another problem is autofluorescence, which can mask signals. For these reasons it is more favorable to measure fluorescence life-time, energy transfer, or anisotropy rather than intensity [38]. The life-time of a fluorescence signal lies in the range of 100 psec to 10 nsec depending on the nature of the system. Presently available fluorescence readers are, to our knowledge, only capable of measuring fluorescence life-time down to the nanosecond range.

Several methods applying fluorescence measurements are known [38, 39]. They serve as monitor for enzyme activity as well as for the interaction between molecules. For example, a peptide library labeled with fluorogenic groups could be used for the monitoring of an aspartic protease activity by intramolecular quenching of fluorescence signals [40]. The homogenous time resolved fluorescence (HTRF) [41] uses Eu^{3+} ions caged in a polycyclic cryptate as a donor. This Eu-cryptate complex can be excited with laser light at 337 nm. The energy absorbed is transferred to an acceptor molecule, allophycocyanin (APC), which emits light at 665 nm over the range of milliseconds. The modulation of the energy transfer (fluorescence resonance energy transfer, FRET) [42] depends strongly on the distance between the donor and the acceptor. The Eu-cryptate itself emits light at 620 nm which can be used as an internal standard. Again, this method is particularly useful in assays of proteases since doubly labeled peptides are easily accessible by solid phase peptide synthesis. The advantages of this method are its sensitivity and the easy labeling procedure. A disadvantage is that pH-values above 7 have to be used for the assays due to the loss of encaged lanthanide at acidic conditions.

Another approach of using fluorimetric assays for screening purposes is the use of coupled enzyme systems. McElroy et al. presented an assay for glutamate

production [43]. This is based on coupling the glutamate production by a carbamoyl phosphate synthase to the enzyme glutamate oxidase. One of the products of glucose oxidase with glutamate is hydrogen peroxide which reacts, catalyzed by horseradish peroxidase, with a substrate, amplex red, producing the fluorescing product resorfin. The fluorescence was detected by conventional microtiter plate readers.

In a number of enzymatic reactions acid is either consumed or produced. The resulting pH-shift can be used as a sensitive monitor for the progress of the reaction. In the pH-stat method acid or base is titrated to maintain a constant pH which is measured by conventional glass electrodes or by chemical pH-indicators [44]. Janes et al. report about a quantitative screening of hydrolyase libraries using a pH-indicator buffer combination with equal pK_a values [45]. The combination of these indicators results in a linear relationship between absorption change and reaction progress. By comparison between the acid consumption of the two enantiomeric substrates they were also able to estimate the enantioselectivity. The inherent limitation of this method, the requirement of equal pK_a values, can be overcome if the dynamics of the system are fully modeled using corresponding material balances and a kinetic model. With the so-called pH-dyn assay [46] numerical simulation and parameter estimation allow the determination of kinetic parameters without linearization of the system.

All the approaches described above used pH-indicators in solution. A new approach uses indicators immobilized at the bottom of microtiter plates [47]. A fluorescence pH-indicator is immobilized in a thin polymer layer. Changes of fluorescence intensity or of fluorescence life-time can be detected and used to calculate pH and further reaction conversion. The method of choice for the detection is the measurement of fluorescence life-time or luminescence decay time. By using a single class of luminophores (ruthenium diimine complexes) immobilized in different polymers, sensors not only for measurement of the pH but also for oxygen, carbon dioxide, various cations, and sugars were developed, creating an important instrument for the screening of a wide range of enzyme catalyzed reactions [48].

A completely different approach for the measurement of enzyme catalyzed reactions is the detection of the reaction heat by IR-thermography [49]. This technique uses a photovoltaic IR-camera equipped with focal plane array detectors to detect emitted infrared radiation. The IR detection system is sensitive to radiation in the wavelength range of 3 – 5 μm and to temperature changes of 10 – 100 mK [49]. Reetz et al. used this technique for the development of a high-throughput screening system for transition metal and enzyme catalyzed kinetic resolution of chiral substrates [49]. As a model reaction for the enzyme catalyzed conversion the lipase catalyzed (immobilized lipase from *Candida antarctica*) acylation of 1-phenylethanol with vinylacetate was investigated. The *R*- and *S*-enantiomers of the alcohols were tested pairwise in separate wells of a microtiter plate, since the use of the racemate would deliver only information about the overall activity. By this approach a clear preference of the lipase for the *R*-configured substrate could be detected. Until now this promising technique delivers only qualitative results. For quantitative measurement, the method still needs to be developed.

4.1.2 *NMR*

Nuclear magnetic resonance (NMR) is another non-invasive method with the potential for the estimation of enantiomeric excess by the use of chiral lanthanide shift reagents [50]. This method has several disadvantages which prevent its use for screening a large number of reactions. Beside the high technological effort, the long time needed for screening is still the main disadvantage even with modern autosampling devices. This limits its use for high-throughput screening. Thus NMR is a method for the testing of the leading compounds found by other screening methods. Only in cases where NMR imaging can be applied to whole microtiter plates has successful application been reported [51].

4.2 Direct-Invasive Methods

The class of direct-invasive methods requires sampling. After sampling any suitable analytical detection method can be used. For screening it has to fulfill especially the criteria of simplicity, speed, and automation. Again, any kind of optical method can be used including those involving derivatizations.

4.2.1 *Mass Spectrometry*

The development of electrospray ionization (ESI) [52] and matrix assisted laser desorption/ionization (MALDI)-techniques [53] has moved mass spectrometry into the focus of almost all fields of biochemistry and biotechnology. Both techniques have several advantages compared to classical methods of mass spectrometry: they are relatively easy to handle, they offer the possibility to measure both low molecular weight compounds and large biopolymers, and can be coupled with separation techniques like HPLC or capillary electrophoresis. For screening purposes mass spectrometry has some general advantages compared to other methods. The amount of sample needed for analysis is in the low picomolar range. Furthermore, in contrast to other methods like optical detection, analytes can be measured which do not carry chromophoric or fluorescent groups. Therefore enzymatic reactions can be monitored with real substrates, and model substrates are not required, which possibly would lead to artifacts during determination of kinetic constants or turnover numbers compared to real substrates. For example, *o*-nitrophenyl-β-D-galactopyranoside, a substrate frequently used to assay β-galactosidase activity, delivers a lower K_M-value and a higher v_{max} than the real substrate lactose itself [54].

Mass spectrometric methods are fast and can be automated. Thus, they are ideal methods for high throughput screening. Compared to ESI-MS, MALDI-MS shows typically higher tolerance against impurities like buffers, for example. Therefore, samples can be measured which are directly taken from a test solution without further pretreatment. On the other hand, electrospray mass

spectrometry is easily coupled to chromatographic devices (LC-MS) allowing a preselection or cleaning of interesting substances. Additionally, different methods of fragmentation are possible (collision induced decomposition (CID), post source decay (PSD)) depending on the nature of mass measurement. These fragmentations deliver additional information about the molecular nature of products. Both ionization techniques are applicable to the measurement of both substrates and products of enzymatic reactions and the enzymes themselves. Thus it is possible to obtain information about the structure of the catalysts. Additionally, these techniques allow the investigation of the decomposition or chemical modification of the enzymes during the catalytic process, e.g. [55].

ESI-MS has been used for the quantification of a number of substrates and products of enzymatic reactions [56, 57]. Hsieh et al. report the use of ion spray mass spectrometry (a technical variation of electrospray ionization) coupled to HPLC for the kinetic analysis of enzymatic reactions in real time [58]. The hydrolysis of dinucleotides with bovine pancreatic ribonuclease A and the hydrolysis of lactose with β-galactosidase were monitored and the resulting data were used for the estimation of K_M and v_{max} of these reactions. Another field of application of electrospray mass spectrometry is the screening of combinatorial libraries for potent inhibitors [31, 59].

Reetz and coworkers developed a highly efficient method for screening of enantioselectivity of asymmetrically catalyzed reactions of chiral or prochiral substrates using ESI-MS [60]. This method is based on the use of isotopically labeled substrates in the form of pseudo-enantiomers or pseudo-prochiral compounds. Pseudo-enantiomers are chiral compounds which are characterized by different absolute configurations and one of them is isotopically labeled. With these labeled compounds two different stereochemical processes are possible. The first is a kinetic separation of a racemic mixture, the second the asymmetric conversion of prochiral substrates with enantiotopic groups. The conversion can be monitored by measuring the relative amounts of substrates or products by electrospray mass spectrometry. Since only small amounts of sample are required for this method, reactions are easily carried out in microtiter plates. The combination of MS and the use of pseudo-enantiomers can be used for the investigation of different kinds of asymmetric conversion as shown in Fig. 3 [60].

The use of MALDI-MS for the measurement of low molecular mass compounds is widely accepted now [61], but quantification remains problematic. The main problem is the inhomogeneous distribution of the analytes within the matrix [62]. This leads to different amounts of ions and therefore to different signal intensities at various locations of a sample spot. The simplest and most effective way to overcome this problem is the use of an appropriate internal standard [63]. The use of deuterated compounds with a high molecular similarity to the analyte as internal standards leads to a linear correlation between relative signal intensities and relative amount of the compound to be quantified (Fig. 4b) [64]. Using this approach it is possible to quantitate substrates and products of enzyme catalyzed reactions. Two examples were shown recently by Kang and coworkers [64, 65]. The first was a lipase catalyzed reaction which produces 2-methoxy-N-[(1*R*)-1-phenylethyl]-acetamide (MET) using *rac*-α-

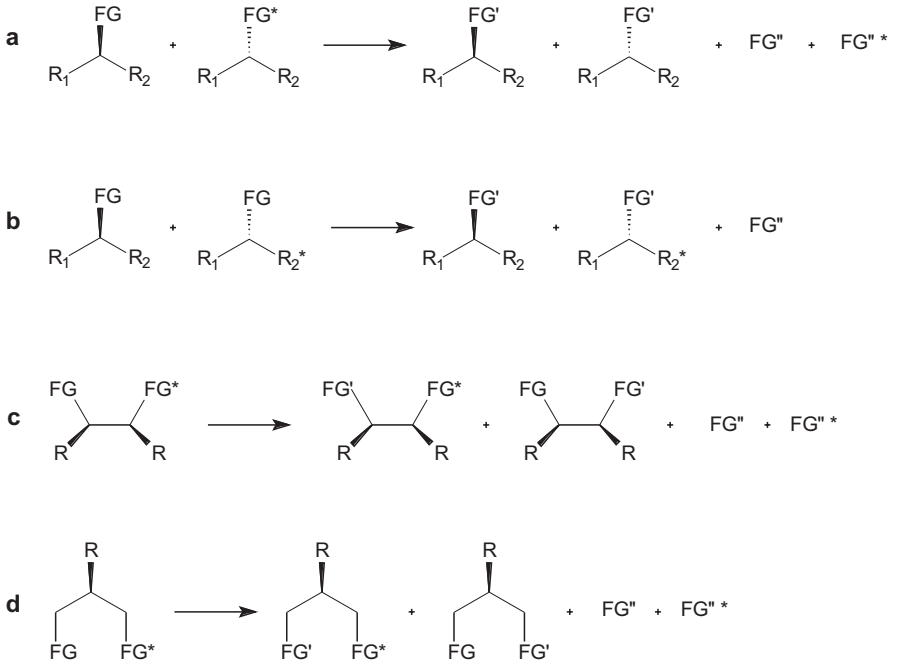

Fig. 3a–d. **a** Principles of asymmetrical transformations which can be followed by electrospray MS: **a** the functional groups FG and the labeled functional groups FG* are cleaved from the molecules. *Primes* mark the functional groups which are created during the reaction from original functional groups (FG), for example in chiral resolution of ester hydrolysis: FG = ester, FG′ = acid, FG′′ = alcohol; **b** cleavage or formation of a new bond on the functional group FG. Residue R_2 is labeled; **c** asymmetrical transformation of a pseudo-meso compound with cleavage of the groups FG or FG*; **d** asymmetrical transformation of a pseudo-prochiral compound (scheme adapted from Reetz et al. [60])

phenylethylamine (PEA) as substrate (Fig. 4a). For this reaction, the kinetics of the enzyme catalyzed conversion could be characterized by quantitative MALDI-MS with comparable results but much faster compared to gas chromatography (Fig. 4c) [65].

The second example was the pyruvate decarboxylase catalyzed formation of (1*R*)-1-hydroxy-1-phenyl-2-propanone (PAC) with benzaldehyde as substrate (Fig. 5a) [64]. This second reaction shows one potential limitation of this method. Some compounds are too volatile for direct measurement by MALDI mass spectrometry or they do not ionize directly due to their nonpolar character. In this case, these compounds have to be derivatized prior to their measurement in order to reduce their volatility and to introduce ionizable functions. This is, however, often very easy using well established quantitative reactions, e.g., formation of oximes from aldehydes and sugars (Fig. 5b).

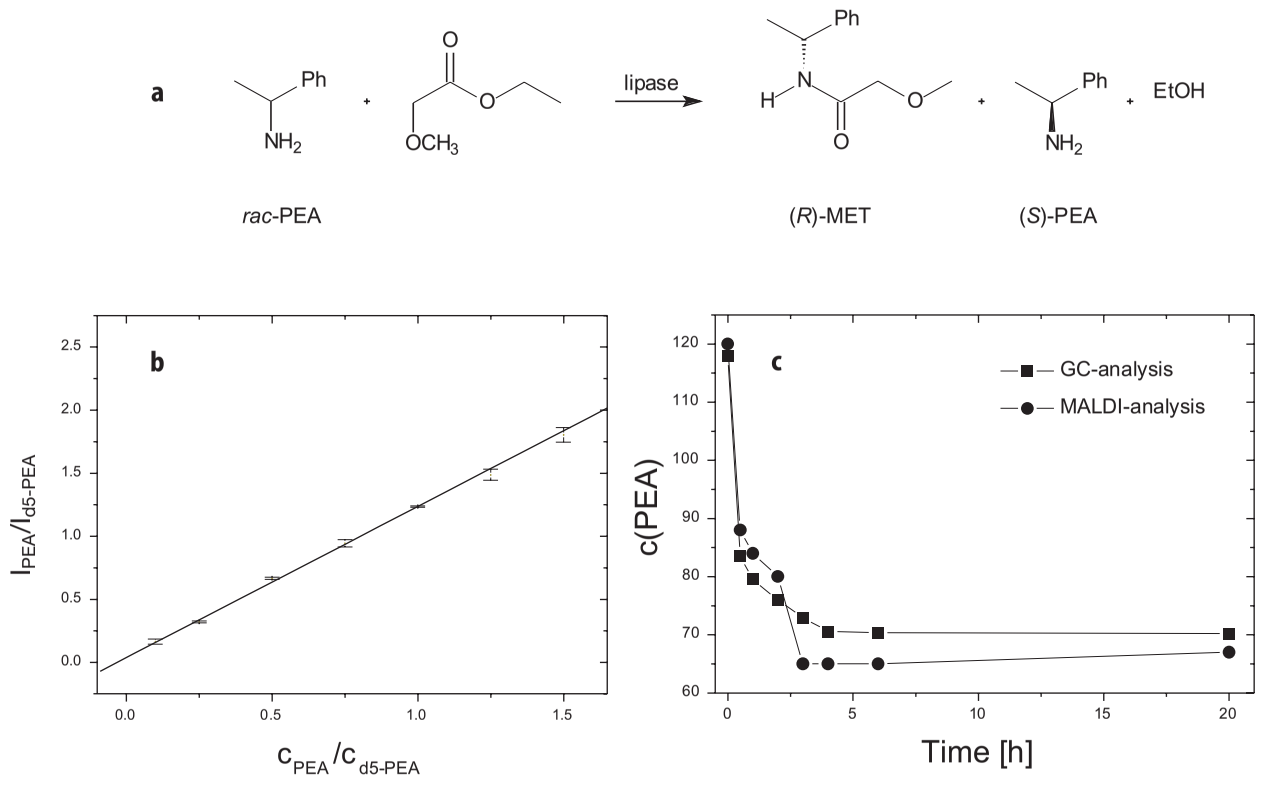

Fig. 4. **a** *rac*-Phenylethylamine (PEA) and 2-methoxy-*N*-[(1*R*)-1-phenylethyl]-acetamide (MET) are substrate and product in a lipase catalyzed transesterification. **b** Linear relationship between relative signal intensities in MALDI-MS and the relative concentrations of PEA/d5-labeled PEA. **c** Comparison of decrease in PEA during enzymatic conversion as measured by quantitative MALDI-MS and gas chromatography (GC)

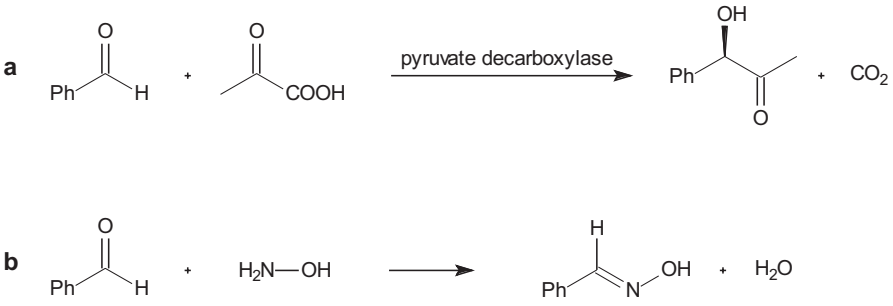

Fig. 5. **a** Pyruvate decarboxylase catalyzed formation of (1*R*)-1-hydroxy-1-phenyl-2-propanone (PAC) using benzaldehyde (BzA) as substrate. **b** Derivatization of benzaldehyde by formation of an oxime

4.3 Separation Methods

Principles of chromatographic methods, e. g., gas chromatography (GC) or high performance/pressure liquid chromatography (HPLC), are well established and do not need any further discussion in this paper. Electrophoretic methods, especially capillary electrophoresis (CE), are still developing quickly and are available even on microchips [66]. This allows a parallel analysis well suited for high throughput screening.

These separation techniques are commonly coupled with detection methods described above, ranging from UV or fluorescence detectors to the coupling with mass spectrometers, especially ESI-MS or – off-line – with MALDI-MS.

The advantage of these methods is that they separate the interesting compounds from the surrounding matrix, allowing the purification of these substances as well as different reaction products or by-products. The disadvantage is the generally low speed of analysis, which prevents their use for the high throughput screening of a large number of substances unless separations are parallelized as mentioned above. Another disadvantage preventing these methods from use in HTS is the high consumption of solvents. Therefore separation methods are only considered in biocatalyst screening when all direct methods fail. This is especially true if enzymatic chiral synthesis is studied. Unlike chiral resolution, where the estimation of enantiomeric excess is possible using techniques described above, there is presently no direct method available to our knowledge which allows estimation of ee in a screening context. The enantioselectivity of an asymmetric reaction is generally determined by conventional GC, HPLC, or CE using chiral stationary phases [67–69]. Another possibility for the estimation of the absolute configuration is the coupling of liquid chromatography with circular dichroism (CD) [70]. Separation techniques are especially useful in the case of investigation of the characteristics of the best candidates already selected by other methods.

5
Future Perspectives

The use of enzymes in industrial processes is a field of growing interest because of the potential it offers for the straightforward selective synthesis of many complex chemicals. The discovery of new catalysts and the optimization as well as modification of those known today will in due course be in the focus of interest. For higher throughput it will be necessary to improve the screening techniques described above. One important point is the automation of these processes. Another important goal is the miniaturization of the methods minimizing the consumption of chemicals – an important economical and ecological factor. The goal of these efforts can be the so-called "lab on a chip" providing the possibility for a very flexible handling of the screening procedures. A major point will be the improvement of data handling. The large amounts of data produced in screening procedures, especially in a high-throughput environment, can only be overviewed by methods to be developed by informatics and especially bioinformatics. The information gained by screening procedures regarding enzyme activities, kinetic constants, and substrate specificities offers the possibility to learn much about the relationship between the structure and the activity of the biocatalysts, thus leading to a deeper understanding of enzymatic processes.

Acknowledgement. We thank G. T. John and C. Wittmann for helpful discussions.

References

1. Liese A, Filho MV (1999) Curr Opin Biotechnol 10:595
2. Bull AT, Bunch AW, Robinson GK (1999) Curr Opin Microbiol 2:246
3. Faber K (2000) Biotransformations in organic chemistry, 4th edn. Springer, Berlin Heidelberg New York
4. Liese A, Seelbach K, Wandrey C (2000) Industrial biotransformation. Wiley-VCH, Weinheim
5. Buchholz K, Kasche V (1997) Biokatalysatoren und Enzymtechnologie. Wiley-VCH, Weinheim
6. Drauz K, Waldmann H (1995) Enzyme catalysis in organic synthesis, vols I and II. VCH, Weinheim
7. Poppe L, Novak L (1992) Selective biocatalysis: a synthetic approach. VCH, Weinheim
8. Theil F (1997) Enzyme in der organischen Synthese. Spektrum Akad, Heidelberg Berlin Oxford
9. Sheldon RA (1993) Chirotechnology: industrial synthesis of optically active compounds. Marcel Dekker, New York Basel Hong Kong
10. Reetz MT, Jaeger KE (2000) Chem Eur J 6:407
11. Sellek GA, Choudhuri JB (1999) Enzyme Microbial Technol 25:471
12. Hertzberg RP, Pope AJ (2000) Curr Opin Chem Biol 4:445
13. Copeland GT, Miller SJ (1999) J Am Chem Soc 121:4306
14. Burbaum JJ, Sigal NH (1997) Curr Opin Chem Biol 1:72
15. Marrs B, Delagrave S, Murphy D (1999) Curr Opin Microbiol 2:241
16. Pedersen H, Holder S, Sutherlin DP, Schwitter U, King DS, Schultz PG (1998) Proc Natl Acad Sci USA 95:10,523
17. Petrounia IP, Arnold FH (2000) Curr Opin Biotechnol 11:325

18. Jaeger KE, Reetz MT (2000) Curr Opin Chem Biol 4:68
19. Arnold FH, Volkov AA (1999) Curr Opin Chem Biol 3:54
20. Altreuther DH, Clark DS (1999) Curr Opin Biotechnol 10:130
21. Leung DW, Chen E, Goeddel DV (1989) Technique 1:11
22. Patten PA, Howard RJ, Stemmer WPC (1997) Curr Opin Biotechnol 8:724
23. Stemmer WPC (1994) Nature 370:389
24. Okahara Y, Mori T (1998) J Mol Catal B: Enz 5:119
25. DeSantis G, Jones JB (1999) Curr Opin Biotechnol 10:324
26. St Clair NL, Navia MA (1992) J Am Chem Soc 114:7314
27. Tischer W, Kasche V (1999) Trends Biotechnol 17:326
28. Beck-Sickinger AG, Weber P (1999) Kombinatorische Methoden in Chemie und Biologie. Spektrum Akad, Heidelberg
29. Demirjian DC, Shah PC, Moris-Varas F (1999) Top Curr Chem 200:2
30. White RE (2000) Annu Rev Pharmacol Toxicol 40:133
31. Cancilla MT, Leavell MD, Chow J, Leary JA (2000) Proc Natl Acad Sci USA 97:12,008
32. Ingham J, Dunn IJ, Heinzle E, Prenosil JE (2000) Chemical engineering dynamics, 2nd edn. Wiley-VCH, Weinheim
33. John RA (1992) Photometric assays. In: Eisenthal R, Danson MJ (eds) Enzyme assays: a practical approach. Oxford University Press, p 59
34. Zocher F, Enzelberger MM, Bornscheuer UT, Hauer B, Schmid RD (1999) Anal Chim Acta 391:345
35. Michal G, Möllering H, Siedel J (1983) In: Bergmeyer HU (ed) Methods of enzymatic analysis, vol I. VCH, Weinheim, p197
36. Ellman GL (1959) Arch Biochem Biophys 82:70
37. Makinen KK, Tenuovo J (1982) Anal Biochem 126:100
38. Pope AJ, Haupts UM, Moore KJ (1999) Drug Discovery Today 4:350
39. Mere L, Bennett T, Coassin, England P, Hamman B, Rink T, Zimmerman S, Negelescu P (1999) Drug Discovery Today 4:363
40. Rosse G, Kueng E, Page MG, Schauer-Vukasinovic V, Giller T, Lahm HW, Hunziker P, Schlatter D (2000) J Comb Chem 2:461
41. Grepin C, Pernelle C (2000) Drug Discovery Today 5:212
42. Mathis G (1995) Clin Chem 41:1391
43. McElroy KE, Bouchard PJ, Harpel MR, Horiuchi KY, Rogers KC, Murphy DJ, Chung TDY, Copeland RA (2000) Anal Biochem 284:382
44. Pantel S (1987) Anal Chim Acta 199:1
45. Janes LE, Löwendahl C, Kazlauskas RJ (1998) Chem Eur J 4:2324
46. John GT, Heinzle E (2001), Biotechnol Bioeng 72:620
47. John GT, Klimant I, Heinzle E (2000) Modeling of enzyme kinetics using microplates with integrated pH-sensing. In: Biotechnology 2000 – 11th International Biotechnology Symposium and Exhibition, Berlin
48. Wolfbeis OS, Klimant I, Werner T, Huber C, Kosch U, Krause C, Neurauter G, Dürktop A (1998) Sensors Actuators B51:17
49. Reetz MT, Becker MH, Kühling KM, Holzwarth A (1998) Angew Chem Int Ed 37:2547
50. Sullivan GR (1978) Top Stereochem 10:287
51. Huisman GW, del Cardayre SB, Selifonov SA, Powell K (2000) Directed molecular evolution for metabolic engineering. In: Metabolic Engineering III, UEF Conference, Colorado Springs
52. Fenn JB, Mann M, Meng CK, Wong SF, Whitehouse CM (1989) Science 246:64
53. Karas M, Hillenkamp F (1988) Anal Chem 60:2299
54. Wallenfels K, Weil R (1972). In: Boyer PD (ed) The enzymes, 3rd edn, vol VII. Academic Press, New York, p 617
55. Treitz G, Maria G, Giffhorn F, Heinzle E (2001) J Biotechnol 85:271
56. Gerber SA, Scott CR, Turecek F, Gelb MH (1999) J Am Chem Soc 121:1102
57. Lee ED, Mück W, Henion JD, Covey TR (1989) J Am Chem Soc 111:4600
58. Hsieh FYL, Tong X, Wachs T, Ganem B, Henion J (1995) Anal Biochem 229:20

59. Wu J, Takayama S, Wong CH, Siuzdak G (1997) Chem Biol 4:653
60. Reetz MT, Becker MH, Klein HW, Stöckigt D (1999) Angew Chem 111:1872
61. Ligard R, Duncan MW (1995) Rapid Commun Mass Spectrom 9:128
62. Garden RW, Sweedler JV (2000) Anal Chem 72:30
63. Ling YC, Lin L, Chen YT (1998) Rapid Commun Mass Spectrom 12:317
64. Kang MJ, Tholey A, Heinzle E (2000) Rapid Commun Mass Spectrom 14:1972
65. Kang MJ, Tholey A, Heinzle E (2000) Quantification of biologically interesting low molecular weight compounds using MALDI-TOF MS. In: Biotechnology 2000 – 11th International Biotechnology Symposium and Exhibition, Berlin
66. Altria KD (1999) J Chromatogr A 856:443
67. König WA (1992) Gas chromatographic enantiomer separation with modified cyclodextrines. Hüthig, Heidelberg
68. Schurig V, Wistuba D (1999) Electrophoresis 20:2313
69. Chankvetadze B (1997) Capillary electrophoresis in chiral analysis. Wiley, Chichester
70. Reetz MT, Kuhling KM, Hinrichs H, Deege A (2000) Chirality 12:479

Received: May 2001

In-Situ-Fluorescence-Probes: A Useful Tool for Non-invasive Bioprocess Monitoring

E. Stärk [1], B. Hitzmann [1], K. Schügerl [1], T. Scheper [1], C. Fuchs [2], D. Köster [2], H. Märkl [2]

[1] Institut für Technische Chemie, Callinstrasse 3, 30167 Hannover, Germany
E-mail: scheper@mbox.iftc.uni-hannover.de
[2] TU Hamburg-Harburg, Biotechnologie I, Denickestr. 15, 21071 Hamburg-Harburg, Germany

Dedicated to Prof. Dr. Wolf-Dieter Deckwer on the occasion of his 60th birthday

Optical sensors appear to be very promising for different applications in modern biotechnology. They offer the possibility to interface all the well known optical analysis techniques to bioprocesses via fiber optical cables. Thus, high sophisticated and sensitive optical analysis techniques can be coupled to a bioprocess via these light signal transporting fibers. A wide variety of sensor types for application in biotechnology has been described [1–4]. Normally these sensors are non-invasive and the response times are nearly instantaneous. In particular, the use of glass fiber technology makes these sensors small, robust and reduces their costs.

Keywords. In-situ, Non-invasive monitoring, Fluorescence, Optical sensor, Bioprocess control

Advances in Biochemical Engineering/ Biotechnology, Vol. 74
Managing Editor: Th. Scheper

List of Abbreviations

DNA	desoxyribonucleic acid
DNP	2,4-dinitrophenol
2D	two-dimensional
FAD	flavin-adenine dinucleotide
$FADH_2$	flavin-adenine dinucleotide (reduced form)
FMN	flavin mononucleotide
HCDC	high-cell-density cultivation
NAD(P)H	nicotinamide-adenine dinucleotide (phosphate) (reduced form)
NIR	near infrared
nm	nanometer
PCA	principal component analysis
PLS	partial least square
rel. units	relative units
RFI	relative fluorescence intensity
RMSEC	root mean square error of calibration
UV	ultra violet

1 Introduction

In the area of nephelometric sensors, a large variety of instruments is commercially available. These sensors monitor the response of turbid samples to light signals [5–14]. In general, turbidity results from suspended solid particles in the liquid. This turbidity is dependent on the physical size and concentration of the particles. In biological systems it might be possible to analyze the cell concentration, when the side effects of suspended solid particles or air bubbles can be excluded. Normally it is not possible to distinguish between viable and nonviable particles with nephelometric methods without any further verification technique. Nephelometric sensors monitor the transmitted light or the scattered light under different angles (e.g., 90° or retro reflective scattering). Most devices use light emitting diodes in the near infrared region as light source.

These optical probes are the most universally applicable in situ devices for on-line biomass monitoring up to now [15, 16]. Konstaninov et al. [17] tested several absorbance and scattering sensors for real-time biomass concentration monitoring in mammalian cell cultivation processes and Hatch and Veilleux [18] compared optical density probes with oxygen uptake rates, packed cell volume, and off-line cell mass monitoring in commercial fed-batch fermentations of *Saccharomyces cerevisiae* [19]. In order to minimize influencing effects, special chemometric data treatment is necessary [20].

2
Optical Chemo- and Biosensors

Fiber optical sensors are popular devices for the design of optical chemosensors. They are based on the change of optical properties (such as adsorption or luminescence) of particular chemical indicators. For example, fiber optical oxygen sensors are produced by the immobilization of oxygen sensitive dyes on the tip of an optical fiber and in an appropriate matrix.

The fluorescence intensity or the decay time of the fluorophor is influenced by the analyte to be measured. Excitation light is guided through the fiber to the chemosensing tip. Here the fluorescence properties of the dye are changed by the interaction with the analyte. The backward fluorescence light (changes in intensity, wave length, or decay time) is guided back through the fiber and is detected by an appropriate light detection unit. A change in the signal can be correlated to the analyte concentration. Different types of oxygen sensors are described in the literature [21, 22]. These sensors have tremendous advantages with regard to the conventional amperometric sensors (Clark) type, since no oxygen is consumed and the signal is not dependent on the stirring rate of the media and no electromagnetic effects interfere with the signals.

If the oxygen sensitive dye is replaced by a pH sensitive dye, optical pH sensors can be produced. Thus miniaturization of these sensors is easy, and multisensing systems can be set up. Different sensor types for biotechnical application are described in the literature (e.g., ethanol and chloride sensors) [23, 24].

Based on these chemosensors, biosensors can be set up such as glucose or H_2O_2 sensors. In this case the appropriate biological compound (glucose oxidase or catalase) must be immobilized on the chemosensor. Different optical sensors are also used as transducer elements for the production of biosensors, especially of immuno-sensors. Here the affinity component is immobilized on the tip of the fiber and all available immuno-sensing assays can be performed using this transducer element. Since these sensors cannot be sterilized and used for on-line monitoring in a bioprocess we refer to other publications [25–27].

3
Infrared Sensors

Infrared spectroscopy has become very popular during the last few years. It offers the possibility of a non-invasive but very specific analysis based on the huge experience in infrared spectroscopy in biochemistry. Thus it is possible to analyze certain organic species even in complex media. Biologically important bonds (aliphatic CH, aromatic or alkene C=H, amine N–H, and hydroxy O–H) absorb in the near infrared range 2.0–2.5 μm. Different spectral regions above 700 nm and the FTIR are also of tremendous interest [28–37]. Each chemical structure is related to a specific position shape and size of the analyte's absorption bands. Because the adsorption bands are interfering and often similar, advanced data analysis is necessary in order to extract the real information from the whole spectrum. Multivaried calibration models generated by using partial least squares (PLS) analysis and other chemometric models are used. Normally

a pre-processing digital Fourier filtering step improves the data treatment and the application of infrared sensors for the determination of glucose, glutamine, ammonia, lactate, and glutamate is reported in different biotechnological application [30]. The short wavelength IR-spectroscopy (700 – 1100 nm) for the detection of ethanol during fermentation processes is reported by Cavinato et al. [34]. The measurements were performed with a photodiode array spectrometer, interfaced via fiber optical cables with a glass fermentor. In high cell density *E. coli* cultivation processes NIR spectroscopy was used for monitoring ammonia, acetate, and glycerol in an industrial process. Different applications in mammalian cell cultivation and in lactic acid production processes and in brewing processes are described [35 – 37]. In general this method can be used for standard fermentation processes in order to monitor the overall productivity of the process.

In general, optical sensor systems based on glass fiber technology offer tremendous advantages for bioprocess monitoring. They offer in general the possibility to couple spectroscopic monitoring techniques which are well established and highly reliable via fiber cables to the bioprocess. These methods are normally non-invasive and do not interfere with the bioprocess. Based on such real-time monitoring, the detailed understanding of the bioprocess is possible allowing an efficient control of the bioprocess.

4 Fluorescence Sensors

Another group of optical sensors, especially designed for application in biotechnology, are in-line, on-line, and in-situ fluorescence. Different types of these sensors have been developed and applied for different purposes such as bioreactor characterization, process monitoring, and process control [38 – 42]. The first devices were developed based on fluorescence studies by Duysens and Amesz in 1957 [43]. They were the first to monitor the reduced form of nicotinamid adenine dinucleotides (NADH or NAD(P)H) in vivo. This coenzyme-dependent fluorescence is measured at 450 nm after excitation at 360 nm. By measuring the emitted light the NAD(P)H-pool inside living organisms can be continuously monitored via this optical technique. The intensity of the fluorescence is effected by the amount of the viable biomass concentration, and the metabolic state of the cells by abiotic factors such as air bubbles or other fluorescent components in the medium.

Different complicated fluorometer devices were developed and interfaced with fermentors over the years. Here the excitation light as well as the emitted fluorescence light was passed through the fermentor walls by Zabriskie and Humphrey in 1978 [45].

Based on these devices, different biomass estimation experiments were performed based on the culture fluorescence monitoring and feeding strategy studies were developed as well as bioreactor characterizations via mixing time experiments. During the next years smaller fluorescence probes were developed which could be interfaced with bioreactors via standard electrode ports. These open end detector systems measured the fluorescence light in the backward di-

rection. Two fluorescence devices were commercially available by BioChem Technology, Malvern, USA [46] and Mettler Toledo, Urdorf, Switzerland (formerly Ingold Messtechnik AG) [47, 48]. Both systems could only measure the NAD(P)H-dependent culture fluorescence or fluorophors with the same fluorescence property. In addition, multi-wavelength systems were described in the literature. A system described by Scheper and Schügerl in 1986 [49] is shown in Fig. 1. Here a low pressure mercury lamp is used as UV light source. Optical filters select the excitation light at 360 nm or an optical system focuses the light on a fiber optical bundle in which the light is guided into the reactor. The retro reflective fluorescence light of the intracellular reduced dinucleotides is measured at 460 nm. In addition, the monitoring of different wavelengths is possible via an appropriate filter system. Photodiodes are used for the monitoring of the fluorescence light. This device offered the possibility to monitor simultaneously two different wavelengths [50–52].

5 Biomass Monitoring

Zabriski and colleagues [45, 46] first used culture fluorescence as an on-line estimate of viable biomass during the batch cultivation of *Saccharomyces cerevisiae*, a species of *Streptomyces*, and a species of *Thermoactinomyces*. They simply linearized the fluorescence to biomass data in order to find a direct function between NADH-dependent culture fluorescence and biomass concentration in the bioreactor. In the following years several other authors reported – on the basis of these results – on the estimation of biomass concentration from culture fluorescence data as shown in Table 1.

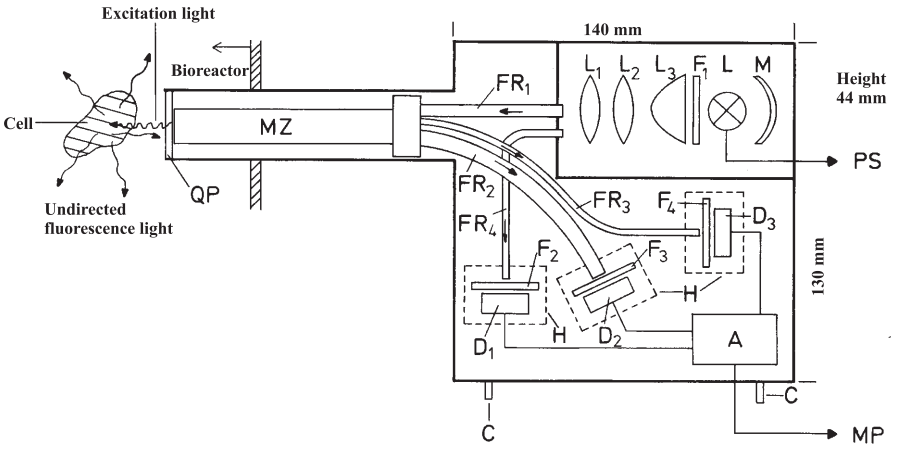

Fig. 1. Schematic design of a fluorescence probe for the simultaneous detection of two different wavelengths. M mirror, L lamp, L1–3 lenses, F1–4 filters, FR1–4 fiber cables, D1–3 photodetectors, H housing, MZ mixing zone of fiber, QP quartz plate, A amplifier, C cooling, MP microprocessor unit, PS power supply

Table 1. On-line estimation of the biomass concentration for different microorganisms by using culture fluorescence

Microorganisms	References
Pseudomonas putida	57, 58
Zymomonas mobilis	59, 60
Sporotrichum thermophile	50
Bacillus subtilis	50, 61
Alcaligenes eutrophus	62
Eschericia coli	50, 63, 64, 65, 71, 72
Clostridium acetobutylicum	39, 54
Pedicoccus sp.	73
Streptomyces sp.	45, 74
Thermoactinomyces sp.	74
Saccharomyces cerevisiae	38, 45, 47, 50, 51, 66, 73, 75
Candida tropicalis	47
Candida utilis	66, 67, 74, 76
Penicillium chrysogenum	49, 56
Cephalosporium acremonium	77
Mucor mucosa	78
Pseudomonas putida	66
Spodoptera frugiperda	77
Plant cells	79
Human melanoma cells	80
Mouse hybridoma cells	53, 73, 81

Different simple correlations between biomass and fluorescence data showed that on-line estimation is possible under strictly defined culture conditions. Even a strictly linear relation between biomass and culture fluorescence was found for the growth of *Zymomonas mobilis*, *Methylomonas mucosa*, and *Pseudomonas putida* under non-limited conditions [47].

As soon as the culture conditions were changed or limiting conditions occurred during the cultivation model deviations occur due to drastic changes of the intracellular coenzyme concentrations.

The monitoring of viable cell mass even in technical media is possible with this technique. However, fluorescence medium components might drastically interfere with the NADH-dependent fluorescence and signal disturbances occur caused by air bubbles (lowering the sensor readings) or large amounts of scattering particles.

While most applications were performed in suspended cell cultures some authors showed that the application of NADH-dependent fluorescence monitoring is also possible in immobilized cell systems. Here the growth of *Clostridium acetobutylicum* and the *Saccharomyces cerevisiae* immobilized in different calcium alginate structures was studied. However, calibration of the culture fluorescence signal with the biomass concentration was not possible but qualitatively an increasing biomass also led to an increase in the fluorescence signals.

In conclusion it can be stated that accurate biomass estimation based on the culture fluorescence monitoring is possible, when the NAD(P)H-pool per cell is

constant and no interfering fluorescence occurs during the monitoring process. Thus, this technique is an excellent device for repeated standard cultivations (e.g., in industry) to provide an on-line monitoring of the biomass concentration. Under these controlled cultivation conditions an accurate estimation of the biomass is still possible, even when metabolic changes occur (aerobic/anaerobic transitions) [52]. It becomes obvious from all the publications that the bottleneck limitation of the fluorescence monitoring in regard to biomass estimation is the restriction to one single wavelength monitoring, since no verification of the signals is possible in regard to interfering fluorophors or disturbing factors (air bubbles, scattering particles).

6
Mixing Time Experiments

In order to quantify the physical environment of a bioreactor, fluorescence assays can be applied for on-line monitoring of the mixing time behavior of all types of bioreactors. In this case the fluorosensor probe can be installed in the bioreactor at different locations of interest. Afterwards, selected fluorophores can be injected in order to study the overall mixing time. These fluorophores must fit to the excitation and emission behavior of the probe and should be selected in regard to the pH-dependency of the bioprocess, and when used during cell cultivation experiments they should not interfere with the cells. Scheper and Schügerl reported on the use of different coumarins for mixing time experiments under bioprocess relevant conditions [49].

7
Cell Metabolism

Since the monitoring of the culture fluorescence is based on the NAD(P)H pools inside the cells, the observation of the fluorescence signals can be used to detect environmental and metabolic changes as a function of the culture conditions. Different applications are presented in the relevant literature as shown in Table 2. Metabolic changes during the growth, such as glycolytic oscillations in yeast or the metabolic shift in *Clostridium acetobutylicum* as a function of the process state, become obvious in the culture fluorescence signals. In chemostat cultures the changes in dilution rates are also reflected in the fluorescence signal, indicating that the metabolic pool and intracellular redox state changes depending on the dilution rate.

The dynamic behavior of the cell metabolism initiated by different external effects (addition of substrates or inhibiting reagents) can be followed via this instantaneous method. These effects can be used to control the overall process and optimize the bioprocess. Meyer and Beyeler [50] developed a control system for a continuous yeast cultivation process. Here the increase up to the optimal dilution rate was controlled via fluorescence monitoring. The dilution rate was only increased when no negative effect on the metabolic state of the cells was observed. During the cultivation of *Candida utilis* the fluorescence signal was used for the addition of substrate ethanol. The addition was started when

Table 2. Metabolic studies on different microorganisms by using culture fluorescence

On-line monitoring	Microorganisms	References
Aerobic-anaerobic transition	*Klebsiella aerogenes*	44
	Saccharomyces cerevisiae	45, 60, 73, 82
	Candida tropicalis	47
	Eschericia coli	50, 65
	C. guilliermondi	83
Aeration rate	*Penicillium chrysogenum*	49, 56
Addition of carbon source to starved cells	*S. cerevisiae*	45, 73, 75, 82
	C. tropicalis	84
	E. coli	50
Diauxic growth	*S. cerevisiae*	82
Dilution rate changes	*S. cerevisiae*	75
	E. coli	64
	Pseudomonas putida	85
Culture synchrony	*S. cerevisiae*	60, 77
Glycolytic oscillations	*S. cerevisiae*	86, 87, 88
Metabolic shifts	*Thermoactinomyces sp.*	45
	Clostridium acetobutylicum	54, 89, 90, 91
	S. cerevisiae	51, 67
	Hybridoma cells	53
	Penicillium chrysogenum	56
Addition of metabolic uncoupler	*S. cerevisiae*	82, 86

the first signal decreased below a certain critical value. In calibration experiments this critical value was determined as an indicator for a low ethanol concentration. The same concept was also used in cultivation of thermo monospora species for optimal growth conditions.

The different applications listed in Table 2 show that culture fluorescence offers the opportunity to have non-invasive insight not only into the fluorophor behavior of the medium but also in the metabolic state. It gives information about the redox status of the cultivation, but still the danger of interference cannot be excluded. Thus, the interpretation of the data measured is often complicated and only successful for a standard cultivation process [51–65].

8 Multi-Wavelength Monitoring

In the early 1990s more and more research groups tried to circumvent the restrictions of single wavelength monitoring by developing different multi-wavelength systems. Again the research group of Humphrey was one of the pioneers in this area [66–68]. They reported on the use of different filter systems or modified spectrofluorometer systems, which were used to study the ethanol fermentation of *Candida utilis* and the phenol fermentation of *Pseudomonas pu-*

tina and the glucose fermentation of *Saccharomyces cerevisiae*. Excitation wavelengths of 289 nm, 313 nm, 365 nm, and 404 nm were used in the experiments. More information was available; however the interpretation was still complex. Based on tryptophan monitoring the amino acid concentration and protein expression could be followed. Even the use of a scanning spectrofluorometer interfaced to a bioreactor was reported; however mostly the restriction to only five or six wavelengths is reported [69, 70]. Tartakovsky and Sheintuch [71] were the first to report the use of the overall spectrum obtained, via the coupling of a spectrofluorometer to a bioreactor using fiber light guide cable. Here the information content of the scanning fluorometry signal during the cultivation of wild type or recombinant *Escherichia coli* and *Saccharomyces cerevisiae* is reported. It becomes obvious that different process parameters can be derived from this highly informative monitoring system.

9
BioView Sensor

The BioView sensor (DELTA Light & Optics, Denmark) was developed especially for industrial applications. It is capable of completely automatic optical measurement for monitoring and control of different bioprocesses. The instrument is conceived to withstand harsh industrial environments (e.g., high temperature, moisture) and electromagnetic interference. For data transfer a single-fiber asynchronous modem is used, which allows a distance between the computer and spectrometer of up to several hundred meters.

For on-line measurement the BioView sensor is connected directly by a 1.5-m bifurcated liquid light conductor (Lumatec, Germany) to a quartz window in a 25-mm electrode standard port of vessel bioreactor (Fig. 2). Contamination and sterilization problems could be avoided, because there is no contact between sensor and fermentation broth.

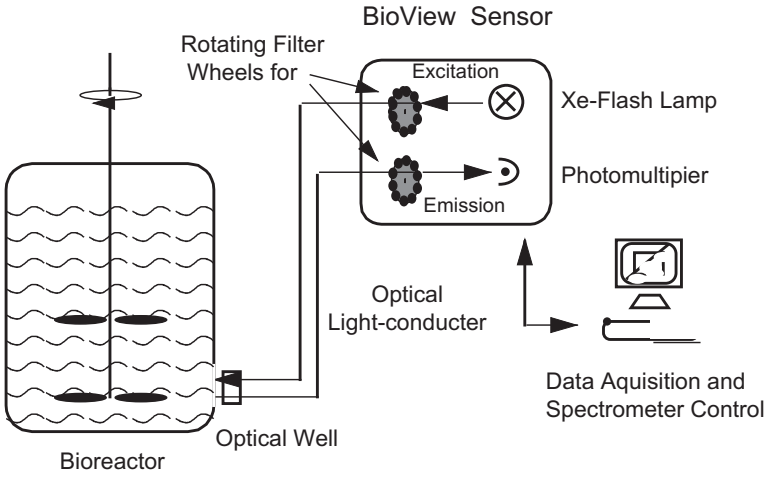

Fig. 2. Schematic set-up of the 2D-fluorescence spectrometer (BioView sensor)

The system uses independent filter wheels (Fig. 2) with up to 16 different filters for excitation (270–550 nm) and emission (310–590 nm) and performs measurements in steps of 20 nm, which was found to be most suitable without any loss of information. The number of measurements for each filter position can be individually chosen. Adapted to the different industrial processes, properties and steps of filters can be designed individually to cover most of the information potential. In addition it is possible to monitor single-wavelength pairs continuously. A high measuring frequency (10/s) enables in situ mixing time experiments for bioreactor characterization [49]. The single-wavelength pairs could be selected dependent of the available or suitable fluorophores.

The BioView sensor includes a software package (CAMO ASA, Norway) for data analysis and on-line estimation of different bioprocess variables simultaneously. Thus, the instrument is able to predict the trends of the concentration courses of different variables during a cultivation and is used to give information about important process steps (e.g., feeding time, harvesting time, etc.). The instrument is able to monitor on-line several fluorophores in situ and non-invasively during cultivation processes and permits an estimation of different bioprocess variables simultaneously. The increasing of cell mass concentration and the product formation as well as the actual metabolic state of the cells is simultaneously detectable by this fluorescence technique.

Problems like overlapping and interfering of fluorophores is overcome by the BioView sensor, which offers a comprehensive monitoring of the wide spectral range. Multivariate calibration models (e.g., partially least squares (PLS), principal component analysis (PCA), and neuronal networks) are used to filter information out of the huge data base, to combine different regions in the matrix, and to correlate different bioprocess variables with the courses of fluorescence intensities.

The potential of the application of 2D-fluorescence spectroscopy has been investigated by the cultivation of various microorganisms [3, 42]. Information about cell growth and metabolism was obtained and correlations to fluorescent product and substrate can be made. Marose et al. [42] correlated the off-line cell mass concentration during *Saccharomyces cerevisiae* cultivation with the culture fluorescence in the different regions of protein, NAD(P)H, riboflavin, and pyridoxine. This method for the on-line detection of biomass is especially suitable if the cells cannot be counted or solid particles in the medium exclude the method of weighing biomass. Even metabolic changes such as aerobic–anaerobic transitions were detected by the 2D-fluorescence spectroscopy. Changes in the relation of oxidized to reduced form of NADH, $FADH_2$ during the aerobic–anaerobic transitions are obvious in the region of NADH fluorescence (Ex350/Em450 nm) and FAD/FMN (Ex450/Em530 nm).

Moreover, uncoupling experiments using *Escherichia coli* cells were described. An addition of glucose to stationary *E. coli* cells leads to an increase of fluorescence intensity in the region of NAD(P)H, because it is formed in the glycolysis. This increase was stopped abruptly by addition of 2,4 dinitrophenol (DNP), which effects a decrease in the fluorescence signal according to the theory of uncoupled oxidative phosphorylation. The dynamics of this process,

which takes place within seconds, can be seen with the 2D-fluorescence spectroscopy by performing the time scan.

During the cultivation of *Claviceps purpurea* the ergot alkaloids formation can be observed as the ergot alkaloids fluoresce by 2D-fluorescence spectroscopy as well. Quantitative analytical techniques for the determination of ergot alkaloids with a modified Van-Urk-assay [107] are invasive and time-consuming. Applying this technique the on-line determination of the exact harvesting time is possible. A further powerful application of BioView sensor is the on-line monitoring of biomass for this organism. Growth in micelles makes it impossible to count cells and also optical density could not be correlated to biomass during C*laviceps purpurea* cultivations. The method of 2D-fluorescence spectroscopy offers a variety of information about this complex organism and the product [42]. Also, for various cultivations of microbial degradation of the pollutant, 2D-fluorescence spectroscopy was used. The decrease of the fluorescence intensity of the substrate phenanthrene during the cultivation of *Sphingomonas yanoikuyae* could be observed on-line.

An on-line monitoring of an industrial chromatographic process was realized by using the BioView sensor. 2D-fluorescence spectroscopy allows automatic real time measurements directly at the outlet of the chromatographic columns. The fluorescence technique for separating different amino acids is faster and more accurate than conventional methods. The application of the BioView sensor will reduce costs and will increased the productivity of further chromatographic separations [92, 93].

10
The Application of a 2D-Spectrofluorometer for the Monitoring of High-Cell-Density Cultivations

High-cell-density cultivation (HCDC) is required to improve microbial biomass yield and product formation substantially. An overview of HCDC is given by Riesenberg and Guthke [94] for different microorganisms (bacteria, archeae, and eukarya) and by Lee and Blanch [95] for different recombinant *Escherichia coli.* The application of on-line fluorescence measurement by the BioView sensor has a favorable effect on the bioprocess monitoring and control, leading to economic and ecological advantages.

Historically, HCDC was first established for yeasts to produce single-cell protein, ethanol, and biomass. Later, dense cultures of other mesophiles producing various types of products were developed, e.g., by Suzuki et al. [96]. The combination of recombinant DNA technology and large-scale culture processes has enabled human proteins to be produced in a number of hosts, in particular in *Escherichia coli* [97 – 100]. Approaches to optimize the production of recombinant proteins are the subject of recent reviews from Winter et al. [101].

A major objective of fermentation in research industry is to maximize the volumetric productivity to obtain the highest possible amount of product in a given volume within in a certain time. The main problems arising from HCDC are limitation and/or inhibition of substrates with respect to growth, accumulation of products or metabolic by-products to a growth-inhibitory level, a high

oxygen demand, as well as an increasing viscosity of the medium in very dense cultures [94]. Different types of bioreactors and fermentation strategies were developed to overcome these problems.

The membrane dialysis reactor designed by Märkl et al. [102] consists of two cylindrical chambers. Each chamber has its own stirrer and accessories for nutrient-split feeding. The main advantage of the dialysis reactor is the continuous removal of inhibitory or toxic low-molecular-mass compounds from the fermentation broth without additional stress to cells [103]. The dialysis technique has turned out to be very efficient and reliable for obtaining high cell densities. If metabolites inhibiting cell growth are eliminated, the efficiency of several microbial or mammalian cell culture processes can be increased significantly. Ogbonna and Märkl [104] suggested a novel "nutrient-split" feeding strategy where the medium is split into a concentrated nutrient solution which is fed directly into the cultivation chamber and a dialyzing buffer solution containing inorganic salts for stabilization of the osmotic pressure. By applying a nutrient-split feeding strategy, the loss of nutrients can be avoided and the medium is used very efficiently.

A scale-up of the dialysis reactor system for suspended cells is feasible by application of external dialysis modules, which are coupled between a culture vessel and a dialysis vessel (Fig. 3). The culture broth and dialysis medium are pumped in an external loop through the dialysis module.

High cell densities are not only a prerequisite for high productivity; additionally an effective on-line control and modeling of the bioprocesses is necessary. For industrial applications, optical measurement methods are more attractive because they are non-invasive and more robust. The potential of the BioView sensor for on-line bioprocess monitoring and control was tested. For high-cell-density cultivation of *Escherichia coli*, maintaining aerobic conditions and removal of inhibitory by-products are essential. Acetic acid is known to be one of the critical metabolites. Information about changes in the cell metabolism and the time of important process operations is accessible on-line for optimization

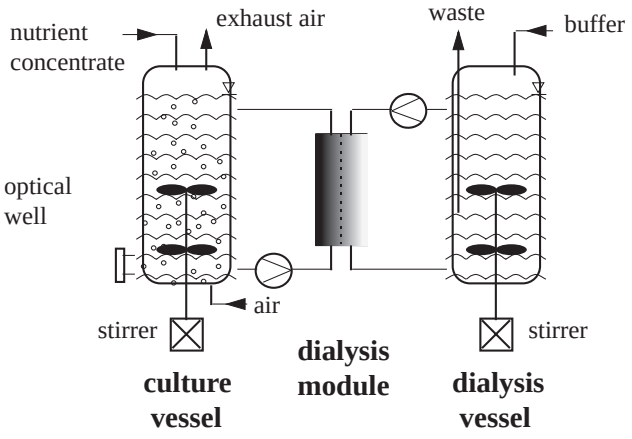

Fig. 3. Schematic design of a two-vessel arrangement for a scale-up of the dialysis technique

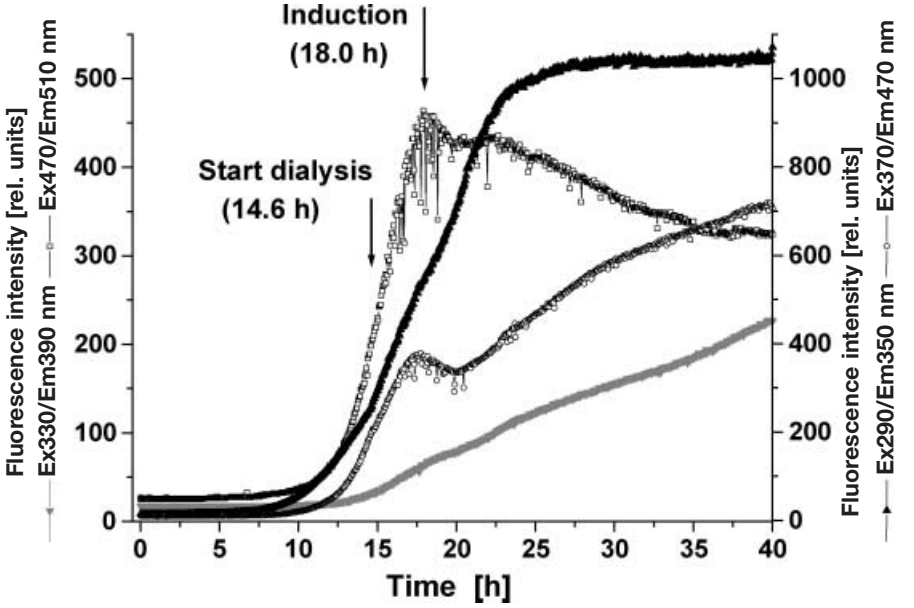

Fig. 4. Courses of culture fluorescence during a high-cell-density cultivation of *E. coli*

of these bioprocesses especially in regard to scale-up. Thus the BioView sensor is interfaced directly to an optical port of a 300-l culture vessel (Fig. 3). For the HCDC a minimal medium was used in a 300-l culture vessel, a pH of 7,1 and a temperature of 35 °C [105].

2D-fluorescence spectra were automatically measured every 3 min. Courses of culture fluorescence during the HCDC of 40 h are shown in Fig. 4. The figure shows the increase of the relative fluorescence intensities (RFI) at the beginning of the exponential growth phase. After 14.6 h the dialysis was started for removal of inhibitory by-products and the slope of the protein dependent RFI at Ex290/Em350 nm increases. The induction of the protein synthesis is performed at an optical density of 100 or a cell dry mass concentration of about 40 g/l. This leads to a change in the cell metabolism after 18 h. The changes in cell physiology become obvious in a decrease of the NAD(P)H (Ex370/Em470 nm) and flavin dependent (Ex470/Em530 nm) fluorescence intensities.

During the process the optical properties of the medium also change in the protein-dependent fluorescence region (Ex290/Em350 nm) due to high intra- and extracellular protein concentration. Thus no further increasing in fluorescence intensity can be observed at Ex290/Em350 nm after 25 h. However, the NAD(P)H and pyridoxine (Ex330/Em390 nm)-dependent RFI increase till the end of the HCDC (40 h), although an optical density of about 400 and a cell dry mass concentration of about 110 g/l was reached.

Fluorescence spectra include information about cell, metabolite, and product concentrations and the actual metabolic state of the cells, leading to a very complex system with interfering signals and overlapping of fluorescence regions.

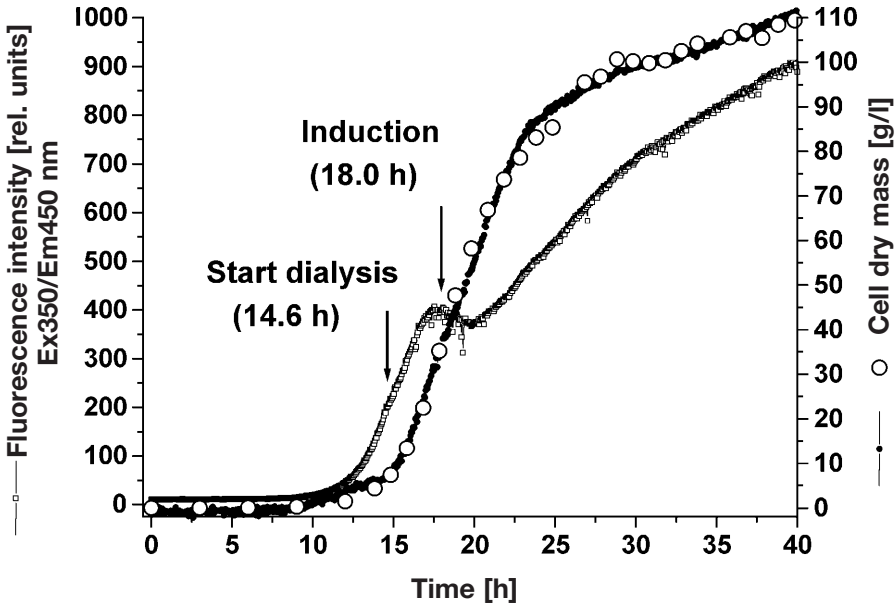

Fig. 5. Courses of predicted and off-line measured cell dry mass concentration and NAD(P)H-dependent relative fluorescence intensity during a high-cell-density cultivation of *E. coli*

This problem is overcome by the BioView sensor, which offers the possibility to monitor the whole spectral range simultaneously, and by using suitable data analysis and mathematical methods like chemometric regression models [106]. Real-time fluorescence measurement can be used more effectively comparing time-consuming off-line methods. Partial least squares (PLS) calibration models were developed for simultaneous on-line prediction of the cell dry mass concentration (Fig. 5), product concentration (Fig. 6), and metabolite concentrations (e.g., acetic acid, not shown) from 2D spectra.

Figure 5 shows a good correlation ($r = 0.9991$) between off-line and predicted cell dry mass concentration. The root mean square error of calibration (RMSEC) amounts to 1.85 g/l. The regression model includes only information about cell growth and cell mass formation, but not about change in cell metabolism recognized in the NAD(P)H dependent RFI at Ex350/Em450 nm. On-line prediction of bioprocess variables offers the possibility to start the dialysis and production steps at optimal process times. Also, Fig. 6 shows a good correlation ($r = 0.9983$) between off-line and predicted product concentration with an RMSEC of 3.07 rel. units. Product formation as well as the end of production could be observed on-line. The exact process time for harvest is recognizable, providing a ideally running bioprocess. The 2D fluorescence spectroscopy offers the possibility of controlling an optimal production run and productivity. Moreover the technique is also able to estimate non-fluorescent variables on-line, for instance the production of acetic acid and citric acid (not shown), de-

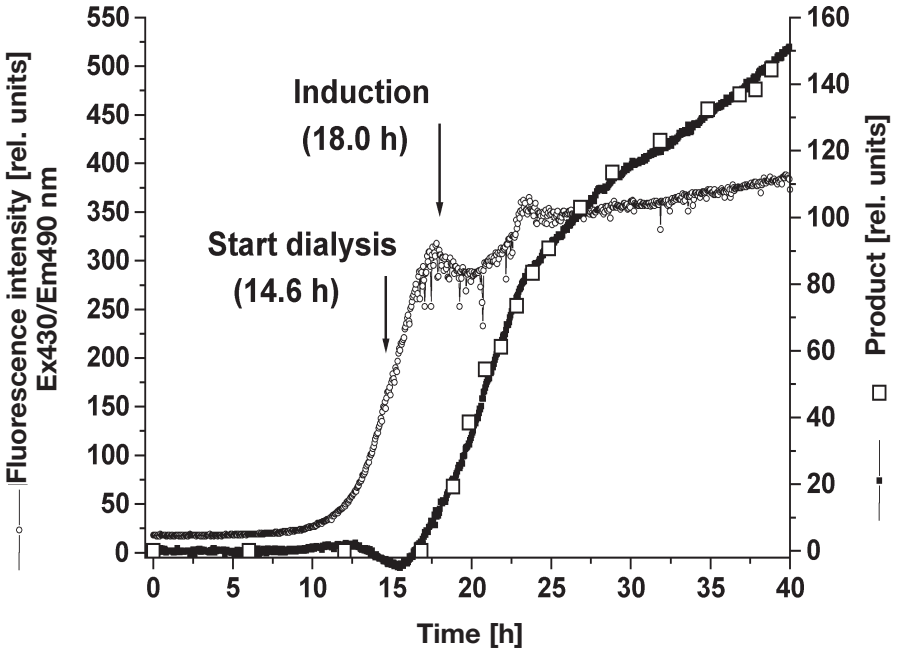

Fig. 6. Courses of predicted and off-line measured product concentration and pyridoxalphosphate-dependent relative fluorescence intensity during a high-cell-density cultivation of *E. coli*

pending on the biological activity of the cells. Riesenberg and Guthke [94] described the dependency of the cell physiology of *Escherichia coli* of the chemical (e.g., pH, medium compounds) and the physical (e.g., temperature, dissolved oxygen) environment. 2D fluorescence spectroscopy supported by mathematical models is even able to monitor the metabolic state of the cells. Based on these data the optimal cultivation conditions for higher production rate and yield can be obtained.

11 Conclusion

Modern optical sensors offer interesting applications in various fields of biotechnology. These sensors measure non-invasively and are able to detect different components inside and outside cells without time delay. Different educt, metabolite, and product concentrations can be monitored simultaneously with the cell count or cell mass and the actual metabolic state of the cells by using these sensitive optical analysis techniques. Based on multivariate calibration models a highly sophisticated process monitoring and control can be achieved, resulting in improved ecological and economical process management. Thus industrial application of optical sensor systems appears bright.

References

1. Wolfbeis OS (1991) Fiber optic chemical sensors and biosensors. CRC Press, Boca Raton
2. Bittner C, Wehnert G, Scheper T (1998) Biotechnol Bioeng 60(1):23–35
3. Scheper T, Hitzmann B, Stärk E, Ulber R, Faurie R, Sosnitza P, Reardon KF (1999) Bioanalytics: detailed insight into bioprocesses, Anal Chim Acta 400:121–143
4. Marose S, Lindemann C, Ulber R, Scheper T (1999) TIBTECH 17:30–34
5. Vaneous RD (1978) Understanding nephelometric instrumentation, Am Lab 6:38–46
6. Hancher CW, Thacker LH, Phares EF (1974) Biotechnol Bioeng 16:475–484
7. Koch AL (1970) Anal Biochem 252–259
8. Lee C, Lim H (1980) Biotechnol Bioeng 22:639–642
9. Lee YH (1981) Biotechnol Bioeng 23:1903–1906
10. Lima Filho JL, Lendingham WM (1987) Biotechnol Tech 1:145–150
11. Kamiyama N, Oikawa Y (1979) Biotechnol Bioeng Symp 9:103–116
12. Metz H (1981) Chem Tech 10:691–696
13. Merten O-W, Palfi GE, Steiner J (1986) Adv Biotechnol 6:111–178
14. Steiner J (1987) Dev Biol Stand 66:357–360
15. Junker BH, Reddy J, Gbewonyo K, Greasham R (1994) Bioprocess Eng 10:95–207
16. Wu P, Ozturk SS, Blackie JD, Thrift JC, Figueroa C, Naveh D (1995) Biotechnol Bioeng 45:495–502
17. Konstantinov K, Chuppa S, Sajan E, Tsai Y, Yoon S, Golim F (1994) Trends Biotechnol 12:324–333
18. Hatch RT, Veilleux BA (1995) Biotechnol Bioeng 46:371–374
19. Kisalita WS (1994) Biotechnol Tech 8:747–750
20. Niamimohasses R, Barnett DM, Green DA, Smith PR (1995) Meas Sci Technol 6:1291–1300
21. Klimant I, Wolfbeis OS (1995) Anal Chem 67:3160–3173
22. Wolfbeis OS (1991) Fiber optic chemical sensors and biosensors, vols 1 and 2. CRC Press, Boca Raton, FL
23. Weigl BH, Holobar A, Trettnak W, Klimant I, Kraus H, O'Leary P, Wolfbeis OS (1994) J Biotechnol 32:127–138
24. Chung H, Arnold MA, Rhiel M, Murhammer DW (1995) Appl Biochem Biotechnol 50:109–125
25. Freitag R (1993) Appl Biosens 4:75–79
26. Watts HJ, Yeung D, Parkes H (1995) Anal Chem 76:4283–4289
27. Chang YH, Chang TC, Kao E-F, Chou C (1996) Biosci Biotechnol Biochem 60:1571–1574
28. Chung H, Arnold MA, Rhiel M, Murhammer DW (1995) Appl Biochem Biotechnol 50:109–125
29. Chung H, Arnold MA, Rhiel M, Murhammer DW (1996) Appl Spectros 50:270–276
30. Riley MR, Rhiel M, Zhou X, Arnold MA, Murhammer DW (1997) Biotechnol Bioeng 55:11–15
31. Zhou X, Chung H, Arnold MA, Rhiel M, Murhammer DW (1995) In: Rogers KR, Mulchandani A, Zhou W (eds) Biosensor and chemical sensor technology. American Chemical Society, Washington, DC
32. Rhiel M, Ziegler T, Ducommun P, von Stockar U, Marison IW (1999) Proceedings of the 16th ESACT Meeting, Lugano, Switzerland, pp 207–209
33. Ducommun P, Bolzonella I, Rhiel M, Pugeaud P, von Stockar U, Marison IW (2001) On-line determination of animal cell concentration. Biotech. Bioeng 72:515–522
34. Cavinato AG, Mayes DM, Ge Z, Callis JB (1990) Anal Chem 62:1977–1982
35. Macalony G, Draper I, Preston J, Anderson KB, Rollins MJ (1996) Food Bioprod Process 71:212–220
36. Vaccari G, Dosi E, Campi AI, Gonzalez-Vara RA, Matteuzzi D, Montovani G (1994) Biotechnol Bioeng 43:913–917
37. Eberl R, Wilke J (1996) Sens Actuat B 32:203–208
38. Srivinas SP, Mutharasan R (1987) Biotechnol Bioeng 30(6):769–774

39. Srivinas SP, Mutharasan R (1987) Biotechnol Lett 9(2):139–142
40. Scheper T, Reardon KF (1991) In: Göpel WG, Hesse JH, Memel JN (eds) Sensors in biotechnology, sensors, vol 2. VCH, Weinheim, pp 1024–1046
41. Schügerl K, Lindemann C, Marose S, Scheper T (1998) In: Berovic M (ed) Bioprocess Engineering Course, 27 Sep–2 Oct 1998, Brac, Croatia. National Institute of Chemistry, Supetar, pp 400–415
42. Marose S, Lindemann C, Scheper T (1998) Biotechnol Prog 14:63–74
43. Duysens LNM, Amesz J (1957) Biochim Biophys Acta 24:19–26
44. Harrison DEF, Chance B (1970) Appl Microbiol 19(3):446–450
45. Zabriskie DW, Humphrey AE (1978) Eur J Appl Microbiol 35(2):337–343
46. Zabriskie DW, Armiger WB, Humphrey AE (1975) Proc ASM Meeting, New York, p 195
47. Beyeler W, Einsele A, Fiechter A (1981) Eur J Appl Microbiol Biotechnol 13:10–14
48. Beyeler W, Gschwend K, Fiechter A (1983) In-situ Fluorometrie: Chem Ing Tech 55(5):869–871
49. Scheper T, Schügerl K (1986) J Biotechnol 3:221–229
50. Meyer C, Beyeler W (1984) Biotechnol Bioeng 26:916–925
51. Siano SA, Mutharasan R (1989) Biotechnol Bioeng 34:660–670
52. Peck MW, Chynoweth DP (1990) Biotechnol Lett 12:17–22
53. Siano SA, Mutharasan R (1991) Biotechnol Bioeng 37:141–159
54. Srivastava AK, Volesky B (1991) Appl Microbiol Biotechnol 34:450–457
55. Kwong SCW, Rao G (1994) Biotechnol Bioeng 44:453–459
56. Nielsen J, Johansen CL, Villadsen J (1994) J Biotechnol 38:51–62
57. Boyer PM, Humphrey AE (1988) Biotechnol Lett 2(3):193–198
58. Samson R, Beaumier D, Beaulieu C (1987) J Biotechnol 6:175–190
59. Gerl K (1986) J Biotechnol 3:231–238
60. Gerl K (1986) Ann NY Acad Sci 506:431–445
60. Heinzle E, Goldschmidt B, Moes J, Dunn IJ (1986) Proc 5th Yugoslavian-Austrian-Italian Chem Eng Conf, Portoroz, Yugoslavia, pp 525–534
62. Groom CA, Luong JHT, Mulchandani A (1988) J Biotechnol 8:271–278
63. Meyer HP, Beyeler W, Fiechter A (1984) J Biotechnol 1(5/6):341–349
64. Scheper T, Gebauer A, Schügerl K (1987) Chem Eng J 34:B7–B12
65. Gebauer A, Scheper T, Schügerl K (1987) Bioprocess Eng 2:13–23
66. Li J-K, Humphrey AE (1991) Biotechnol Bioeng 37:1043–1049
67. Li J-K, Asali EC, Humphrey AE (1991) Am Chem Soc Eng 21–27
68. Li J-K, Humphrey AE (1992) J Fermentat Bioeng 74:104–111
69. Horvath JJ, Glazier SA, Spangler CJ (1993) Biotech Prog 9:666–670
70. Lipton AJ, Domach MM (1992) Biotechnol Bioeng 39:13–19
71. Tartakovsky B, Sheintuch M (1996) Biotechnol Prog 12:126–135
72. Walker CC, Dhurjati P (1989) Biotechnol Bioeng 33:500–505
73. Armiger WB, Lee JF, Montalvo LM, Forro JR (1985) Proc 190th ACS Meeting, Chicago, MBTD 40
74. Zabriskie DW (1979) Biotechnol Bioeng Symp 9:117–123
75. Scheper T, Schügerl K (1986) Appl Microbiol Biotechnol 23:440–444
76. Watteeuw C, Armiger WB, Ristroph D, Humphrey AE (1979) Biotechnol Bioeng 21:1221–1237
77. Scheper T, Wehnert G, Schügerl K (1997) DECHEMA Biotechnology Conferences, vol 1, pp 63–66
78. Luong JHT, Carrier DJ (1986) Appl Microbiol Biotechnol 24:65–70
79. Forro JR, Maenner GF, Armiger WB (1984) Proc 188th ACS National Meeting, Philadelphia, MBTD 79
80. Leist C, Meyer HP, Fiechter A (1986) J Biotechnol 4, 235–246
81. MacMichael G, Armiger WB, Lee JF, Mutharasan R (1987) Biotechnol Tech 1:213–218
82. Müller W, Wehnert G, Scheper T (1988) Anal Chim Acta 213:47–53
83. Maneshin SK, Arevshatyan AA (1972) Appl Biochem Microbiol 8:273–275
84. Einsele A, Ristroph DL, Humphrey AE (1979) Eur J Appl Microbiol Biotechnol 6:335–339

85. Li J, Humphrey AE (1989) Biotechnol Lett 11(3):177–182
86. Betz A, Chance B (1965) Arch Biochem Biophys 109:579–584
87. Chance B, Estabrook RW, Gosh A (1964) Natl Acad Sci USA 51:1244–1251
88. Doran PM, Bailey JE (1987) Biotechnol Bioeng 29:892–897
89. Reardon KF, Scheper T, Bailey JE (1986) Biotechnol Lett 8(11):817–822
90. Reardon KF, Scheper T, Bailey JE (1987) Biotechnol Progr 3(3):153–167
91. Rao G, Mutharasan R (1989) Appl Microbiol Biotechnol 30:59–66
92. Ulber R, Faurie R, Sosnitza P, Fischer L, Stärk E, Harbeck C, Scheper T (2000) J Chromatogr A 882:329–334
93. Stärk E, Harbeck C, Faurie R, Lindemann C, Scheper T, Proceedings of SPIE, 10 Sept 1999, Boston, Massachusetts, USA, pp 42–48
94. Riesenberg D, Guthke R (1999) Appl Microbiol Biotechnol 51:422–430
95. Lee YL, Blanch HW (1993) Biotechnol Bioeng 46:579–587
96. Suzuki T, Yamane T, Shimizu S (1987) Appl Microbiol Biotechnol 25:526–531
97. Riesenberg D (1991) Curr Opin Biotechnol 34:380–384
98. Kleman GL, Strohl WR (1994) Curr Opin Biotechnol 5:180–186
99. Lee L, Blanch HW (1993) Biotechnol Bioeng 41:781–790
100. Lee SY (1996) Trends Biotechnol 14:98–105
101. Winter J, Neubauer P, Glockshuber R, Rudolph R (2000) J Biotechnol 84(2):175–185
102. Märkl H, Lechner M, Götz F (1990) J Fermentat Bioeng 69(4):244–249
103. Pörtner R, Märkl H (1998) Appl Microbiol Biotechnol 50:403–414
104. Ogbonna JC, Märkl H (1993) Biotechnol Bioeng 41:1092–1100
105. Nakano K, Rischke M, Sato S, Märkl H (1997) Appl Microbiol Biotechnol 48:597–601
106. Hitzmann B, Pekelev T, Marose S, Lindemann C, Scheper T (1998), Conference in Osaka. Elsevier Science, Oxford, pp 451–456
107. Michelon LE, Kelleher WJ (1963) Lloydia 26:192–201

Received: May 2001

Metabolic Flux Analysis Using Mass Spectrometry

C. Wittmann

Biochemical Engineering Institute, Saarland University, 66123 Saarbruecken, Germany
E-mail: c.wittmann@mx.uni-saarland.de

Dedicated to Prof. Dr. Wolf-Dieter Deckwer on the occasion of his 60th birthday

Detailed knowledge on carbon flux distributions is crucial for the understanding and targeted optimization of cellular systems. Analytical methods to identify the topology of metabolic networks and to quantify fluxes through its different pathways are therefore in the core of metabolic engineering. An elegant approach for metabolic flux analysis is provided by tracer experiments. In such studies tracer substrates with stable isotopes such as ^{13}C are applied and the labeling pattern of metabolites is subsequently measured. Detailed flux distributions can be obtained by a combination of tracer experiments and stoichiometric balancing. In recent years, mass spectrometry (MS) has emerged as an interesting method for labeling measurements in metabolic flux analysis and provided valuable insights into the cellular metabolism. The present review provides an overview on current experimental and modeling tools for metabolic flux analysis by MS. The application of MS for flux analysis is illustrated by examples from the literature for various biological systems, including bacteria, fungi, tissue cultures and *in vivo* studies in humans.

Keywords. Metabolic flux analysis, mass spectrometry, ^{13}C tracer experiments, modeling, experimental design

Advances in Biochemical Engineering/
Biotechnology, Vol. 74
Managing Editor: Th. Scheper

List of Symbols and Abbreviations

c	molar cumomer fraction
Φ	flux parameter, flux partitioning ratio
$I_{m1/m2}$	intensity ratio of mass isotopomer pools m_1 and m_2
s	sum of squares of relative deviations
S	flux sensitivity
x	molar fraction
AMM	atom mapping matrix
CI	chemical ionization
CID	collision induced decay
EI	electron impact
ESI	electrospray ionization
FAB	fast atom bombardment
FMDV	fragment mass isotopomer distribution vector
GC	gas chromatography
HPLC	high pressure liquid chromatography
ICP	inductively coupled plasma
IDV	isotopomer distribution vector
IR MS	isotope ratio mass spectrometry
IMM	isotopomer mapping matrix
MALDI	matrix-assisted laser desorption ionization
MCP	microchannel plate
MDV	mass distribution vector
ME	molar enrichment
MI MS	membrane inlet mass spectrometry
MS	mass spectrometry
NMR	nuclear magnetic resonance
PPP	pentose phosphate pathway
SEM	secondary electron multiplier
SIM	selective ion monitoring, single ion monitoring

TCA tricarboxylic acid
TOF time-of-flight
TSQ triple stage quadrupole

1 Introduction

Metabolic engineering aims at a targeted improvement of cellular properties. To achieve such improvements in an efficient way, a fundamental knowledge of intracellular distributions of carbon fluxes and their regulation in the metabolism is needed. The identification of the network topology and the quantification of carbon fluxes through the different reactions of the network are important tasks in this context. Information on carbon fluxes is provided by measuring rates of substrate consumption and product and biomass formation. Usually the number of measured rates is smaller than the number of parameters in the model. In stoichiometric balancing, also called metabolite balancing, this is overcome by the introduction of additional constraints on the metabolism such as balances of ATP or reduction equivalents. These constraints may be uncertain and are therefore controversially discussed. Separate balances of NADPH and NADH are inappropriate, if the organism studied is capable of interconversion of the two reduction equivalents by transhydrogenase activity [1]. Interconversion of NADPH and NADH is also possible in bidirectional reactions that cannot be quantified by metabolite balancing such as the mannitol cycle operating in fungi [2] or the interconversion of isocitrate and α-ketoglutarate recently suggested to take place in liver mitochondria [3]. Markedly different flux distributions for *Bacillus subtilis* obtained by different authors applying metabolite balancing underlined that the result of the flux calculation is very sensitive towards changes in the NADPH balance [4]. Moreover, alternative pathways with identical overall stoichiometry cannot be discriminated by metabolite balancing, and cyclic pathway activities cannot be quantified with this technique. The use of tracer substrates and the subsequent analysis of labeling patterns in metabolites of the regarded network is an elegant way to increase the number of known quantities. The benefits of ^{13}C labeling analysis in addition to metabolite balancing were recently discussed [5, 6]. The comprehensive application of both metabolite balancing and tracer studies allows a most detailed examination of metabolic networks with respect to pathway identification, metabolite channeling, compartmentation or quantification of flux partitioning ratios and bidirectional fluxes [7].

Several studies recently underlined the great potential of MS for the labeling measurements in metabolic network characterization [8–10]. Among the most attractive properties of MS for bioanalysis are (i) the high informational content of data, (ii) the high sensitivity, (iii) the high accuracy, (iv) the versatility, (v) the robustness and (vi) the rapidity of data accumulation [11]. In comparison to NMR, which is the other main method in flux analysis [4], especially the high sensitivity and the fast data generation are major advantages of MS. The characteristics mentioned for MS fulfil important criteria for efficient metabolic flux analysis, which is most valuable, if a number of comparative experi-

ments, e.g. for the change of flux distributions during batch-culture or for different mutants of a producer strain, can be efficiently performed in short time. This requires measurement of labeling patterns and subsequent data processing to be fast. The high sensitivity is a crucial point due to two main aspects: (i) small experimental volumes – resulting in small sample volumes – are desired due to the high costs of the tracer substrates, and (ii) amounts of analytes from biological systems, such as intracellular metabolites, are often rather low.

Generally, metabolic flux analysis by ^{13}C labeling experiments requires a known topology of the biochemical network and a justified neglection of isotope effects on rates and equilibria of metabolic rates. It is usually performed as stationary flux analysis, whereby the metabolism has to be in an isotopic steady-state. Phenomena, such as metabolite channeling may influence the fate of metabolites in the network and should be therefore potentially considered, when interpreting obtained labeling data. Evidence for metabolite channeling was recently obtained for mitochondrial tricarboxylic acid (TCA) cycle enzymes in mammalian cells [12] and for pentose phosphate pathway (PPP) enzymes in yeast [13]. For eucaryotic cells, compartmentation has to be taken into account.

The present review gives an overview on experimental and modeling approaches for metabolic network analysis by MS. Available MS techniques are briefly characterized. Different methodologies used for model generation, experimental design and parameter estimation are discussed. The broad range of application examples of MS in metabolic flux analysis chosen from the literature, including cultivations of bacteria, fungi, tissue cultures and in vivo studies in humans on the whole body level underlines the great versatility of MS in this area.

2
Modeling of Biochemical Networks and Experimental Design of Tracer Studies

2.1
Definition of Labeling Patterns

Commonly used isotope labels in metabolic flux analysis and pathway identification are ^{2}H, ^{13}C, ^{15}N, and ^{18}O. The most prominent stable isotope is ^{13}C. The transfer of carbons from substrates to products in the network is exactly defined by the specificity of the enzymes. The reactions of the central metabolism are linked to the cleavage and formation of C-C bonds of the metabolites and cause a rearrangement of their carbon skeleton, leading to significant labeling patterns in tracer experiments. The major developments of modeling approaches are found for the mainly used ^{13}C labeling. The chapter on modeling and experimental design therefore focuses on this type of label in tracer studies. A clear and straightforward mathematical formulation of labeling states of metabolites and of the transfer of label in metabolic networks is the prerequisite for accurate and efficient metabolic flux analysis. As follows, clear definitions used in the literature for the description of the ^{13}C labeling state of a compound are given. They are given for carbon, but are generally applicable also for other isotope labels.

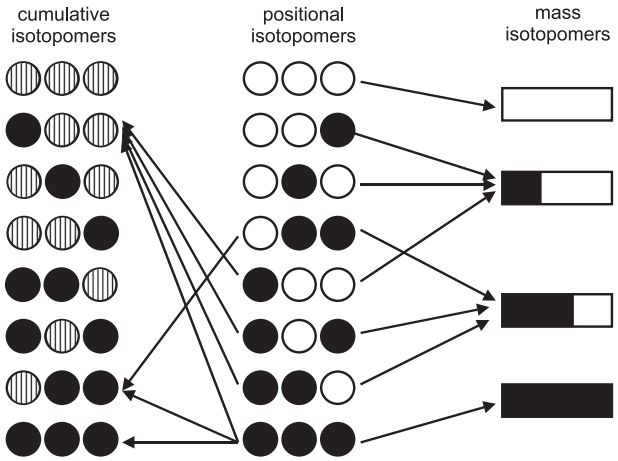

Fig. 1. Pools of cumulative isotopomers (cumomers), positional isotopomers and mass isotopomers exemplified for a molecule with 3 carbon atoms either ^{12}C (white) or ^{13}C (black) or not specified (hatched). The arrows indicate the grouping of positional isotopomers into different cumomer fractions, and different mass isotopomer fractions, respectively

A *positional isotopomer* has an exactly determined labeling pattern, described by a specific number of ^{13}C atoms in specific positions of the molecule. Generally, 2^n isotopomers are possible for a compound with n carbon atoms. The 8 different positional isotopomers of a compound with 3 carbon atoms are shown in Fig. (1).

Schmidt et al. suggested isotopomer distribution vectors (IDV) to quantitatively describe distributions of positional isotopomers, whereby the elements of an IDV contain molar fractions of single positional isotopomers [14]. The indexing of positional isotopomers as elements of an IDV is based on the binary code with ones for labeled and zeros for non-labeled carbons following the standard rules of numbering the carbons within a molecule. The positional isotopomers in Fig. (1) are ordered in this way. The sum of all elements in the IDV equals 1. The IDV of pyruvate can serve as an example (Eq. 1).

$$\mathrm{IDV}_{\mathrm{Pyruvate}} = \begin{bmatrix} x(1) \\ x(2) \\ x(3) \\ x(4) \\ x(5) \\ x(6) \\ x(7) \\ x(8) \end{bmatrix} = \begin{bmatrix} x_{000} \\ x_{001} \\ x_{010} \\ x_{011} \\ x_{100} \\ x_{101} \\ x_{110} \\ x_{111} \end{bmatrix} \tag{1}$$

A *mass isotopomer* x_{m+i} is specified by the number i of ^{13}C atoms in the molecule, but not by their positions. A compound with n carbons has $n+1$ different mass isotopomers, ranging from the non-labeled U-^{12}C mass isotopomer (x_m)

to the fully labeled U-^{13}C mass isotopomer (x_{m+n}). Thus, four different mass isotopomers, comprising non-labeled, single-labeled, double-labeled and triple-labeled form, can occur for the C_3 compound in the given example (Fig. 1). The non-labeled and fully-labeled mass fractions contain one positional isotopomer, whereas 3 positional isotopomers belong to the $m+1$ and to the $m+2$ fraction, respectively. The sum of molar fractions of all mass isotopomers is equal to 1. The molar fraction of a mass isotopomer is also called fractional abundance [15]. Mass isotopomer distributions can be represented in the form of vectors, called mass isotopomer distribution vectors (MDV) [9]. The different fractions of mass isotopomers in a MDV are ordered with increasing masses as shown for the example of pyruvate (Eq. 2).

$$\mathrm{MDV}_{\mathrm{Pyruvate}} = \begin{bmatrix} x_m \\ x_{m+1} \\ x_{m+2} \\ x_{m+3} \end{bmatrix} \tag{2}$$

As discussed above, fragments of the analyte molecule can be obtained by MS. Fragment analysis can provide useful information about the labeling pattern of the analyte and allow the calculation of pools of single or at least a selected group of positional isotopomers. A compound with n carbon atoms theoretically can form (2^n-1) different fragments containing different numbers and combinations of carbons. The mass isotopomer distribution of each fragment can be also described by vectors. The indexing of the corresponding fragment mass isotopomer distribution vector (FMDV) follows the same rules for MDV.

In their approach of applying transition matrices for the description of the carbon transfer in metabolic networks, Wiechert et al. [16] defined the labeling pattern of a molecule via cumulated isotopomer (cumomer) fractions, whereby the isotopomers belonging to the same cumomer fraction share labelings at specific carbon positions. For a C_3 compound, three 1-cumomer fractions (c_{1xx}, c_{x1x} and c_{xx1}) occur, in which all isotopomers are at least labeled in position C_1, C_2 or C_3 and which are identical to the fractional enrichment. Besides three 2-cumomer fractions (c_{11x}, c_{1x1} and c_{x11}), only one 3-cumomer fraction (c_{111}) exists identical to the corresponding fully-labeled positional isotopomer. The grouping of positional isotopomers into their corresponding cumomer fractions is exemplified for c_{1xx}, c_{x11} and c_{111} in Fig (1).

The ^{13}C labeling state of a molecule with n carbons can be also expressed as molar enrichment (ME) [15] or summed fractional labeling [17], describing the weighted sum of mass isotopomer fractions (Eq. 3).

$$\mathrm{ME} = \sum_{i=1}^{n} i \cdot x_{m+i} \tag{3}$$

To calculate the ^{13}C labeling of a molecule from a mass spectrometric measurement, the data have to be corrected for natural isotopes present in the analyzed ion of the target molecule. Hereby, the atoms of the analyte and of added derivatization residues have to be considered. Additionally, elements that form ad-

ducts with the analyte in the MS analysis, such as protons or potassium ions in MALDI MS, can be important [18]. Mathematically, the presence of natural isotopes can be considered by correction matrices [9, 19, 20]. It is important to note for *in vivo* studies with animals or humans with low degrees of labeling applied, that the natural background of ^{13}C in tissue varies for different parts of the world and with different dietary habits [21].

2.2 Modeling of Carbon Transfer in Biochemical Networks

Two formal approaches have been established to solve isotopomer balances for biochemical networks in a generally applicable way: (i) the transition matrix approach by Wiechert [22] and (ii) the isotopomer mapping matrix (IMM) approach by Schmidt et al. [14]. The matrix transition approach is based on a transformation of isotopomer balances into cumomer balances exhibiting a much greater simplicity. As shown, non-linear isotopomer balances can always be analytically solved by this approach [16]. The matrix transition approach was applied for experimental design of tracer experiments and for parameter estimation from labeling data [16, 23].

The isotopomer mapping matrix approach is based on the concept of atom mapping matrices, AMM, previously developed by Zupke and Stephanopoulos [24]. AMM are straightforward generated from the biochemical knowledge typically available in textbooks. The IMM of a reaction exactly defines which positional isotopomers of the product can be generated from each individual positional isotopomer of the substrate. It is generated automatically from the corresponding AMM, saving time and preventing the introduction of typing errors. With the IMM approach, positional isotopomer distributions are calculated for all metabolites of the network, specified by the used tracer substrate and its flux distributions. Using the approach with MS requires the subsequent transformation of the obtained metabolite IDV into MDV, which can be carried out by matrix calculus [9]. The IMM approach can be implemented into mathematical software such as Matlab. It was further developed to be used for model generation, experimental design and parameter estimation of ^{13}C tracer experiments with MS, respectively [9, 25–27].

These two types of modeling frameworks represent a clear, systematic and general approach for the quantitative description of the transfer of labeled ^{13}C atoms in metabolic networks. In most cases available from the literature, specific approaches were used to describe the carbon transfer in the network. These included only part of the isotopomer balances and were set up specifically related to the treated flux problem with certain assumptions on the labeling pattern of the applied tracer substrate and on the bidirectionality of fluxes and simplifications as for example the neglection of $^{13}CO_2$ incorporation in carboxylating reactions [28–31]. A broad application of such approaches to other networks, other flux situations or other tracer substrates is difficult due to their high specificity. A general modeling framework with different tools for model generation, experimental design, parameter estimation and statistical analysis is highly desired [16].

2.3 Experimental Design of Tracer Experiments

The aim of experimental design is to obtain maximal information on metabolic flux distributions with requested accuracy and minimal costs for labeled substrates. Admittedly, the metabolic networks are usually complex. The complexity is increased by various experimental parameters that have to be chosen. These can be grouped into tracer substrate and measurement design. Tracer substrate design includes position and labeling degree in the tracer substrate which can be singly or multiply labeled or a mixture of differently labeled compounds. The right choice of label in the tracer substrate is very critical for the quality of the obtained information on intracellular flux distributions [23, 26]. In the measurement design those labels are selected which are most informative to determine the flux parameter of interest. This can significantly reduce the experimental effort in tracer experiments [27]. ^{13}C tracer experimental design is illustrated for the flux partitioning ratio between PPP and glycolysis (Φ_{PPP}). This flux parameter is of central interest in different biotechnological processes with industrial relevance. The PPP is the major source for NADPH formation, which is required in substantial amounts in lysine or penicilline production. In other cases the product itself, e.g. riboflavine, or an important precursor of the product, e.g. in phenylalanine production, is synthesized via the PPP. For simplicity reasons, the reactions in the PPP and the reaction of glucose 6-phosphate isomerase are assumed to be irreversible, and natural isotopes are neglected in the example. The key for the determination of Φ_{PPP} is the specificity of 6-phosphogluconate dehydrogenase, which exclusively releases the C_1 from its substrate 6-phosphogluconate, equal to the C_1 of the applied glucose, as CO_2. With 1-^{13}C glucose as tracer substrate the ^{13}C label from position C_1 is thus quantitatively removed in the initial PPP reactions, whereas it is conserved in the glycolysis (Fig. 2).

The labeling of pyruvate can be used to visualize Φ_{PPP}. 100 % flux through the glycolysis results in the formation of equimolar amounts of non-labeled and single labeled pyruvate, whereas for 100 % flux through the PPP an exclusive formation of non-labeled pyruvate occurs. Flux partitioning ratios between these two extremes cause a defined ratio between non-labeled and single labeled pyruvate. With the simplifications and assumptions chosen, the relative flux into the PPP can be obtained from the pyruvate labeling $I_{m+1/m}$ by a rather simple equation (Eq. 4).

$$\Phi_{PPP} = \frac{1 - I_{m+1/m,\,\text{Pyruvate}}}{1 + \frac{2}{3} I_{m+1/m,\,\text{Pyruvate}}} \tag{4}$$

The calculation of corresponding analytical equations for realistic conditions, considering bidirectional fluxes, natural isotopes, or other tracer substrates such as multiply labeled compounds is much more complex or even impossible, with respect to the non-linearity of such systems. The same holds for alternative metabolites applied for the labeling measurement, such as glutamate or lysine, which are located in the network at a far distance to the flux node of inte-

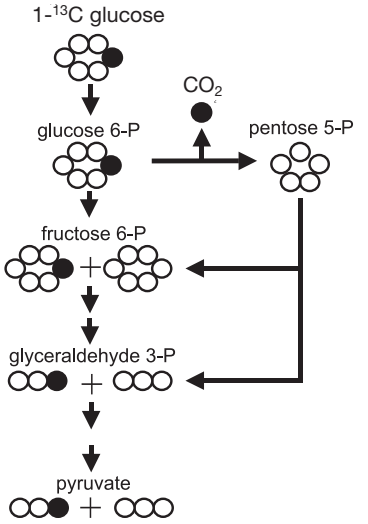

Fig. 2. Experimental design of a ^{13}C tracer experiment for the determination of the flux partitioning ratio between pentose phosphate pathway and glycolysis (Φ_{PPP}): ^{13}C label distribution from 1-^{13}C glucose through the network with ^{13}C atoms (black) and ^{12}C atoms (white)

rest and of which the carbon skeleton is subjected to substantial alterations in the metabolic reactions in between. Computer based tools for efficient experimental design of ^{13}C tracer experiments have been recently developed. They are implemented in general modeling frameworks of metabolic networks and allow the optimal design of tracer experiments [23, 26]. As a great advantage, the design can be carried out under realistic flux situations including all isotopomer balances of the network and bidirectional fluxes. With such tools, a large number of different experimental approaches can be compared in short time. As an example, the dependence of $I_{m+1/m}$ of pyruvate on Φ_{PPP} under realistic flux conditions, including bidirectional fluxes in the network, 99% 1-^{13}C glucose and natural isotopes can be easily calculated (Fig. 3).

Obviously, the behavior of the network under realistic conditions is significantly different from the one, predicted in the simplified example in Eq. (4). Calculation of Φ_{PPP} from the pyruvate labeling via the simplified approach thus leads to errors in the result.

An important task of experimental design studies is the characterization and visualization of the identified optimal experimental approach. For this purpose, quantitative parameters were suggested as output from such simulation studies, that directly provide quantitative information on the suitability of a certain experimental design and easily allow the identification of the optimal one among a large number [23, 26]. Wiechert and coworkers have developed a statistical tool for the design of tracer experiments. Considering measurement errors of the labeling data and parameter covariance matrices, different experimental approaches can be compared by statistical quality measures and approaches of choice can be computed [23]. Wittmann and Heinzle [26] suggested flux sensi-

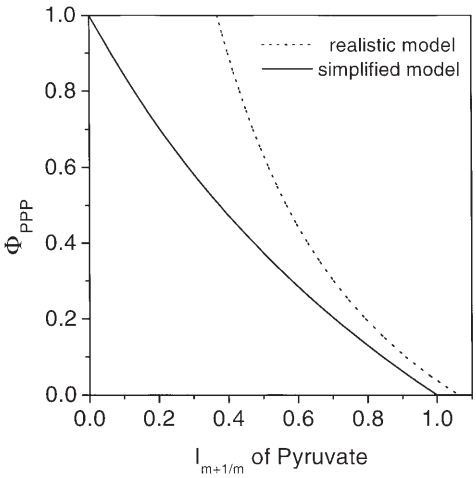

Fig. 3. Change of the intensity ratio $I_{m+1/m}$ of pyruvate with variation of the flux partitioning ratio between pentose phosphate pathway and glycolysis (Φ_{PPP}). The curves were calculated from the analytical expression (Eq. 4) of a simplified model and from computer based modeling considering a realistic flux situation with partitioning ratios and bidirectional fluxes and natural isotopes (Wittmann and Heinzle, 2001b)

tivities *S* for the quantitative evaluation of a experimental design. The flux sensitivity *S* for the quantification of a flux parameter Φ via an intensity ratio *I* can be expressed via the corresponding partial derivative for a certain flux situation (Eq. 5).

$$S_{\Phi_i}^{I} = \left| \frac{\partial I}{\partial \Phi_i} \right|_{\Phi_1, \Phi_2 \ldots \Phi_i} \tag{5}$$

Using this approach, general guidelines for experimental design of ^{13}C-tracer studies with MS could be shown for the central metabolism of *Corynebacterium glutamicum* comprising various flux scenarios and tracer substrates [26].

To summarize, among the benefits of general experimental design approaches are (i) the comparison of various different experimental approaches, (ii) the identification of an optimal approach by quantitative means, (iii) the possible consideration of the influence of MS measurement errors on the predicted precision of flux analysis, and (iv) the possible extension of the design to various flux scenarios of the regarded network and (v) the applicability to different networks. Unfortunately, the chosen modeling approaches in the literature are often rather specific and based on analytical equations. With such frameworks only a limited experimental design of tracer experiments can be carried out. The identification of a suitable experimental approach is then restricted to qualitative criteria. The quantitative evaluation and comparison of various different experimental conditions and the identification of an optimal experimental design is usually not possible.

Besides ^{13}C, also other stable isotopes, such as ^{18}O, ^{2}H, or ^{15}N have been applied. An example for the use of ^{18}O is the quantification of the flux partitioning

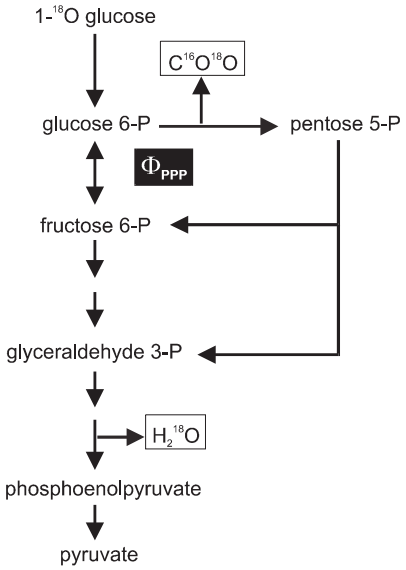

Fig. 4. Experimental design of an ^{18}O tracer experiment for the determination of the flux partitioning ratio between pentose phosphate pathway and glycolysis (Φ_{PPP}): ^{18}O label distribution from 1-^{18}O glucose through the network

ratio Φ_{PPP} with 1-^{18}O glucose. The estimation of Φ_{PPP} is based on the measurement of mass isotopomer pools of CO_2 [32]. As shown in Fig. (4), the ^{18}O label is exclusively released as $C^{16}O^{18}O$ in the initial reactions of the PPP, whereas it ends up in $H_2{}^{18}O$ in the glycolytic enolase reaction from 2-phosphoglycerate to phosphoenolpyruvate. Information on the relative flux of carbon through the PPP can be obtained from the intensity ratio between $C^{16}O^{18}O$ and $C^{16}O_2$.

^{15}N labeled tracers are frequent substrates for in vivo studies on amino acid metabolism and protein synthesis [33–36]. Deuterium labeled compounds are comparably cheap, but care has to be taken concerning exchange reactions with hydrogen atoms from the surrounding solvents [37]. 6,6-$^2H_2$ and 2-^2H labeled glucose [38] and 1-^2H-galactose [39] were used as substrates for *in vivo* tracer experiments on the hepatic glucose metabolism in humans. Deuterium labeled water (D_2O) was applied for *in vivo* studies of fatty acid and cholesterol synthesis [40]. D_2O incorporation studies can also serve for flux analysis of gluconeogenesis [41].

2.4 Parameter Estimation

The flux parameters are usually estimated from the ^{13}C tracer studies data by minimization of the deviations between experimental and modeled labeling data corresponding to the optimized set of fluxes. In general, the isotopomer balance equations are non-linear and numerical routines are used for their so-

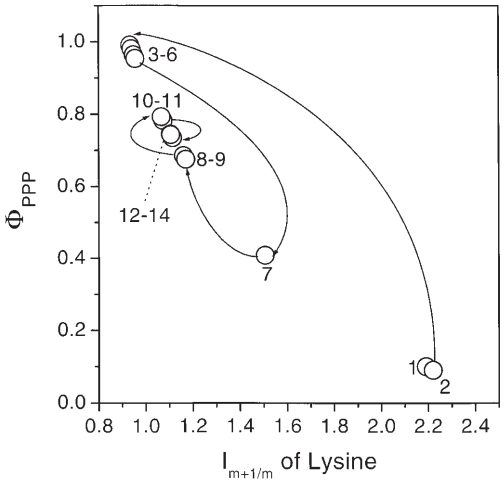

Fig. 5. Estimation of the flux partitioning ratio between pentose phosphate pathway and glycolysis (Φ_{PPP}) from the lysine intensity ratio $I_{m+1/m}$ = 1.11 using the optimization function *fmincon* implemented in Matlab. The numbered data points indicate the results obtained through the different iterations. Starting from Φ_{PPP} = 0.1, the optimal fit of experimental and calculated labeling was obtained after 14 iterations

lution. In the used iterative algorithms the flux parameters of interest, such as flux partitioning ratios or reversibilities of bidirectional fluxes, are varied by the optimization function starting from initial values until an acceptable agreement between measured and calculated labeling pattern is achieved. Usually, the optimization problem with several parameters estimated simultaneously from different labelings is multidimensional. The procedure of parameter estimation is illustrated by a simple example with only one parameter to be determined, which can be easily displayed in graphical form, the estimation of the flux partitioning ratio Φ_{PPP} from the experimental lysine intensity ratio $I_{m+1/m}$ = 1.11, taken from [27], using the optimization function *fmincon* implemented in MATLAB via minimization of the relative deviation (s) between experimental and modeled labeling. All other flux parameters are held constant in this example. Starting with an initial guess (data point no. 1 with Φ_{PPP} = 0.1) the optimization function calculates the corresponding labeling data, which is $I_{m+1/m,\,\mathrm{Lysine}}$ = 2.19 and compares it to the experimental value (Fig. 5).

The result of Φ_{PPP} = 0.744 corresponding to the best fit of experimental to calculated lysine labeling is obtained within 14 iterations. Using MS, the labeling data are mainly molar enrichments [17] or intensity ratios of mass isotopomers [26, 27]. Different optimization functions such as gradient or adaptive random search functions are available. To increase the probability of the identification of a global optimum for the solution, the convergence is usually tested for different initial guesses. If several intensity ratios are fitted simultaneously, the sum of the squares of the relative deviations (s) between experimental (I_{exp}) and modeled (I_{mod}) intensity ratios of mass isotopomers corresponding to the optimized set of fluxes is minimized (Eq. 6).

$$s = \sum \left(\frac{I_{\text{exp}} - I_{\text{mod}}}{I_{\text{mod}}} \right)^2 \quad (6)$$

In case, the network is overdetermined a least square approach is possible. The information obtained by MS from ^{13}C tracer studies can be combined with metabolite balancing for the estimation of flux parameters [25, 27]. Measurement errors can be included to predict uncertainties for the obtained flux parameters [23].

3 Mass Spectrometry Methods

Mass spectrometry (MS) has changed its appearance in the scientific world considerably during recent years. At the beginning of the 20th century first applications in physics were described. Gradually MS methods entered more and more into the fields of biology, biochemistry and biomedicine and became a major tool in life sciences. Mass spectrometers consist of a sequence of functional units for sample introduction, ion formation, mass separation, and detection. The data handling is carried out by computers. Currently, a variety of different mass spectrometric techniques are used for the analysis of biomolecules (Fig. 6).

To illustrate and evaluate the different methods available, the following chapter gives a short overview on the most important methods for sample introduction, ion formation, and mass separation with respect to metabolic flux analysis. For a more detailed insight into modern MS methods the reader is addressed to recent overviews [e.g. 42–44].

3.1 Sample Introduction and Ion Formation

The dominating method of ion formation in metabolic flux analysis is electron impact. It might be supplemented in the future by novel methods, such as matrix assisted laser desorption and electrospray. Additional techniques such as chemical ionization, fast atom bombardment or inductively coupled plasma ionization are only of minor importance and not further discussed in this context.

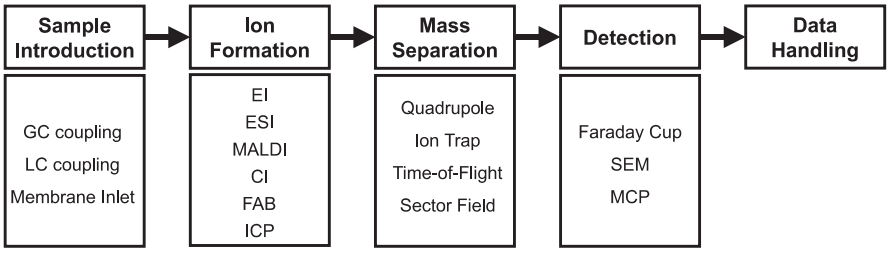

Fig. 6. Overview on different mass spectrometry methods

3.1.1 *Electron Impact*

Electron impact (EI) is probably the most widely used technique for ionization in MS. It is characterized by a high sensitivity, reproducibility and stability. The ionization is based on thermally produced electrons, which orthogonally cross the analyte stream and create mainly positive ions by extracting electrons from the analyte molecules (Fig. 7).

The resulting spectra from EI usually contain a number of fragments, providing extensive structural information about the analyte. A disadvantage of the observed fragmentation is eventually occurring isobaric overlay from different compounds in the analysis of sample mixtures, which often requires a separation step prior to the MS analysis. For this purpose the coupling of a GC with the ion source of the mass spectrometer via capillary inlet is a well established technique. Volatiles can be selectively introduced into EI mass spectrometers via pervaporation membranes. The principle and application of this technique, called membrane introduction (MI) MS was recently reviewed [45]. The accuracy of intensity ratio measurements by EI MS is about 0.1 – 0.5 % [4, 8].

A specific variant of EI MS is isotope ratio (IR) MS [46]. It is based on electron impact ionization with maximized ionization probability. IR MS is limited to the analysis of gases of high volatility and low reactivity such as CO_2, N_2 or SO_2. The analytes of interest thus have to be transformed into one of these gases before introduction into the IR MS. Information on the position of ^{13}C labelings in the analyte can be only obtained, if all carbons are isolated position specific and subsequently combusted. In this context Corso and Brenna [47] showed position specific ^{13}C analysis by IR MS for methylpalmitate through pyrolytic fragmentation. IR MS exhibits an extremely high precision of ±0.00001 % for the isotope ratio measurement and is optimal to quantify low label enrichments [48]. This is especially important for *in vivo* studies with ani-

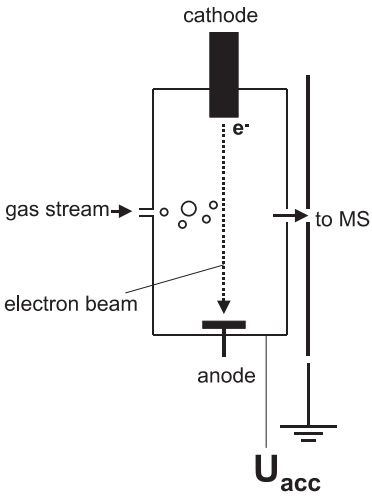

Fig. 7. Schematic view of electron impact ionization

mals or humans. IR MS is often applied in combination with gas chromatography combustion. Recently LC coupling has been also realized [49].

3.1.2 *Laser Desorption Ionization*

A breakthrough in laser desorption techniques was reached by the observation, that compounds, that were not ionized in pure form, could be ionized in a mixture with a compound of high absorption capacity for the laser energy. This enhancement of ionization efficiency by selected, so called matrix compounds, initiated the development of matrix assisted laser desorption ionization (MALDI) [50, 51], which is nowadays broadly applied for the analysis of biomolecules [52]. For sample preparation, usually 0.1 to 1 µl droplets of sample and matrix solution are mixed and pipetted on selected positions of a plate, normally made of stainless steal, gold or glass, and subsequently dried. The plates with the crystallized sample spots are then introduced into the vacuum chamber of the instrument. The procedure of sample preparation can be automated. The crystals are irradiated by a pulsed laser. As a result a plasma is formed, causing vaporization and ionization of the analyte molecules. The ions are then accelerated by a strong electric field. The ionization procedure is soft and fragmentation does usually not occur. MALDI MS can be operated alternatively in positive or in negative mode by appropriate setting of the voltages of the accelerating electric field. The operation mode of choice depends on the target analyte. Compounds with electronegative or negatively charged functional groups, such as hydroxyl or carboxyl groups, respectively, are better ionized in the negative mode, whereas the positive mode is more suitable for basic compounds. MALDI MS is nowadays almost exclusively applied for the analysis of biopolymers. However, it has also been successfully used for low molecular weight compounds [18, 53, 54]. MALDI MS is a rapid, convenient and robust method. Automatization techniques for sample preparation and data accumulation are available. Due to the pulsed laser, it is mainly combined with time-of-flight analyzers. MALDI is not as easily compatible with liquid chromatography, as ESI. However, LC coupling has been established [55]. The accuracy of MALDI MS with standard deviations of about 1–5% for intensity ratio measurements is currently lower compared for example to EI MS, but will be surely increased during further improvements of this novel approach.

3.1.3 *Electrospray Ionization*

Different types of instrumentation have been developed to introduce liquid samples into the MS. Since Fenn has shown that molecular ions can be formed from liquids sprayed at atmospheric pressure in high electric fields, electrospray ionization (ESI) MS has gained increasing popularity for the analysis of biological samples [56]. In an electrospray inlet, the liquid sample is usually emitted as a spray from a capillary at a high potential compared to the mass analyzer into the electric field in front of the mass analyzer (Fig. 8).

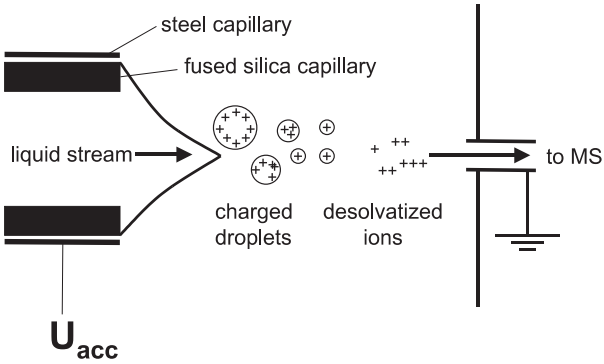

Fig. 8. Schematic view of electrospray ionization

The optimization of the process in recent years, led to defined ion formation with solvent evaporation and complete desolvatation of analyte ions, which are then accelerated towards the mass separator. Analyte molecules often form multiply charged ions. ESI can be carried out both in positive and in negative mode. The sample introduction can be performed with microscale tips mainly made of fused silica capillaries, which are inexpensive and available in various sizes and geometric forms. Recently, nanospray technologies as microvariants of ESI with increased sensitivity were developed, which allowed the analysis of extremely small sample amounts [57].

Alternatively, the mobile phase of a high pressure liquid chromatography or a capillary electrophoresis system can be directly sprayed into the MS [58, 59]. An advantage of ESI MS is its compatibility with tandem MS techniques. ESI is most suitable for charged analytes, whereby uncharged and unpolar compounds may be difficult to be analyzed. ESI MS is limited by its high sensitivity to contaminants such as alkali metals or basic compounds. Non-volatile buffers frequently applied in liquid chromatography and detergents can cause efficiency problems in the subsequent ionization and require frequent cleaning.

3.2 Mass Separation

The most commonly used mass separators are quadrupoles, ions traps and time-of-flight analyzers, for which the principle of mass separation is discussed below. Additionally, other types such as magnetic sector field or Fourier-transform cyclotron-resonance instruments are available.

3.2.1 *Quadrupole*

Quadrupoles are the most commonly used type of mass separator in MS. The operation of quadrupoles is based on the motion of ions in oscillating electric fields. A quadrupole consists of four parallel rods of about 25 cm length each,

whereby opposite rods are electrically connected. At a certain voltage between the rods, only analyte molecules of a distinct mass to charge ratio can pass, whereas ions of different mass to charge ratios are subjected to oscillations, which cause their collision with the rods. Variation of the voltage between the rods creates an oscillating radio-frequency field. The quadrupole thus works as a mass filter. It allows a fast scan over the whole mass range of the instrument within a few seconds. The short time needed for a full scan is especially important, when the MS is coupled to a GC eluting narrow peaks, that have to be scanned several times each. The sensitivity of a quadrupole detector can be significantly enhanced by selected ion monitoring (SIM), whereby only selected masses are sequentially measured with frequencies of 0.1 to 2 seconds each. The number of collected ions for the selected masses is increased by a factor of $10^2 - 10^3$ in comparison to the scan mode. MS/MS can be performed by operating three quadrupoles in series, named triple stage quadrupole (TSQ) MS. In a TSQ isolation, collision and mass analysis of ions are taking place in different parts of the instrument (tandem in space). The first and the third quadrupole operate with a combination of direct current voltages and radio frequency, whereas the second stage quadrupole is only operated in the RF mode, mainly serving as collision cell. Parent ions selected by the first stage quadrupole are subjected to collision induced dissociation (CID) by collision with inert gas molecules (such as argon or helium) in the second stage. From the daughter ions formed through unimolecular fragmentation selected ones can be monitored.

3.2.2 *Ion Trap*

Ion traps are quadrupoles with a specific operation mode, by which ions can be trapped inside the high frequency field for a short time [60]. The field is usually formed via a ring shaped electrode. By varying the amplitude of the frequency, ions can be extracted from the field and directed towards a detector. The amplitude corresponds to the mass of the ions that loose their stability in the field. Limitations of ion traps are the limited dynamic range, the dependence of the quality of the mass spectrum on many operational parameters and possible artifacts in the mass spectra. Ion traps can be applied in combination with MALDI or ESI techniques. Manipulating the ions by using current voltage and radiofrequency electric fields in a series of carefully timed events provides some unique capabilities, such as extended MS/MS experiments, high resolution, and high sensitivity. In MS/MS analysis with ion traps a series of different steps are performed sequentially in the same space (tandem in time). Ions entering the trap e.g. from an ESI source, are trapped and allowed to "cool" by collision with the bath gas of the trap, followed by additional manipulation steps for collisional activation and isolation. MS^n techniques with multiple stages of isolation and fragmentation can be applied.

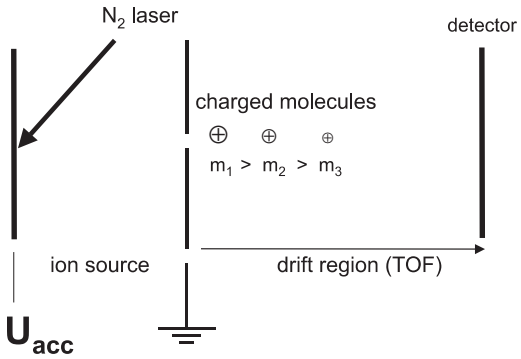

Fig. 9. Schematic view of a linear MALDI-TOF MS instrument

3.2.3
Time-of-Flight

In a time-of-flight (TOF) analyzer the time of flight of ions between the ion source and the detector is measured [61]. This requires that the time at which the ions leave the ion source is well-defined. Therefore, ions are either formed by a pulsed ionization method or various kinds of rapid electric field switching. The single discontinuous laser pulses at distinct time points used in MALDI can be ideally combined with time-of-flight mass separation. TOF analyzers thus received increasing interest with the development of MALDI MS. The schematic draw of a linear MALDI-TOF MS is shown in Fig. (9).

Ions formed in the ion source are accelerated in a short electric field of 2 to 20 mm length to a high kinetic energy of about 20 – 30 keV, whereby ions of the same charge receive the same kinetic energy. During the acceleration phase, ions with lower masses therefore reach higher velocities, compared to ions with higher masses and need a shorter time to reach the detector. The mass to charge ratio is determined from the time elapsed from ion formation to ion arrival at the detector. It is proportional to the square of the time of flight. Flight tubes of TOF analysators are about 0.5 to 3 m in length.

4
Analysis of Metabolite Labeling by MS

The analytes of interest in ^{13}C tracer studies are mainly low molecular metabolites from the cell interior or low molecular weight products excreted into the cell surrounding. The samples from biological systems for labeling measurements frequently exhibit different characteristics that impose specific constraints on the MS techniques used for their analysis. Generally, they are complex mixtures of diverse substances, which may require a separation step prior to MS analysis. The compounds of interest are generally extracted from the biological system, single cells, blood, urine or other biological fluids or obtained from culture supernatants by lyophilization. Often, amounts and concentrations

of these analytes in the samples are rather low. In addition to small molecules, also biopolymers such as proteins, glycogen or DNA, are compounds of interest, because they potentially carry valuable labeling information in their monomeric subunits. Their analysis is mainly carried out on the level of the subunits, obtained after hydrolysis of the polymer. The analysis of the labeling of a compound depends on the desired content of information on the labeling degree. The information content increases in the order molar enrichment, mass isotopomer distributions and positional isotopomer distributions. This chapter describes their direct measurement. The molar enrichment can be calculated from the mass or positional isotopomer distribution, and the mass isotopomer distribution itself can be calculated from the positional isotopomer distribution.

4.1 Measurement of Molar Enrichment

The molar enrichment of a compound can be directly measured by IR MS. The ^{13}C molar enrichment can be obtained from the labeling of CO_2, formed after complete combustion of the analyte.

4.2 Measurement of Mass Isotopomer Distributions

MS can measure the ratio between molar fractions of mass isotopomers. The ratio between two mass isotopomer pools of masses m_1 and m_2 is defined in the present work as intensity ratio $I_{m1/m2}$. It is identical with a mass spectral intensity ratio. If more than two mass isotopomer pools are assessed, their relative ratios, normalized to the sum, are named mass isotopomer distribution. The mass distribution of a compound can be thus obtained from the analysis of ions, which contain the intact carbon skeleton of the analyte. In the area of metabolic flux analysis, mass distributions of various metabolites have been assessed by MS. The major method used is GC/MS, whereby the analytes are derivatized into forms with desired physico-chemical properties such as increased volatility, thermal stability and suitable MS properties [62]. The mass of the formed derivate must be sufficiently high (usually above 175 apparent mass units) to avoid background interference [48]. To obtain the ^{13}C mass distribution of a compound, ions with the entire carbon skeleton of the analyte have to be present. For accurate quantification of the mass distribution of such ions, they should occur in high abundance and preferably be unique species, thus being formed by only one fragmentation pathway.

The compounds analyzed by GC/MS comprise e.g. amino acids [34, 39, 64–69], organic acids [33, 63, 65, 66, 69], sugars [39, 70, 71], lipids and fatty acids [72, 73]. Moreover, mass distributions of polymers and their building blocks, obtained via hydrolysis of the polymer, were assessed. Examples are glycogen [39, 70], cell protein [8, 10, 17], or DNA [74]. Most of the analytical methods have been developed for tissue samples. Since most of the compounds studied are polar or even charged molecules, derivatization is necessary in most of the cases of GC/MS analysis. The derivatization method of choice clearly depends

on the chemical nature of the analyte of interest. Often used derivatizations are methylation, acetylation, silylation and acylation. Instable metabolites such as oxaloacetate can be transformed into stable derivates by suitable derivatization such as oximation, whereby the reagent can be directly supplied in the extraction solvent [75].

In addition to GC/MS, also MALDI MS can be applied for labeling measurements of low molecular weight compounds related to the metabolism. Successful analysis of amino acids, organic acids, and sugars has been demonstrated [18, 25, 27]. Usually, derivatization is not required, which is a major advantage compared to GC/MS. To our knowledge, ESI MS has so far not been directly used for labeling measurements in metabolic flux analysis. However, its application for the analysis of low molecular weight metabolites has been demonstrated by several authors [e.g. 76, 77]. Membrane introduction MS has been used for the quantification of intensity ratios of labeled to non-labeled gases in bioprocesses such as CO_2 or CH_4 [32, 78].

4.3 Measurement of Positional Isotopomer Distributions

More detailed information on the labeling of a compound can be obtained with MS via additional analysis of fragment ions, which contain only specific parts of the carbon skeleton of the analyte. It should be noticed that the resolution of single positional isotopomer pools not necessarily leads to an increase in information for flux quantification [16]. Mathematically, isotopomer distributions can be obtained from mass distributions of the molecular ion, and the different assessed fragment ions via matrix calculus [8, 9]. By this approach, positional isotopomer distributions can be partially, in some cases even completely resolved. As example, the entire positional isotopomer distribution of pyruvate can be achieved via analysis of the molecular ion and three additional fragments formed in GC/MS analysis of pyruvate as methylester [9] or via analysis of the molecular ion and one fragment ion of derivatized alanine and one fragment ion of derivatized valine, both formed in the metabolism from pyruvate [8]. More complex protocols may be required for analytes containing more carbon atoms, thus exhibiting a substantially increased number of possible positional isotopomers. Di Donato et al. [64] determined 24 out of 32 possible positional isotopomers of glutamate by GC/MS, which was linked to an enormous experimental effort, requiring the synthesis and MS analysis of five different derivates in addition to glutamate. Also other protocols for the partial resolution of positional isotopomer pools are laborious, include various steps for purification and chemical or enzymatic conversion of the analytes [65, 66]. This impedes the broad and routine use of such techniques.

As underlined, the success of positional isotopomer analysis by MS is based on the availability of suitable fragments. Using hard ionization techniques such as EI ionization usually yields a number of fragments automatically. If the information content from the available fragments is too low, other derivates of the analyte, with a different fragmentation pattern, can be analyzed in addition. A major tool to obtain additional fragments is targeted fragmentation. A pro-

mising approach for positional isotopomer measurements is MS/MS, also called tandem MS, where selected ions can be isolated, subsequently fragmented and the fragments can be analyzed for their mass distribution (see chapter 2).

5
Application of MS to Metabolic Flux Analysis

The following chapter shows the application of MS to metabolic flux analysis with different examples. Whereas some of them focus on flux quantification of only a single or a few selected reactions, others aim at the analysis of larger parts of the metabolism. The overview given should illustrate the broad application potential of MS for metabolic flux analysis by examples from different fields of research. The majority of studies belongs to the medical field, whereas so far only few examples can be found in the area of biochemical engineering.

5.1
Microorganisms and Fungi

Park et al. showed the activity of pyruvate carboxylase in a pyruvate kinase deficient strain of lysine producing *Corynebacterium glutamicum* by ^{13}C tracer experiments with NMR and GC/MS [68]. Wittmann and Heinzle [25, 27] applied MALDI-TOF MS to batch cultivations of lysine producing *C. glutamicum* either on 1-^{13}C glucose or on a mixture of U-^{13}C and naturally labeled glucose, respectively, in combination with metabolite balancing. From stoichiometric data and from selected intensity ratios of secreted lysine, alanine and trehalose, the flux distribution of the central metabolism was determined. During maximum lysine production, the strain exhibited high relative fluxes of 71% into the pentose phosphate pathway and significant anaplerotic formation of oxaloacetate 37%. The two alternative lysine producing branches, the succinylase and the dehydrogenase pathway, respectively were found active, whereby 63% of lysine were formed via the dehydrogenase branch. Glucose 6-phosphate isomerase was found highly reversible. Moreover significant backfluxes from the TCA cycle to the glycolysis causing a withdrawal of the lysine precursor oxaloacetate, were found. The benefits of ^{13}C experiments and MS in addition to metabolite balancing are underlined by the comparison with a study applying only metabolite balancing for flux analysis of the same strain [79]. As described below, metabolite balancing alone does not provide sufficient information to resolve key fluxes in the central metabolism of *C. glutamicum*. As example metabolite balancing cannot discriminate between the two alternative routes in the lysine biosynthesis. In contrast, sufficient information on the flux partitioning in the lysine biosynthesis is provided by MS measurement of only one lysine intensity ratio [27]. The flux partitioning ratio between glycolysis and pentose phosphate pathway is accessible via metabolite balancing including a balance of NADPH, which is often found uncertain as described above. The flux distribution between glycolysis and PPP can be sensitively quantified by MS from only one measured intensity ratio of lysine [27]. In contrast to tracer experiments with MS, no information could be obtained by metabolite balancing on bidirectional

fluxes catalyzed by reversible enzymes such as glucose 6-phosphate isomerase or on cycling fluxes between C_4 units of the TCA cycle and C_3 units of the glycolysis.

Christensen et al. [17] determined flux distributions in the central metabolism of low and high-yielding strains of *Penicillium chrysogenum* applying chemostat cultures with 1-^{13}C glucose. The authors analyzed the labeling pattern of amino acids in hydrolyzed cell protein by GC/MS, which provides a high amount of labeling information. Recently Gombert et al. [80] applied GC/MS for labeling analysis and quantified metabolic fluxes in the central metabolism of *S. cerevisiae* with ^{13}C glucose as substrate. The authors found significant differences between cells grown in batch and in continuous culture. The relative flux through the pentose phosphate pathway was markedly higher in continuous culture compared to batch culture. A knockout of the *MIG1* gene caused no changes in the intracellular flux distribution. A combined approach of ^{13}C labeled fructose, glutamate or aspartate and NMR and GC/MS for labeling analysis was used to study the metabolism of actinomycin producing *Streptomyces parvulus* [81]. Labeling analysis of the actinomycin D peptide ring allowed the specification of the origin of its five amino acids. Kinetic studies in anaerobic mixed cultures were performed by Dornseiffer et al. [82] in a miniaturized bioreactor equipped with a membrane mass spectrometer with ^{13}C labeled bicarbonate and subsequent measurement of $^{12}CH_4$ and $^{13}CH_4$ by membrane MS. Flux analysis of *Saccharomyces cerevisiae* with ^{13}C and ^{18}O labeled glucose as tracer substrate and measurement of different mass isotopes of CO_2 was carried out in the same measurement cell [32].

5.2 Tissue Cultures

A number of authors have applied ^{13}C labeling experiments with MS to metabolic flux analysis in tissues such as liver, kidney, brain, and heart [83]. The inherent complexity of the networks including phenomena such as compartmentation, metabolite channeling and complex dilution effects of the labeling usually allow the determination of only selected flux parameters by a tracer experiment. One application of stable isotopes and MS is the *in vivo* quantification of the biosynthesis of polymers. For this purpose, a mathematical approach, recently reviewed by Hellerstein and Neese [84], was developed, that allows the determination of the labeling of the actual precursor molecules of a particular polymer. With this approach, the biosynthesis of proteins [85], lipids [86], and steroids [87] was studied. It was also applied to quantify gluconeogenesis [88]. Extensive work has been carried out on quantifying fluxes in the central metabolism of tissue cultures as exemplified by studies on the pentose phosphate pathway in human hepatoma cells [89], or on anaplerosis and the TCA cycle in perfused rat liver [64, 66, 69], and rat heart [90, 91]. Fluxes in the central metabolism of different mammalian cell lines were quantified by Lin et al. [71].

5.3
In vivo Studies in Animals and Humans

Tracer studies with stable isotopes have a long tradition in medical biochemistry. ^{13}C, ^{15}N or ^{18}O do not cause adverse physiological effects even at higher enrichments and are therefore especially suitable for *in vivo* studies in animals and humans. The quantification of metabolite turnover rates *in vivo* is a typical application field as reviewed by Wolfe [92]. *In vivo* studies on the glucose metabolism including gluconeogenesis, hepatic glucose cycling, glycogen synthesis and breakdown were conducted by several authors [e.g. 38, 39, 65, 70, 93, 94]. Additional studies were performed on the fatty acid and lipoprotein metabolism [46].

6
Conclusion and Future Perspectives

As shown in this review tracer experiments and MS are valuable tools for the analysis of metabolic fluxes in various different biological systems. Metabolic flux analysis by MS plays a central role in biochemical network characterization. Future perspectives of this rapidly developing field are seen in different areas. The first attributes to the fact that the real value of metabolic flux analysis is its comparative application, e.g. to different physiological situations or to different strains. However, metabolic flux analysis as a routine tool is currently not available. Thus, alterations of fluxes during industrially relevant batch or fed-batch cultivations or differences of flux distributions between wild type and genetically engineered over-producing strains are still widely unknown. Concerning the experimental methods, a major challenge will be therefore the simplification, miniaturization and automatization of the MS measurements for flux analysis, whereby especially novel techniques such as ESI MS or MALDI-TOF MS exhibit a high potential. An important requirement for broad and efficient flux analysis is the availability of general modeling frameworks with tools for model generation, experimental design, parameter estimation and statistical analysis. An interesting future direction is the elucidation of metabolic fluxes under dynamic conditions aiming at the determination of *in vivo* kinetics of enzymes and of metabolic regulation. MS exhibits a high sensitivity and an excellent applicability to both concentration and labeling measurements of intracellular metabolites, providing information on intracellular pool sizes and flux distributions, which makes it a promising tool to study flux dynamics, including the resolution of time-dependent flux alterations linked to the cell cycle or cell differentiation.

References

1. Sauer U, Hatzimanikatis V, Hohmann HP, Manneberg M, Van Loon AP, Bailey JE (1996) Appl Env Microbiol 62:3687
2. Hult K, Veide A, Gatenbeck S (1980) Arch Microbiol 128:253
3. Sazanov LA, Jackson JB (1994) FEBS Lett 344:109
4. Szyperski T (1998) Q Rev Biophys 31:41
5. Schmidt K, Marx A, de Graaf AA, Wiechert W, Sahm H, Nielsen J, Villadsen J (1998) Biotechnol Bioeng 58:254
6. Bonarius HP, Timmerarends B, de Gooijer CD, Tramper J (1998) Biotechnol Bioeng 58: 258
7. Christensen B, Nielsen J (2000) Adv Biochem Eng Biotechnol 66:209
8. Christensen B, Nielsen J (1999) Metab Eng 1:282
9. Wittmann C, Heinzle E (1999) Biotechnol Bioeng 62:739
10. Dauner M, Sauer U (2000) Biotechnol Prog 16:642
11. Spengler B (2001) The basics of matrix-assisted laser desorption ionization time-of flight mass spectrometry and post source decay. In: James P (ed) (2001) Proteome research: Mass spectrometry. Springer, New York, p 33
12. Sherry AD, Sumegi B, Miller B, Cottam GL, Gavva S, Jones JG, Malloy CR (1994) Biochemistry 33:6268
13. Debnam PM, Shearer G, Blackwood L, Kohl DH (1997) Eur J Biochem 246:283
14. Schmidt K, Carlsen M, Nielsen J, Villadsen J (1997) Biotechnol Bioeng 55:831
15. Kelleher JK (1999) Am J Physiol 277:E395
16. Wiechert W, Moellney M, Isermann N, Wurzel M, de Graaf AA (1999) Biotechnol Bioeng 66:69
17. Christensen B, Thykaer J, Nielsen J (2000) Appl Microbiol Biotechnol 54:212
18. Wittmann C, Heinzle E (2001) Biotechnol Bioeng 72:642
19. Lee WN, Byerley LO, Bergner EA, Edmond J (1991) Biol Mass Spectrom 20:451
20. Fernandez CA, Des Rosiers C, Previs SF, David F, Brunengraber H (1996) J Mass Spectrom 1996 31:255
21. Jones PJ, Leatherdale ST (1991) Clin Sci (Colch) 80:277
22. Wiechert W (1996) Habilitation Thesis, University of Bonn, Jülicher Forschungsbericht 3301, ISSN 0944-2952 (in German)
23. Moellney M, Wiechert W, Kownatzki D, de Graaf AA (1999) Biotechnol Bioeng 66:86
24. Zupke C, Stephanopoulos G (1994) Biotechnol Prog 10:489.
25. Wittmann C, Heinzle E (2000) Metabolic flux analysis of lysine producing *Corynebacterium glutamicum* by MALDI-TOF MS, 3rd European Symposium on Biochemical Engineering Sciences, Copenhagen, Denmark
26. Wittmann C, Heinzle E (2001) Metab Eng 3:171 – 190
27. Wittmann C, Heinzle E (2001) Eur J Biochem 268:2441 – 2455
28. Malloy CR, Sherry AD, Jeffrey FMH (1988) J Biol Chem 263:6964
29. Lee WN (1993) J Biol Chem 268:25522
30. Szyperski T (1995) Eur J Biochem 232:433
31. Klapa MI, Park SM, Sinskey AJ, Stephanopoulos G (1999) Biotechnol Bioeng 62:375
32. Luxenburger H, Wittmann C, Heinzle E (1998) Metabolic flux studies in *Saccharomyces cerevisiae* using dynamic membrane mass spectrometry. 2nd Conference on Metabolic Engineering, Elmau, Germany.
33. Erecinska M, Zaleska MM, Nissim I, Nelson D, Dagani F, Yudkoff M (1988) J Neurochem 51:892
34. Schadereit R, Krawielitzki K (1998) Isotopes Environ Health Stud 34:127
35. Doumit J, Le J, Frey J, Chamson A, Perier C (1999) Amino Acids 16:107
36. Yudkoff M, Daikhin Y, Nissim I, Nissim I (2000) Neurochem Int 36:329
37. Ben-Yoseph O, Kingsley PB, Ross BD (1994) Magn Reson Med 32:405
38. Weber JM, Klein S, Wolfe RR (1990) J Appl Physiol 68:1815
39. Hellerstein MK, Neese RA, Linfoot P, Christiansen M, Turner S, Letscher A (1997) J Clin Invest 1997 100:1305

40. Lee WN, Bassilian S, Ajie HO, Schoeller DA, Edmond J, Bergner EA, Byerley LO (1994) Am J Physiol 266:E699
41. Landau BR, Wahren J, Chandramouli V, Schumann WC, Ekberg K, Kalhan SC (1995) J Clin Invest 95:172
42. Costello CE (1997) Biophys Chem 68:173
43. Matsuo T, Seyama Y (2000) J Mass Spectrom 35:114
44. James P (ed) (2001) Proteome research: Mass spectrometry, Springer New York
45. Johnson RC, Cooks RG, Allen TM, Cisper ME, Hemberger PH (2000) Mass Spectrom Rev 19:1
46. Brenna JT (1994) Acc Chem Res 27:340
47. Corso TN, Brenna JT (1997) Proc Natl Acad Sci 94:1049
48. Thompson GN, Pacy PJ, Ford GC, Halliday D (1989) Biomed Environ Mass Spectrom 18:321
49. Caimi RJ, Brenna JT (1993) Anal Chem 65:3497
50. Karas M, Hillenkamp F (1988) Anal Chem 60:2299
51. Tanaka K, Waki H, Ido Y, Akita S, Yashida Y, Yoshida Y (1988) Rap Comm Mass Spectrom 8:151
52. Moore WT (1997) Methods Enzymol 289:520
53. Duncan MW, Matanovic G, Cerpa-Poljak A (1993) Rapid Commun Mass Spectrom 7:1090
54. Kang MJ, Tholey A, Heinzle E (2000) Rapid Commun Mass Spectrom 14:1972
55. Zhan Q, Gusev A, Hercules D M (1999) Rapid Commun Mass Spectrom 13:2278.
56. Fenn JB, Mann M, Meng CK, Wong SF, Whitehouse CM (1989) Science 246:64
57. Emmet MR, Caprioli RM (1994) J Am Soc Mass Spectrom 5:605
58. Edmonds CG, Loo JA, Loo RR, Udseth HR, Barinaga CJ, Smith RD (1991) Biochem Soc Trans 19:943
59. Parker CE, Perkins JR, Tomer KB, Shida Y, O'Hara K (1993) J Chromatogr 616:45
60. Cooks RG, Kaiser RE (1990) Acc Chem Res 23:213
61. Cotter RJ (1989) Biomed Environ Mass Spectrom 18:513
62. Tsikas D (1998) J Chromatogr B Biomed Sci Appl 717:201
63. Nissim I, Nissim I, Yudkoff M (1990) Biochim Biophys Acta 1033:194
64. Di Donato L, Des Rosiers C, Montgomery JA, David F, Garneau M, Brunengraber H (1993) J Biol Chem 268:4170
65. Katz J, Wals P, Lee WN (1993) J Biol Chem. 268:25509
66. Des Rosiers C, Di Donato L, Comte B, Laplante A, Marcoux C, David F, Fernandez CA, Brunengraber H (1995) J Biol Chem 270:100 27
67. Neese RA, Schwarz JM, Faix D, Turner S, Letscher A, Vu D, Hellerstein M (1995) J Biol Chem 270:14452
68. Park SM, Shaw-Reid C, Sinskey AJ, Stephanopoulos G (1997) Appl Microbiol Biotechnol 47:430
69. Des Rosiers C, Fernandez CA, David F, Brunengraber H (1994) J Biol Chem 269:27179
70. Katz J, Lee WN, Wals PA, Bergner EA (1989) J Biol Chem 264:12994
71. Lin YY, Cheng WB, Wright CE (1993) Anal Biochem 209:267
72. Lligona Trulla L, Magistrelli A, Salmona M, Tacconi MT (1992) Melanoma Res 2:235
73. Hellerstein MK, Schwarz JM, Neese RA (1996) Annu Rev Nutr 16:523
74. Macallan DC, Fullerton CA, Neese RA, Haddock K, Park SS, Hellerstein MK (1998) Proc Natl Acad Sci USA 95:708
75. Laplante A, Comte B, Des Rosiers C (1995) Anal Biochem 224:580
76. Gerber SA, Scott CR, Turecek F, Gelb MH (1999) J Am Chem Soc 121:1102
77. Reetz MT, Becker MH, Klein HW, Stöckigt D (1999) Angew Chem 111:1872
78. Meyer B, Heinzle E (1998) Biotechnol Bioeng 57:127
79. Vallino JJ, Stephanopoulos G (1993) Biotechnol Bioeng 41:633
80. Gombert AK, Moreira Dos Santos M, Christensen B, Nielsen J (2001) J Bacteriol 183:1441
81. Inbar L, Lapidot A (1991) J Bacteriol 173:7790
82. Dornseiffer P, Meyer B, Heinzle E (1995) Biotechnol Bioeng 45:219
83. Lee K, Berthiaume F, Stephanopoulos G, Yarmush ML (1999) Tissue Eng 5:347

84. Hellerstein MK, Neese RA (1999) Am J Physiol 276:E1146
85. Papageorgopoulos C, Caldwell K, Shackleton C, Schweingrubber H, Hellerstein MK (1999) Anal Biochem 267:1
86. Hellerstein MK, Christiansen M, Kaempfer S, Kletke C, Wu K, Reid JS, Mulligan K, Hellerstein NS, Shackleton CH (1991) J Clin Invest 87:1841
87. Kelleher JK, Kharroubi AT, Aldaghlas TA, Shambat IB, Kennedy KA, Holleran AL, Masterson TM (1994) Am J Physiol 266:E384
88. Neese RA, Schwarz JM, Faix D, Turner S, Letscher A, Vu D, Hellerstein MK (1995) J Biol Chem 270:14452
89. Lee WN, Boros LG, Puigjaner J, Bassilian S, Lim S, Cascante M (1998) Am J Physiol 274:E843
90. Comte B, Vincent G, Bouchard B, Des Rosiers C (1997) J Biol Chem 272:26117
91. Laplante A, Vincent G, Poirier M, Des Rosiers C (1997) Am J Physiol 272:E74
92. Wolfe RR (1992) Radioactive and stable isotope tracers in biomedicine: Principle and practice of kinetic analysis. Whiley-Liss, New York
93. Kalderon B, Korman SH, Gutman A, Lapidot A (1989) Am J Physiol 257:E346
94. Katz J, Lee WN (1991) Am J Physiol 261:E332

Received: April 2001

The Molecular Mechanism of ATP Synthesis by F_1F_0-ATP Synthase: A Scrutiny of the Major Possibilities

Sunil Nath

Department of Biochemical Engineering and Biotechnology, Indian Institute of Technology, Hauz Khas, New Delhi 110 016, India
E-mail: sunath@dbeb.iitd.ernet.in

Dedicated to Prof. Dr. Wolf-Dieter Deckwer on the occasion of his 60th birthday

There is a complicated hypothesis which usually entails an element of mystery and several unnecessary assumptions. This is opposed by a more simple explanation which contains no unnecessary assumptions. The complicated one is always the popular one at first, but the simpler one, as a rule, eventually is found to be correct. This process frequently requires 10 to 20 years. The reason for this long time lag was explained by Max Planck. He remarked that "Scientists never change their minds, but eventually die."

J. H. Northrop

A critical goal of metabolism in living cells is the synthesis of adenosine triphosphate (ATP). ATP is synthesized by the enzyme F_1F_0-ATP synthase. This enzyme, the smallest-known molecular machine, couples proton translocation through its membrane-embedded, hydrophobic domain, F_0, to the synthesis of ATP from adenosine diphosphate (ADP) and inorganic phosphate (P_i) in its soluble, hydrophilic headpiece, F_1. Animals, plants and microorganisms all capture and utilize energy by this important chemical reaction. How does it occur? The binding change mechanism and the torsional mechanism of energy transduction and ATP synthesis are two mechanisms that have been proposed in the literature. According to the binding change mechanism (which considers reversible catalysis and site-site cooperativity), energy is required primarily for release of synthesized ATP, but not for its synthesis. On the other hand, according to the torsional mechanism (which considers an irreversible mode of catalysis and absence of cooperativity), all the elementary steps require energy, and the ion-protein interaction energy obtained from the ion gradients is used to synthesize ATP, for P_i binding, and for straining the β-ε bond in order to enable ADP to bind. The energy to release preformed ATP from the tight catalytic site (β_{DP}) is provided by the formation of the β-ε ester linkage. First, the central features of these mechanisms are clearly delineated. Then, a critical scrutiny of these mechanisms is undertaken. The predictions of the torsional mechanism are listed. In particular, how the torsional mechanism deals with the specific difficulties associated with other mechanisms, and how it seeks to explain a wealth of structural, spectroscopic, and biochemical data is discussed in detail. Recent experimental data in support of the mechanism are presented. Finally, in view of the molecular machine nature of energy transduction, the indispensability of applying engineering tools at the molecular level is highlighted. This paves the way for the development of a new field: Molecular Physiological Engineering.

Keywords. ATP synthase, Oxidative phosphorylation, Binding change mechanism, Torsional mechanism, Molecular physiological engineering

Advances in Biochemical Engineering/
Biotechnology, Vol. 74
Managing Editor: Th. Scheper

Symbols and Abbreviations

A_O	affinity of oxidation
A_P	affinity of phosphorylation
a,b,c	subunits of the F_0 portion of ATP synthase enzyme
α,β,γ,δ,ε	subunits of the F_1 portion of ATP synthase enzyme
$\beta_O, \beta_C, \beta_{TP}, \beta_{DP}$	open, closed, loose, tight conformations, respectively, of the catalytic site
d	channel width
ε	dielectric constant
ξ	frictional coefficient
C	closed
E	enzyme
F	Faraday
F_0	hydrophobic, membrane-bound portion of ATP synthase
F_1	hydrophilic, extra-membrane portion of ATP synthase
f	fraction
I	moment of inertia
I	ion concentration
K	equilibrium constant
K_{qss}	quasi-steady state constant
k	torsional constant (modulus of rigidity)
$k_r, k_{r'}$	rate constants
k_s	constant of proportionality
k_t	transport rate constant
L	loose
l	horizontal distance
Λ	electrostatic coupling strength
λ	screening distance
$\Delta\mu_H$	electrochemical potential difference
n	exponent
O	open
θ	angle, angular displacement
ΔpH	pH difference
Δψ	electrical potential difference
Δ(Δψ)	change in electrical potential
q	Coulombic charge, degree of coupling
R	radial distance
r	radial distance, vertical distance
T	tight
t	time
τ_M	machine electrostatic torque
V	electrostatic potential
V_{max}	maximum velocity
v_{hyd}	rate of ATP hydrolysis
v_{syn}	rate of ATP synthesis
ω	angular velocity

x	distance, phosphate potential
y	distance
Z	mechanistic stoichiometry
ADP	adenosine diphosphate
AMP-PNP	non-hydrolyzable ATP analog
Asp	aspartic acid
ATP	adenosine triphosphate
DELSEED	seven-residue amino acid sequence in the β subunit
Glu	glutamic acid
Met	methionine
P/O	ATP/oxygen ratio
P_i	inorganic phosphate
Phe	phenylaniline
Val	valine

1 Introduction and Brief History

From knowledge of metabolic pathways and the extent of the world's biomass, it is estimated that the energy currency of the cell, the molecule adenosine triphosphate (ATP) and the adenosine diphosphate (ADP) and inorganic phosphate (P_i) from which it is formed, participate in more chemical reactions than any other compound on the surface of the earth with the exception of water. ATP was co-discovered by Fiske and SubbaRow and independently by Lohmann in 1929 [1, 2]. Over 60 years ago, the vital cellular process of oxidative phosphorylation was demonstrated by Belitzer and Kalckar. It was recognized that this was the major pathway by which our bodies captured energy from foodstuffs and used it to carry out a variety of essential cellular functions, but how it took place was largely unknown. In 1941, Lipmann postulated the key role of ATP in cellular metabolism and suggested that it possessed a "high group transfer potential" [3]. Lehninger identified the site of this reaction as the mitochondrion in 1948.

The synthesis of ATP is catalyzed by the enzyme ATP synthase (or F_1F_0-ATP synthase); the F_1 portion of this enzyme was first isolated by Racker and coworkers in 1960 [4]. ATP synthase is present in abundance in the membranes of animal mitochondria, plant chloroplasts, bacteria and other organisms. ATP synthesized by our ATP synthase is transported out of mitochondria and used for the function of muscle, brain, nerve, liver and other tissues, for active transport, and for synthesizing myriad compounds needed by the cell. Since the pool of adenosine phosphates in the body is limited, the use of ATP must be continually compensated by its synthesis, and an active person synthesizes his own body weight of ATP every day. The synthesis of ATP is the most prevalent chemical reaction in the body [5]. This is indeed a very important reaction. How exactly does it occur?

Historically, a first step towards resolution of this problem was taken by Slater in 1953 through his formulation of the chemical hypothesis [6]. Un-

fortunately, no chemical intermediate between oxidation and phosphorylation could be isolated despite frenzied efforts by several groups. Between 1961 and 1966, Mitchell formulated his then radical chemiosmotic hypothesis of oxidative phosphorylation [7, 8], while Williams proposed localized models coupling oxidation and ATP synthesis [9, 10]. Boyer presented the salvage conformational hypothesis in 1965 in which oxidation was directly coupled to phosphorylation via protein-protein conformational interactions [11]. In 1973, Boyer and colleagues proposed a precursor [12] to what later became the binding change mechanism of ATP synthesis, which he reviewed in great detail in 1993 [13]. Cross modified the mechanism and presented it in a review in 1996 [14], but still referred to it as the binding change mechanism.

Exactly a decade ago, after a long, rigorous and thorough education in both the engineering and biological sciences at IIT Kanpur, Princeton University, MIT, GBF/TU Braunschweig (under the inspiring guidance of Prof. Dr. W.-D. Deckwer), I decided, as a young Assistant Professor at IIT Delhi, to "work on something really challenging." Basic studies in bioenergetics had intrigued scientists for a long time; yet the molecular mechanism of biological energy transduction remained an enigma. It appeared that a completely fresh and original hypothesis was needed that could explain the wealth of existing data and better withstand further experimental challenge. In a series of papers during 1998–2001, Nath and co-workers proposed the torsional mechanism of energy transduction and ATP synthesis [16–20, 56].

In this review, I shall attempt to critically examine, as best as I can in the limited space available, some of the major candidate molecular mechanisms of ATP synthesis.

2
The ATP Synthase

2.1
Subunit Composition

ATP is synthesized by the enzyme ATP synthase (or F_1F_0 ATPase), which transforms energy from a transmembrane gradient of protons, or, in some cases, Na^+ ions into the chemical energy of ATP. This enzyme, the smallest known molecular machine, consists of two major parts: a membrane-extrinsic, hydrophilic F_1 containing three α, three β, and one copy each of γ, δ, and ε subunits, and a membrane-embedded, hydrophobic F_0 composed of one a, two b, and twelve c subunits (Fig. 1). The molecular masses of the α, β, γ, δ, and ε subunits in *E. coli* measure about 55, 50, 31, 19, and 15 kDa, while the a, b, and c subunits have molecular masses of 30, 17, and 8 kDa, respectively [21–30]. The F_0 and F_1 domains are linked by two slender stalks [21–30]. The central stalk is formed by the ε subunit and part of the γ subunit, while the peripheral stalk is constituted by the hydrophilic portions of the two b subunits of F_0 and the δ subunit of F_1. The ion channel is formed by the interacting regions of the a and c subunits in F_0, while the catalytic binding sites are predominantly located in the β subunits of F_1 at the α-β interface [21, 22, 28].

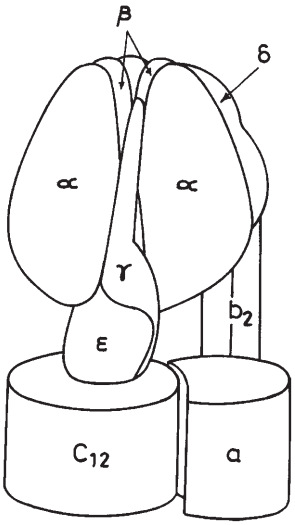

Fig. 1. Schematic diagram of the *Escherichia coli* ATP synthase enzyme

2.2 Molecular Machine Characteristics

ATP synthesis takes place by conformational changes at the catalytic binding sites. Recent structural [21, 27], biochemical [13, 28, 31], spectroscopic [32, 33] and microscopic [34, 35] studies indicate that these conformational changes arise from rotation of the γ-ε subunit in a static barrel of $\alpha_3\beta_3$ subunits in ATP synthase, making it the world's smallest molecular machine with a rotor radius of ≈1 nm (Fig. 1).

2.3 Structure

2.3.1 *The Walker Structure*

The X-ray crystal structure of bovine heart mitochondrial F_1 was solved by the group of Walker to 2.8 Å resolution in 1994, and represents the largest asymmetric structure ever solved [21]. The elongated α and β subunits are arranged alternately in the form of a hexagon. A 9-nm long α-helix of the γ subunit (comprising of residues 209–272 at the carboxy terminal) extends from top to bottom of the central cavity of the hexagon. The lower part of the carboxy terminal helix forms a coiled coil with a α-helix consisting of residues 1–45 at the amino terminus of the γ subunit. A short α-helix consisting of residues 73–90 of the γ subunit projects from the bottom. The δ and ε subunits, and 145 residues of the γ subunit (~50%), were not sufficiently ordered to diffract to high resolution and were not located in the electron density map.

In the Walker crystal structure of F_1-ATPase, the three non-catalytic α sites are liganded with the non-hydrolyzable ATP analog MgAMP-PNP. In contrast, the three catalytic β sites possess different conformations. One of the catalytic sites in the structure binds the analog MgAMP-PNP and is designated as β_{TP}; another site binds MgADP and is denoted by β_{DP}, while the third site is empty and distorted and is called β_E [21]. In further contrast, the nucleotide-free $\alpha_3\beta_3$ subcomplex of ATP synthase is a symmetric trimer [36].

2.3.2
The Pedersen-Amzel Structure

In 1998, Pedersen, Amzel, and colleagues solved the X-ray structure of rat liver mitochondrial F_1-ATPase to 2.8 Å resolution and obtained a more symmetrical structure of the α and β subunits [27]. In this structure, catalytic as well as non-catalytic sites are occupied with bound nucleotide and the three α subunits and the three β subunits are in very similar but distinct closed conformations, with no indication of an open conformation as found in the Walker structure. The rat liver crystals were grown in the presence of substantially higher concentrations of nucleotides, and the crystallization medium contained only ATP (and not AMP-PNP), but no Mg^{2+}.

3
Molecular Mechanism of ATP Synthesis in the F_1 and F_0 Portions of ATP Synthase

3.1
The Binding Change Mechanism

According to the binding change mechanism proposed by Boyer (Fig. 2, where O, L, T refer to open, loose and tight conformations, respectively), the synthesis of ATP occurs reversibly with an equilibrium constant close to unity in the high-affinity enzyme catalytic binding site; energy input from the so-called protonmotive force is needed not for synthesis of ATP at the catalytic site (which occurs spontaneously), but for the release of synthesized ATP from the high-affinity catalytic site [5, 13, 22, 37]. Thus, the step of chemistry is not an energy-requiring step according to this mechanism, while the high-affinity catalytic site opens due to provision of energy by the protonmotive force. Another

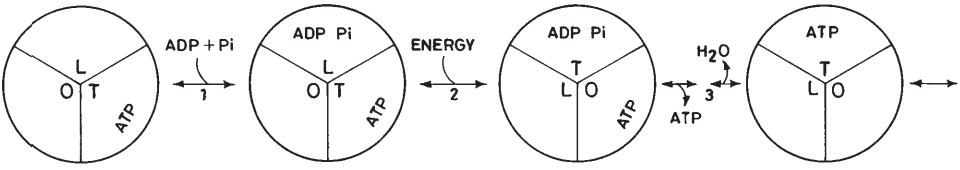

Fig. 2. Depiction of the binding change mechanism of ATP synthesis (simplified diagram redrawn from [13])

central feature of the binding change mechanism is that the catalytic sites interact with each other, i.e., cooperativity exists among catalytic sites [5, 13]. Thus, substrate ($ADP + P_i$) binding at a low-affinity catalytic site promotes product ATP release from the high-affinity catalytic site; hence, substrate binding must precede product release or be simultaneous with it during steady operation. Moreover, a simultaneous negative cooperativity of binding and positive cooperativity of catalysis is hypothesized to occur in the F_1 portion of ATP synthase in the physiological mode of operation [13]. Another tenet is the free rotation of the γ subunit in the cavity of the $\alpha_3\beta_3$ barrel in F_1. According to the binding change mechanism, physiological rates of ATP synthesis occur when two of the three catalytic sites contain bound nucleotide (Fig. 2).

3.1.1
Modification of the Binding Change Mechanism

In the version of the binding change mechanism (1993) described in Sect. 3.1 (bi-site catalysis, Fig. 2) [13], ($ADP + P_i$) enter in the loose catalytic site (L), ATP forms spontaneously in the tight site (T) and is released from the open site (O). In the 1997 version, the mechanism remains bi-site, but now ($ADP + P_i$) enters in O, ATP forms in T and is released in L [22]. In the modification of the binding change mechanism by Cross and co-workers, all three catalytic sites were used (though bound nucleotide still occurs in only two sites, thereby making this modification effectively still a bi-site mechanism), and an intermediate enzyme state containing loosely bound ($ADP + P_i$) in L as well as tightly bound ($ADP + P_i$) in T was envisaged [14] (Fig. 3). Cross envisaged that ATP forms from tightly bound ($ADP + P_i$) in T only after ATP release has taken place from O (Fig. 3, steps 1, 2). However, recently [5, 13], the concept of the tightly bound ($ADP + P_i$) intermediate was abandoned by Boyer, though all the tenets given in Sect. 3.1 were still retained. A quasi-equilibrium of a catalytic site containing ($ADP + P_i$) (form 2-H) and ATP (form 2-S) was envisaged. In the latest modification in the year 2000, the requirement of ($ADP+P_i$) in the L site was deemed unnecessary as it "introduces another control", and the conformation that a single catalytic site passes through during ATP synthesis was proposed to be O to T to L [37]. All other tenets were as in Sect. 3.1.

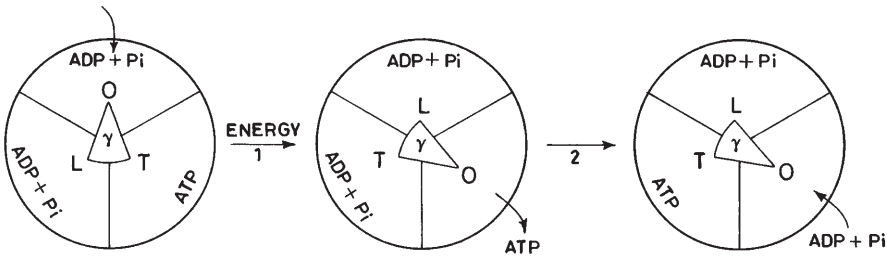

Fig. 3. Modified model of the binding change mechanism highlighting cooperativity and including tightly bound ADP and P_i as intermediates (simplified and redrawn from [14])

3.2
Latest Experimental Evidence not in Agreement with any Version of the Binding Change Mechanism

Recently, in a significant development, Senior and colleagues designed an optical probe by inserting a tryptophan residue to directly monitor, for the first time, the occupancy of the catalytic sites by nucleotides [28, 38]. Their tryptophan fluorescence experiments in the hydrolysis mode established definitively that V_{max} activity is attained by F_1-ATPase only when all three catalytic sites are occupied by bound nucleotide, i.e., an enzyme species with all three β subunits occupied is the only catalytically competent species [38]. Due to the inviolability of microscopic reversibility, this result holds for ATP synthesis also, and agrees with an earlier assessment based on enzyme kinetic and radioactive nucleotide binding data [39]. This experimental evidence is in complete disagreement with the fundamental tenets of the binding change mechanism. Further, the tryptophan fluorescence experiments showed that P_i binding can not be spontaneous, as suggested in diagrams illustrating the binding change mechanism (e.g., Figs. 2 and 3). The recent X-ray structure of mitochondrial F_1-ATPase in the transition state [39a] shows nucleotide bound to all three catalytic sites, which can never be explained by the binding charge mechanism.

Direct visualization of F_1-ATPase by sophisticated single molecule spectroscopy techniques such as epifluorescence/confocal microscopy clearly and unequivocally demonstrates *unidirectional and discrete* motion of the γ subunit in steps of 120° [34, 35, 40]. In various disciplines, from quantum chemistry to chemical/biochemical and mechanical engineering, such motion is considered irreversible. It is very difficult to conceive how a unidirectional, discrete motion can take place by a reversible mode of catalysis ($E.ATP \rightleftharpoons E.ADP.P_i$), i.e., how can a subunit of a single enzyme molecule oscillate back and forth in the presence of a driving force in one direction? This irreversibility of operation in a single molecule mode contradicts the fundamental tenet of the binding change mechanism that ATP synthesis occurs reversibly (and spontaneously) in a catalytic site of the enzyme. In my view, it is imperative to relate the *chemical kinetics* (the arrows representing an elementary step in the kinetic scheme) to the *mechanical aspects* (structure and dynamics of the molecular machine). It is interesting to note that our approach to the problem, in contrast, has incorporated irreversibility from the very outset [16–20, 41, 42, 56].

3.3
Further Specific Difficulties Associated with the Binding Change Mechanism

In addition to the very serious recent evidence in total disharmony with the binding change mechanism discussed above (Sect. 3.2), we pointed out several other specific difficulties in a paper published in January 2000, and stated that it was most important "to recognize and understand the imperative need to consider novel ideas with an open mind, and to overcome the limitations imposed on our own thinking by currently accepted mechanisms, by paradigms that are no longer applicable" [18]. For instance, since the loose conformation, L (β_{TP}), con-

tains bound (MgADP + P_i), and the open site, O (β_E), contains no bound nucleotide or P_i (Fig. 2), we found it difficult to conceive how both the binding steps could take place in the same catalytic site conformation (β_{TP}), especially keeping in mind that the binding of P_i is not spontaneous and requires energy [18]. The spontaneity of inorganic phosphate binding was emphasized as a serious defect. In the latest version [37], in addition to competent binding of ADP and P_i to O, even ATP is synthesized in a single O $\rightarrow$ T binding change, which is even more problematic. We considered it highly unlikely that nucleotide could bind to the catalytic site in the O conformation as proposed by Boyer [13, 22, 37], because of the absence of a proper nucleotide binding site [18]. This is even more difficult to reconcile in the hydrolysis mode, as pointed out by other workers [27]. Moreover, in this mode, in Boyer's bi-site mechanism, MgATP binds to the low affinity O site, but the medium affinity L site is left unfilled, which is a problem, as discussed [43]. Further, negative binding cooperativity and positive catalytic cooperativity need not occur simultaneously, as discussed by us [19], and as shown by recent experimental evidence [44]. We have also shown from first principles that there is absence of site-site cooperativity in ATP synthase under physiological steady state operating conditions [19]; in fact, there is no need for cooperativity [18]. Moreover, the molecular basis of cooperativity in ATP synthase remains unelucidated, despite almost three decades of experimental effort! Finally, our kinetic analysis necessitates that in the steady state physiological mode of ATP synthesis, product ATP release must precede substrate ADP binding [19], in agreement with the latest experimental evidence by direct optical probes [38], while, according to all versions of the binding change mechanism from 1973 to 2000, ADP binding must precede ATP release or be simultaneous with it. In the latest modification [37], the L site has no real role to play. It appears to be there just to accommodate the existence of three catalytic sites. Further, in the synthesis mode, T contains bound ATP while in the hydrolysis mode, L has bound ATP. If, in the synthsis mode, release of ATP takes place from O, then, at any instant, there exist two bound ATP molecular in F_1. This contradicts experimental data [bottom of p. 255 in 37]. If, in the synthesis mode, ATP is released from L, why is it that in the hydrolysis mode [39a] the ATP, entering in O, is not released from L itself? A logical explanation of these numerous discrepancies is that the basic tenets of the binding charge mechanism are incorrect.

Cross's modification of the binding change mechanism (Fig. 3) is also inadequate; in addition to the difficulties detailed above, it is beset with other serious problems. For instance, the open conformation (O) causes release of ATP, therefore, how can it cause binding of ADP, as envisaged? Moreover, it is hypothesized that ATP forms from tightly bound (ADP + P_i) in T only *after* ATP release has taken place from O (Fig. 3; steps 1, 2); since these conformational changes are caused by rotation of γ-ε, they should logically occur simultaneously at the different catalytic sites. How substrate (MgADP) binding enhances product (MgATP) release at a different catalytic site, which in turn promotes ATP synthesis at a third site, has never been proposed, i.e., how is this signal communicated, and, above all, how is the energy transmitted from one β subunit to another through the intervening α subunits? Further, in the nonequilibrium mode of functioning, tightly bound (ADP + P_i) should not be present in T; instead,

bound MgATP should be present. Finally, in this mechanism, the loose (L) site is serving no real function; it contains loosely bound ($ADP + P_i$) throughout the cycle (Fig. 3). Moreover, the O site also contains ($ADP + P_i$), and the T site also has bound ($ADP + P_i$) at a particular instant!

In view of the numerous serious difficulties discussed above, it seemed clear that only by questioning our fundamental beliefs would it be possible to truly understand how ATP is made.

3.4
The Torsional Mechanism of ATP Synthesis

In a series of papers, we have proposed the torsional mechanism of energy transduction and ATP synthesis, the only unified and detailed molecular mechanism of ATP synthesis to date [16–20, 56] which addresses the issues of ion translocation in F_0 [16, 20, 56], ionmotive torque generation in F_0 [16, 20, 56], torque transmission from F_0 to F_1 [17, 18], energy storage in the enzyme [17], conformational changes in F_1 [18], and the catalytic cycle of ATP synthesis [18, 19]. We have also studied the thermodynamic and kinetic aspects of ATP synthesis [19, 20, 41, 42, 56]. A kinetic scheme has been developed and mathematically analyzed to obtain a kinetic model relating the rate of ATP synthesis to pH_{in} and pH_{out} in the F_0 portion and the adenine nucleotide concentrations in the F_1 portion of ATP synthase. Analysis of these kinetic models reveals a wealth of mechanistic details such as the absence of cooperativity in the F_1 portion of ATP synthase, order of substrate binding and product release events, and kinetic inequivalence of ΔpH and $\Delta\psi$.

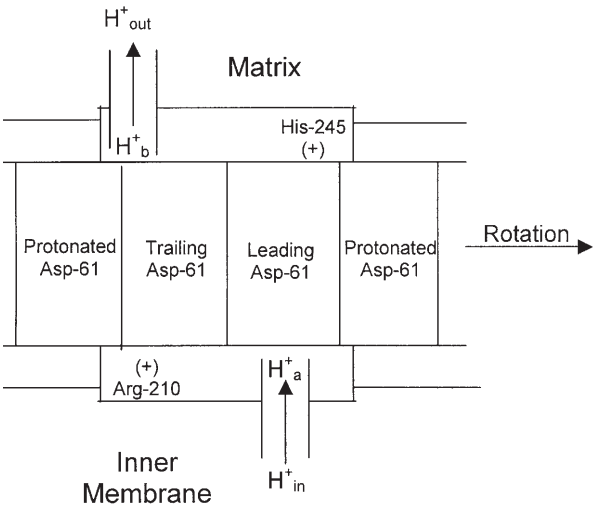

Fig. 4. Schematic diagram of the $\Delta pH - \Delta\psi$ two mutually non-colinear half-channel model for torque generation by the F_0 portion of ATP synthase forming a part of the torsional mechanism of energy transduction and ATP synthesis [16–20, 56]

Our molecular mechanism for torque generation in the F_0 portion of ATP synthase [16, 20, 56] considers (and highlights) the roles of both ΔpH and $\Delta\psi$ using two mutually non-colinear half-channels (Fig. 4); torque generation is a result of change in electrostatic potential, $\Delta(\Delta\psi)$, brought about by the binding of protons flowing along their concentration gradient to their binding sites in the c-subunit. In our model, entry and exit of protons through the corresponding half-channels are separated by the time it takes the c-rotor to rotate by 15°. We have shown that ΔpH and $\Delta\psi$ are kinetically inequivalent in driving ATP synthesis, and $\Delta\mu_H$ (defined as $F\,\Delta\psi - (2.303RT)\,\Delta pH$) is not the true driving force for ATP synthesis [20, 56].

According to the torsional mechanism of ATP synthesis, ΔpH supplies only *half* the energy requirement for ATP synthesis; the rest has to be supplied by an *independent* source of $\Delta\psi$. Further, we have proposed that $\Delta\psi$ is created in the vicinity of the ATP synthase enzyme complex, i.e., $\Delta\psi$ *is localized*, and we have postulated a dynamically electrogenic but overall electroneutral ion transport involving membrane-permeable anions (such as succinate) and protons. In order to utilize the energy of the anion gradient, the anion flows through the membrane along its concentration gradient in the vicinity of the enzyme complex and creates a localized $\Delta\psi$ (negative inside) of –60 mV. This is *followed* by the transport of protons (symsequenceport) through the proton half-channel along its concentration gradient. (In general, according to postulates of the torsional mechanism, cations penetrate the inner mitochondrial membrane following a negative internal electrical potential generated by the diffusion of anions.) Hence, the true driving forces for ATP synthesis are ΔpH and $\Delta\psi$, not $\Delta\mu_H$. The proton binds to the essential Asp (or Glu) residue of the c-rotor resulting in a change in the overall $\Delta\psi$, $\Delta(\Delta\psi)$, of approximately 60 mV (30 mV due to ΔpH across the entry proton half-channel, and 30 mV due to change in $\Delta\psi$ upon proton binding to the Asp residue). This value is estimated based on energy balance and our molecular mechanism which predicts a proton/ATP ratio of 4, and each proton binding and unbinding step to release nearly $\sim 480/4 = \sim 120$ meV of energy in total, i.e., ~60 meV (or equivalently creation of a $\Delta(\Delta\psi)$ of ~60 mV) during each elementary step of binding and unbinding. The energy released in this step rotates the c-rotor by 15°. The incoming Asp residue releases its bound proton at the a-c interface, resulting in a $\Delta(\Delta\psi)$ of ~60 mV (30 mV due to ΔpH across the exit proton half-channel, and 30 mV due to change in $\Delta\psi$ upon proton unbinding from the Asp residue) and a consequent rotation of the c-rotor by 15°. During each 15° rotation of the c-rotor, the ion-protein interaction energy is transiently stored as a twist in the helices of the ten membrane-bound c subunits. The simultaneous untwisting of the c-subunit helices drives the rotation of the ε subunit and the bottom of the γ subunit by 15°, and the ion-protein interaction energy is now stored as *torsional energy* in the γ subunit. Hence, the energy transiently stored in ΔpH and $\Delta\psi$ is converted to torsional energy through the process of ion-protein interactions. In this way, through cation binding *within* the electrostatic potential field created by the transport of anions, the enzyme is able to *utilize* the energy of both the delocalized ΔpH and the localized $\Delta\psi$.

Thus, a central feature of the torsional mechanism is the development of a torsional strain in the γ subunit due to rotation of the bottom of the central

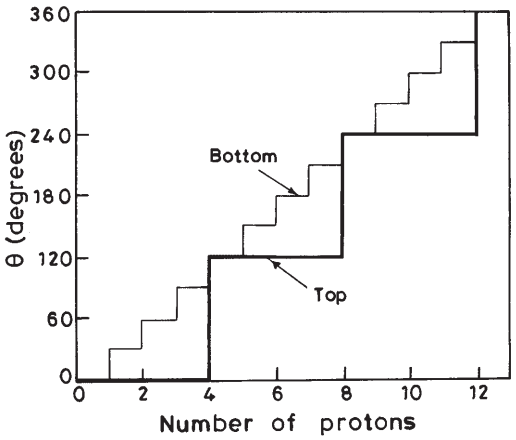

Fig. 5. Rotation of the top and bottom of the central stalk as a function of the number of protons as predicted by the torsional mechanism of energy transduction and ATP synthesis [17–20, 56]

stalk of ATP synthase in discrete steps of 30° (considering translocation of a proton across the membrane) or in two discrete steps of 15°, corresponding to each elementary step of proton unbinding from and binding to its binding site on the c subunit in our $\Delta pH - \Delta\psi$ two mutually non-colinear half-channel model (Fig. 4), while the top of the γ subunit remains stationary due to its interactions with the catalytic sites (Fig. 5). The rotation arises from the change in electrostatic potential $\Delta(\Delta\psi)$ caused by ion-protein interactions in an electrostatic potential field defined by $\Delta\psi_{intrinsic}$, the electrical potential difference due to the charge geometry of the c-rotor–a-stator [16, 20], and the diffusion potential generated as a result of diffusion of organic anions that are permeable to the membrane (e.g., succinate), the transport of which *precede* the translocation of cations (e.g., protons). The torsional strain is responsible for storage of torsional energy in the γ subunit and causes conformational changes at the catalytic sites [17, 18]. During rotation of the bottom of the central stalk (consisting of the ε subunit and the lower portion of the γ subunit), the ε-β_E ester bond gets strained, and Mg^{2+} interacts with its ligands in the open conformation (β_E) and creates a site with the correct conformation for ADP binding. The substrate MgADP binds and the binding energy breaks the strained ε-β_E interaction, causing the catalytic site to adopt a closed conformation (β_C). Rotation of the top of the γ subunit by 120° (Fig. 5) causes a change in the conformation of β_C to the loose conformation β_{TP} that enables entry and binding of P_i in β_{TP} [18]. Upon another 120° rotation of the top of the γ subunit, the γ-β_{TP} interactions break, leading to the establishment of the tight conformation, β_{DP}, resulting in synthesis of MgATP by nucleophilic attack involving ADP-O^- as the nucleophile and P_i [18]. A further rotation and interaction of the ε subunit with the catalytic site leads to opening of the catalytic site (β_E) and release of the bound MgATP. The energy for release of preformed MgATP is provided by the formation of the ε-β_{DP} ester bond,

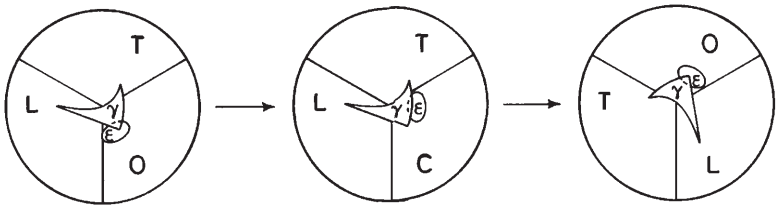

Fig. 6. One-third of the catalytic cycle according to our proposed torsional mechanism of ATP synthesis by ATP synthase (viewed from the F_1 side) [18]. The conformations of the F_1 catalytic sites in the diagram on the left are: open, O (β_E), tight, T (β_{DP}), and loose, L (β_{TP}). The rotating ε subunit has caused β_{DP} to open (see text), thereby releasing the bound MgATP from the previous one-third of the enzyme cycle. MgADP diffuses into this open conformation, but in the absence of a binding site it cannot bind to it. Thus, the open conformation (β_E) contains no *bound* nucleotide. The middle diagram is drawn for the case when the driving force has caused the ε subunit to rotate 60° counterclockwise (in two 30° steps, if translocation of one ion through F_0 all the way *across* the membrane is taken as the basis [16, 20], or by four 15° steps, corresponding to each elementary step of proton unbinding from and binding to its binding site on the c subunit, if the ion half-channel is taken as the basis); the top of the γ subunit remains stationary in this interval of time because of constraints arising from its interactions with the catalytic sites [17–19]. The substrate has bound and its binding energy has broken the strained ε-β_E interactions, and the open catalytic site has changed to a closed conformation (β_C). β_C therefore contains bound MgADP. The tight and the loose catalytic sites contain bound MgATP and bound (MgADP+P_i), respectively. With the passage of four ions through F_0, sufficient *torsional energy* is accumulated in the γ subunit to enable the constraints at the top to be broken, and the top of the γ subunit rotates 120° counterclockwise in a single step [17, 18] (i.e., while the bottom of the γ subunit, together with ε, rotates from 90° to 120°, the top of the γ subunit rotates from 0° to 120°), leading to the enzyme conformation depicted in the diagram on the right. This rotation of the top of the γ subunit converts the L site (β_{TP}) to the T site (β_{DP}), and the C site (β_C) to the L site (β_{TP}). Interaction of the ε subunit converts the T site (β_{DP}) to the open site (β_E), and an enzyme conformation similar to the diagram on the left appears, but shifted counterclockwise by 120°, and the entire cycle repeats. Thus, the sequence of conformations that a particular catalytic site (β subunit) passes through during ATP synthesis is O to C to L to T

whereas P_i binding and ATP synthesis are driven by rotation of the top of the γ subunit by 120° as a consequence of relaxation of the γ subunit due to breaking of the constraints at the top of the 'shaft' upon accumulation of torsional energy [16–19].

One-third of the catalytic cycle of ATP synthase as proposed by the torsional mechanism of ATP synthesis is shown in Fig. 6. Extension of the sequence of events at a single catalytic site to the enzyme as a whole is shown in Fig. 7. The switching of the enzyme from the two-nucleotide ground state to the three-nucleotide catalytic state and back to the ground state is clearly depicted in this figure.

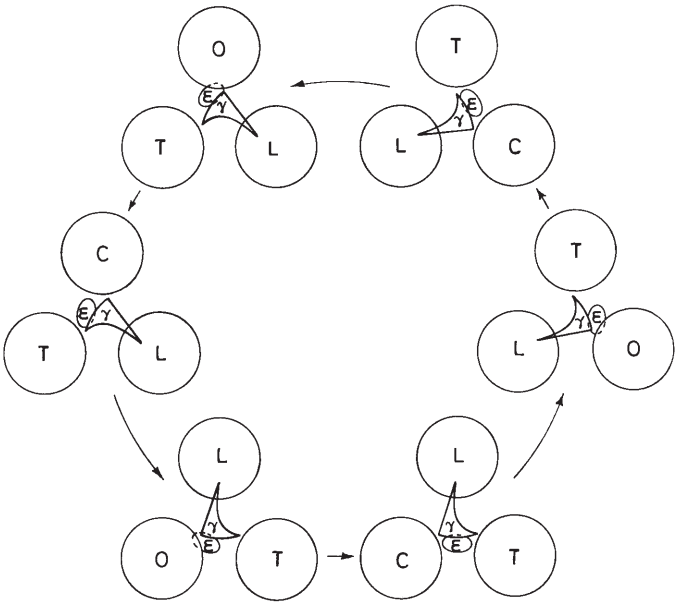

Fig. 7. Extension of the sequence of events at a single β subunit to the ATP synthase enzyme as a whole during ATP synthesis, as proposed by the torsional mechanism. The diagram is drawn at 60° intervals of the movement of the ε subunit. Binding of substrate converts the two-nucleotide state (the resting or ground state) to the three-nucleotide state. Catalysis takes place in the three-nucleotide state, which converts back to the two-nucleotide state with release of product [18]

3.4.1 *Some Novel Predictions of the Torsional Mechanism of ATP Synthesis*

Some of the predictions made by the torsional mechanism are:

1. Torque generation is a result of a change in electrostatic potential brought about by the ion gradients.
2. ΔpH and $\Delta\psi$ are kinetically inequivalent in driving ATP synthesis, and $\Delta\mu_H$ is not the true driving force for ATP synthesis.
3. Energy storage takes place in the γ subunit of ATP synthase.
4. Differential rotation of the top of the γ subunit exists with respect to the bottom of the γ subunit and the ε subunit.
5. The true driving forces for ATP synthesis are ΔpH and $\Delta\psi$, while for the oxidative phosphorylation process, the overall driving forces are the ion gradients of protons as well as anions or cations, which are transported across the membrane via symsequenceport or antisequenceport, accordingly, followed by ion-protein interactions involving creation of $\Delta(\Delta\psi)$ as an intermediate step for rotation of the c-rotor and subsequent storage of torsional energy in the γ subunit to be used thereafter for synthesizing ATP.

6. K^+ ions in the presence of valinomycin do not distribute passively at electrochemical equilibrium; rather, this represents a nonequilibrium state in which K^+ creates a diffusion potential following which protons move.
7. Unisite catalysis is a non-physiological mode of operation of the synthase; the two-nucleotide state is the resting (ground) state of the enzyme. Physiological rates of ATP synthesis occur only when all three catalytic sites are filled by bound nucleotide.
8. The sequence of conformations that a particular β subunit cycles through during ATP synthesis is O (open, β_E) to C (closed, β_C) to L (loose, β_{TP}) to T (tight, β_{DP}). The order of conformations that a catalytic site passes through during ATP hydrolysis is O to C to T to L.
9. The bound nucleotide occupancies of the catalytic sites during ATP synthesis are: no bound nucleotide in β_E (open), MgADP in β_C (closed), MgADP + P_i in β_{TP} (loose), and MgATP in β_{DP} (tight). The bound nucleotide occupancies of the catalytic sites during ATP hydrolysis are: no bound nucleotide in β_E (open), MgATP in β_C (closed), MgATP in β_{DP} (tight), and MgADP + P_i in β_{TP} (loose).
10. The ε subunit plays a crucial role in release of product.
11. The ε subunit (in *E. coli*) is always closest to the catalytic site with the least affinity for ATP (β_E, defined only for the two-nucleotide state).
12. P_i binding is not spontaneous but requires energy.
13. A single molecule of ATP synthase catalyzes ATP synthesis by an irreversible mode of catalysis.
14. Product ATP release precedes substrate ADP binding under physiological steady state operating conditions for ATP synthesis.
15. There is no site-site cooperativity in ATP synthase in the physiological steady state mode of operation.

3.4.2 *Quantification of the Torsional Mechanism*

We focus only on selected results of our quantitative analysis of the torsional mechanism of energy transmission in this section. In the charge geometry of Fig. 4, let l_{23} be the distance between the two negatively charged rotor residues and d the channel distance between the rotor and the stator. We represent the vertical offset between the leading negatively charged rotor residue and the upper positively charged stator residue by r_{12}. The vertical offset between the trailing negatively charged rotor residue and the lower positively charged stator residue is represented by r_{34}, while the horizontal offset is denoted by l_{34}. Let θ be the angle swept by the imaginary line joining the trailing rotor residue and the upper stator residue at any instant of time with respect to the equilibrium position [16, 20]. Thus, we can write the distance x between the trailing rotor residue and the lower stator residue at any instant of time as:

$$x = [d^2 + r_{34}^2 + \{l_{23} + l_{34} - r_{12} \tan(\tan^{-1}(l_{23}/r_{12}) - \theta)\}^2]^{1/2} \quad (1)$$

and the distance y between the trailing rotor residue and the upper stator residue at any time as:

$$y = [d^2 + r_{12}^2 + \{r_{12} \tan (\tan^{-1}(l_{23}/r_{12}) - \theta)\}^2]^{1/2} \quad (2)$$

After a proton hop, the leading rotor residue is neutralized [16, 20] and the electrostatic potential, V, between the two pairs of oppositely charged point charges in the resulting charge configuration can be written as:

$$V = \Lambda[\exp(-\lambda x)/x + \exp(-\lambda y)/y] \quad (3)$$

where Λ is the coupling strength $-q_1q_2/(4\pi\varepsilon_0\varepsilon)$, and the charges q_1 and q_2 are taken with the appropriate sign.

The machine electrostatic torque is given by the expression:

$$\tau_M = -\partial V/\partial\theta = -(\partial V/\partial x)(\partial x/\partial\theta) - (\partial V/\partial y)(\partial y/\partial\theta) \quad (4)$$

Evaluating the partial differentials in Eq. (4) using Eqs. (1)–(3) leads to the angular dependence of the electrostatic torque, i.e.:

$$\begin{aligned}\tau_M = -[\Lambda\{\exp(-\lambda x)\}\{1+\lambda x\}\{l_{23}+l_{34}-r_{12}\tan(\tan^{-1}(l_{23}/r_{12}) - \theta)\} \\ \cdot \{r_{12}\sec^2(\tan^{-1}(l_{23}/r_{12}) - \theta)\}/x^3] + [\Lambda\{\exp(-\lambda y)\}\{1+\lambda y\} \\ \cdot \{r_{12}\tan(\tan^{-1}(l_{23}/r_{12}) - \theta)\}\{r_{12}\sec^2(\tan^{-1}(l_{23}/r_{12}) - \theta)\}/y^3]\end{aligned} \quad (5)$$

Using the equation of motion for a system with differential rotation taking into account the inertial, frictional, torsional and electrostatic forces:

$$Id^2\theta/dt^2 + \xi d\theta/dt + k\theta = \tau_M \quad (6)$$

with the boundary conditions

$$\omega = 0 \quad \text{at} \quad x = R^2 + r^2 - 2Rr\cos 30 \quad (7)$$

and

$$\theta = 0 \quad \text{at} \quad t = 0, \quad (8)$$

numerical results were obtained. Figure 8 shows the results of this computation in the form of a θ vs. time plot for a range of θ from 0 to 120° for the bottom of the shaft, which corresponds to the sequential passage of four protons, and represents one-third of the catalytic cycle of ATP synthesis. As seen from Fig. 8, each proton hop leads to a rapid rise in the angular displacement (the transient nonequilibrium state or phase) and subsequently reaches a new local equilibrium, as indicated by the charge configuration shown in Fig. 4. Energy storage in the γ subunit takes place rapidly during the transient nonequilibrium phase that minimizes losses due to dissipation and leads to very high efficiencies of energy transfer. Due to the presence of torsion in the shaft with a piecewise linear stress-strain relationship, the time taken by the bottom of the shaft to traverse an angular displacement of 30° increases with the passage of each proton in the 0–90° range. Passage of the fourth proton achieves the break-through stress and causes the constraints at the top of the shaft to be broken, leading to a very rapid movement of the entire shaft (Fig. 8). For the conditions of our

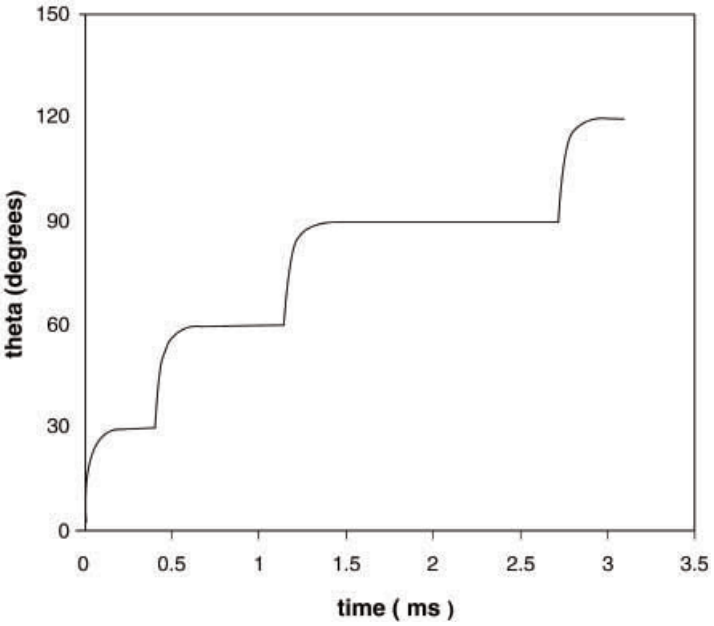

Fig. 8. Quantification of the dynamics of the bottom of the γ-ε shaft as proposed by the torsional mechanism of energy transmission. Angular displacement vs. time in the 0–120° interval obtained by numerical simulation of the equations of motion in the presence of differential rotation is shown. The values of the parameters employed in the simulation are: $\xi = 3.3\times10^{-25}$ kg m^2 s^{-1}; $k = 12.40\times10^{-20}$ kg m^2 s^{-2} (0–30°), 6.21×10^{-20} kg m^2 s^{-2} (30–60°), 4.14×10^{-20} kg m^2 s^{-2} (60–90°), 8.0×10^{-20} kg m^2 s^{-2} (90–120°); $d = 0.5\times10^{-9}$ m; $l_{23} = 1.3\times10^{-9}$ m; $l_{34} = 1.8\times10^{-9}$ m; $r_{12} = 0.20\times10^{-9}$ m; $r_{34} = 0.85\times10^{-9}$ m; $\lambda = 1\times10^{-9}$ m; $\Lambda = 1.152\times10^{-28}$ kg m^3 s^{-2}; $q = 1.6\times10^{-19}$ C; $\varepsilon = 2$

simulation, the bottom of the shaft reaches 30° at 0.571 ms, 60° at 1.364 ms, 90° at 3.395 ms, and 120° at 3.859 ms, i.e., it takes 0.571, 0.793, 2.031, and 0.464 ms to traverse successive 30° displacements in the 0–120° range. An average value of angular velocity of approximately 100 revolutions per second is obtained, which is well within the expected range [21, 28].

3.4.3 Resolution of Difficulties Achieved and Experimental Evidence Supporting the Torsional Mechanism

Without exception, none of the specific difficulties discussed in Sects. 3.2 and 3.3 arise in the torsional mechanism. For instance, there is no requirement that nucleotides bind (and stay bound) to the catalytic site in the open conformation in the torsional mechanism; nor does binding of both MgADP and P_i take place in the same catalytic site. In fact, the presence of torsional strain ensures that another conformation (β_C) is attained between β_E and β_{TP}, where MgADP gets bound. Furthermore, upon rotation and interaction of γ with the DELSEED sequence of β_C caused by the proton gradient, the conformation of the catalytic

site is altered (slightly loosened) to β_{TP} and access of inorganic phosphate to the site is created. Binding of P_i takes place in this altered conformation, β_{TP}. Since the torsional mechanism is a tri-site mechanism, substrate enters (and binds) to the same catalytic site from which product had been released earlier; therefore, the problem of leaving a higher-affinity catalytic site unfilled never arises. Each catalytic site serves its particular function in the torsional mechanism, unlike in Boyer's [37] or Cross's [14] modification.

3.4.3.1
Optical Probes

The mechanism is in complete agreement with results from recent tryptophan fluorescence experiments (which, due to the inviolability of microscopic reversibility, also hold in the synthesis mode) that establish definitively that (i) P_i cannot simply bind spontaneously, (ii) an enzyme species with all three catalytic sites occupied is the only catalytically competent species, and (iii) release of product and binding of substrate cannot be simultaneous, rather product release must precede substrate binding [38].

3.4.3.2
Electron Microscopy and Image Analysis

In a very recent important development, Böttcher and Gräber carried out a laborious investigation of the structure of chloroplast ATP synthase by electron microscopy and obtained vastly improved interpretation of the data by introducing sophisticated image analysis techniques [45]. 3300 ATP synthase molecules were imaged, classified into 16 classes by difference analysis using multivariate statistical techniques, and the signal-to-noise ratio enhanced by averaging images of molecules within the same class. The class average from electron microscopic data was interpreted based on the Walker structure. The final result (their Fig. 2D) showed the ε subunit lying closest to β_E and the γ subunit interacting with β_{TP}, in complete agreement with the predictions of the torsional mechanism made in 1998 [16, 18]. The small structural detail detected in the form of the tiny third stalk/connection in the electron microscopy data, "formed presumably by a single α helix [45]", would then correspond to the interaction of the Ser 108 of the ε subunit with the DELSEED sequence (β-Glu 381) of the catalytic site proposed in the torsional mechanism [16–20].

3.4.3.3
Single Molecular Spectroscopy

The observed unidirectional (no reversal of rotation) and discrete rotation of the γ subunit in steps of 120° during ATP hydrolysis by single molecule spectroscopy [34, 35, 40] supports the irreversible mode of operation of a single enzyme molecule that has been envisaged for the formulation of the thermody-

namics and the molecular mechanism right since inception [16, 41, 42]. According to the torsional mechanism, during ATP synthesis, the γ subunit rotates counter-clockwise when viewed from the F_1 side. Thus, during ATP hydrolysis, the γ subunit should rotate clockwise when viewed from the F_1 side, which agrees with the direction observed by single molecule epifluorescence microscopy experiments [34]. Moreover, reversing the direction of motion of the γ subunit during ATP synthesis, the torsional mechanism predicts that, during ATP hydrolysis, the rotating γ subunit will sequentially encounter β subunits in the conformations O followed by L followed by T, in agreement with that determined experimentally [34].

3.4.3.4
Biochemical Nucleotide Site Occupancy Experiments

For ATP hydrolysis, in our view, the bound nucleotide occupancies are: no bound nucleotide in β_E (O, open), MgATP in β_C (C, closed), MgATP in β_{DP} (T, tight), and MgADP+P_i in β_{TP} (L, loose). The order of conformations that a *particular* β subunit cycles through during ATP hydrolysis is O to C to T to L. Thus, from the point of view of the order of conformations that a catalytic site passes through, ATP hydrolysis is not simply the reverse of ATP synthesis. Hence, ATP synthesis cannot be understood adequately by merely reversing the reaction arrows in a mechanism for ATP hydrolysis; this point of view has also been expressed by another group recently [43, 46]. This is logical, because the driving force for ATP hydrolysis is the hydrolysis step itself, while, in ATP synthesis, the rotation of γ-ε is induced by F_0 which is driven by the ion gradients. Further, recent studies demonstrate that isolated F_1 and F_0F_1 do not bind P_i to any extent at physiological concentrations (5 mM) in the absence of a proton gradient [38], and the effect of the proton gradient increases the affinity of the catalytic site for P_i by orders of magnitude during ATP synthesis, as discussed earlier, again pointing clearly to irreversibility. This does not conflict with the recent observation that both synthesis and hydrolysis reactions proceed through the same transition state [47]; thus, in our view, the L to T transformation of a β subunit during ATP synthesis and the T to L transformation of the subunit during ATP hydrolysis are the exact reverse of each other and will employ the same reaction pathway and pass through the same transition state.

3.4.3.5
Biochemical Acid Quench/Cold Chase Experiments

In classical acid quench/cold chase experiments [48] with mitochondrial F_1 in "unisite" catalysis mode, [γ-^{32}P]ATP was used as substrate and the ratio of bound $^{32}P_i$/total bound ^{32}P, where total bound ^{32}P includes both bound $^{32}P_i$ and bound [γ-^{32}P]ATP, was measured at different concentrations of F_1 and [γ-^{32}P]ATP and at different incubation times of the reaction mixture. A kinetic scheme based on a general sequence of events leading to ATP hydrolysis which considers irreversibility of the catalysis steps, as proposed recently by some researchers [16–20, 43, 46, 49], was developed. k_r and k_r' represent the rate con-

stants for consumption of E.ATP to E.ADP.P_i and of E.ADP.P_i to E.ADP + P_i respectively. We define

$$f = \text{bound } {}^{32}P_i/\text{total bound } {}^{32}P = [E.ADP.P_i]/([E.ATP]+[E.ADP.P_i]) \quad (9)$$

Unisite catalysis is a non-physiological mode of catalysis in which a very small fraction of the enzyme population contains bound nucleotide in all three catalytic sites. According to the torsional mechanism, only this fraction will contribute to the measured ATPase activity. Based on the site occupancies predicted by the torsional mechanism during ATP hydrolysis (two catalytic sites contain bound MgATP, while one contains bound MgADP + P_i), the fraction f in Eq. (9) is predicted to be 0.33, which is in perfect agreement with experiment [48].

Because of the irreversibility of the catalysis steps, once ATP is bound to the F_1-ATPase it has to be hydrolyzed to ADP and P_i and subsequently release the products from the catalytic site. As E.ADP.P_i is an intermediate in ATP hydrolysis, quasi-steady state considerations imply that the rate of formation of E.ADP.P_i is equal to its rate of consumption, i.e.:

$$v_{hyd} = k_r[E.ATP] = k_r'[E.ADP.P_i] \quad (10)$$

This implies that

$$[E.ADP.P_i] = [E.ATP](k_r/k_r') \quad (11)$$

Substituting Eq. (11) into Eq. (9) leads to

$$f = k_r/(k_r + k_r') \quad (12)$$

Since f = 0.33 by experiment as well as by theory,

$$k_r/(k_r + k_r') = 0.33, \text{ or } k_r' = 2k_r \quad (13)$$

From Eq. (12) we see that f is independent of both the concentrations of the enzyme and the substrate as well as the incubation time, as observed in the experiments. Since k_r and k_r' are rate constants, the fraction f is a characteristic property of the system. Similar to the equilibrium constant for reversible hydrolysis [48], we define a quasi-steady state constant for irreversible hydrolysis as:

$$K_{qss} = \text{rate constant for formation of E.ADP.}P_i\text{/rate constant for consumption of E.ADP.}P_i = k_r/k_r' = 0.5 \quad (14)$$

Hence, an irreversible mode of catalysis (where catalysis refers to rotation of the c-rotor in the F_0 portion of ATP synthase, and to ADP, P_i binding and ATP synthesis and release in the F_1 portion of ATP synthase) may also be employed to explain these experimental observations.

3.4.3.6 Structural Considerations

The Pedersen-Amzel structure revealed a state of the enzyme in which all six α,β subunits adopt a similar closed conformation, and it was argued that this

represents the active conformation of the enzyme. In their view, the Walker structure is a non-physiological state induced by crystallization without sufficient total nucleotide present to occupy all three catalytic sites [27]. In a recent X-ray structure of the *E. coli* F_1-ATPase at 4.4 Å resolution [50], the departure from exact threefold symmetry was confirmed, in agreement with the Walker structure. The crystallization conditions used in this study employed a higher (5 mM) concentration of nucleotide, which is above the physiological level (~3 mM). Hence, the asymmetry of F_1 is not caused by an artificially low concentration of nucleotide as stated [27] but is an intrinsic property of the enzyme, as proposed [21], and as considered in the formulation of the torsional mechanism. Moreover, the crystallization medium employed for solving the Pedersen-Amzel structure contained 5 mM ATP but no Mg^{2+}, and these workers proposed that "Mg^{2+} binding to ATP in the β subunits causes no major conformational changes" [27], and that the main difference between the two structures, the presence of the closed conformation in the rat liver enzyme [27], could not be attributed to the absence of Mg^{2+}, as suggested [22]. According to the torsional mechanism [18], "Mg^{2+} is critical for the structure and mechanism, and, as shown and emphasized, Mg^{2+} has a crucial role in catalysis." We therefore could not conceive "how a closed catalytic site conformation can occur in the absence of Mg^{2+}" [18]. In fact, our argument implies that, since a closed conformation of the catalytic sites is indeed observed in the Pedersen-Amzel structure [27], Mg^{2+} *must* be present. Since no Mg^{2+} was contained externally in the crystallization medium, a possibility is that the Mg^{2+} may have been present internally in the rat liver enzyme source itself. A physiologically functional rat liver mitochondrial enzyme would be expected to contain enough Mg^{2+} to fill all sites. It is very interesting to note that the α subunits have been clearly shown to contain bound Mg^{2+} (Figs. 1, 5 of ref. 27) from careful analysis of the electron density in the Pedersen-Amzel X-ray structure. Thus, it can be inferred logically that the Mg^{2+} in the β subunits has originated from the same source (whatever that might be) that caused the α subunits of the rat liver enzyme to contain Mg^{2+}, as observed in the structure [27]. This point may be responsible for the confusion and controversy that has been expressed in the bioenergetics literature, and our interpretation would readily explain and reconcile various conflicting viewpoints, without disregarding any of the experimental facts, all of which, in our view, have the capacity to significantly contribute to our understanding of the molecular mechanism of ATP synthesis.

3.4.3.7
Site-Site Cooperativity in ATP Synthase

The molecular basis of site-site cooperativity in ATP synthase still remains unelucidated [46], and the absence of any direct evidence for cooperativity (despite almost three decades of effort) is explained, within the framework of the torsional mechanism, by the fact that site-site cooperativity does not exist in the physiological, steady state mode of functioning. Since, according to the torsional mechanism, no rotation takes place in uni-site or bi-site catalysis

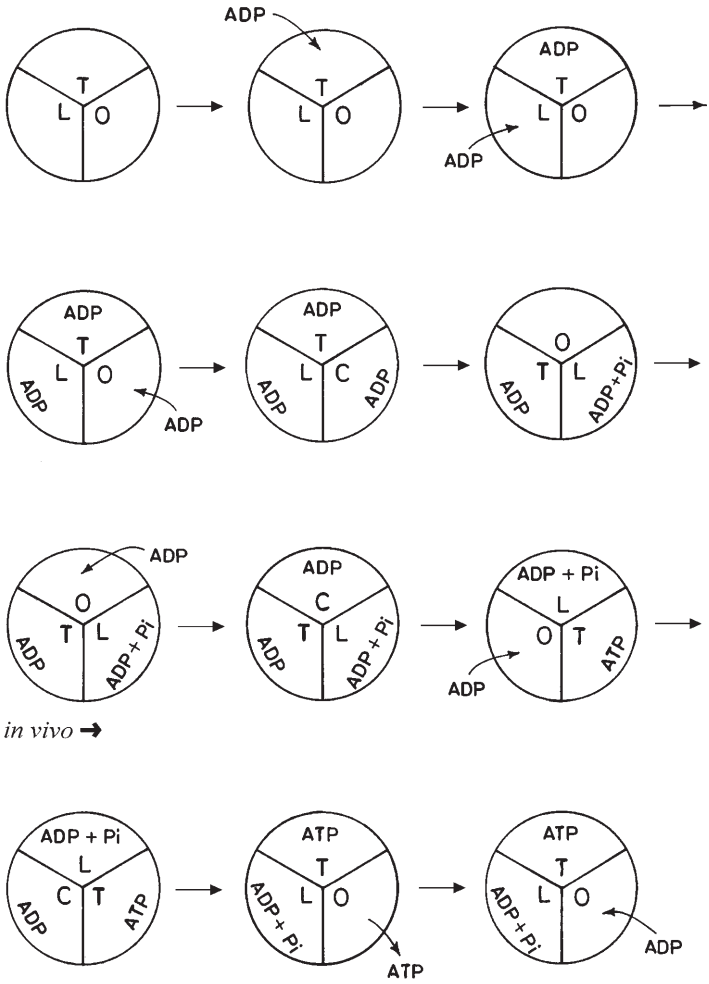

Fig. 9. Unsteady state start-up leading to physiological steady state operation of ATP synthase based on the torsional mechanism

modes of ATP synthesis, each substrate molecule enters and binds to the enzyme system that is in the same (unchanging) state in each catalytic cycle. Hence, there is no question of change in rate constant with substrate concentration in the physiological steady state mode of operation, and hence there can be no cooperativity in this mode of operation. The unsteady state (in vitro) filling up of the catalytic sites (start-up) and the progression to steady state operation are depicted in Fig. 9. Finally, the Michaellian nature of the results of our recent kinetic model of ATP synthesis based on the torsional mechanism (Eq. 11 of ref. 19 and Eq. 12 of ref. 20) clearly indicates the absence of site-site cooperativity during steady state ATP synthesis and suggests the presence of competitive inhibition of ATP synthase by product ATP as the inhibitor in the

synthesis mode. An important consequence of the competitive product inhibition is the order imposed on binding and release events, i.e., product release must precede substrate binding [19].

3.4.3.8 Irreversible Mode of Catalysis

In the kinetic scheme for ATP synthesis (Fig. 2 of ref. 19), if the catalytic steps resulting in the formation of E.ADP.P_i and E.ATP are made reversible with equilibrium constants K_r and K_r', mathematical analysis of this modified kinetic scheme leads to the result:

$$v_{syn} = k_t\,[ADP_{cy}\,(K_2K_rK_r'/K_1) - ATP_{cy}]/(1 + K_2K_rK_r'/K_1) \qquad (15)$$

which predicts a linear (and not hyperbolic) relationship between the rate of ATP synthesis and the substrate ADP concentration, which is not in agreement with the experimental observations [51, 52]. A similar result is obtained for the F_0 portion (Eq. 16), after similar modification of the kinetic scheme (Fig. 2 of ref. 20) to incorporate reversible catalysis.

$$v_{syn} = k_sk_t\,[H^+_{in}\,(K_rK_2/K_1) - H^+_{out}]/(1 + K_rK_2/K_1) \qquad (16)$$

Hence, the analysis reveals an irreversible mode of catalysis in both F_0 and F_1 portions of ATP synthase.

4 Further Insights into the Molecular Mechanism in the F_0 Portion of ATP Synthase

To reach a delocalized $\Delta\psi$ of ~200 mV for the macroscopic process of chemiosmotic coupling, Mitchell [8] estimated the charge transfer to be 0.8 μeq H^+/g protein in rat liver mitochondria. From classical data [53], 1 mg mitochondrial protein contains 7.2×10^9 mitochondria. To generate a delocalized $\Delta\psi$ of 120 mV, the number of protons transferred per mitochondrion is $\{0.8 \times (120/200) \times 10^{-9} \times 6 \times 10^{23}\}/7.2 \times 10^9 = 40{,}000$ H^+/mitochondrion. Thus, the creation of a macroscopic, delocalized electrical potential difference of 120 mV across the inner mitochondrial membrane (to maintain the thermodynamic potential needed for ATP synthesis) requires the transfer of 40,000 protons in each mitochondrion, i.e., of 3333 cycles of electron transfer! Transfer of only 2 e^- will create a negligible delocalized $\Delta\psi$ in Mitchell's chemiosmotic model. Hence, it may not be realistic to retain the analogy of the energy transduction process with a fuel cell [54]. In our conception, the ATP synthase should be viewed, not as a fuel cell, but as an enthalpic nonequilibrium molecular machine and mechano(electro)chemical transducer [17, 18]. Note that on taking the experimental value of 20,000 molecules per mitochondrion [53], we obtain a potential of 60 mV by translocation of one H^+ discretely, in perfect agreement with our value obtained by energy balance. Our proposed mechanism postulates that the energy supplied by translocation of each ion is due to transport of a charge

discretely irrespective of the rate of ion transport. The rate of ion transport itself is determined by the corresponding ion concentration gradient. Moreover, the commonly employed expression $RTln(I_{in}/I_{out})$ for any ion I is a measure of the total energy available to the system through that ion I; it does not represent the energy per ion of I translocated. If the ion concentration gradient is increased, the fraction of the enzyme complexes involved in ATP synthesis in its population and/or the rate of ion transport increases, and this is responsible for the experimentally observed increase in the rate of ATP synthesis with an increase in the ion concentration gradient. However, it should be emphasized that the energy obtained per ion translocated still remains the same.

The molecular mechanism and the kinetic model for the F_0 portion of ATP synthase show that ΔpH and $\Delta\psi$ are kinetically inequivalent driving forces for ATP synthesis [16, 20, 56]. This kinetic inequivalence has also been demonstrated by recent experiments [55]. $\Delta\mu_H$ cannot be taken as the true driving force for ATP synthesis. Inequivalence can also be seen from the fact that ΔpH and $\Delta\psi$ act at different elementary steps in our kinetic scheme [20, 56] as well as in our molecular mechanism [16, 20, 56]. Further, the diffusion potential generated as a result of diffusion of organic anions that are permeable to the membrane (e.g., succinate) (included in $\Delta\psi_{intrinsic}$, see Sect. 3.4) or that generated due to K^+-valinomycin transport ($\Delta\psi_{extrinsic}$) may be predicted to precede the translocation of protons along their concentration (pH) gradient. In such a situation, each component of the driving force, ΔpH and $\Delta\psi$, can alter the rate of ATP synthesis independently of each other. A possible cause of this inequivalence is the existence of a delocalized ΔpH and a localized $\Delta\psi$, as conceived originally by us, though our molecular mechanism applies irrespective of the source of this $\Delta\psi$, whether localized or delocalized. This inequivalence has further implications that have been analyzed in detail [56]. Since protons that have been transported across the membrane to the matrix are transported back to the inner membrane by the redox enzyme complexes, ΔpH is delocalized. Similarly, Δp anion is delocalized. The energy of the anion gradient is converted to a $\Delta\psi$; both the components of $\Delta\psi$ discussed here – $\Delta\psi_{intrinsic}$ and $\Delta\psi_{extrinsic}$ – are created in the vicinity of the ATP synthase enzyme complex, in which case the $\Delta\psi$ is a localized phenomenon. If this is the case, then it is incorrect to combine ΔpH and $\Delta\psi$ as is done in the definition of $\Delta\mu_H$. Also, a delocalized and a localized driving force cannot compensate for each other and have to be inequivalent. In such a situation, $\Delta\mu_H$ is a mathematically defined quantity that does not have any physical meaning.

A more detailed molecular mechanism incorporating the above concepts is represented diagramatically in Fig. 10. Possibilities include the electrogenic movement of protons, on one hand, and the movement of a proton (along its concentration gradient) following a negative interior potential created by diffusion along its concentration gradient of a permeant anion, or by K^+-valinomycin transport, on the other. The former will lead to a $\Delta(\Delta\psi)$ of ~60 mV per unbinding and binding step, while the latter will yield ~30 mV (due to the ΔpH across the inlet half-channel) + ~30 mV due to the $\Delta(\Delta\psi)$ caused by proton binding and a similar contribution from the exit half-channel, providing in all ~120 mV in both cases per proton translocated across the membrane

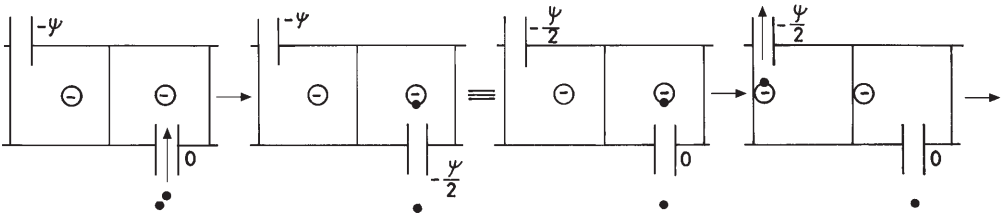

Fig. 10. Interaction of the ions with protein-in-the-membrane in the F_0 portion of ATP synthase. *Black dots* are protons; the negative charge represents the Asp-61 residue in the c subunit. ψ is 120 mV for the electrogenic case or 60 mV for the dynamically electrogenic, overall electroneutral case discussed in the text. In the left most panel, the $-\psi$ potential has been created either by the redox enzymes or by organic anions respectively. Following the rightmost arrow, a state is reached (not shown) when the entire potential has been discharged. This potential is re-created, and the cycle repeats

(Fig. 10). If respiration does not generate the delocalized $\Delta\psi$, then we strongly suggest consideration of the alternative, that the transport is dynamically electrogenic but electroneutral overall (i.e., transiently electrogenic, but electroneutral in the steady state). In such a situation, one cannot use the term "electrogenic" indiscriminately. Key sets of experiments to unambiguously distinguish between these possibilities need to be systematically designed and conducted.

Previous models of F_0 place the essential Asp-61 carboxyl group at the interface of the a and c subunits [30, 57, 58]. However, the protonated carboxyl in the membrane, in its resting state, is positioned at the center of four α-helices of two interacting c subunits [59, 60]. In our view, the ε subunit and the bottom of the γ subunit do not move simultaneously with c; rather, movement of the latter precedes that of the former. As c rotates by 15° due to ion binding, the helices rotate and tilt, and the ion-protein interaction energy is stored as twist in the α-helices of the 10 membrane-embedded c subunits. The polar residues of c that are interacting with the γ subunit remain more or less stationary, and the bottom of the c subunits move by 15°, thereby bringing the Asp-61 residues of all the c subunits to the periphery. The H^+ in the membrane cannot exit, and the helices of the ten c subunits, present in their high energy state, will almost instantaneously untwist and return to their resting state. This impulse moves the polar residues by 15° thereby causing the c subunits to straighten.

The electrostatic interactions between the polar residues of these c subunits and the γ subunit causes the bottom of the γ subunit to rotate by 15°. Exposure of residues of the new c subunit to the aqueous medium at the a-c interface (helped by the bend in the C-terminal helix beyond Pro-64) and non-exposure of the helical face due to the excessive energy penalty in hydrating the hydrophobic residues such as Val-74, Met-75, or Phe-76 ensures that this tilted C-terminal helix of the c subunit is not allowed to untwist. The protonated Asp-61 lying in the middle of the helix is still not at the a-c interface; movement of the bottom of the γ subunit forces this new trailing c subunit to straighten and expose the proton to the interface. The H^+ exposed at the a-c interface now unbinds, rotates c, and the cycle of energy storage and release continues (Figs. 11, 12). In

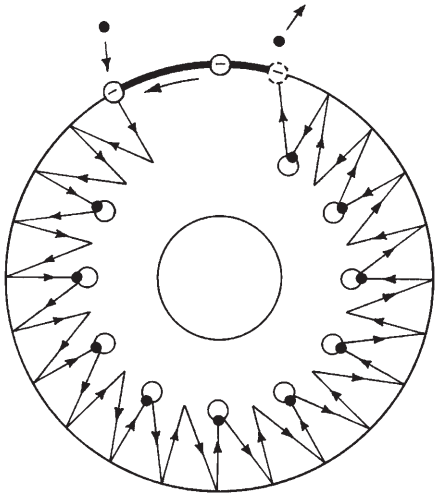

Fig. 11. Proposed schematic representation of the swiveling movement of helices in the F_0 portion of ATP synthase. Since deprotonation of the Asp-61 residue can only occur at the periphery of the c-rotor at the a-c interface, twisting and swiveling of the helices composing the c subunits is caused by the rotation of the c-rotor. Since all protonated c subunits are identical, untwisted (protonated) c subunit helices should twist when the c-rotor rotates as a result of proton binding and unbinding during ATP synthesis

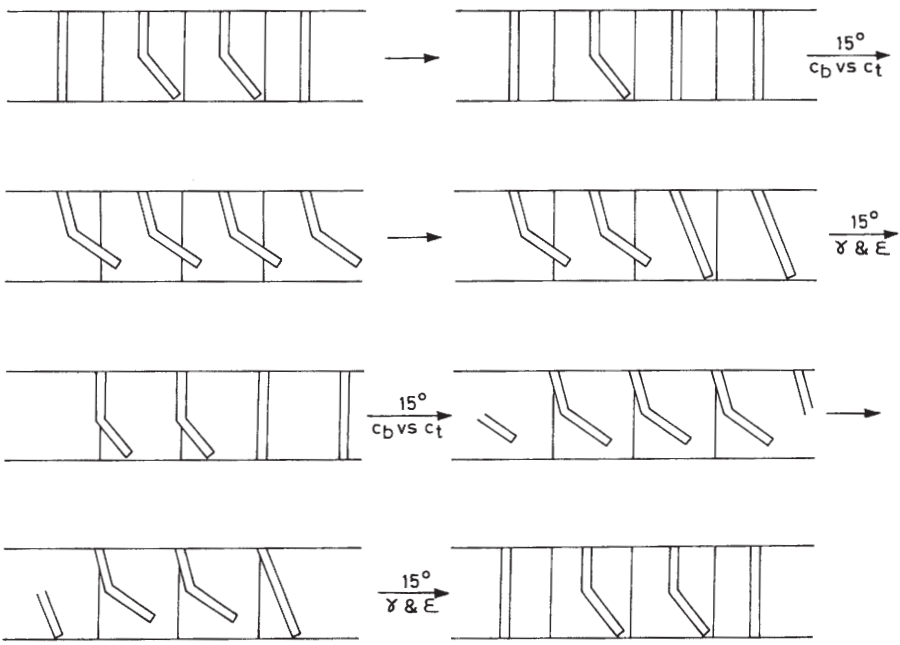

Fig. 12. *Legend see page 92*

Fig. 12. Details of the torsional mechanism within F_0. The c subunits facing the a subunit are twisted and bent, while the remaining ten c subunits inside the membranous region being protonated, are untwisted, i.e. in their normal/resting state for the protonated Asp residues which lie in the interior of the c-rotor. In this state, the exposed Asp residues interact with the charges on the a-stator, and the system is in a local equilibrium (Fig. 4). When the incoming proton, which is transported along its concentration gradient, through the proton half channel facing the inner membrane (or outside) binds to the leading Asp-61 residue, the leading c subunit immediately attains an untwisted conformation characteristic of a protonated c subunit, and the now-protonated Asp-61 residue moves towards the center of the c-rotor. This alters the electrostatic interactions in the system and in order to attain a new local equilibrium state, the c-rotor rotates by 15°. As a result of this 15° rotation of the c-rotor, all the protonated c subunits get twisted and bent, keeping the polar residues of the c subunits, which are in contact with the bottom of the γ subunit, stationary while the bottom of the c subunits move by a full 15° displacement thereby bringing all the Asp-61 residues to the periphery of the c-rotor. However, since this state is a metastable high-energy state for all the eleven *protonated* c subunits, all these c subunits except the new, incoming c subunit untwist simultaneously carrying all the Asp-61 residues of the ten protonated c subunits inside. The impulse thus created moves the polar residues of these ten protonated and untwisted c subunits by 15°, thereby causing these c subunits to straighten (untilt). The electrostatic interactions between the polar residues of these ten c subunits and the γ subunit cause the bottom of the γ subunit to rotate by 15°. Hence, the energy released during the proton binding step is transiently stored as strain energy in the c subunits as twist and is later stored as strain energy in the γ subunit as torsion. The final state of the F_0 portion attained after the 15° rotation has the c subunit immediately before the trailing c subunit at the interface of the membranous and the non-membranous region, and the leading c subunit at the other interface. The *Escherichia coli* c subunit contains a Pro-64 and a series of hydrophobic residues toward the end of the C-terminal helix. The portion of the C-terminal helix beyond Pro-64 bends such that the new, incoming trailing c subunit has part of the c subunit protruding out of the membranous region, with the rest of the helix still inside the membranous region. The twist causes the hydrophobic residues to face the N-terminal helix and keeps them away from the aqueous medium. When the remaining ten protonated c subunits untwist to release the strain, this c subunit is unable to do so, as this would require the hydrophobic residues to be in direct contact with the aqueous medium, which is energetically highly unfavorable. The untwisting of the ten c subunits drives the rotation of the bottom of the γ subunit by 15°; rotation of the bottom of the γ subunit forces this new, trailing c subunit to straighten. The straightening of this new, trailing c subunit brings its Asp-61 residue to the a-c interface. This Asp-61 residue then loses its proton to the matrix (or inside) through the exit half-channel to become unprotonated. The deprotonation of this Asp-61 residue keeps the already twisted c subunit in the same conformation characteristic of the unprotonated c subunit. The change in the electrostatics of the system again results in a rotation of the c-rotor by 15° in order to attain a new local equilibrium position. As a result of this 15° rotation, all the protonated and therefore untwisted c-subunits get twisted and tilted (keeping the polar residues and the γ subunit stationary), thereby bringing their Asp-61 residues to the periphery of the c-rotor. As this state is a high-energy state for all the ten protonated c subunits, they untwist, and the impulse created causes these protonated c subunits to untilt by moving their polar residues by 15°. The movement of the polar residues causes the bottom of the γ subunit to rotate by an equal 15° angular displacement. The ε subunit interacts with the bottom of the γ subunit and the polar residues of the c subunits, and therefore the ε subunit rotates together with the bottom of the γ subunit. In this way, each proton translocation drives the rotation of the ε subunit and the bottom of the γ subunit by 30° (in two steps of 15° each) and the consequent storage of energy as torsional strain in the γ subunit. The final state of the system after these elementary steps is the same as the initial state, i.e. with both the Asp-61 residues facing the a-stator unprotonated, except that the ε subunit and the bottom of the γ shaft have rotated by 30° relative to the initial state.

this schematic representation, the need for dynamic cyclical changes in protein structure in membrane-bound F_0 is emphasized. Thus, the energy transduction processes can be represented as the energy of ion-protein interactions getting converted [via $\Delta(\Delta\psi)$] to twist in the c-subunit helices, which is converted to torsional energy in γ, and thereafter to the chemical energy of ATP by ATP synthase.

5 Thermodynamic Analysis of Molecular Mechanisms for ATP Synthesis

An extensive study is needed to understand the energetics of coupling in the F_0 portion of ATP synthase. ATP synthesis has been demonstrated with the enzyme molecule isolated, purified, and reconstituted into liposomes, which do not contain any redox complexes [49, 51, 55]. Therefore, either $\Delta\psi$ is not created, or it is created in the vicinity of the ATP synthase enzyme complex, i. e., $\Delta\psi$ is localized. Since ΔpH supplies only half the energy requirement for mitochondrial ATP synthase, the rest has to be supplied by a locally present but independent source of $\Delta\psi$. One possible explanation suggested by several research groups is electroneutral transport of ions [61–64]; however, we postulate a dynamically electrogenic but overall electroneutral ion transport involving membrane-permeable anions (such as succinate), and protons, as discussed. In this way, through cation binding *within* the electrostatic potential field created by the transport of anions, the enzyme is able to utilize the energy of both the delocalized ΔpH and the localized $\Delta\psi$.

When the K^+-valinomycin system is used, the H^+ moves *following* K^+ transport (antisequenceport), and, therefore, as the concentration of K^+-valinomycin is increased, H^+ transport increases and the rate of ATP synthesis correspondingly increases. However, when the K^+ transport attains a maximum limit upon saturation, the rate of ATP synthesis also becomes constant. This is in complete agreement with the experimental observations that the K^+/ATP ratio increases with an increase in K^+ concentration and becomes constant at 4 for very high concentrations of K^+ [61, 62]. The dynamically electrogenic but overall electroneutral ion transport implies that, if the transmembrane potential ($\Delta\psi$) is measured with nano/microelectrodes, the potential should be close to zero, as found by direct measurements on giant mitochondria [63, 64]. The anion and the proton are transported back to the outside against the concentration gradients by the redox complexes, thereby storing the energy of oxidative phosphorylation as proton and anion gradients. In this context, we predict that complex II in the respiratory chain (succinate ubiquinone oxidoreductase) transports anions against the concentration gradient and thus plays a key role in energy coupling.

5.1 Mechanistic P/O Stoichiometry in Oxidative Phosphorylation

The question of mechanistic P/O stoichiometries has been the subject of extensive studies for over 50 years [65, 66]; yet it remains an unresolved issue [67]. To address this aspect, we consider the dynamically electrogenic but overall electroneutral ion transport for the complete process of oxidative phosphorylation in mitochondria. ATP synthesis is regulated by its demand for various cellular processes; when ATP^{4-} is required, it is transported out from the matrix to the cytoplasm along its concentration gradient. The electrical potential thus created drives ADP^{3-} along its concentration gradient to the mitochondrial matrix in exchange for ATP^{4-} by the adenine nucleotide transporter. The resulting unbalanced potential causes HPO_4^{2-} to move into the matrix, and the OH^- produced during ATP synthesis in the F_1 portion of ATP synthase [18, 68] is driven out of the mitochondria in exchange for the HPO_4^{2-} by the HPO_4^{2-}/OH^- antiporter. The OH^- released per ATP produced is neutralized by a proton from the external medium, forming water. Thus, we need four protons to synthesize one molecule of ATP and one proton to neutralize the released OH^-, i. e., 5 H^+/ATP overall. In each cycle of oxidative phosphorylation, twelve protons are pumped out by the redox complexes with NADH-related substrates such as 3-hydroxybutyrate, and eight protons are transported from the matrix to the inner membrane against the concentration gradient with succinate as substrate. This implies that the mechanistic P/O ratio equals 12/5 (= 2.4) and 8/5 (= 1.6) for 3-hydroxybutyrate and succinate, respectively, for the *overall* oxidative phosphorylation process. This P/O ratio corresponds to the physiological steady state mode of operation. However, if only the *coupling* between the redox complexes and ATP synthase is considered, then the mechanistic P/O ratio equals 12/4 (= 3) and 8/4 (= 2) for 3-hydroxybutyrate and succinate, respectively [41, 42]. The experimentally observed P/O ratio will be lower than the mechanistic P/O due to the presence of proton leak through the membrane, as found [42, 69, 70]. It is worthwhile to note that if unsteady state experiments (pulse mode experiments) are carried out, the observed P/O ratios will depend on the time of incubation with 2.4 (complete neutralization of OH^-) and 3.0 (no neutralization of OH^-) as the theoretical lower and upper limits (without considering proton leaks). Thus, if the system is incubated for short durations (<1 min), all the OH^- released by the *population* of the ATP synthase molecules will not be neutralized by H^+, and the observed P/O ratio will be higher than that observed for steady state operation or for systems incubated for long durations (>2 min). According to the above analysis, the observed P/O (or J_P/J_O) should show a continuously decreasing trend with time during the state 3 to state 4 transition due to the progressive neutralization by protons of the hydroxyl ions released into the external medium. This is in complete agreement with classical experimental data recorded by Slater and colleagues for respiring mitochondria [69]. The consistently observed increase in the magnitude of the phosphorylation affinity (A_P) with time [69] during the state 3 to state 4 transition is explained by the progress of the system from the initial unsteady state non-optimal operation to its steady state optimal operation. The decrease of the P/O ratio with increase in (the magni-

tude) of A_P agrees with the nonequilibrium thermodynamic analysis of oxidative phosphorylation also [42]. In a systematic experimental investigation of mechanistic P/O ratios for mitochondrial oxidative phosphorylation [70], long incubation times of 4.5 min led to the lower values of the P/O stoichiometries of 2.27 for 3-hydroxybutyrate and 1.48 for succinate as substrate, as predicted by our analysis above. The same analysis can also be employed to explain the variation in observed P/O ratios with successive additions of substrate ADP to mitochondria [71]. In this study, for pyruvate + malate as substrates, P/O ratios as high as 3 and 2.6 were observed in the presence of EDTA and $MgCl_2$, respectively, for short incubation times of less than 60 s. The observed decrease in the P/O ratios (from 3.01 to 2.87 and from 2.58 to 2.51) occurs due to un-neutralized OH^- remaining in the medium from the previous incubation. The longer incubation time during the second incubation (e.g. ~100 s instead of ~50 s for the EDTA case and ~75 s instead of ~50 s for $MgCl_2$) step led to partial neutralization of the OH^- remaining in the medium from the first and the second incubation steps, which was reflected in a slight increase (2.87 to 2.91 for EDTA) or a constant value (2.51 for $MgCl_2$) of the P/O ratio during the third incubation step. Our mechanistic stoichiometry is also in agreement with experimental studies carried out by the engineering community [72].

One view to explain different P/O ratios for different classes of organisms is to consider variability in both the molecular mechanism as well as the stoichiometry of proton transport and ATP synthesis with the source of the enzyme [67]. However, considering our molecular mechanism and the energetics of the oxidative phosphorylation process, we believe that a universality in the mechanistic, kinetic and thermodynamic characteristics of the system is operative.

Since the phosphate potential ($x = A_P/A_O$) can be looked at as the fraction of the oxidative phosphorylation energy for synthesizing each ATP molecule, x can be taken as 1/3 and 1/2 for 3-hydroxybutyrate and succinate, respectively, which is in accordance with the experimental measurements for the state 3 phosphate potential in rat liver mitochondria [73, 74]. Hence, for short incubation times, the mechanistic stoichiometry in the absence of proton leak, Z, equals 3 for 3-hydroxybutyrate, which corresponds to a degree of coupling, q, of 0.982 [42, 73] or $n = 5$ [73], which implies that the system optimizes output power, efficiency, and developed phosphate potential. On the other hand, for steady state operation or for long incubation times, Z equals 2.4 for 3-hydroxybutyrate which corresponds to a q of 0.986 or $n = 6$, which implies that the system optimizes output power, efficiency, and developed phosphate potentials due to protons as well as anions. The occurrence of $n = 6$ for steady state operation, which is the physiological mode of operation, supports the dynamically electrogenic but overall electroneutral ion transport discussed in the previous section. Hence, knowledge of the underlying molecular mechanism of ion translocation permits the assessment of the final mechanistic stoichiometries for the oxidative phosphorylation process.

6
Molecular Physiological Engineering: a New Frontier

The cell can be considered as a complex network of interacting molecular machines. Traditionally, molecular and cellular processes have been studied by biochemists, microbiologists and molecular biologists, with virtually no input of engineering knowledge. Our research of the past 10 years unambiguously demonstrates that the *in vivo* dynamic, nonequilibrium mode of operation of biological molecular machines cannot be understood without the application of the principles of thermodynamics, kinetics and transport. The key effects of elastic strain in molecular energy conversion processes cannot be quantitatively described without a sound knowledge of mechanics and dynamics. The application of engineering tools to biology and physiology at the *molecular* level has led to the development of a new field that I have called "Molecular Physiological Engineering" [15]. Storage of energy within a single molecule (as internal energy) plays a central role in the torsional mechanism of ATP synthesis. Energy storage within single molecules, and its subsequent utilization, via specific mechanisms of the type proposed and detailed in earlier papers and in this work may prove to be one of the great unifying principles of biology: in photo- and oxidative phosphorylation, muscle contraction and other related energy transductions. These properties make the above topics very attractive for contemporary interdisciplinary research. Finally, in our view, the aspects dealt with in this work constitute the key elements whose lack of detailed consideration has held back the progress of research in this important field. Thus, it is well known (and generally accepted) that science is indispensable to engineering; however, our research shows that *engineering is also indispensable to science, to fundamental science*, and this indispensability will, in my opinion, manifest itself even more poignantly in this century as biology becomes increasingly dominated by computation.

Acknowledgement. I am much indebted to my students H. Rohatgi, A. Saha and S. Jain who have greatly contributed to bring our knowledge of the torsional mechanism to this point; their names are to be found in most of our papers on this subject. I thank Dr. N. Pant, in whose classes I sat as a student over many years, for teaching me so much. It is a pleasure to acknowledge Prof. W.-D. Deckwer's continual encouragement of our approach to bioenergetics. I thank Profs. P. Balaram and M. Saraste for their real help as editors, and Profs. E. H. Battley and L. D. Hansen for their faith in me. I am grateful to the Department of Science and Technology, India, and the All-India Council of Technical Education for funding my research. I am deeply indebted to my father, Prof. M.V. Ranganath for all that he has given me.

References

1. Fiske CH, SubbaRow Y (1929) Science 70:381
2. Lohmann K (1929) Naturwissenschaften 17:624
3. Lipmann F (1941) Adv Enzymol 1:99
4. Penefsky HS, Pullman ME, Datta A, Racker E (1960) J Biol Chem 235:3330
5. Boyer PD (1998) Angew Chem Int Ed Engl 37:2296
6. Slater EC (1953) Nature 172:975
7. Mitchell P (1961) Nature 191:144

8. Mitchell P (1966) Biol Rev 41:445
9. Williams RJP (1961) J Theor Biol 1:1
10. Williams RJP (1962) J Theor Biol 3:209
11. Boyer PD (1965) In: King TE, Mason HS, Morrison M (eds) Oxidases and related redox systems. Wiley, New York, p 994
12. Boyer PD, Cross RL, Momsen W (1973) Proc Natl Acad Sci USA 70:2837
13. Boyer PD (1993) Biochim Biophys Acta 1140:215
14. Cross RL, Duncan TM (1996) J Bioenerg Biomembr 28:403
15. Nath S (2000) Molecular Physiological Engineering: A New Frontier. 41st Annual Conference of the Association of Microbiologists of India, Jaipur, India, p 3
16. Rohatgi H, Saha A, Nath S (1998) Curr Sci 75:716; erratum (2000) 78:201
17. Nath S, Rohatgi H, Saha A (1999) Curr Sci 77:167
18. Nath S, Rohatgi H, Saha A (2000) Curr Sci 78:23
19. Nath S, Jain S (2000) Biochem Biophys Res Commun 272:629
20. Jain S, Nath S (2000) FEBS Lett 476:113
21. Abrahams JP, Leslie AGW, Lutter R, Walker JE (1994) Nature 370:621
22. Boyer PD (1997) Annu Rev Biochem 66:717
23. Ramasarma T (1998) Curr Sci 74:953
24. Nakamoto RK, Ketchum CJ, Al-Shawi MK (1999) Annu Rev Biophys Biomol Struct 28:205
25. Allison WS (1998) Acc Chem Res 31:819
26. Fillingame RH, Jiang W, Dmitriev OY, Jones PC (2000) Biochim Biophys Acta 1458:387.
27. Bianchet MA, Hullihen J, Pedersen PL, Amzel LM (1998) Proc Natl Acad Sci USA 95:11065.
28. Weber J, Senior AE (1997) Biochim Biophys Acta 1319:19
29. Wilkens S, Capaldi RA (1998) Nature 393:29.
30. Zhou Y, Duncan TM, Cross RL (1997) Proc Natl Acad Sci USA 94:10583
31. Ogilvie I, Aggeler R, Capaldi RA (1997) J Biol Chem 272:16652
32. Sabbert D, Engelbrecht S, Junge W (1996) Nature 381:623
33. Sabbert D, Junge W (1997) Proc Natl Acad Sci USA 94:2312
34. Noji H, Yasuda R, Yoshida M, Kinosita K (1997) Nature 386:299
35. Yasuda R, Noji H, Kinosita K, Yoshida M (1998) Cell 93:1117
36. Shirakihara Y, Leslie AGW, Abrahams JP, Walker JE, Ueda T, Sekimoto Y, Kambara M, Saika K, Kagawa Y, Yoshida M (1997) Structure 5:825
37. Boyer PD (2000) Biochim Biophys Acta 1458:252
38. Löbau S, Weber J, Senior AE (1998) Biochemistry 37:10846
39. Hatefi Y (1993) Eur J Biochem 218:759
39a. Menz RI, Walker JE, Leslie AGW (2001) Cell 106:331
40. Adachi K, Yasuda R, Noji H, Itoh H, Harada Y, Yoshida M, Kinosita K (2000) Proc Natl Acad Sci USA 97:7243
41. Nath S (1994) A fundamental thermodynamic principle for coupling in oxidative phosphorylation. 16th Int Congr Biochemistry and Molecular Biology, New Delhi, India, vol II, p 390
42. Nath S (1998) Pure Appl Chem 70:639
43. Weber J, Senior AE (2000) Biochim Biophys Acta 1458:300
44. Garcia JJ, Capaldi RA (1998) J Biol Chem 273:15940
45. Böttcher B, Gräber P (2000) Biochim Biophys Acta 1458:404
46. Senior AE, Nadanaciva S, Weber J (2000) J Exp Biol 203:35
47. Al-Shawi MK, Ketchum CJ, Nakamoto RK (1997) Biochemistry 36:12961
48. Grubmeyer C, Cross RL, Penefsky HS (1982) J Biol Chem 257:12092
49. Fischer S, Gräber P (1999) FEBS Lett 457:327
50. Hausrath AC, Grüber G, Matthews BW, Capaldi RA (1999) Proc Natl Acad Sci USA 96:13697
51. Possmayer FP, Gräber P (1994) J Biol Chem 269:1896
52. Pänke O, Rumberg B (1996) FEBS Lett 383:196
53. Estabrook W, Holowinski A (1960) J Biophys Biochem Cyt 9:19
54. Mitchell P (1979) Science 206:1148

55. Kaim G, Dimroth P (1999) EMBO J 18:4118
56. Jain S, Nath S (2001) Thermochim Acta 378:35
57. Elston T, Wang H, Oster G (1998) Nature 391:510
58. Vik SB, Antonio BJ (1994) J Biol Chem 269:30364
59. Dmitriev OY, Jones PC, Fillingame RH (1999) Proc Natl Acad Sci USA 96:7785
60. Rastogi VK, Girvin ME (1999) Nature 402:263
61. Massari S, Azzone GF (1970) Eur J Biochem 12:301
62. Azzone GF, Massari S (1971) Eur J Biochem 19:97
63. Tedeschi H (1975) FEBS Lett 59:1
64. Tupper JT, Tedeschi H (1969) Science 166:1539
65. Ochoa S (1943) J Biol Chem 151:493
66. Ernster L (1993) FASEB J 7:1520
67. Ferguson SJ (2000) Curr Biol 10:R804
68. Lodish H, Berk A, Zipursky SL, Matsudaira P, Baltimore D, Darnell J (2000) Molecular cell biology, 4th edn. W.H. Freeman, New York, p 647
69. Slater EC, Rosing J, Mol A (1973) Biochim Biophys Acta 292:534
70. Hinkle PC, Kumar MA, Resetar A, Harris DL (1991) Biochemistry 30:3576
71. Lee CP, Gu Q, Xiong Y, Mitchell RA, Ernster L (1996) FASEB J 10:345
72. Zeng AP, Ross A, Deckwer W-D (1990) Biotechnol Bioeng 36:965
73. Stucki JW (1980) Eur J Biochem 109:269
74. Lemasters JJ (1984) J Biol Chem 259:13123

Received: April 2001

Bioreactor Developments for Tissue Engineering Applications by the Example of the Bioartificial Liver

Inka Jasmund[1], Augustinus Bader[1,2]

[1] Experimental Radiology, Hepatic Tissue Engineering, Medical School Hannover, Carl-Neuberg-Str. 1, 30625 Hannover, Germany
E-mail: jasmund.inka@mh-hannover.de
[2] National Research Institute for Biotechnology (GBF), Mascheroder Weg 1B, 38124 Braunschweig, Germany
E-mail: Augustinus.Bader@t-online.de, Augustinus.Bader@GBF.de

Dedicated to Prof. Dr. Wolf-Dieter Deckwer on the occasion of his 60th birthday

Tissue engineering is the application of the principles and methods of engineering and the life sciences towards the development of biological substitutes to restore, maintain or improve functions. It is an area which is emerging in importance worldwide. This article is to show the developments in tissue engineering research by the example of the bioartificial liver. As an alternative to liver transplantation, numerous researchers have been working towards the goal of development of a fully functional artificial liver. Liver support systems based on detoxification alone have proven ineffective because they cannot correct biochemical disorders. An effective artificial liver support system should be capable of carrying out the liver's essential processes, such as synthetic and metabolic functions, detoxification, and excretion. It should be capable of sustaining patients with fulminant hepatic failure and preparing patients for liver transplantation when a donor liver is not readily available. Although several hepatocyte-based liver support systems have been proposed, there is no current consensus on its eventual design configuration.

Keywords. Bioartificial liver, cell culture, hollow fiber bioreactor, flat membrane bioreactor, spheroids

Advances in Biochemical Engineering/
Biotechnology, Vol. 74
Managing Editor: Th. Scheper

1 Introduction

Health care for patients with tissue loss or end-stage organ failure is becoming increasingly expensive. For example the estimated costs in the U.S. for such patients exceed $400 billion p.a. [1]. Transplantation is severely limited by a critical donor shortage, and as a consequence, there has been a rapidly growing interest in the field of tissue engineering - the manufacture of biological substitutes that can restore, maintain or improve tissue function. Tissue engineering offers the possibility of substantial future savings in health care budgets by providing substitutes that are more cost efficient than donor organ transplantations, are life saving, or provide the means of intervention before patients become critically ill.

In the past product development regarding the engineering of hybrid tissues using all cells in an hierarchical and tissue specific arrangement has been plagued by a shortage of bioreactors that could fulfill these expectations. In addition, storage, handling and applications in a clinical environment pose significant hurdles, as live tissues cannot be easily shipped. In contrast, prohibitive costs and time dependent dedifferentiation or infection risks are looming logistical obstacles at present to the shipment of viable artificial organs.

One of the key problems in the in vitro engineering of transplantable bioartificial tissues is the lack of a bioreactor and corresponding bioengineering technology that could solve such limitations [2]. Primary cells need a lead structure supplied in a bioreactor to grow on, no matter what the targeted structure is, it has to provide a unique 3-D matrix structure. The bioreactor should act as a containment, a GMP compatible production unit, and preferably as a transport device with cryostorage capacity. Currently available bioreactor devices cannot fulfill these requirements due to design limitations.

Current technologies do not permit the generation of a full liver in vitro, and full bioartificial organ transplantation still remains an unrealistic dream. As shown previously by Nyberg et al. endogenous retroviruses from animals such as PERV might be transmitted as well [3]. In this context the development of a bioreactor technology to grow organs or parts thereof in vitro represents a clean and working alternative to both, the use of animals as living bioreactors for human embryonal cells and xenotransplantation. Probably, the generated tissue interacts with the human host, i.e. the recipient after transplantation or extracorporeal contact. The extracorporeal liver induces liver regeneration and thus transplantation is not required.

With the goal of mimicking the cellular environment of the native organ, it is fair to assume that pure monolayer cultures are not suitable to reproduce the necessary conditions to induce and maintain differentiation and function of a complex organ [4]. A detailed analysis of the fundamental conditions is therefore necessary to distinguish between a microenvironment that is in a way rather artificial such as the monolayer culture, and a more organotypical 3D situation that contributes to the signal pattern necessary to induce the expression of specific cellular functions. Only with this knowledge, a tissue-like culture device can be constructed and improved to potentially serve as a bioartifi-

cial organ that might be used not only in basic research but also for therapeutic purposes such as artificial organ support.

2 State of the Art

There have already been clinical trials of porcine hepatocyte-based bioartificial livers [5, 6]. However, we believe these systems to represent temporary and short-lived approaches. Compelling evidence from recent experiments show that primary porcine liver cells express and release endogenous retroviral particles that are able to infect human cells. However, long term in vivo investigations of patients previously exposed to porcine tissues over a period of 12 year did not show any porcine endogenous retrovirus (PERV) viremia [7]. Therefore, we consider the further pursuit of porcine bioartificial livers the only solution at present with regard to the cell source. However, as an intermediate term alternative human cell sources are in development [8]. Expansion technologies for human fetal cells may contribute to resolve these limitations in the future.

Hepatocyte-based bioartificial livers will have two major uses: to provide a) short term support for liver-failure patients in the clinic and b) a tool for the pharmaceutical industry to produce drug metabolites for subsequent toxicological studies in vitro.

To be useful to both, clinicians and the pharmaceutical industry, a bioartificial liver will need to maintain a large number of hepatocytes at high cell densities and in a fully differentiated state for prolonged periods of time. Development of such a system has been impeded by three principal problems: a) a requirement for large numbers of cells ($>25 \cdot 10^9$); b) loss of liver-specific functions in cultured cells (primary and immortalized); c) nutrient and waste product gradients in high density cultures leading to lowered cell viability and impaired function.

There is a general consensus that human life can be sustained with 10% of normal liver mass [9] or estimated $25 \cdot 10^9$ cells. Therefore, in constructing a bioartificial liver there is an enormous requirement for functional hepatocytes. The use of primary human hepatocytes is limited by the scarcity of human liver tissue and by their poor proliferative potential. Currently available cell lines are limited in that they only display a limited repertoire of liver-specific functions and furthermore, like primary cells, may also lose these during prolonged periods in culture. There is, therefore, a pressing need to develop new human liver cell bioreactor technologies which provide a good proliferative potential and maintain a broad spectrum of liver-specific functions during cultivation time. A new approach is to develop immortalized cell lines by deriving them from human fetal liver cells. These can then be expanded in culture to give the large number of cells required to produce a functional bioartificial liver.

A bioartificial liver will need to maintain a large number of hepatocytes at high cell densities over a prolonged period of time. The metabolic requirements of hepatocytes, particularly the high rates of oxygen consumption, place strin-

gent demands on the bioreactor system. This problem is exacerbated if the cells are maintained in a 3D matrix, since the matrix material can represent a significant diffusion barrier for nutrients, especially oxygen. Intensive reactor systems are intrinsically inaccessible to conventional monitoring techniques and therefore improvements in design and operation of these systems require new non-invasive methods for assessing reactor performance. A successful bioartificial liver will need to maintain a broad spectrum of liver-specific activities.

3 Types of Hepatocytes

Generally there are two approaches in the incorporation of cells in bioreactors for liver support. One is the use of cell lines [10]. The other is to isolate and use primary hepatocytes from animal livers [11] or human livers [12].

3.1 Cell Lines

Cell lines established from human liver cancer cells can be derived from primary hepatocellular carcinoma or hepatoblastoma cells [10]. For example, the well known HepG2 line was derived from hepatoblastoma cells. Such cells can be employed effectively if the function of normal liver cells has been highly preserved. In practice, however, such cells contain a high proportion of abnormal genetic component, which inhibits their ability to express normal protein synthesis and enzyme activity. Potential problems, such as the loss of liver specific functions and the possibility of metastasis, which could arise from the use of hepatoma cells have not yet been satisfactorily discussed [13].

Artificially immortalized human liver cells would be an ideal source if genetic engineering or other methods could be used to imbue the cells with the highly differentiated functions and proliferative capacity observed in normal cells. At present, cultures of such immortalized cells have not demonstrated long-term viability and the hepatocyte-specific characteristics, such as albumin secretion, disappear quickly. In addition, these cells suffer from a high incidence of malignant change and dedifferentiation. A promising new cell line (HepZ) was created by Werner et al. [14]. The cell line was immortalized through transfection of albumin-promotor-regulated antisense constructions against the negative controlling cell cycle proteins Rb and p53. Furthermore, plasmids including genes coding for the cellular transcription factor E2F and D1 cyclin were cotransfected to overcome the G1-restriction point. The cell line HepZ retains liver-specific functions and is appropriate for a mass cell cultivation. Further investigations have to show whether the biochemical spectrum is sufficient. Research continues to be carried out in this field, however, and promising results are expected in the future [13].

3.2
Primary Hepatocytes

Freshly isolated hepatocytes can be obtained from animal or human liver. Hepatocytes taken from these sources, however, are very vulnerable to contamination and technically difficult to preserve in a fresh state. Although it is not generally possible until now to proliferate human hepatocytes in vitro, the advantages of homology and human-specific functions demand that resources continue to be directed towards the elucidation of the conditions necessary for maintaining viable human hepatocyte cultures.

Methods of collagenase perfusion for hepatocyte isolation were developed on rat livers [15, 16]. Berry and Friend [15] made first experiments with collagenase-perfusion in rats, essentially comprising three processes: exposure to a medium very low in Ca^{2+}, digestion with collagenase, and gentle mechanical disruption. The two-step procedure [16, 17] was introduced by Seglen as a consequence of his studies of the effects of Ca^{2+} and collagenase on the isolated perfused liver. The essential feature of the two-step approach is that the liver is first flushed with Ca^{2+}-free medium after which the perfusion medium is changed to one containing Ca^{2+} and collagenase. This method achieves a good viability and yield in rats.

Because of the need for isolation techniques applicable to other species, Hoogenboom et al [18] investigated the isolation of hepatocytes from porcine livers and developed an enzymatic method with closed-loop and open-loop perfusion stages for the perfusion of liver lobes. We investigated a method to perfuse the whole organ to receive a great amount of liver cells (up to $25 \cdot 10^9$ cells per pig liver) and a viability higher than 90%.

4
Bioreactor Design

The cultivation of hepatocytes in a stationary suspension culture is actually ineffective. The hepatocytes lose their differentiation within hours. An improvement was the attachment culture. Thereby, the cells are cultivated either in self- or microcarrier-induced multicellular aggregates or on membranes. When standard monolayer culture was adequate to maintain the cell viability for 1 to 2 weeks the differentiation was lost after a few days. Different modifications as described beneath allowed the maintenance of differentiation for 2 to 3 weeks.

4.1
Spheroids

It has become increasingly evident that three dimensional rather than monolayer growth is particularly important for maintaining differentiated hepatocyte function in culture. One means of establishing three dimensional hepatocyte growth is the creation of multicellular spheroid aggregates. Sakai et al. have shown that multicellular spheroids can be rapidly created by rotational culture systems [19, 20] or by incubation with a small number of collagen-coated dextran, polystyrene or glass microcarriers as a center for cell aggregation [21].

Naruse et al. proposed another bioreactor design [22, 23], in which porcine hepatocyte spheroids are immobilized on non-woven polyester fabric. This device allows more direct contact between hepatocytes and perfused medium and improves, therefore, the mass transfer capacity. The non-woven fabric module expressed better metabolic and synthetic functions at 24 hours than a hollow fiber module containing spheroids in suspension culture. Longer term results are not yet available and the immunoexclusion properties of this fabric have not been addressed.

Isolated rat hepatocytes were immobilized in cellulose multiporous microcarriers by Kino et al. [24]. The microcarriers had a pore size of 100 μm and protected the cells from external shear stress. A newly developed stirred tank reactor contained the microcarrier-immobilized hepatocytes. The O_2-supply was improved by using an oxygenator. The performance of microcarrier-immobilized hepatocytes in the reactor was as good as that in floating culture and they demonstrated good ammonia metabolism.

Demetriou et al. [25] described a capillary hollow fiber membrane based bioreactor in which microcarrier-attached hepatocytes are placed in the extracapillary space on the exterior surface of the capillary hollow fiber membranes as shown in Fig. 1. Recent experimental studies with this device have demonstrated its efficacy in animal models. By using cryopreserved microcarrier-attached hepatocytes this system offers the convenience of being readily available when needed.

A new concept based on a fluidized bed bioreactor was proposed by Dore et al. [26, 27]. This type of reactor is well known in chemical engineering applications to promote interactions and exchanges between solid and liquid phases. An alginate bead structure provides the hepatocytes with a three-dimensional anchorage framework. Scaling-up only depends on the number of beads employed. The efficacy of this system was tested in vitro and ex vivo in the acute liver failure model of pig [28]. The alginate-embedded hepatocytes maintain most liver-specific functions including ammonia removal and urea synthesis in vitro. The animal data suggest that the system arrests the increase of serum ammonia and intracranial pressure significantly in the acute liver failure model of pig.

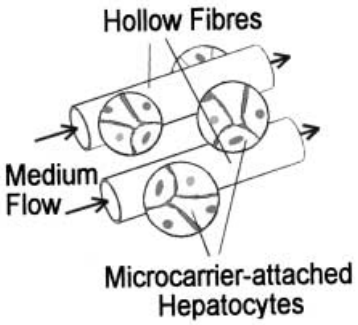

Fig. 1. Schematic illustration of a hepatocyte bioreactor with microcarrier-attachted hepatocytes. The capillary membranes are perfused with medium. (Modified from Dixit et al. [29])

4.2
Hollow Fiber Bioreactors

Several innovative membrane-based bioreactor designs have recently been proposed, including that by Sussman et al. [10], which involves the cultivation of hepatoma cells on the exterior surfaces of semipermeable capillary hollow fiber membranes which are bundled together with an enclosing plastic shell (Fig. 2). Required nutrient medium is circulated within the capillaries. After the hepatocytes have attached and formed a mass of liver tissue, the capillary membranes are perfused with the media.

Another modification has been described by Nyberg et al. [30]. In this design primary hepatocytes are entrapped in cylindrical collagen gels inside the lumen of the hollow fibres as shown in Fig. 3. The gel entrapment technique reported by this group enables a large number of hepatocytes to be employed in the bioreactor. Additionally, this technique also provides a three-dimensional frame-

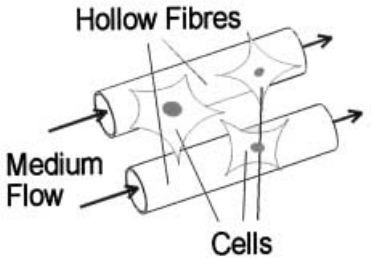

Fig. 2. Hepatoma cells are cultivated on the exterior surfaces of semipermeable capillary hollow fiber membranes. After the hepatocytes have attached and formed a mass of liver tissue, the capillary membranes are perfused with medium. (Modified from Dixit et al. [29])

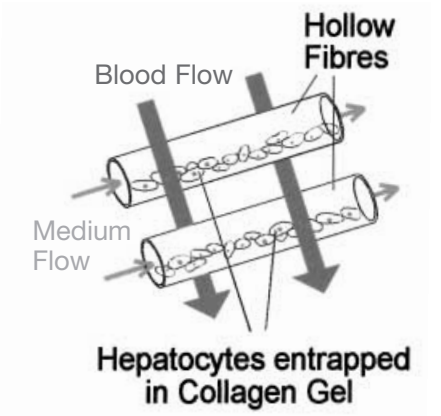

Fig. 3. The gel-entrapped hepatocytes are located in the intra-luminal capillary space of the device. Culture medium is perfused through and over the gel-entrapped hepatocytes. The host animal's blood is circulated in the extracapillary compartment between the capillary hollow fibers. (Modified from Dixit et al. [29])

work for cultured hepatocytes, allowing close contact between adjacent hepatocytes, which may be important in maintaining normal hepatocyte function within the bioartificial liver. Recent in vitro studies have reported significant albumin production and cytochrome P-450 activity by the hepatocytes [31].

In the HepatAssist 2000 system the patient's plasma is perfused through a hollow fiber bioreactor containing primary porcine hepatocytes [32]. It is outfitted with a complete cartridge tubing set, integrated oxygenator and heat exchanger, plasma reservoir, and BAL2000 hollow fiber cartridge. Cryopreserved hepatocytes are thawed and inoculated in the bioreactor with Cytodex-3 microcarriers. A protocol has been developed to simulate the function of the system during a patient's treatment. It has been used to determine rates of oxygen consumption and liver cell function (metabolism of diazepam) and was set up to study its performance in vitro and simulate its performance in vivo.

Gerlach et al. [33] have described a system which features porcine hepatocytes cultured in adhesion on the outer surface of and between four interwoven, biomatrix-coated hollow fiber membrane systems arranged in three planes at 90° to each other and which serve independent functions. This design incorporates sinusoidal endothelial cell co-cultures and allows decentralized cell perfusion and the independent supply of oxygen, nutrients and metabolite exchange at low gradients. Solute transport through the cell mass is appreciably enhanced. Hepatocytes spontaneously form aggregates and assume a three-dimensional structure during culture within the bioreactor and have been shown to express differentiated function in vitro for up to 4 weeks.

We have designed a new bioreactor on the basis of a hollow fiber membrane oxygenator [34]. The hollow fiber bioreactor, therefore, enables an optimized oxygen support. It consists of two membrane packages. In the first chamber, sheets of heat exchange (polyethylene) and sheets of microporous oxygenation fibers (polypropylene) are arranged crosswise as shown in Fig. 4. In the second chamber only sheets of oxygenation fibers are arranged. The hepatocytes are placed in the extrafibrous space on the surface of the hollow fibers. Medium is perfused through the extrafiber space and therefore in direct contact with the hepatocytes. The hollow fiber oxygenator offers different advantages. A high cell density of up to $50 \cdot 10^6$ cells/ml can be obtained and because no incubator is

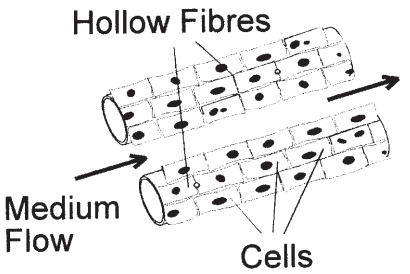

Fig. 4. Primary liver cells are cultivated on the exterior surfaces of semipermeable capillary hollow fiber membranes. Medium is perfused through the extrafiber space. Through the fibers oxygen supply is supported

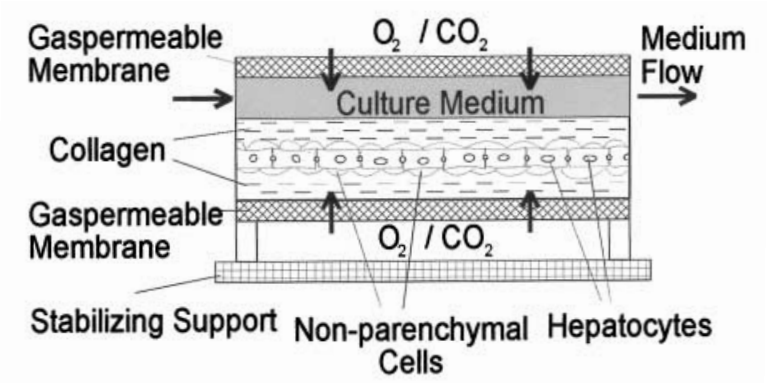

Fig. 5. The primary hepatocytes are co-cultivated with non-parenchymal cells between two layers of extracellular matrix. Medium and cells are oxygenated in the incubator across the gaspermeable membrane

necessary and the limited size of the oxygenator a good handling is achieved. Cultivations with primary porcine hepatocytes demonstrate that the cells preserve their viability and primary metabolism over the complete period of study of about three weeks.

4.3 Flat Membrane Bioreactor

Bader et al. [35] and De Bartolo et al. [36] developed the flat membrane bioreactor which consists of a multitude of stackable flat membrane modules as shown in Fig. 5. Each module has an oxygenating surface area of 1150 cm^2. Up to 50 modules can presently be run in parallel mode. Isolated hepatocytes are co-cultured with non-parenchymal cells. Liver cells are located of a distance of 20 µm of extracellular matrix from a supported polytetrafluorethylene (PTFE) film. Medium and cells in the modules are oxygenated in the incubator by molecular diffusion of air across the non-porous PTFE membrane. The design of the bioreactor is also the basis for its proven potential for cryostorage with fully differentiated adult primary human liver cells.

5 Conclusions

Human donor tissue is scarce and therefore the requirement for large numbers of cells cannot be met easily by the use of primary cells. The cell isolation procedures are time consuming and typically yield cells with limited lifespan. Furthermore the conditions that promote long term survival of highly differentiated cells also inhibit cell growth and thus there is little opportunity to increase cell numbers by expanding them in vitro.

Loss of tissue-specific functions and lack of appropriate differentiation during the culture of primary cells is a major problem. Extracellular matrix com-

position and topology can have a profound influence on the physiology of cultured cells in bioreactors and can be used to help maintain their differentiated state.

Immortalization of human hepatocytes would help to overcome the limited availability of human cells, thereby avoiding the use of malignant-derived cell lines; however, care will still be required with these cells. A better approach would be to develop methods for the culture of primary human hepatocytes using hormonally defined media containing growth factors in which cells are stimulated to undergo division.

A clinically useful bioreactor system will need to be compact and capable of maintaining a large number of cells at relatively high densities over a prolonged period of time. Engineering intensive bioreactor systems to have the appropriate 3D matrix geometries exacerbates the problems associated with ensuring adequate nutrient delivery, particularly oxygen, in these high density cultures.

The development of cryotechnologies for the bioreactor represents one of the core goals. Although cryopreservation is a standard technique for preserving different kinds of primary cells as well as various cell lines, standard cryopreservation procedures can inflict considerable injury to hepatocytes. It is envisaged that the technology will be developed to cryopreserve bioreactors together with the respecting bioartificial tissues. This will significantly contribute towards the clinical applicability of the bioartificial organs as a ready to use treatment option.

Although several hepatocyte-based liver support systems have been proposed, there is no current consensus on its eventual design configuration. The most devices used currently are based on conventional hollow fiber membranes, and there are many opportunities for bioengineers to design new bioreactors that will optimize device function, particularly with regard to oxygen and nutrient provision.

References

1. Langer R, Vacanti JP (1993) Science 260:920
2. Dixit V, Gitnick G (1998) Eur J Surg Suppl 582:71
3. Nyberg SL, Hibbs JR, Hardin JA, Germer JJ, Persing DH (1999) Transplantation 67:1251
4. Bader A, Knop E, Kern A, Boker K, Frühauf N, Crome O, Esselmann H, Pape C, Kempka G, Sewing KF (1996) Exp Cell Res 226:223
5. McLaughlin B, Tosone CM, Custer LM, Mullon C (1999) Ann N Y Acad Sci 875:310
6. Busse B, Gerlach JC (1999) Ann N Y Acad Sci 875:326
7. Paradis K, Langford G, Long Z, Heneine W, Sandstrom P, Switzer WM, Chapman LE, Lockey C, Onions D, The XEN 111 Study Group, Otto E (1999) Science 285:1236
8. Kobayashi N, Fujiwara T, Westerman KA, Inoue Y, Sakaguchi M, Noguchi H, Miyazaki M, Cai J, Tanaka N, Fox IJ, Leboulch P (2000) Science 287:1258
9. Riordan S, Williams R (1997) Br Med Bull 53:730
10. Sussman NL, Chong MG, Koussayer T, He DE, Shang TA, Whisennand HH, Kelly JH (1992) Hepatology 16:60
11. Neuzil DF, Rozga J, Moscioni AD, Ro MS, Hakim R, Arnaout WS, Demetriou AA (1993) Surgery 113:340
12. Gerlach JC, Brombacher J, Kloppel K, Schnoy N, Neuhaus P (1994) Transplantation 57:1318

13. Nagamori S, Hasumura S, Matsuura T, Aizaki H, Kawada M (2000) J Gastroenterol 35:493
14. Werner A, Duvar S, Müthing J, Büntemeyer H, Lünsdorf H, Strauss M, Lehmann J (2000) Biotechnol Bioeng 68:59
15. Berry MN, Friend DS (1969) J Cell Biol 43:506
16. Seglen PO, Jervell KF (1969) Hoppe Seylers Z Physiol Chem 350:308
17. Seglen PO (1976) Methods Cell Biol 13:29.
18. Hoogenboom LA, Pastoor FJ, Clous WE, Hesse SE, Kuiper HA (1989) Xenobiotica 19:1207
19. Sakai Y, Furkawa K, Suzuki M (1992) Biotechnol Tech 6:527
20. Sakai Y, Naruse K, Nagashima I, Muto T, Suzuki M (1999) Cell Transpl 8:531
21. Kong LB, Chen S, Demetriou AA, Rozga J (1996) Int J Artif Organs 19:72
22. Naruse K, Sakai Y, Nagashima I, Jiang GX, Suzuki M, Muto T (1995) Int J Art Organs 19:347
23. Naruse K, Nagashima I, Sakai Y, Harihara Y, Jiang GX, Suzuki M, Muto T, Makuuchi M (1998) Artif Organs 22:1031
24. Kino Y, Sawa M, Kasai S, Mito M (1998) J Surg Res 79:71
25. Arnaout WS, Moscioni AD, Barbour RL, Demetriou AA (1990) J Surg Res 48:379
26. Dore E, Legallais C (1999) Ther Apher 3:264
27. Legallais C, Dore E, Paullier P (2000) Artif Organs 24:519
28. Hwang YJ, Kim YI, Lee JG, Lee JW, Kim JW, Chung JM (2000) Tranplant Proc 32:2349
29. Dixit V, Gitnick G (1996) Scand J Gastroenterol Suppl 220:101
30. Nyberg SL, Platt JL, Shirabe K, Payne WD, Hu WS, Cerra FB (1992) Asaio J 38:M463
31. Nyberg SL, Shirabe K, Peshwa MS, Sielaff TD, Crotty PL, Mann HJ (1993) Cell Transplantation 2:241
32. Custer L, Mullon CJ (1998) Adv Exp Med Biol 454:261
33. Gerlach J C, Encke J, Hole O, Muller C, Courtney JM, Neuhaus P (1994) Int J Artif Organs 17:301
34. Jasmund I, Schmidt-Richter I., Simmoteit R., Bader A. (2000) Int J Artif Organs 23:535
35. Bader A, De Bartolo L, Haverich A (2000) J Biotech 81:95
36. De Bartolo L, Jarosch-von Schweder G, Haverich A, Bader A (2000) Biotechnol Prog 16:102

Received: April 2001

Cultivation of Hematopoietic Stem and Progenitor Cells: Biochemical Engineering Aspects

Thomas Noll[1,*], Nanni Jelinek[2], Sebastian Schmidt[1,3], Manfred Biselli[1,4], Christian Wandrey[1]

[1] Institut für Biotechnologie 2, Forschungszentrum Jülich GmbH, 52425 Jülich, Germany
E-mail: th.noll@fz-juelich.de
[2] Biogenerix, Janderstr. 3, 68199 Mannheim, Germany
[3] Bayer AG, ZT-TE 5.6, 51368 Leverkusen, Germany
[4] University of Applied Sciences Aachen, Ginsterweg 1, 52428 Jülich, Germany

Dedicated to Prof. Dr. Wolf-Dieter Deckwer on the occasion of his 60th birthday

The ex vivo expansion of hematopoietic cells is one of the most challenging fields in cell culture. This is a rapidly growing area of tissue engineering with many potential applications in bone marrow transplantation, transfusion medicine or gene therapy. Over the last few years much progress has been made in understanding hematopoietic differentiation, discovery of cytokines, isolation and identification of cellular subtypes and in the development of a variety of bioreactor concepts. All this has led to a number of (preliminary) clinical trials that gave a hint of the benefits that can be obtained from the use of expanded hematopoietic cells in therapy. Moreover, as we understand the complexity and the regulation of hematopoiesis, it becomes obvious that highly sophisticated cultivation techniques and bioreactor concepts are needed: a new challenge for bioprocess engineering in cell culture.

Keywords. Hematopoietic cell culture, Stem and progenitor cells, Ex vivo expansion, Bioprocess engineering

* To whom all correspondence should be adressed.

Advances in Biochemical Engineering/
Biotechnology, Vol. 74
Managing Editor: Th. Scheper

Abbreviations

BFU-E	burst-forming unit erythroid
BM	bone marrow
CAFC	cobblestone-area-forming cell
CB	cord blood
CD	cluster of differentiation
CFC	colony-forming cell
CFU	colony-forming unit
CFU-Ba	CFU basophil
CFU-Eo	CFU eosinophil
CFU-E	CFU erythrocyte
CFU-G	CFU granulocyte
CFU-GEMM	CFU granulocyte/erythrocyte/macrophage/megacaryocyte
CFU GM	CFU granulocyte/macrophage
CFU-M	CFU macrophage
CFU-Meg	CFU megacyryocyte
CMV	cytomegalovirus
EBV	Epstein-Barr virus
Epo	erythropoietin
G-CSF	granulocyte-colony-stimulating factor
GM-CSF	granulocyte-macrophage colony-stimulating factor
GVHD	graft-versus-host disease
HSC	hematopoietic stem cell
IL	interleukin
LTC-IC	long-term-culture initiating cell
mM	millimole per liter
MNC	mononuclear cell
MPB	mobilized peripheral blood
MRC	mouse-repopulating cell
M-CSF	macrophage colony-stimulating factor
NK	natural killer
NOD-SCID	non-obese diabetic severe combined immune deficiency
PS	polystyrene
SCEPF	stem cell expansion promoting factor
SCF	stem cell factor
SCM	stromal-conditioned medium
SDF-1	stromal-derived factor 1

TGF-β	transforming-growth factor β
TPO	thrombopietin
VEGF-2	vascular endothelial growth factor 2

1 Introduction

Hematopoiesis, the process of generating mature blood cells, is mainly located in the red bone marrow, predominantly in the sternum, femur and pelvic bones [1]. In the marrow the hematopoietic cells are embedded in stromal tissue. This consists of different cell types (e.g., fibroblasts, endothelial cells, adipocytes, macrophages) that provide soluble and membrane-bound growth factors and produce an extracellular matrix consisting of collagen, laminin, fibronectin, and glycosaminoglycans [2, 3]. The interactions between hematopoietic cells, stromal cells and extracellular matrix are indicated in Fig. 1 [4, 5].

Everyday, almost 400 billion hematopoietic cells of different subtypes are produced in an average human to replace the natural loss of cells [6]. Despite this tremendous proliferation, the balance between the different lineages is very efficiently controlled to guarantee the many functions of the blood (Table 1). If necessary (e.g., in the case of an infection or blood loss caused by an injury) the overall production of blood cells or the maturation of specific subpopulations can even be further significantly increased.

2 The Hematopoietic System

Despite enormous progress, even today the hematopoietic system is not completely understood. However, it is agreed that all hematopoietic cells originate from a small population of pluripotent stem cells that proliferate and differentiate into the whole spectrum of mature blood cells (see Fig. 2) [1]. The pluri-

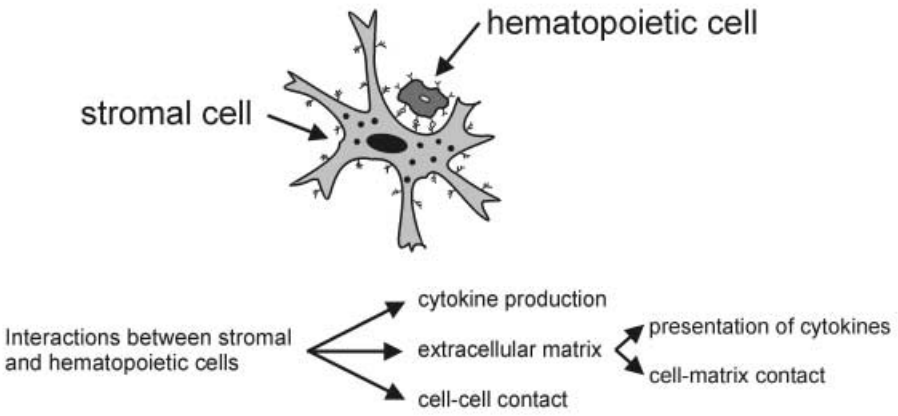

Fig. 1. Interactions between hematopoietic cells and the stroma

Table 1. Function, concentration and life-span of different mature cells in the blood

Cell type	Function	Concentration (cells/ml)	Life span
NK-cells	Kill virus-infected cells and some tumor cells	1×10^5	7–500 d
T-lymphocytes	Antigen-specific, cell-mediated immuneresponse	1×10^6	7–500 d
B-lymphocytes	Antigen-specific, antibody-mediated immuneresponse	2×10^6	Unknown
Basophilic granulocytes	Release of histamine and serotonine in certain immune reactions	4×10^4	Few hours
Eosinophilic granulocytes	Destroy larger parasites and modulate allergic inflammatory responses	2×10^5	3–8 h
Neutrophilic granulocytes	Phagocytose and destroy invading bacteria	5×10^6	6–9 h
Monocytes	Differentiate to macrophages, which phagocytose damaged cells and bacteria	4×10^5	3–6 d
Thrombocytes	Initiate blood clotting	3×10^8	1 week
Erythrocytes	Transport of O_2 and CO_2	5×10^9	4 months

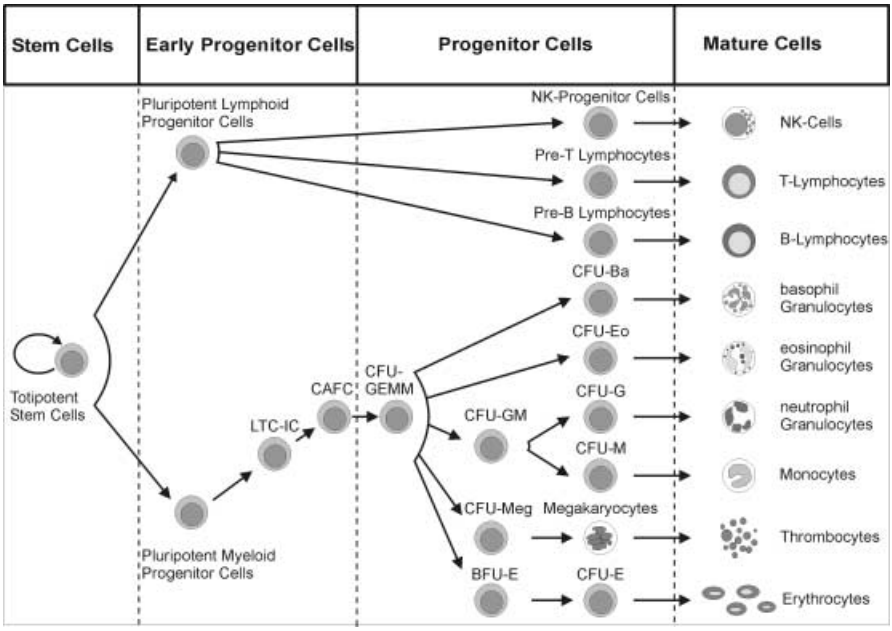

Fig. 2. Structure of the hematopoietic system

potent stem cells are the only ones with self-renewable capacity and for all other cells proliferation is inevitably combined with a lineage-specific differentiation and loss of immaturity. Every step of differentiation and maturation is regulated and controlled in vivo by the cell's microenvironment. This means that a cell cultivation technique that aims at generating a specific subpopulation has to meet the cells specific environmental requirements.

A great challenge in hematopoietic cell culture is the identification of the cells. While mature blood cells can easily be detected by their morphology and by flow cytometric analysis of characteristic surface molecules, the identification of progenitor cells needs time-consuming in vitro assays like colony-forming cell (CFC) assay, cobblestone-area-forming cell (CAFC) assay or long-term-culture initiating-cell (LTC-IC) assay. In the CFC assay a small number of cells are cultivated for 2 weeks in a semi-solid medium containing cytokines. Colony-forming cells generate a colony of more differentiated cells depending on their lineage specificity (e.g., a CFU-G forms a colony of granulocytes). For the detection of more primitive progenitor cells, the CAFC or LTC-IC assay is used. Here a small number of cells are placed on a stromal cell layer for 6–8 weeks. During this period the early progenitor CAFC and LTC-IC differentiate and, in the case of CAFC, cobblestone-area-like cells are formed that can be easily identified. In the case of LTC-IC the early progenitor cells differentiate into CFC, which are detected using a subsequent CFC assay [7, 8]. By extension of the cultivation time up to 14 weeks (extended long-term culture), even more immature cells than LTC-IC can be identified [9, 10]. For the detection of the pluripotent stem cells only in vivo assays are available, which use the potential of these cells to repopulate irradiated, immunodeficient mice (NOD-SCID), sheep or monkeys [11–13].

The identification of stem and progenitor cells using flow cytometry has intrinsic difficulties as some surface molecules vanish while others occur during differentiation and true stem cell markers are still unknown. It was long thought that CD34 could act as a marker of stem cells as the CD34+ population contains a high amount of CFC, LTC-IC and MRC [14]. However, some publications describe a mouse-repopulating capacity for a population of cells which are CD34– but do not have markers of more mature states [15, 16]. One of the most recent theories describes the stem cell population as CD34–, which, after activation, can develop the CD34 molecule in a reversible process [17, 18]. Other surface molecules that are supposed to identify the stem cell or at least very early progenitors are AC133, KDR and CXCR-4 [19–21]. However, as the cellular phenotype determined by flow cytometry and the biological function of the cells do not coincide in every case, as shown by Dorrell [22], functional in vitro assays are strongly recommended.

2.1 Sources of Hematopoietic Cells

There are three sources of hematopoietic stem and progenitor cells available: bone marrow (BM), peripheral blood after stem cell mobilization (MPB) and umbilical cord blood (CB).

Bone marrow is the natural site of hematopoiesis and was therefore the first source of hematopoietic stem and progenitor cells. In addition to the hematopoietic cells primary stroma can also be collected simultaneously from this source. However, as the harvesting of cells from bone marrow is an invasive procedure that requires manual extraction under spinal or general anesthesia, alternative sources are preferred whenever possible, although, for allogeneic stem cell transplantation, bone marrow is still the source of choice [23].

Peripheral blood normally does not contain significant amounts of stem and progenitor cells but, after administration of G-CSF or GM-CSF or a light chemotherapy protocol, stem and progenitor cells circulate in higher numbers and can be isolated by leukaphoresis [24]. This is the standard procedure to collect hematopoietic stem and progenitor cells from patients for autologous transplantation after high-dose chemotherapy [23].

Umbilical cord blood as a source of hematopoietic stem and progenitor cells has many advantages. It is easily accessible by a procedure noninvasive for the mother or the neonate and contains a significant amount of progenitor cells with high proliferative potential [25]. The burden of CB with common viral contaminations like EBV and CMV is lower than that of MPB or BM and, as the lymphocytes are more naive, the risk of a graft-versus-host disease (GVHD) is reduced [24]. The main disadvantage of cord blood is the low number of cells obtained due to the small volume of blood collectable from umbilical cords. Without an expansion of the stem and progenitor cells, a transplantation is limited to a body weight of about 40 kg making this therapy only available for juvenile patients [26].

2.2 Potential Medical Applications

Expanded hematopoietic (stem and progenitor) cells have widespread potential in therapy and this will only be briefly described here. For a comprehensive overview, the review by Schindhelm and Nordon [27] is recommended. Potential applications include 'graft engineering' in stem cell transplantation [24], gene and immunotherapy and the production of mature blood cells for transfusion medicine.

Both chemotherapy and radiation therapy in cancer treatment are based on the fact that tumor cells are continuously proliferating and these procedures are therefore aimed at cells in mitosis. All other cells that undergo rapid proliferation are also damaged and this applies especially to the hematopoietic system [28]. In high-dose chemotherapy doses of cytotoxic drugs are increased to a level that is supposed to also eradicate residual tumor cells. This also leads to a total loss of all hematopoietic stem cells, making an autologous or allogeneic stem cell transplantation obligatory. Expansion of stem and progenitor cells can either increase the number of umbilical cord blood derived cells, making this source also available for adult patients, or result in a reduction in the number of leukaphoresis procedures necessary for the collection of autologous cells. The transplantation of lineage-restricted progenitor cells can help to reduce the period of neutropenia after chemotherapy, and, in

the case of megacaryocytes, alleviate post-transplant-associated thrombocytopenia [29].

Expansion of specific T-lymphocytes or natural killer cells gives access to cell-mediated immunotherapy, while the generation and specific loading of dendritic cells offers possibilities for the in vivo induction of antigen-specific immunity [30]. Furthermore, the generation of erythrocytes or thrombocytes can lead to blood transfusions without a risk of viral contaminants. Finally, stem cells are an appropriate target for somatic gene therapy as they can offer a chance of a lifelong cure from genetic disorders due to their self-renewing capacity.

3 Cultivation Parameters

As outlined earlier every single step of hematopoiesis is regulated and controlled in vivo by the cell's microenvironment. This not only includes the composition and concentration of growth factors, but also the local oxygen concentration, the pH, the osmolality, the supply of nutrients and the cellular and molecular surrounding of the cells (cell-cell contact, adhesion molecules and extracellular matrix). All these parameters affect the fate of the cell and, to establish a cell culture process to cultivate or generate a specific subpopulation, the influence of all these factors has to be considered in the experimental set-up. In the following sections these parameters will be discussed in brief.

3.1 Cytokines

In the bone marrow, cytokines are produced predominantly from stromal cells, although accessory and hematopoietic cells themselves have also been shown to secrete growth factors [31–33]. Cytokines affect nearly all processes of hematopoiesis, like proliferation, differentiation, adhesion and functional properties of the cells, while, in the absence of cytokines, HSC suffer apoptosis [34]. The effects of hematopoietic cytokines are very complex and show synergistic as well as antagonistic interactions. Changes in the cytokine concentrations during cultivation can cause significant changes in the proliferation and the differentiation of the cells. Therefore, the control of cytokine composition is an extremely important element of the bioprocess strategy. For the expansion of stem and progenitor cells, interleukin 3 (IL-3), interleukin 6 (IL-6), stem cell factor (SCF), thrombopoietin (TPO) and flt3 ligand (FL) are thought to play major roles [35–37] and are mostly used in the expansion of hematopoietic stem and progenitor cells.

The number of cytokines known to influence hematopoiesis is steadily growing. The most recently identified cytokines are SDF-1 [38], VEGF2 [39] and SCEPF [40], but there are still growth factors in the stromal environment to be identified. This has been proven by the additional growth-supportive effects of stroma-conditioned medium on the proliferation of hematopoietic stem cells.

Due to the complexity and the manifold interactions between cytokines, determination of an optimum cytokine mix for stem cell cultivation is difficult and most optimization algorithms are inefficient. Significant progress can be made using genetic algorithms, as shown by Thoma et al. [41].

3.2 Culture Media and Feeding Schedules

The choice of the culture medium, especially the use of serum, directly influences the differentiation of the cells and therefore the aims of the cultivation should be considered when determining the medium to be used [1]. Serum normally contains TGF-β, which is known to inhibit the erythroid and megacaryocytic lineage, therefore promoting the granulocytic and macrophage differentiation [42]. In stroma-containing culture, serum strengthens the adhesion of the cells and stabilizes the feeder layer. A further aspect which has to be considered in the use of animal serum (e.g., fetal bovine or horse) is the clinical applicability, as media containing components from animal sera will face more regulatory hurdles than serum-free compositions [43].

Because hematopoiesis in the bone marrow takes place under static conditions [1], with a continuous feed of nutrients and a simultaneous removal of waste products, several feeding strategies have been developed in the cultivation of hematopoietic cells. In static cultivations feeding schedules have been described, which range from half medium exchange per week up to a total daily exchange [44, 45]. Most perfused cultures were not continuously supplied with fresh medium. From a reservoir the medium is fed into the cultivation chamber containing the cells and then back into the reservoir, which is intermittently replaced by fresh medium, leading to exchange rates between half a medium exchange three times per week and a total daily exchange [46–48]. Palsson et al. [49] and Meissner et al. [50] have both described cultivations using a continuous supply with a fresh culture medium.

Feeding of fresh medium prevents the limitation of growth from a lack of substrates as well as inhibition from the accumulation of metabolic by-products. This has recently been investigated in detail for lactate, when Patel et al. found that a lactate concentration of more than 20 mM inhibits cell proliferation and metabolism, although it has little effect on cell differentiation [51].

3.3 Oxygen Tension

Oxygen tension plays an important role in hematopoietic cell culture as it directly influences the cellular proliferation and differentiation [1]. In the bone marrow, oxygen concentrations of 5%–30% of air saturation have been described [52]. Low oxygen levels (5%) support the proliferation of colony-forming cells (CFC), probably due to decreased oxidative damage and an increased responsiveness to growth factors like Epo or M-CSF [53, 54]. This has been demonstrated in the cultivation of cord blood MNC with and without stromal feeder layers. High oxygen tension (20%–30%) promotes the growth of

mature erythroid and megacaryocytic cells, while mature granulocytes show higher proliferation at low oxygen levels [1]. Together with the choice of cytokine combination, this can be used to control and direct the proliferation and differentiation of the culture towards the cells of interest. This is a challenge for bioprocess engineering, as the oxygen concentration in the medium has to be measured accurately and controlled exactly to avoid oxygen limitations. This is especially important in the cultivation of stem and progenitor cells at low oxygen levels. According to the growth of the cells the oxygen transfer has to be adjusted by increasing the oxygen concentration in the gas phase, increasing the perfusion or increasing the agitation rates.

3.4 pH

The regulation of hematopoiesis in the bone marrow is not only controlled by the cytokine composition, the cells microenvironment and the oxygen tension, but, as shown recently [55], also by the local pH. For cells of different lineages deviating pH optima have been described. While CFU-GM proliferate best in a pH range 7.2–7.4 (the normal pH of blood), for erythroid cells an optimum of pH 7.6 was found. Below an acidic pH of 6.7 no differentiation or proliferation of any hematopoietic cell was observed. Cells of the erythroid lineage are even strongly inhibited at a pH below 7.1 [56].

To avoid inhibition of proliferation and differentiation the pH in hematopoietic cell cultures has to be controlled carefully. Especially in non-perfused culture the pH shifts during the cultivation due to secreted acidic metabolites like lactate. However is has been reported recently that pH control alone is not sufficient to eliminate inhibition of cell growth and metabolism as other inhibitory factors also accumulate in un-fed cultures [51].

3.5 Osmolality

Hematopoietic cells like all mammalian cells are quite sensitive to changes in osmolality. We have recently examined the effect of osmolality (0.26–0.38 mOsmol/kg) on human hematopoietic proliferation and differentiation and found an optimum for the expansion of MNC and CD34+ cells in a range between 0.31 and 0.32 mOsmol per kg, as described earlier by McAdams [57]. While MNC show a symmetric decrease in proliferation for osmolalities beyond this range, for CD34+ cells a much greater sensitivity for hypertonic conditions was found [58]. At the level of colony-forming cells distinct differences have been observed. Progenitors of the granulocytic and macrophage lineage show maximum proliferation at slightly hypotonic osmolalities (0.29 mOsmol/kg), while BFU-E proliferation is enhanced at hypertonic levels (0.34 mOsmol/kg). This finding might offer an additional opportunity to direct the proliferation and differentiation by adjusting the appropriate culture conditions.

3.6 Biocompatibility of Materials

As outlined earlier, hematopoiesis is a complex process that is influenced and affected by a multitude of factors. Thus, the biocompatibility of materials is an important issue in hematopoietic culture. It has to be ensured that all materials that are in contact with hematopoietic cells or their culture medium do not leach any toxins or adhere medium components. In case of cell immobilization, additional effects of the materials surface (e.g., charge) have to be considered. LaIuppa investigated the influence of a wide range of materials on the proliferation and differentiation of hematopoietic cells in comparison to polystyrene (the standard material in cell culture) [59, 60]. She found that colony-forming-cell expansion is more affected than total cell expansion and CD34+ cells are more sensitive than MNC. In our own studies we compared different materials that are commonly used in the construction of bioreactors for their influences in hematopoietic culture, with and without serum [58]. Direct contact was investigated, as well as their potential to release toxins into the culture medium and to adhere essential medium components. By preincubating medium with a sample of the materials, it was clearly demonstrated that the inhibitory effects are much stronger in direct contact, and in the absence of serum. The protective effect of serum is probably caused by the material's surface being coated with protein. A direct correlation was found between the inhibitory effect and the ratio of the material's surface to medium volume (cm^2/ml). For example, glass with a ratio of 1 showed no inhibitory effects either on the expansion of MNZ or CD34+ cells or on the CFC. If one increases the ratio to 3.8 the expansion of colony-forming cells compared to polystyrene (PS) dropped about 50%, while MNZ and CD34 expansion only slightly decreased. A further increase in the surface-to-volume ratio (11.3) resulted in a 95% decrease of CFC expansion when compared to PS. Expansion of mononuclear and CD34+ cells was also significantly reduced (75% and 85%, respectively). In most bioreactor concepts the material surface to medium volume is in a range that makes inhibitory effects unlikely, but this should be evaluated when developing a new hematopoietic culture system.

4 Concepts of Cultivation

As outlined earlier, hematopoietic cells have a widespread potential in medicine, but all of the envisaged applications necessitate the generation of large amounts of cells. This is true for stem and progenitor cells as well as for mature hematopoietic cells. In every case the bioprocess has to meet the following requirements:

Large Cell Expansion in Short Time. Most of the cells needed for therapy have to be patient-specific and therefore must be provided 'on demand' and in a number sufficient for one patient. A billion-fold expansion in a timeframe of months fails to meet the clinical requirements. For example, in the case of a

stem cell transplantation after high-dose chemotherapy, the expansion of the cells has to be performed during the chemotherapy protocol, giving the cultivation no more than 7–10 d. An exception might be megacaryocytes, used for the treament of thrombocytopenia, which can be cryopreserved and thawed in the necessary amount prior to transfusion.

Considering the normally small amount of cells in the early stage of culture and the significant increase during cultivation, the bioreactors used should enable not only an increase in cell density but also in culture volume without changing the culture system.

Easy Cell Harvest. In this type of bioprocess the cells are the products so a method for an easy cell harvest must be provided. Neither a substantial loss in cell number nor damage to the cells is acceptable, because this would directly affect the therapeutic value of the transplant. A large number of labor-intensive isolation and purification steps is also unacceptable. This is not only because of the increase in time and costs, but also due to the increasing risk of contamination.

Controlled Culture Conditions. As described above, the culture conditions have an enormous influence on the proliferation and differentiation of hematopoietic (stem and progenitor) cells. Slight changes in the oxygen tension, the pH or the medium and growth factor composition can result in significant alterations in the differentiation pattern and the proliferative potential. This, in combination with the small starting volume in the early stage of culture, is a great challenge for bioprocess engineering. The materials used for the bioreactor setup, as well as the mechanical forces occurring during cultivation, have to be adapted to the intended subtype of cells.

Clinical Applicability. The regulatory conditions for cell therapy directly refer to the cells and the materials utilized during the cultivation. The use of cell lines, especially those of animal origin (e.g. stromal cell lines in cocultivation), and the use of animal serum should carefully be reconsidered, as this will make the seeking of clinical approval a difficult task.

In case of stem and progenitor cells, which are the focus of this review, many strategies for cultivation and expansion have been developed, as shown in Fig. 3.

4.1
Cultivation of Isolated Stem and Progenitor Cells

Since the development of recombinant human cytokines, cultivation and significant expansion of isolated hematopoietic stem and progenitor cells is possible without a supporting feeder-layer of stromal cells. It is the simplicity of these culture systems that is their main attraction [29]. The cells are cultivated in chemically defined culture medium containing defined combinations of cytokines and without any stromal products. On the one hand this enables a better control of the culture and the investigation of the influence of single cytokines or culture conditions. On the other hand, as our understanding of stem cell regu-

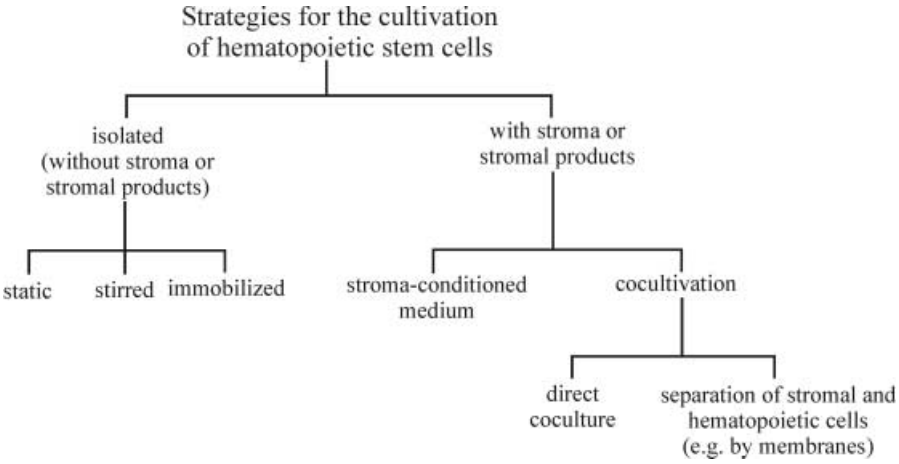

Fig. 3. Strategies for the cultivation of hematopoietic stem and progenitor cells

lation is still incomplete and it is hypothesized that stromal influences regulate in vivo hematopoiesis, it is likely that the cultivation of isolated hematopoietic cells results in suboptimal expansion. This is supported by our own results, which show significantly better expansion, especially of early progenitors, in the presence of stromal cells [61].

Three different approaches for the cultivation of isolated hematopoietic cells have been described, the static, the stirred and the immobilized culture. Static cultivation takes place in very simple culture systems like well plates, tissue-culture flasks or gas-permeable culture bags [62, 63]. As the first two systems do not allow cell cultivation on a clinical scale, the latter is actually the most often used technique for stem cell expansion. All these systems have the advantage of being easy to handle, single-use devices, which enable an uncomplicated cell harvest. But all of them do not offer possibilities for process control or continuous feeding. This causes variations in culture conditions during fermentation (e.g., oxygen tension, pH, substrate, metabolite and cytokine concentrations).

Stirred bioreactors are common in animal cell culture, as they offer a homogenous environment, representative sampling, better access to process control and an increased oxygen transfer. Several of these techniques (spinner flasks and stirred vessel bioreactors) have been tested successfully for the cultivation of hematopoietic cells [58, 64–67].

The immobilization of stem and progenitor cells is an attempt to reach local high cell densities and to imitate the three-dimensional structure of the bone marrow without the use of stroma. A number of porous microcarriers with and without additional coating of components of an extracellular matrix (e.g., collagen, fibronectin, laminin) have been investigated for this purpose. Bagley et al. compared different porous materials and described a greater than sixfold expansion of CFC in a long-term cultivation of CD34+ cells in tantalum-coated porous carriers, even without adding exogenous cytokines [68]. However, stem cell immobilization, especially in porous materials, requires a technique for

detaching the cells from the matrix prior to transplantation, a significant disadvantage compared to suspension culture.

Hollow fiber modules and the microencapsulation of progenitor cells have been used in hematopoietic culture with less success [69, 70]. Furthermore, these approaches do not fit the clinical requirements, as the harvest of the cells is almost impossible.

The most sophisticated technique for stem cell expansion is the Aastrom-Replicell system (Aastrom Biosciences Inc., Ann Arbor, MI, USA), which is an automated clinical system for the onsite expansion of stem cells in cancer therapy. It consists of a grooved perfusion chamber for the retention of the hematopoietic cells, with the medium flow perpendicular to the channel grooves resulting in a continuous supply of fresh nutrients while metabolites are simultaneously removed [47, 71, 72]. This technique has already been used in a number of clinical studies [73, 74]. No incompatibility of the expanded cells was found, but the expansion of the early progenitor cells was rather low [75].

Local high cell densities, as they are realized in the pores of microcarriers or in the grooves of the AastromReplicell, have been described to make bone marrow MNC essentially stroma-independent in terms of LTC-IC maintenance and expansion [44]. This might also be the reason for the good expansion of progenitors in the culture bags, where the cells accumulate in the wrinkles of the bag and reach local high cell densities.

4.2 Cultivation with Stromal Cells or Stroma-Derived Factors

Before the discovery and development of recombinant human cytokines, a feeder layer of stromal cells was essential for the cultivation of hematopoietic cells. The first system for the successful expansion of hematopoietic cells from murine origin was described by Dexter more than 20 years ago [76, 77]. Some years later this principle was transferred to human cells [78]. Stromal culture of hematopoietic cells is a generic term that covers a variety of cultivation concepts, as indicated in Fig. 3.

The most simple strategy is the application of exogenous stromal-conditioned medium [79, 80]. Stromal cells secrete numerous different growth factors necessary for the maintenance and expansion of stem and progenitor cells and many of these substances are still unknown. Some attempts have already been made to characterize them [81] and, in the future, significant progress can be expected using techniques developed for proteomics analysis. The use of conditioned medium enables the application of all bioreactor systems developed for the cultivation of isolated stem and progenitor cells and allows the culture to be supplied with (unidentified) growth factors secreted from the stroma. The conditioned medium can be produced in large amounts exogenously and stored until application.

A variation of this approach is the in situ generation of stromal-conditioned medium in a stroma non-contact co-culture (e.g., seperated by microporous membranes). This permits an interaction between stromal and hematopoietic cells mediated by secreted molecules, which has been described to support the

expansion of the early progenitor cells more efficiently than the use of exogenous conditioned medium [82]. Disadvantageous in this technique is the increase in the technical requirements for the set-up and process control.

One important element in the in vivo regulation of hematopoiesis is missing in the approaches using conditioned medium: the cell-cell contact between hematopoietic and stromal cells. This mimicry of the bone marrow has been reproduced in several types of bioreactors providing direct coculture of progenitors on a two- or three-dimensional stromal feeder layer. Tissue-culture flasks were used as well as microcarriers (in spinner flasks, airlift or fixed-bed bioreactors), nonwoven fabrics disks, large pore-size cubes or nylon screens [50, 61, 70, 76, 83–85]. In many of these cultivations expansion of the early progenitors is superior to that obtained in stroma-free culture. In our own study we reached a 100-fold expansion of MNC and CFC and a more than 6-fold expansion of CAFC in a fixed-bed bioreactor within 14 d [61]. Köhler et al. described a trend toward decreased apoptosis in culture with bone marrow stroma indicating the supportive character of the feeder layer [86].

For stromal culture, besides primary stroma from bone marrow, a variety of stromal cell lines are available. However, most are from murine origin, and human cell lines that support hematopoiesis are not efficiently available (Table 2). The human cell lines L87/4 and L88/5 are difficult to irradiate and favor differentiation and maturation over the expansion of early progenitors [87, 88].

The main attraction of stromal culture of hematopoietic cells is their superior ability for stem cell expansion especially in direct co-culture. However, despite this, a clinical use has not been realized until now. The major drawback is the origin of the stromal support. While autologous stroma would be feasible, in many cases this is not realizable. Furthermore, the use of cell lines (although irradiated to prevent further proliferation) is problematic as all stromal cells have to be removed completely prior to transplantation, a demand which is difficult to fulfill. In the case of murine cell lines a transfer of residue cells into a patient would be a xenotransplantation, which is faced with extensive regulatory hurdles.

Recently, a new approach has been reported that may offer co-culture a chance to be clinical applicable. Kawada et al. described a co-cultivation of stromal and hematopoietic cells separated by a porous membrane that enables a di-

Table 2. Stromal cell lines used in the cultivation of hematopoietic stem and progenitor cells

Cell line	Origin	Application	References
AC6.21	Murine	Co-culture and SCM	40, 89
FBMD-1	Murine	Co-culture and SCM	79, 90, 91
HESS-5	Murine	Co-culture	92–94
L87/4, L88/5	Human	Co-culture and SCM	79, 87, 95
MS-5	Murine	Co-culture and SCM	96–99
M2-10B4	Murine	Co-culture	50, 87, 100, 101
M2-10B4mod	Murine	Co-culture	61, 102
Sl/Sl	Murine	Co-culture	61, 102

rect contact between the cells by their extracellular matrix, but prevents the stromal cells from entering the hematopoietic compartment [94]. This work was carried out on small scale in a transwell, but a scale-up to a clinical level seems possible.

5 Conclusions and Outlook

The ex vivo expansion of hematopoietic cells is a rapidly growing area of tissue engineering with many potential applications in medicine. During the last few years a variety of bioreactor concepts and cultivation strategies have been developed, but no final decision has been made about the optimal system for hematopoietic culture.

The cultivation of isolated stem and progenitor cells has some distinct advantages like its simplicity, clinical applicability and the possibility to use standard cell culture techniques, but the expansion of the early progenitor cells shown in different clinical studies was rather low. The use of stromal-conditioned medium promises better expansion and lower costs due to the reduced need for exogenous cytokine supplementation, but the culture medium is chemically undefined, which will render reproducibility more difficult and complicate the clinical permission. Co-cultivation of stromal and hematopoietic cells results in the best expansion of early progenitor cells, but, as nearly all stromal cell lines are of murine origin, a clinical application of this approach is hardly possible. Membrane-separated co-cultivation may offer a possibility to avoid this disadvantage.

What can be expected from the future? The cultivation of isolated hematopoietic cells will benefit from the identification of new cytokines, making the use of stromal-conditioned medium unnecessary. The recent development of proteomics techniques will expediate this process. The prospects of the co-cultivation will depend on the development of human stromal cell lines supporting the expansion of early progenitor cells, and the membrane approach has to prove its potential on a clinical scale.

In summary, for the near future it can be expected that culture systems of sufficient simplicity, productivity and reliablity will be developed and tested in clinical studies, making transplantation therapies utilizing cultured hematopoietic cells a more common application in medicine.

Acknowledgement. We thank Dr. Joy Burchell for careful revision of the manuscript.

References

1. McAdams TA, Miller WM, Papoutsakis ET (1996) TIBTECH 14:341
2. Wilkins BS (1992) J Clin Pathol 45:645
3. Verfaillie C, Hurley R, Bhatia R, McCarthy JB (1994) Crit Rev Oncol/Hematol 16:201
4. Mayani H, Guilbert LJ, Janowska-Wieczorek A (1992) Eur J Hematol 49:225
5. Deryugina EI, Muller-Sieburg CE (1993) Crit Rev Immunol 13:115
6. Koller MR, Palsson BO (1993) Biotechnol Bioeng 42:909

7. Sutherland HJ, Lansdorp PM, Henkelman DH, Eaves AC, Eaves CJ (1990) Proc Natl Acad Sci 87:3584
8. Breems DA, Blokland EAW, Neben S, Ploemacher RE (1994) Leukemia 8:1095
9. Ploemacher RE (1997) Baillière's Clinical Hematology 10:429
10. Ramsfjell V, Bryder D, Björgvinsdottir H, Kornfält S, Nilsson L, Borge OJ, Jacobsen SEW (1999) Blood 94:4093
11. Lapidot T, Pflumio F, Doedens M, Murdoch B, Williams DE, (1992) Science 255:1137
12. Shimizu Y, Ogawa M, Kobyashi M, Almeida-Porada G, Zanjani ED (1998) Blood 91:3688
13. Brandt JE, Bartholomew AM, Fortman JD, Nelson MC, Brumo E, Chen LM, Turian FV, Davis TA, Chute JP, Hoffman R (1999) Blood 94:106
14. Krause DS, Fackler MJ, Civin CI, Stratford W (1996) Blood 87:1
15. Bhatia M, Bonnet D, Murdoch B, Gan OI, Dick JE (1998) Nature Med 4:1038
16. Zanjani ED, Almeida-Porada G, Livingston AG, Flake AW, Ogawa M (1998) Exp Hematol 26:353
17. Goodell MA (1999) Blood 94:2545
18. Sato T, Laver JH, Ogawa M (1999) Blood 94:2548
19. Yin AH, Miraglia S, Zanjani ED, Almeida-Porada G, Ogawa M, Leary AG, Olweus J, Kearney J, Buck DW (1997) Blood 90:5002
20. Ziegler BL, Valitieri M, Almeida-Porada G, De Maria R, Muller R, Masella B, Gabbianekki M, Casella I, Pelosi E, Bock T, Zanjani ED, Peschle C (1999) Science 285:1553
21. Kawabata K, Ujikawa M, Egawa T, Kawamoto H, Tachibana K, Iizasa H, Katsura Y, Kishimoto T, Nagasawa T (1999) Proc Natl Acad Sci 96:5663
22. Dorrell C, Gan OI, Pereira DS, Hawley RG, Dick JE (2000) Blood 95:102
23. Rowlings PA (1999) In: Schindhelm K, Norton R (eds) Ex vivo cell therapy. Academic Press, San Diego, p 85
24. McAdams TA, Winter JN, Miller WM, Papoutsakis ET (1996) TIBTECH 14:388
25. Kim DK, Fujiki Y, Fukushima T, Ema H, Shibuya A, Nakauchi H (1999) Stem Cells 17:286
26. Cairo MS, Wagner JE (1997) Blood 90:4665
27. Schindhelm K, Nordon R (1999) (eds) Ex vivo cell therapy. Academic Press, San Diego
28. Collins PC, Papoutsakis ET, Miller WM (1996) Curr Opin Biotechnol 7:223
29. Alcorn MJ, Holyoake TL (1996) Blood Rev 10:167
30. Bremers AJA, Parmiani G (2000) Crit Rev Oncol/Hematol 34:1
31. Linenberger ML, Jacobsen FW, Bebbett LG, Broudy VC, Martin FH, Abkowitz JL (1995) Exp Hematol 23:1104
32. Lisovsky M, Braun SE, Ge Y, Takahari H, Lu L, Savchenko VG, Lyman SD, Broxmeyer HE (1996) Leukemia 10:1012
33. Guerriero A, Worford L, Holland HK, Guo GR, Sheehan K, Walle EK (1997) Blood 90: 3444
34. Cottner TG, Fernandes RS, Verhaegen S, McCarthy JV (1994) Immunol Rev 142:93
35. Piacibello W, Sanavio F, Garetto L, Severino A, Bergandi D, Ferrario J, Fagioli F, Berger M, Aglietta M (1997) Blood 89:2644
36. Murray LJ, Young JC, Osborne LJ, Luens KM, Scollary R, Hill BL (1999) Exp Hematol 27:1019
37. Ramsfjell V, Bryder D, Björgvinsdottir H, Kornfält S, Nilsson L, Borge OJ, Jacobsen SEW (1999) Blood 94:4093
38. Möhle R, Bautz F, Rafii S, Moore MAS, Brugger W, Kanz L (1998) Blood 91:4523
39. Eichmann A, Corbel C, Nataf V, Vaigot P, Breánt C, LeDouarin N (1997) Proc Natl Acad Sci 94:5141
40. Shih CC, Hu MC, Wenig Y, Yazaki PJ, Medeiros J, Forman SJ (2000) Blood 95:1957
41. Thoma S, Schmidt S, Jelinek N, Herfurth C, Takors R, Wandrey C, Biselli M (1999) Onkologie 22 (suppl 1):180
42. Dybedal I, Jacobsen SE (1995) Blood 86:949
43. Sandstrom CE, Miller WM, Papoutsakis ET (1994) Biotechnol Bioeng 43:706
44. Koller MR, Manchel I, Palsson MA, Maher RJ, Palsson BO (1996) Biotechnol Bioeng 50:505

45. Schwartz RM, Palsson BO, Emerson SG (1991) Proc Natl Acad Sci 88:6760
46. Sandstrom CE (1995) PhD thesis, Northwestern University, Evanston
47. Sandstrom CE, Bender JE, Miller WM, Papoutsakis ET (1996) Biotechnol Bioeng 50: 493
48. Wang TY, Brennan JK, Wu JHD (1995) Exp Hematol 23:26
49. Palsson BO, Paek SH, Schwartz RM, Palsson MA, Lee GM, Silver S, Emerson SG (1993) Bio/Technology 11:368
50. Meissner P, Schroeder B, Herfurth C, Biselli M (1999) Cytotechnology 30:227
51. Patel SD, Papoutsakis ET, Winter JN, Miller WM (2000) Biotechnol Prog 16:885
52. Ishikawa Y, Ito T (1988) Eur J Hematol 40:126
53. Rich IN, Kubanek B (1986) Br J Hematol 52:579
54. Broxmeyer HE, Cooper S, Lu L, Miller ME, Langefeld CD, Ralph P (1990) Blood 76:323
55. Hehevan DL, Papoutsakis ET, Miller WM (2000) Exp Hematol 28:267
56. McAdams TA, Papoutsakis ET, Miller WM (1995) Blood (suppl. 1) 86:674a
57. McAdams TA (1997) PhD thesis, Northwestern University, Evanston
58. Schmidt S (2000) PhD thesis, University RWTH, Aachen
59. LaIuppa JA, McAdams TA, Miller WM, Papoutsakis ET (1995) Blood (Suppl. 1) 86:231a
60. LaIuppa JA, McAdams TA, Papoutsakis ET, Miller WM (1997) Biomed Mat Res 36:347
61. Jelinek N (2000) PhD Thesis University RWTH Aachen
62. Brugger W, Heimfeld S, Berenson RJ, Mertelsmann R, Kanz L (1995) N Eng J Med 333:283
63. Alcorn MJ, Holyoake TL, Richmond L (1996) J Clin Oncol 14:1839
64. Collins PC, Miller WM, Papoutsakis ET (1998) Biotechnol Bioeng 59:534
65. Kim BS (1998) Biotechnol Lett 20:595
66. Zandstra PW, Petzer AL, Eaves CJ, Piret JM (1997) Biotechnol Bioeng 54:58
67. De León A, Mayani H, Ramirez OT (1998) Cytotechnology 28:127
68. Bagley J, Rosenzweig M, Marks DF, Pykett MJ (1999) Exp Hematol 27:496
69. Levee MG, Lee GM, Paek SH, Palsson BO (1994) Biotechnol Bioeng 43:734
70. Sardonini CA, Wu YJ (1993) Biotechnol Prog 9:131
71. Sandstrom CE, Bender JG, Papoutsakis ET, Miller WM (1995) Blood 86:958
72. Koller MR, Maher RJ, Manchel I, Oxender M, Smith AK (1998) J Hematotherapy 7:413
73. Bachier CR, Gokmen E, Teale J, Lanzkron S, Childs C, Franklin W, Shpall E, Douville J, Weber S, Muller T, Armstrong D, Lemaistre CF (1999) Exp Hematol 27:615
74. Chabannon C, Novakovitch G, Blache JL, Olivero S, Camerlo J, Genre D, Maraninchi D, Viens P (1999) Hematol Cell Ther 41:78
75. Chabannon C, Blache JL, Sielleur I, Douville J, Faucher C, Gravis G, Arnoulet C, Oziel-Taieb S, Blaise D, Novakovitch G, Camerlo J, Chabbert I, Genre D, Appel M, Armstrong D, Maraninchi D, Viens P (1999) Int J Oncol 15:511
76. Dexter TM, Wright EG, Krizsa F, Lajtha LG (1977) Biomedicine 27:344
77. Dexter TM, Allen TD, Laijtha LG (1977) J Cell Physiol 91:335
78. Gartner S, Kaplan HS (1980) Proc Natl Acad Sci 77:4756
79. Breems DA, Blokland EAW, Ploemacher RE (1997) Leukemia 11:142
80. Bhatia R, McGlave PB, Lin W, Wissink S, Miller JS, Verfaillie CM (1995) Blood (Suppl. 1) 86:294a
81. Gupta P, McCarthy JB, Verfaillie CM (1996) Blood 87:3229
82. Verfaillie CM, Catanzarro PM, Li W (1994) J Exp Med 179:643
83. Highfill JG, Haley SD, Kompala DS (1995) Biotechnol Bioeng 50:514
84. Naughton BA, Naughton GK (1991) J Biomech Eng 113:171
85. Tomimori Y, Tagaki M, Yoshida T (2000) Cytotechnology 34:121
86. Köhler T, Plettig R, Wetzstein W, Schaffer B, Ordemann R, Nagels HO, Ehninger G, Bornhauser M (1999) Stem Cells 17:19
87. Schroder B (1997) PhD thesis, University of Bonn
88. Bertolini F, Battaglia M, Soligo D, Corsini C, Curioni C, Lazzari L, Pedrazzoli P, Thalmeier K (1997) Exp Hematol 25:350
89. Shih CC, Hu MCT, Hu J, Medeiros J, Forman SJ (1999) Blood 94:1623

90. Breems DA, Van Driel EM, Hawley RG, Siebel KE, Ploemacher RE (1998) Leukemia 12:951
91. Breems DA, Blokland EAW, Siebel KE, Mayen AEM, Engels LJA, Ploemacher RE (1998) Blood 91:111
92. Tsuji T, Nishimura-Morita Y, Watanbe Y, Hirano D, Nakanishi S, Mori KJ, Yatsunami K (1999) Growth Factors 16:225
93. Nakamura Y, Ando K, Chargui J, Kawada H, Sato T, Tsuji T, Hotta T, Kato S (1999) Blood 94:4053
94. Kawada H, Ando K, Tsuji T, Shimakura Y, Nakamura Y, Chargui J, Hagihara M, Itagaki H, Shimizu T, Nokuchi S, Kato S, Hotta T (1999) Exp Hematol 27:904
95. Thalmeier K, Meissner P, Reisbach G, Falk M, Brechtel A, Dormer P (1994) Blood 83:1799
96. Bennaceur-Griscelli A, Tourino C, Izac B, Vainchenker W, Coulombel L (1999) Blood 94:529
97. Tordjman R, Ortega N, Coulombel L, Plouet J, Romeo PJ, Lemarchandel V (1999) Blood 94:2301
98. Nishi N, Ishikawa R, Inoue H, Bishikawa M, Yoneya T, Kakeda M, Tsumara H, Ohashi H, Mori LJ (1997) Leukemia (suppl. 3) 11:468
99. Kanai M, Ikeda H, Ikebuchi K (2000) Bone Marrow Trans 26:837
100. Lemoine FM, Humphries RK, Abraham SD, Krystal G, Eaves CJ (1988) Exp Hematol 16:708
101. Sutherland HJ, Eaves CJ, Landsdorp PM, Thaker JD, Hogge DE (1991) Blood 78:666
102. Sutherland HJ, Hogge DE, Cook D, Eaves CJ (1993) Blood 81:1465

Received: April 2001

Cultivation of Hematopoietic Stem and Progenitor Cells: Biochemical Engineering Aspects

Thomas Noll[1,*], Nanni Jelinek[2], Sebastian Schmidt[1,3], Manfred Biselli[1,4], Christian Wandrey[1]

[1] Institut für Biotechnologie 2, Forschungszentrum Jülich GmbH, 52425 Jülich, Germany
E-mail: th.noll@fz-juelich.de
[2] Biogenerix, Janderstr. 3, 68199 Mannheim, Germany
[3] Bayer AG, ZT-TE 5.6, 51368 Leverkusen, Germany
[4] University of Applied Sciences Aachen, Ginsterweg 1, 52428 Jülich, Germany

Dedicated to Prof. Dr. Wolf-Dieter Deckwer on the occasion of his 60th birthday

The ex vivo expansion of hematopoietic cells is one of the most challenging fields in cell culture. This is a rapidly growing area of tissue engineering with many potential applications in bone marrow transplantation, transfusion medicine or gene therapy. Over the last few years much progress has been made in understanding hematopoietic differentiation, discovery of cytokines, isolation and identification of cellular subtypes and in the development of a variety of bioreactor concepts. All this has led to a number of (preliminary) clinical trials that gave a hint of the benefits that can be obtained from the use of expanded hematopoietic cells in therapy. Moreover, as we understand the complexity and the regulation of hematopoiesis, it becomes obvious that highly sophisticated cultivation techniques and bioreactor concepts are needed: a new challenge for bioprocess engineering in cell culture.

Keywords. Hematopoietic cell culture, Stem and progenitor cells, Ex vivo expansion, Bioprocess engineering

* To whom all correspondence should be adressed.

Advances in Biochemical Engineering/
Biotechnology, Vol. 74
Managing Editor: Th. Scheper

Abbreviations

BFU-E	burst-forming unit erythroid
BM	bone marrow
CAFC	cobblestone-area-forming cell
CB	cord blood
CD	cluster of differentiation
CFC	colony-forming cell
CFU	colony-forming unit
CFU-Ba	CFU basophil
CFU-Eo	CFU eosinophil
CFU-E	CFU erythrocyte
CFU-G	CFU granulocyte
CFU-GEMM	CFU granulocyte/erythrocyte/macrophage/megacaryocyte
CFU GM	CFU granulocyte/macrophage
CFU-M	CFU macrophage
CFU-Meg	CFU megacyryocyte
CMV	cytomegalovirus
EBV	Epstein-Barr virus
Epo	erythropoietin
G-CSF	granulocyte-colony-stimulating factor
GM-CSF	granulocyte-macrophage colony-stimulating factor
GVHD	graft-versus-host disease
HSC	hematopoietic stem cell
IL	interleukin
LTC-IC	long-term-culture initiating cell
mM	millimole per liter
MNC	mononuclear cell
MPB	mobilized peripheral blood
MRC	mouse-repopulating cell
M-CSF	macrophage colony-stimulating factor
NK	natural killer
NOD-SCID	non-obese diabetic severe combined immune deficiency
PS	polystyrene
SCEPF	stem cell expansion promoting factor
SCF	stem cell factor
SCM	stromal-conditioned medium
SDF-1	stromal-derived factor 1

TGF-β	transforming-growth factor β
TPO	thrombopietin
VEGF-2	vascular endothelial growth factor 2

1 Introduction

Hematopoiesis, the process of generating mature blood cells, is mainly located in the red bone marrow, predominantly in the sternum, femur and pelvic bones [1]. In the marrow the hematopoietic cells are embedded in stromal tissue. This consists of different cell types (e.g., fibroblasts, endothelial cells, adipocytes, macrophages) that provide soluble and membrane-bound growth factors and produce an extracellular matrix consisting of collagen, laminin, fibronectin, and glycosaminoglycans [2, 3]. The interactions between hematopoietic cells, stromal cells and extracellular matrix are indicated in Fig. 1 [4, 5].

Everyday, almost 400 billion hematopoietic cells of different subtypes are produced in an average human to replace the natural loss of cells [6]. Despite this tremendous proliferation, the balance between the different lineages is very efficiently controlled to guarantee the many functions of the blood (Table 1). If necessary (e.g., in the case of an infection or blood loss caused by an injury) the overall production of blood cells or the maturation of specific subpopulations can even be further significantly increased.

2 The Hematopoietic System

Despite enormous progress, even today the hematopoietic system is not completely understood. However, it is agreed that all hematopoietic cells originate from a small population of pluripotent stem cells that proliferate and differentiate into the whole spectrum of mature blood cells (see Fig. 2) [1]. The pluri-

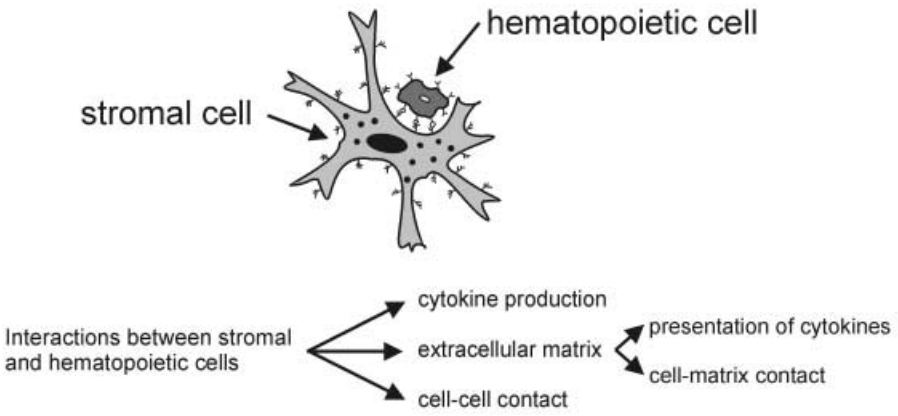

Fig. 1. Interactions between hematopoietic cells and the stroma

Table 1. Function, concentration and life-span of different mature cells in the blood

Cell type	Function	Concentration (cells/ml)	Life span
NK-cells	Kill virus-infected cells and some tumor cells	1×10^5	7–500 d
T-lymphocytes	Antigen-specific, cell-mediated immuneresponse	1×10^6	7–500 d
B-lymphocytes	Antigen-specific, antibody-mediated immuneresponse	2×10^6	Unknown
Basophilic granulocytes	Release of histamine and serotonine in certain immune reactions	4×10^4	Few hours
Eosinophilic granulocytes	Destroy larger parasites and modulate allergic inflammatory responses	2×10^5	3–8 h
Neutrophilic granulocytes	Phagocytose and destroy invading bacteria	5×10^6	6–9 h
Monocytes	Differentiate to macrophages, which phagocytose damaged cells and bacteria	4×10^5	3–6 d
Thrombocytes	Initiate blood clotting	3×10^8	1 week
Erythrocytes	Transport of O_2 and CO_2	5×10^9	4 months

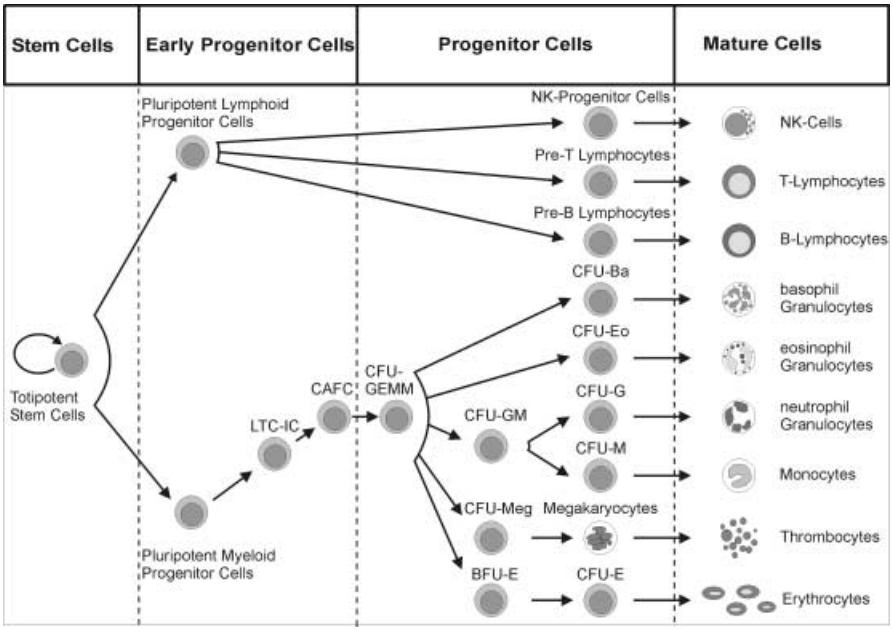

Fig. 2. Structure of the hematopoietic system

potent stem cells are the only ones with self-renewable capacity and for all other cells proliferation is inevitably combined with a lineage-specific differentiation and loss of immaturity. Every step of differentiation and maturation is regulated and controlled in vivo by the cell's microenvironment. This means that a cell cultivation technique that aims at generating a specific subpopulation has to meet the cells specific environmental requirements.

A great challenge in hematopoietic cell culture is the identification of the cells. While mature blood cells can easily be detected by their morphology and by flow cytometric analysis of characteristic surface molecules, the identification of progenitor cells needs time-consuming in vitro assays like colony-forming cell (CFC) assay, cobblestone-area-forming cell (CAFC) assay or long-term-culture initiating-cell (LTC-IC) assay. In the CFC assay a small number of cells are cultivated for 2 weeks in a semi-solid medium containing cytokines. Colony-forming cells generate a colony of more differentiated cells depending on their lineage specificity (e.g., a CFU-G forms a colony of granulocytes). For the detection of more primitive progenitor cells, the CAFC or LTC-IC assay is used. Here a small number of cells are placed on a stromal cell layer for 6–8 weeks. During this period the early progenitor CAFC and LTC-IC differentiate and, in the case of CAFC, cobblestone-area-like cells are formed that can be easily identified. In the case of LTC-IC the early progenitor cells differentiate into CFC, which are detected using a subsequent CFC assay [7, 8]. By extension of the cultivation time up to 14 weeks (extended long-term culture), even more immature cells than LTC-IC can be identified [9, 10]. For the detection of the pluripotent stem cells only in vivo assays are available, which use the potential of these cells to repopulate irradiated, immunodeficient mice (NOD-SCID), sheep or monkeys [11–13].

The identification of stem and progenitor cells using flow cytometry has intrinsic difficulties as some surface molecules vanish while others occur during differentiation and true stem cell markers are still unknown. It was long thought that CD34 could act as a marker of stem cells as the CD34+ population contains a high amount of CFC, LTC-IC and MRC [14]. However, some publications describe a mouse-repopulating capacity for a population of cells which are CD34– but do not have markers of more mature states [15, 16]. One of the most recent theories describes the stem cell population as CD34–, which, after activation, can develop the CD34 molecule in a reversible process [17, 18]. Other surface molecules that are supposed to identify the stem cell or at least very early progenitors are AC133, KDR and CXCR-4 [19–21]. However, as the cellular phenotype determined by flow cytometry and the biological function of the cells do not coincide in every case, as shown by Dorrell [22], functional in vitro assays are strongly recommended.

2.1 Sources of Hematopoietic Cells

There are three sources of hematopoietic stem and progenitor cells available: bone marrow (BM), peripheral blood after stem cell mobilization (MPB) and umbilical cord blood (CB).

Bone marrow is the natural site of hematopoiesis and was therefore the first source of hematopoietic stem and progenitor cells. In addition to the hematopoietic cells primary stroma can also be collected simultaneously from this source. However, as the harvesting of cells from bone marrow is an invasive procedure that requires manual extraction under spinal or general anesthesia, alternative sources are preferred whenever possible, although, for allogeneic stem cell transplantation, bone marrow is still the source of choice [23].

Peripheral blood normally does not contain significant amounts of stem and progenitor cells but, after administration of G-CSF or GM-CSF or a light chemotherapy protocol, stem and progenitor cells circulate in higher numbers and can be isolated by leukaphoresis [24]. This is the standard procedure to collect hematopoietic stem and progenitor cells from patients for autologous transplantation after high-dose chemotherapy [23].

Umbilical cord blood as a source of hematopoietic stem and progenitor cells has many advantages. It is easily accessible by a procedure noninvasive for the mother or the neonate and contains a significant amount of progenitor cells with high proliferative potential [25]. The burden of CB with common viral contaminations like EBV and CMV is lower than that of MPB or BM and, as the lymphocytes are more naive, the risk of a graft-versus-host disease (GVHD) is reduced [24]. The main disadvantage of cord blood is the low number of cells obtained due to the small volume of blood collectable from umbilical cords. Without an expansion of the stem and progenitor cells, a transplantation is limited to a body weight of about 40 kg making this therapy only available for juvenile patients [26].

2.2 Potential Medical Applications

Expanded hematopoietic (stem and progenitor) cells have widespread potential in therapy and this will only be briefly described here. For a comprehensive overview, the review by Schindhelm and Nordon [27] is recommended. Potential applications include 'graft engineering' in stem cell transplantation [24], gene and immunotherapy and the production of mature blood cells for transfusion medicine.

Both chemotherapy and radiation therapy in cancer treatment are based on the fact that tumor cells are continuously proliferating and these procedures are therefore aimed at cells in mitosis. All other cells that undergo rapid proliferation are also damaged and this applies especially to the hematopoietic system [28]. In high-dose chemotherapy doses of cytotoxic drugs are increased to a level that is supposed to also eradicate residual tumor cells. This also leads to a total loss of all hematopoietic stem cells, making an autologous or allogeneic stem cell transplantation obligatory. Expansion of stem and progenitor cells can either increase the number of umbilical cord blood derived cells, making this source also available for adult patients, or result in a reduction in the number of leukaphoresis procedures necessary for the collection of autologous cells. The transplantation of lineage-restricted progenitor cells can help to reduce the period of neutropenia after chemotherapy, and, in

the case of megacaryocytes, alleviate post-transplant-associated thrombocytopenia [29].

Expansion of specific T-lymphocytes or natural killer cells gives access to cell-mediated immunotherapy, while the generation and specific loading of dendritic cells offers possibilities for the in vivo induction of antigen-specific immunity [30]. Furthermore, the generation of erythrocytes or thrombocytes can lead to blood transfusions without a risk of viral contaminants. Finally, stem cells are an appropriate target for somatic gene therapy as they can offer a chance of a lifelong cure from genetic disorders due to their self-renewing capacity.

3 Cultivation Parameters

As outlined earlier every single step of hematopoiesis is regulated and controlled in vivo by the cell's microenvironment. This not only includes the composition and concentration of growth factors, but also the local oxygen concentration, the pH, the osmolality, the supply of nutrients and the cellular and molecular surrounding of the cells (cell-cell contact, adhesion molecules and extracellular matrix). All these parameters affect the fate of the cell and, to establish a cell culture process to cultivate or generate a specific subpopulation, the influence of all these factors has to be considered in the experimental set-up. In the following sections these parameters will be discussed in brief.

3.1 Cytokines

In the bone marrow, cytokines are produced predominantly from stromal cells, although accessory and hematopoietic cells themselves have also been shown to secrete growth factors [31–33]. Cytokines affect nearly all processes of hematopoiesis, like proliferation, differentiation, adhesion and functional properties of the cells, while, in the absence of cytokines, HSC suffer apoptosis [34]. The effects of hematopoietic cytokines are very complex and show synergistic as well as antagonistic interactions. Changes in the cytokine concentrations during cultivation can cause significant changes in the proliferation and the differentiation of the cells. Therefore, the control of cytokine composition is an extremely important element of the bioprocess strategy. For the expansion of stem and progenitor cells, interleukin 3 (IL-3), interleukin 6 (IL-6), stem cell factor (SCF), thrombopoietin (TPO) and flt3 ligand (FL) are thought to play major roles [35–37] and are mostly used in the expansion of hematopoietic stem and progenitor cells.

The number of cytokines known to influence hematopoiesis is steadily growing. The most recently identified cytokines are SDF-1 [38], VEGF2 [39] and SCEPF [40], but there are still growth factors in the stromal environment to be identified. This has been proven by the additional growth-supportive effects of stroma-conditioned medium on the proliferation of hematopoietic stem cells.

Due to the complexity and the manifold interactions between cytokines, determination of an optimum cytokine mix for stem cell cultivation is difficult and most optimization algorithms are inefficient. Significant progress can be made using genetic algorithms, as shown by Thoma et al. [41].

3.2 Culture Media and Feeding Schedules

The choice of the culture medium, especially the use of serum, directly influences the differentiation of the cells and therefore the aims of the cultivation should be considered when determining the medium to be used [1]. Serum normally contains TGF-β, which is known to inhibit the erythroid and megacaryocytic lineage, therefore promoting the granulocytic and macrophage differentiation [42]. In stroma-containing culture, serum strengthens the adhesion of the cells and stabilizes the feeder layer. A further aspect which has to be considered in the use of animal serum (e.g., fetal bovine or horse) is the clinical applicability, as media containing components from animal sera will face more regulatory hurdles than serum-free compositions [43].

Because hematopoiesis in the bone marrow takes place under static conditions [1], with a continuous feed of nutrients and a simultaneous removal of waste products, several feeding strategies have been developed in the cultivation of hematopoietic cells. In static cultivations feeding schedules have been described, which range from half medium exchange per week up to a total daily exchange [44, 45]. Most perfused cultures were not continuously supplied with fresh medium. From a reservoir the medium is fed into the cultivation chamber containing the cells and then back into the reservoir, which is intermittently replaced by fresh medium, leading to exchange rates between half a medium exchange three times per week and a total daily exchange [46–48]. Palsson et al. [49] and Meissner et al. [50] have both described cultivations using a continuous supply with a fresh culture medium.

Feeding of fresh medium prevents the limitation of growth from a lack of substrates as well as inhibition from the accumulation of metabolic by-products. This has recently been investigated in detail for lactate, when Patel et al. found that a lactate concentration of more than 20 mM inhibits cell proliferation and metabolism, although it has little effect on cell differentiation [51].

3.3 Oxygen Tension

Oxygen tension plays an important role in hematopoietic cell culture as it directly influences the cellular proliferation and differentiation [1]. In the bone marrow, oxygen concentrations of 5%–30% of air saturation have been described [52]. Low oxygen levels (5%) support the proliferation of colony-forming cells (CFC), probably due to decreased oxidative damage and an increased responsiveness to growth factors like Epo or M-CSF [53, 54]. This has been demonstrated in the cultivation of cord blood MNC with and without stromal feeder layers. High oxygen tension (20%–30%) promotes the growth of

mature erythroid and megacaryocytic cells, while mature granulocytes show higher proliferation at low oxygen levels [1]. Together with the choice of cytokine combination, this can be used to control and direct the proliferation and differentiation of the culture towards the cells of interest. This is a challenge for bioprocess engineering, as the oxygen concentration in the medium has to be measured accurately and controlled exactly to avoid oxygen limitations. This is especially important in the cultivation of stem and progenitor cells at low oxygen levels. According to the growth of the cells the oxygen transfer has to be adjusted by increasing the oxygen concentration in the gas phase, increasing the perfusion or increasing the agitation rates.

3.4 pH

The regulation of hematopoiesis in the bone marrow is not only controlled by the cytokine composition, the cells microenvironment and the oxygen tension, but, as shown recently [55], also by the local pH. For cells of different lineages deviating pH optima have been described. While CFU-GM proliferate best in a pH range 7.2–7.4 (the normal pH of blood), for erythroid cells an optimum of pH 7.6 was found. Below an acidic pH of 6.7 no differentiation or proliferation of any hematopoietic cell was observed. Cells of the erythroid lineage are even strongly inhibited at a pH below 7.1 [56].

To avoid inhibition of proliferation and differentiation the pH in hematopoietic cell cultures has to be controlled carefully. Especially in non-perfused culture the pH shifts during the cultivation due to secreted acidic metabolites like lactate. However is has been reported recently that pH control alone is not sufficient to eliminate inhibition of cell growth and metabolism as other inhibitory factors also accumulate in un-fed cultures [51].

3.5 Osmolality

Hematopoietic cells like all mammalian cells are quite sensitive to changes in osmolality. We have recently examined the effect of osmolality (0.26–0.38 mOsmol/kg) on human hematopoietic proliferation and differentiation and found an optimum for the expansion of MNC and CD34+ cells in a range between 0.31 and 0.32 mOsmol per kg, as described earlier by McAdams [57]. While MNC show a symmetric decrease in proliferation for osmolalities beyond this range, for CD34+ cells a much greater sensitivity for hypertonic conditions was found [58]. At the level of colony-forming cells distinct differences have been observed. Progenitors of the granulocytic and macrophage lineage show maximum proliferation at slightly hypotonic osmolalities (0.29 mOsmol/kg), while BFU-E proliferation is enhanced at hypertonic levels (0.34 mOsmol/kg). This finding might offer an additional opportunity to direct the proliferation and differentiation by adjusting the appropriate culture conditions.

3.6 Biocompatibility of Materials

As outlined earlier, hematopoiesis is a complex process that is influenced and affected by a multitude of factors. Thus, the biocompatibility of materials is an important issue in hematopoietic culture. It has to be ensured that all materials that are in contact with hematopoietic cells or their culture medium do not leach any toxins or adhere medium components. In case of cell immobilization, additional effects of the materials surface (e.g., charge) have to be considered. LaIuppa investigated the influence of a wide range of materials on the proliferation and differentiation of hematopoietic cells in comparison to polystyrene (the standard material in cell culture) [59, 60]. She found that colony-forming-cell expansion is more affected than total cell expansion and CD34+ cells are more sensitive than MNC. In our own studies we compared different materials that are commonly used in the construction of bioreactors for their influences in hematopoietic culture, with and without serum [58]. Direct contact was investigated, as well as their potential to release toxins into the culture medium and to adhere essential medium components. By preincubating medium with a sample of the materials, it was clearly demonstrated that the inhibitory effects are much stronger in direct contact, and in the absence of serum. The protective effect of serum is probably caused by the material's surface being coated with protein. A direct correlation was found between the inhibitory effect and the ratio of the material's surface to medium volume (cm^2/ml). For example, glass with a ratio of 1 showed no inhibitory effects either on the expansion of MNZ or CD34+ cells or on the CFC. If one increases the ratio to 3.8 the expansion of colony-forming cells compared to polystyrene (PS) dropped about 50%, while MNZ and CD34 expansion only slightly decreased. A further increase in the surface-to-volume ratio (11.3) resulted in a 95% decrease of CFC expansion when compared to PS. Expansion of mononuclear and CD34+ cells was also significantly reduced (75% and 85%, respectively). In most bioreactor concepts the material surface to medium volume is in a range that makes inhibitory effects unlikely, but this should be evaluated when developing a new hematopoietic culture system.

4 Concepts of Cultivation

As outlined earlier, hematopoietic cells have a widespread potential in medicine, but all of the envisaged applications necessitate the generation of large amounts of cells. This is true for stem and progenitor cells as well as for mature hematopoietic cells. In every case the bioprocess has to meet the following requirements:

Large Cell Expansion in Short Time. Most of the cells needed for therapy have to be patient-specific and therefore must be provided 'on demand' and in a number sufficient for one patient. A billion-fold expansion in a timeframe of months fails to meet the clinical requirements. For example, in the case of a

stem cell transplantation after high-dose chemotherapy, the expansion of the cells has to be performed during the chemotherapy protocol, giving the cultivation no more than 7–10 d. An exception might be megacaryocytes, used for the treament of thrombocytopenia, which can be cryopreserved and thawed in the necessary amount prior to transfusion.

Considering the normally small amount of cells in the early stage of culture and the significant increase during cultivation, the bioreactors used should enable not only an increase in cell density but also in culture volume without changing the culture system.

Easy Cell Harvest. In this type of bioprocess the cells are the products so a method for an easy cell harvest must be provided. Neither a substantial loss in cell number nor damage to the cells is acceptable, because this would directly affect the therapeutic value of the transplant. A large number of labor-intensive isolation and purification steps is also unacceptable. This is not only because of the increase in time and costs, but also due to the increasing risk of contamination.

Controlled Culture Conditions. As described above, the culture conditions have an enormous influence on the proliferation and differentiation of hematopoietic (stem and progenitor) cells. Slight changes in the oxygen tension, the pH or the medium and growth factor composition can result in significant alterations in the differentiation pattern and the proliferative potential. This, in combination with the small starting volume in the early stage of culture, is a great challenge for bioprocess engineering. The materials used for the bioreactor setup, as well as the mechanical forces occurring during cultivation, have to be adapted to the intended subtype of cells.

Clinical Applicability. The regulatory conditions for cell therapy directly refer to the cells and the materials utilized during the cultivation. The use of cell lines, especially those of animal origin (e.g. stromal cell lines in cocultivation), and the use of animal serum should carefully be reconsidered, as this will make the seeking of clinical approval a difficult task.

In case of stem and progenitor cells, which are the focus of this review, many strategies for cultivation and expansion have been developed, as shown in Fig. 3.

4.1
Cultivation of Isolated Stem and Progenitor Cells

Since the development of recombinant human cytokines, cultivation and significant expansion of isolated hematopoietic stem and progenitor cells is possible without a supporting feeder-layer of stromal cells. It is the simplicity of these culture systems that is their main attraction [29]. The cells are cultivated in chemically defined culture medium containing defined combinations of cytokines and without any stromal products. On the one hand this enables a better control of the culture and the investigation of the influence of single cytokines or culture conditions. On the other hand, as our understanding of stem cell regu-

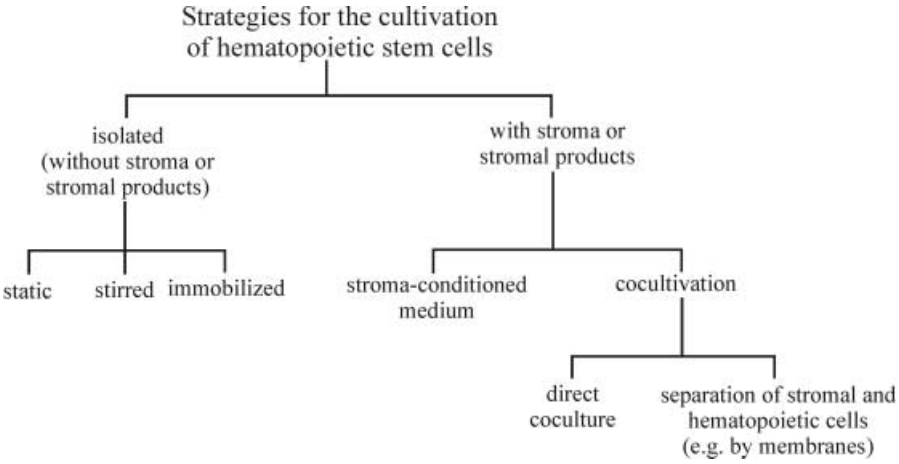

Fig. 3. Strategies for the cultivation of hematopoietic stem and progenitor cells

lation is still incomplete and it is hypothesized that stromal influences regulate in vivo hematopoiesis, it is likely that the cultivation of isolated hematopoietic cells results in suboptimal expansion. This is supported by our own results, which show significantly better expansion, especially of early progenitors, in the presence of stromal cells [61].

Three different approaches for the cultivation of isolated hematopoietic cells have been described, the static, the stirred and the immobilized culture. Static cultivation takes place in very simple culture systems like well plates, tissue-culture flasks or gas-permeable culture bags [62, 63]. As the first two systems do not allow cell cultivation on a clinical scale, the latter is actually the most often used technique for stem cell expansion. All these systems have the advantage of being easy to handle, single-use devices, which enable an uncomplicated cell harvest. But all of them do not offer possibilities for process control or continuous feeding. This causes variations in culture conditions during fermentation (e.g., oxygen tension, pH, substrate, metabolite and cytokine concentrations).

Stirred bioreactors are common in animal cell culture, as they offer a homogenous environment, representative sampling, better access to process control and an increased oxygen transfer. Several of these techniques (spinner flasks and stirred vessel bioreactors) have been tested successfully for the cultivation of hematopoietic cells [58, 64–67].

The immobilization of stem and progenitor cells is an attempt to reach local high cell densities and to imitate the three-dimensional structure of the bone marrow without the use of stroma. A number of porous microcarriers with and without additional coating of components of an extracellular matrix (e.g., collagen, fibronectin, laminin) have been investigated for this purpose. Bagley et al. compared different porous materials and described a greater than sixfold expansion of CFC in a long-term cultivation of CD34+ cells in tantalum-coated porous carriers, even without adding exogenous cytokines [68]. However, stem cell immobilization, especially in porous materials, requires a technique for

detaching the cells from the matrix prior to transplantation, a significant disadvantage compared to suspension culture.

Hollow fiber modules and the microencapsulation of progenitor cells have been used in hematopoietic culture with less success [69, 70]. Furthermore, these approaches do not fit the clinical requirements, as the harvest of the cells is almost impossible.

The most sophisticated technique for stem cell expansion is the Aastrom-Replicell system (Aastrom Biosciences Inc., Ann Arbor, MI, USA), which is an automated clinical system for the onsite expansion of stem cells in cancer therapy. It consists of a grooved perfusion chamber for the retention of the hematopoietic cells, with the medium flow perpendicular to the channel grooves resulting in a continuous supply of fresh nutrients while metabolites are simultaneously removed [47, 71, 72]. This technique has already been used in a number of clinical studies [73, 74]. No incompatibility of the expanded cells was found, but the expansion of the early progenitor cells was rather low [75].

Local high cell densities, as they are realized in the pores of microcarriers or in the grooves of the AastromReplicell, have been described to make bone marrow MNC essentially stroma-independent in terms of LTC-IC maintenance and expansion [44]. This might also be the reason for the good expansion of progenitors in the culture bags, where the cells accumulate in the wrinkles of the bag and reach local high cell densities.

4.2 Cultivation with Stromal Cells or Stroma-Derived Factors

Before the discovery and development of recombinant human cytokines, a feeder layer of stromal cells was essential for the cultivation of hematopoietic cells. The first system for the successful expansion of hematopoietic cells from murine origin was described by Dexter more than 20 years ago [76, 77]. Some years later this principle was transferred to human cells [78]. Stromal culture of hematopoietic cells is a generic term that covers a variety of cultivation concepts, as indicated in Fig. 3.

The most simple strategy is the application of exogenous stromal-conditioned medium [79, 80]. Stromal cells secrete numerous different growth factors necessary for the maintenance and expansion of stem and progenitor cells and many of these substances are still unknown. Some attempts have already been made to characterize them [81] and, in the future, significant progress can be expected using techniques developed for proteomics analysis. The use of conditioned medium enables the application of all bioreactor systems developed for the cultivation of isolated stem and progenitor cells and allows the culture to be supplied with (unidentified) growth factors secreted from the stroma. The conditioned medium can be produced in large amounts exogenously and stored until application.

A variation of this approach is the in situ generation of stromal-conditioned medium in a stroma non-contact co-culture (e.g., seperated by microporous membranes). This permits an interaction between stromal and hematopoietic cells mediated by secreted molecules, which has been described to support the

expansion of the early progenitor cells more efficiently than the use of exogenous conditioned medium [82]. Disadvantageous in this technique is the increase in the technical requirements for the set-up and process control.

One important element in the in vivo regulation of hematopoiesis is missing in the approaches using conditioned medium: the cell-cell contact between hematopoietic and stromal cells. This mimicry of the bone marrow has been reproduced in several types of bioreactors providing direct coculture of progenitors on a two- or three-dimensional stromal feeder layer. Tissue-culture flasks were used as well as microcarriers (in spinner flasks, airlift or fixed-bed bioreactors), nonwoven fabrics disks, large pore-size cubes or nylon screens [50, 61, 70, 76, 83–85]. In many of these cultivations expansion of the early progenitors is superior to that obtained in stroma-free culture. In our own study we reached a 100-fold expansion of MNC and CFC and a more than 6-fold expansion of CAFC in a fixed-bed bioreactor within 14 d [61]. Köhler et al. described a trend toward decreased apoptosis in culture with bone marrow stroma indicating the supportive character of the feeder layer [86].

For stromal culture, besides primary stroma from bone marrow, a variety of stromal cell lines are available. However, most are from murine origin, and human cell lines that support hematopoiesis are not efficiently available (Table 2). The human cell lines L87/4 and L88/5 are difficult to irradiate and favor differentiation and maturation over the expansion of early progenitors [87, 88].

The main attraction of stromal culture of hematopoietic cells is their superior ability for stem cell expansion especially in direct co-culture. However, despite this, a clinical use has not been realized until now. The major drawback is the origin of the stromal support. While autologous stroma would be feasible, in many cases this is not realizable. Furthermore, the use of cell lines (although irradiated to prevent further proliferation) is problematic as all stromal cells have to be removed completely prior to transplantation, a demand which is difficult to fulfill. In the case of murine cell lines a transfer of residue cells into a patient would be a xenotransplantation, which is faced with extensive regulatory hurdles.

Recently, a new approach has been reported that may offer co-culture a chance to be clinical applicable. Kawada et al. described a co-cultivation of stromal and hematopoietic cells separated by a porous membrane that enables a di-

Table 2. Stromal cell lines used in the cultivation of hematopoietic stem and progenitor cells

Cell line	Origin	Application	References
AC6.21	Murine	Co-culture and SCM	40, 89
FBMD-1	Murine	Co-culture and SCM	79, 90, 91
HESS-5	Murine	Co-culture	92–94
L87/4, L88/5	Human	Co-culture and SCM	79, 87, 95
MS-5	Murine	Co-culture and SCM	96–99
M2-10B4	Murine	Co-culture	50, 87, 100, 101
M2-10B4mod	Murine	Co-culture	61, 102
Sl/Sl	Murine	Co-culture	61, 102

rect contact between the cells by their extracellular matrix, but prevents the stromal cells from entering the hematopoietic compartment [94]. This work was carried out on small scale in a transwell, but a scale-up to a clinical level seems possible.

5 Conclusions and Outlook

The ex vivo expansion of hematopoietic cells is a rapidly growing area of tissue engineering with many potential applications in medicine. During the last few years a variety of bioreactor concepts and cultivation strategies have been developed, but no final decision has been made about the optimal system for hematopoietic culture.

The cultivation of isolated stem and progenitor cells has some distinct advantages like its simplicity, clinical applicability and the possibility to use standard cell culture techniques, but the expansion of the early progenitor cells shown in different clinical studies was rather low. The use of stromal-conditioned medium promises better expansion and lower costs due to the reduced need for exogenous cytokine supplementation, but the culture medium is chemically undefined, which will render reproducibility more difficult and complicate the clinical permission. Co-cultivation of stromal and hematopoietic cells results in the best expansion of early progenitor cells, but, as nearly all stromal cell lines are of murine origin, a clinical application of this approach is hardly possible. Membrane-separated co-cultivation may offer a possibility to avoid this disadvantage.

What can be expected from the future? The cultivation of isolated hematopoietic cells will benefit from the identification of new cytokines, making the use of stromal-conditioned medium unnecessary. The recent development of proteomics techniques will expediate this process. The prospects of the co-cultivation will depend on the development of human stromal cell lines supporting the expansion of early progenitor cells, and the membrane approach has to prove its potential on a clinical scale.

In summary, for the near future it can be expected that culture systems of sufficient simplicity, productivity and reliablity will be developed and tested in clinical studies, making transplantation therapies utilizing cultured hematopoietic cells a more common application in medicine.

Acknowledgement. We thank Dr. Joy Burchell for careful revision of the manuscript.

References

1. McAdams TA, Miller WM, Papoutsakis ET (1996) TIBTECH 14:341
2. Wilkins BS (1992) J Clin Pathol 45:645
3. Verfaillie C, Hurley R, Bhatia R, McCarthy JB (1994) Crit Rev Oncol/Hematol 16:201
4. Mayani H, Guilbert LJ, Janowska-Wieczorek A (1992) Eur J Hematol 49:225
5. Deryugina EI, Muller-Sieburg CE (1993) Crit Rev Immunol 13:115
6. Koller MR, Palsson BO (1993) Biotechnol Bioeng 42:909

7. Sutherland HJ, Lansdorp PM, Henkelman DH, Eaves AC, Eaves CJ (1990) Proc Natl Acad Sci 87:3584
8. Breems DA, Blokland EAW, Neben S, Ploemacher RE (1994) Leukemia 8:1095
9. Ploemacher RE (1997) Baillière's Clinical Hematology 10:429
10. Ramsfjell V, Bryder D, Björgvinsdottir H, Kornfält S, Nilsson L, Borge OJ, Jacobsen SEW (1999) Blood 94:4093
11. Lapidot T, Pflumio F, Doedens M, Murdoch B, Williams DE, (1992) Science 255:1137
12. Shimizu Y, Ogawa M, Kobyashi M, Almeida-Porada G, Zanjani ED (1998) Blood 91:3688
13. Brandt JE, Bartholomew AM, Fortman JD, Nelson MC, Brumo E, Chen LM, Turian FV, Davis TA, Chute JP, Hoffman R (1999) Blood 94:106
14. Krause DS, Fackler MJ, Civin CI, Stratford W (1996) Blood 87:1
15. Bhatia M, Bonnet D, Murdoch B, Gan OI, Dick JE (1998) Nature Med 4:1038
16. Zanjani ED, Almeida-Porada G, Livingston AG, Flake AW, Ogawa M (1998) Exp Hematol 26:353
17. Goodell MA (1999) Blood 94:2545
18. Sato T, Laver JH, Ogawa M (1999) Blood 94:2548
19. Yin AH, Miraglia S, Zanjani ED, Almeida-Porada G, Ogawa M, Leary AG, Olweus J, Kearney J, Buck DW (1997) Blood 90:5002
20. Ziegler BL, Valitieri M, Almeida-Porada G, De Maria R, Muller R, Masella B, Gabbianekki M, Casella I, Pelosi E, Bock T, Zanjani ED, Peschle C (1999) Science 285:1553
21. Kawabata K, Ujikawa M, Egawa T, Kawamoto H, Tachibana K, Iizasa H, Katsura Y, Kishimoto T, Nagasawa T (1999) Proc Natl Acad Sci 96:5663
22. Dorrell C, Gan OI, Pereira DS, Hawley RG, Dick JE (2000) Blood 95:102
23. Rowlings PA (1999) In: Schindhelm K, Norton R (eds) Ex vivo cell therapy. Academic Press, San Diego, p 85
24. McAdams TA, Winter JN, Miller WM, Papoutsakis ET (1996) TIBTECH 14:388
25. Kim DK, Fujiki Y, Fukushima T, Ema H, Shibuya A, Nakauchi H (1999) Stem Cells 17:286
26. Cairo MS, Wagner JE (1997) Blood 90:4665
27. Schindhelm K, Nordon R (1999) (eds) Ex vivo cell therapy. Academic Press, San Diego
28. Collins PC, Papoutsakis ET, Miller WM (1996) Curr Opin Biotechnol 7:223
29. Alcorn MJ, Holyoake TL (1996) Blood Rev 10:167
30. Bremers AJA, Parmiani G (2000) Crit Rev Oncol/Hematol 34:1
31. Linenberger ML, Jacobsen FW, Bebbett LG, Broudy VC, Martin FH, Abkowitz JL (1995) Exp Hematol 23:1104
32. Lisovsky M, Braun SE, Ge Y, Takahari H, Lu L, Savchenko VG, Lyman SD, Broxmeyer HE (1996) Leukemia 10:1012
33. Guerriero A, Worford L, Holland HK, Guo GR, Sheehan K, Walle EK (1997) Blood 90: 3444
34. Cottner TG, Fernandes RS, Verhaegen S, McCarthy JV (1994) Immunol Rev 142:93
35. Piacibello W, Sanavio F, Garetto L, Severino A, Bergandi D, Ferrario J, Fagioli F, Berger M, Aglietta M (1997) Blood 89:2644
36. Murray LJ, Young JC, Osborne LJ, Luens KM, Scollary R, Hill BL (1999) Exp Hematol 27:1019
37. Ramsfjell V, Bryder D, Björgvinsdottir H, Kornfält S, Nilsson L, Borge OJ, Jacobsen SEW (1999) Blood 94:4093
38. Möhle R, Bautz F, Rafii S, Moore MAS, Brugger W, Kanz L (1998) Blood 91:4523
39. Eichmann A, Corbel C, Nataf V, Vaigot P, Breánt C, LeDouarin N (1997) Proc Natl Acad Sci 94:5141
40. Shih CC, Hu MC, Wenig Y, Yazaki PJ, Medeiros J, Forman SJ (2000) Blood 95:1957
41. Thoma S, Schmidt S, Jelinek N, Herfurth C, Takors R, Wandrey C, Biselli M (1999) Onkologie 22 (suppl 1):180
42. Dybedal I, Jacobsen SE (1995) Blood 86:949
43. Sandstrom CE, Miller WM, Papoutsakis ET (1994) Biotechnol Bioeng 43:706
44. Koller MR, Manchel I, Palsson MA, Maher RJ, Palsson BO (1996) Biotechnol Bioeng 50:505

45. Schwartz RM, Palsson BO, Emerson SG (1991) Proc Natl Acad Sci 88:6760
46. Sandstrom CE (1995) PhD thesis, Northwestern University, Evanston
47. Sandstrom CE, Bender JE, Miller WM, Papoutsakis ET (1996) Biotechnol Bioeng 50: 493
48. Wang TY, Brennan JK, Wu JHD (1995) Exp Hematol 23:26
49. Palsson BO, Paek SH, Schwartz RM, Palsson MA, Lee GM, Silver S, Emerson SG (1993) Bio/Technology 11:368
50. Meissner P, Schroeder B, Herfurth C, Biselli M (1999) Cytotechnology 30:227
51. Patel SD, Papoutsakis ET, Winter JN, Miller WM (2000) Biotechnol Prog 16:885
52. Ishikawa Y, Ito T (1988) Eur J Hematol 40:126
53. Rich IN, Kubanek B (1986) Br J Hematol 52:579
54. Broxmeyer HE, Cooper S, Lu L, Miller ME, Langefeld CD, Ralph P (1990) Blood 76:323
55. Hehevan DL, Papoutsakis ET, Miller WM (2000) Exp Hematol 28:267
56. McAdams TA, Papoutsakis ET, Miller WM (1995) Blood (suppl. 1) 86:674a
57. McAdams TA (1997) PhD thesis, Northwestern University, Evanston
58. Schmidt S (2000) PhD thesis, University RWTH, Aachen
59. LaIuppa JA, McAdams TA, Miller WM, Papoutsakis ET (1995) Blood (Suppl. 1) 86:231a
60. LaIuppa JA, McAdams TA, Papoutsakis ET, Miller WM (1997) Biomed Mat Res 36:347
61. Jelinek N (2000) PhD Thesis University RWTH Aachen
62. Brugger W, Heimfeld S, Berenson RJ, Mertelsmann R, Kanz L (1995) N Eng J Med 333:283
63. Alcorn MJ, Holyoake TL, Richmond L (1996) J Clin Oncol 14:1839
64. Collins PC, Miller WM, Papoutsakis ET (1998) Biotechnol Bioeng 59:534
65. Kim BS (1998) Biotechnol Lett 20:595
66. Zandstra PW, Petzer AL, Eaves CJ, Piret JM (1997) Biotechnol Bioeng 54:58
67. De León A, Mayani H, Ramirez OT (1998) Cytotechnology 28:127
68. Bagley J, Rosenzweig M, Marks DF, Pykett MJ (1999) Exp Hematol 27:496
69. Levee MG, Lee GM, Paek SH, Palsson BO (1994) Biotechnol Bioeng 43:734
70. Sardonini CA, Wu YJ (1993) Biotechnol Prog 9:131
71. Sandstrom CE, Bender JG, Papoutsakis ET, Miller WM (1995) Blood 86:958
72. Koller MR, Maher RJ, Manchel I, Oxender M, Smith AK (1998) J Hematotherapy 7:413
73. Bachier CR, Gokmen E, Teale J, Lanzkron S, Childs C, Franklin W, Shpall E, Douville J, Weber S, Muller T, Armstrong D, Lemaistre CF (1999) Exp Hematol 27:615
74. Chabannon C, Novakovitch G, Blache JL, Olivero S, Camerlo J, Genre D, Maraninchi D, Viens P (1999) Hematol Cell Ther 41:78
75. Chabannon C, Blache JL, Sielleur I, Douville J, Faucher C, Gravis G, Arnoulet C, Oziel-Taieb S, Blaise D, Novakovitch G, Camerlo J, Chabbert I, Genre D, Appel M, Armstrong D, Maraninchi D, Viens P (1999) Int J Oncol 15:511
76. Dexter TM, Wright EG, Krizsa F, Lajtha LG (1977) Biomedicine 27:344
77. Dexter TM, Allen TD, Laijtha LG (1977) J Cell Physiol 91:335
78. Gartner S, Kaplan HS (1980) Proc Natl Acad Sci 77:4756
79. Breems DA, Blokland EAW, Ploemacher RE (1997) Leukemia 11:142
80. Bhatia R, McGlave PB, Lin W, Wissink S, Miller JS, Verfaillie CM (1995) Blood (Suppl. 1) 86:294a
81. Gupta P, McCarthy JB, Verfaillie CM (1996) Blood 87:3229
82. Verfaillie CM, Catanzarro PM, Li W (1994) J Exp Med 179:643
83. Highfill JG, Haley SD, Kompala DS (1995) Biotechnol Bioeng 50:514
84. Naughton BA, Naughton GK (1991) J Biomech Eng 113:171
85. Tomimori Y, Tagaki M, Yoshida T (2000) Cytotechnology 34:121
86. Köhler T, Plettig R, Wetzstein W, Schaffer B, Ordemann R, Nagels HO, Ehninger G, Bornhauser M (1999) Stem Cells 17:19
87. Schroder B (1997) PhD thesis, University of Bonn
88. Bertolini F, Battaglia M, Soligo D, Corsini C, Curioni C, Lazzari L, Pedrazzoli P, Thalmeier K (1997) Exp Hematol 25:350
89. Shih CC, Hu MCT, Hu J, Medeiros J, Forman SJ (1999) Blood 94:1623

90. Breems DA, Van Driel EM, Hawley RG, Siebel KE, Ploemacher RE (1998) Leukemia 12:951
91. Breems DA, Blokland EAW, Siebel KE, Mayen AEM, Engels LJA, Ploemacher RE (1998) Blood 91:111
92. Tsuji T, Nishimura-Morita Y, Watanbe Y, Hirano D, Nakanishi S, Mori KJ, Yatsunami K (1999) Growth Factors 16:225
93. Nakamura Y, Ando K, Chargui J, Kawada H, Sato T, Tsuji T, Hotta T, Kato S (1999) Blood 94:4053
94. Kawada H, Ando K, Tsuji T, Shimakura Y, Nakamura Y, Chargui J, Hagihara M, Itagaki H, Shimizu T, Nokuchi S, Kato S, Hotta T (1999) Exp Hematol 27:904
95. Thalmeier K, Meissner P, Reisbach G, Falk M, Brechtel A, Dormer P (1994) Blood 83:1799
96. Bennaceur-Griscelli A, Tourino C, Izac B, Vainchenker W, Coulombel L (1999) Blood 94:529
97. Tordjman R, Ortega N, Coulombel L, Plouet J, Romeo PJ, Lemarchandel V (1999) Blood 94:2301
98. Nishi N, Ishikawa R, Inoue H, Bishikawa M, Yoneya T, Kakeda M, Tsumara H, Ohashi H, Mori LJ (1997) Leukemia (suppl. 3) 11:468
99. Kanai M, Ikeda H, Ikebuchi K (2000) Bone Marrow Trans 26:837
100. Lemoine FM, Humphries RK, Abraham SD, Krystal G, Eaves CJ (1988) Exp Hematol 16:708
101. Sutherland HJ, Eaves CJ, Landsdorp PM, Thaker JD, Hogge DE (1991) Blood 78:666
102. Sutherland HJ, Hogge DE, Cook D, Eaves CJ (1993) Blood 81:1465

Received: April 2001

Cell Retention Devices for Suspended-Cell Perfusion Cultures

Leda R. Castilho[1,*], Ricardo A. Medronho[2]

[1] GBF-German National Research Center for Biotechnology, Biochemical Engineering Division, Mascheroder Weg 1, 38124 Braunschweig, Germany
E-mail: ledacastilho@ieg.com.br
[2] Federal University of Rio de Janeiro, Department of Chemical Engineering, School of Chemistry, Centro de Tecnologia, Bloco E, Ilha do Fundão, 21949-900 Rio de Janeiro – RJ, Brazil
E-mail: medronho@ufrj.br

Dedicated to Prof. Dr. Wolf-Dieter Deckwer on the occasion of his 60th birthday

Perfusion cultures of animal cells have several advantages over batch or fed-batch cultures. They give, for instance, higher productivities and a consistent product quality, and allow steady state operation and better cell physiology control. However, one of the main aspects limiting performance and scale-up of perfusion processes is the need for an adequate cell retention device. The devices currently in use for stirred perfusion bioreactors are continuous centrifuges, tangential flow membrane filters, dynamic filters, spin-filters, ultrasonic and dielectrophoretic separators, gravity settlers and, more recently, hydrocyclones. The advantages and disadvantages of each of these methods will be discussed.

Keywords. Perfusion cultures, mammalian cell retention devices, filtration, centrifugation, sedimentation

* Current address:
Federal University of Rio de Janeiro, COPPE-Chemical Engineering Program, Centro de Tecnologia, sala G-116, 21945-970 Rio de Janeiro/RJ, Brazil

Advances in Biochemical Engineering/
Biotechnology, Vol. 74
Managing Editor: Th. Scheper

Abbreviations

A	area (m^2)
b	field force intensity ($m\ s^{-2}$)
d	cell diameter (m)
D	perfusion rate (s^{-1})
$d_{bioreactor}$	bioreactor diameter (m)
d_c	cut size (m)
d_{hf}	hollow fiber internal diameter (m)
d_{sf}	spin-filter diameter (m)
E	cell separation efficiency (–)
E′	reduced total efficiency (–)
g	gravity acceleration ($m\ s^{-2}$)
$h_{bioreactor}$	bioreactor height (m)
h_{sf}	spin-filter height (m)
J_p	perfusion flux ($m\ s^{-1}$)
k	ratio of particle radius to channel width (–)
Q	feed volumetric flow rate ($m^3\ s^{-1}$)
Q_o	overflow volumetric flow rate ($m^3\ s^{-1}$)
Q_u	underflow volumetric flow rate ($m^3\ s^{-1}$)
r	cell radius (m)
R	radial position of the particle (m)
r_{cf}	ratio of permeation drag to lift drag in cross-flow filtration (–)
Re	Reynolds number (–)
R_f	flow ratio (–)
r_{sf}	ratio of permeation drag to lift drag in spin-filters (–)
t	time (s)
V	bioreactor volume (m^3)
v_p	velocity due to perfusion flux ($m\ s^{-1}$)
$v_{permeation}$	permeation velocity ($m\ s^{-1}$)
v_t	terminal settling velocity ($m\ s^{-1}$)
v_{tang}	tangential velocity ($m\ s^{-1}$)
X	cell concentration in the feed suspension (m^{-3})
X_o	cell concentration in the overflow (m^{-3})
X_u	cell concentration in the underflow (m^{-3})
β	cell passage factor (–)
ε	porosity (–)
η	liquid viscosity (Pa s)
μ	specific growth rate (s^{-1})
μ_{app}	apparent specific growth rate (s^{-1})
ρ	density of the liquid ($kg\ m^{-3}$)
ρ_s	density of the cells ($kg\ m^{-3}$)
ω	angular velocity (s^{-1})

1 Introduction

Mammalian cells are commonly employed for the production of therapeutic and diagnostic proteins, since they are able to correctly synthetize the large and complex structures that the human body requires as medicine [1]. Nowadays, they are employed for the large-scale production of recombinant therapeutic proteins, monoclonal antibodies (MAbs) and viruses used in the preparation of vaccines (e.g. against rabies, hepathytis B, polio, etc) [2]. An overview of some licensed/approved products derived from mammalian cell culture is given in Table 1.

Although the initial focus was on diagnostic products, the emphasis in animal cell biotechnology has been increasingly shifting to therapeutic proteins [3]. Furthermore, among the newer products, especially MAbs, a visible trend is that doses are becoming larger. While doses of the earlier rDNA products were in the sub-milligram range, nowadays various new products are administered in tens or hundreds of milligrams [4]. These facts not only enhance the importance of process quality and higher purity levels, but also imply a continuing search for even more efficient ways to grow cells, express and purify proteins. Besides physiological studies and medium optimization, further development of engineering aspects of production systems is a fundamental key for manufacturers to improve productivity and thus cope with the kilogram quantities of product needed nowadays.

Commercial scale cultivation of mammalian cells is accomplished using different technologies: roller bottles, microcarriers, suspension (batch, fed-batch or perfusion mode) and hollow fiber bioreactors (Table 2). However, especially for products needed in large amounts, suspension cultivation seems to be the most effective system [4, 5]. Suspension-based systems are characterized by a homogeneous concentration of cells, nutrients, metabolites and product, thereby facilitating scale-up [6] and enabling an accurate monitoring and control of the culture [7].

Suspension systems can be operated in different modes: batch, fed-batch, chemostat, and perfusion (Fig. 1). These operation modes differ basically in the way nutrient supply and metabolite removal are accomplished, which in turn determines cell concentration, product titer and volumetric productivity that can be achieved [8]. The intrinsic limitation of batch processes, where cells are exposed to a constantly changing environment, limits full expression of growth and metabolic potentials. This aspect is partially overcome in fed-batch cultures, where a special feeding strategy prolonges the culture and allows an increase in cell concentration to be achieved. In perfusion and chemostat processes nutrients are continuously fed to the bioreactor, while the same amount of spent medium is withdrawn. However, in perfusion cultures the cells are retained within the bioreactor, as opposed to continuous-flow culture (chemostat), which washes cells out with the withdrawn medium [9].

Batch, fed-batch and perfusion processes are commonly used in large-scale cultivation of mammalian cells. Chemostat cultures are a valuable tool for cell physiology studies but not a serious contender as a production process [3].

Table 1. Some licensed/approved biologicals produced by mammalian cells [2, 4, www.fda.gov/cber/cberac.htm]

Product	Protein or MAb/immunogen	Indication	Cells	First approval	Countries
Activase	t-PA	acute ischemic stroke	CHO	1987	various
Avonex	β-interferon	multiple sclerosis	CHO	1996	USA
Bene Fix	factor IX	hemophilia B	CHO	1997	USA
Cerezyme	glucocere-broxidase	Gaucher disease	CHO	1994	USA, Austria, New Zealand
Enbrel/Etanercept	fusion protein (TNFR/hIgG1)	rheumatoid arthritis	CHO	1998	USA
Epogen/Procrit	EPO	anemia	CHO	1989	various
Epogin/Recormon	EPO	anemia	CHO	1990	Japan, Europe
GenHevac B Pasteur	HBsAg	hepatitis	CHO	1989	France
Gonal-F	FSH	female infertility	CHO	1995	Sweden, Finland, USA
Granocyte	g-CSF	anemia, neutropenia	CHO	1991	Japan, Europe
HB Gamma	HBsAg	hepatitis	CHO	1990	Japan
Herceptin/ Trastuzumab[a]	MAb/HER2	metastatic breast cancer	CHO	1998	USA
Infliximab/ Remicade[a,b]	MAb/TFNα	Crohn's disease	n. a.	1998	USA
Kogenate[b]	factor VIII	hemophilia A	BHK	1993	various
MAbs for *in vitro* diagnostic	about 100 different	various	various	from 1980	various
Myoscint[c]	MAb/myosin	cardiac imaging agent	n. a.	1989	Europe, USA
Novo Seven	factor VIIa	hemophilia A and B	BHK	1996	Switzerland, Europe, USA
Panorex[a]	MAb/n.a.	colorectal cancer	n. a.	1995	Germany
Prosta Scint[c]	MAb/PSMA	prostate cancer	n. a.	1996	USA
Pulmozyme	DNAse I	cystic fibrosis	CHO	1993	Sweden, USA, Switzerland
Puregon	FSH	female infertility	n. a.	1996	Denmark
Recombinate	factor VIII	hemophilia A	CHO	1992	various
Refacto	antihemophilic factor	hemophilia A	CHO	2000	USA
ReoPro[a]	MAb/Platelet IIb/IIIa	cardiac schemic complications	n. a.	1994	USA
Rituxan[a]	MAb/CD20	B cell non-Hodgkin's lymphoma	CHO	1997	USA
Simulect/ Basiliximab[a]	MAb/IL2Rα	acute kidney transplant rejection	mouse myeloma	1998	USA
TNKase/ Tenecteplase	t-PA	acute myocardial infarction	CHO	2000	USA
Verluma[c]	MAb/n.a.	small cell lung cancer	n. a.	1996	USA
Wellferon	interferon α-N1	hepatitis C	human lympho-blastoid	1999	USA

n. a.: Information not available.
[a] Therapeutic monoclonal antibody.
[b] Produced by continuous perfusion process.
[c] Monoclonal antibody for *in vivo* diagnostic.

Table 2. Technologies used for commercial-scale cultivation of mammalian cells [4]

Technology	Product(s)
Roller bottles	EPO, h-GH, HbsAg
Microcarriers	glucocerebrosidase
Suspension	t-PA, factor VIII, factor IX, α interferon, several MAbs
Perfused suspension	factor VIII, several MAbs
Hollow fiber	*in vivo* diagnostic MAb

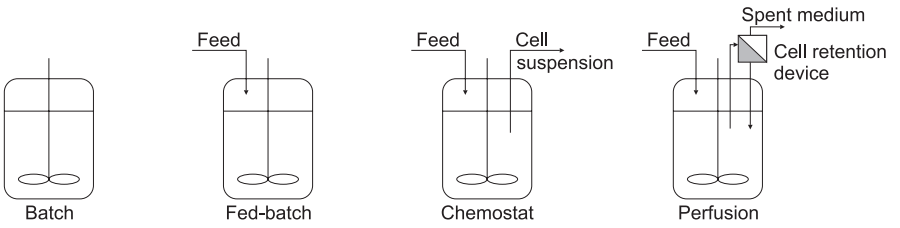

Fig. 1. Schematic view of the different operation modes of suspended-cell processes: batch, fed-batch, chemostat and perfusion

Kadouri and Spier [10] presented the various factors that should be considered before choosing a particular operation mode and proposed a decision tree to facilitate the choice between batch and perfusion processes.

Perfusion is not a modern technique, since it was already employed in 1912 [11] to keep small pieces of tissue viable for extended microscopic observations. It was a result of the observation that in vivo cells are continuously supplied with blood, lymph or another body fluid to keep them in a constant physiological environment, supporting cell concentrations as high as 10^9 cells/mL [9].

By using a perfusion system, in situ medium exchange is accomplished, and a better control of the culture environment (dissolved oxygen tension, pH, substrate concentration) is possible. Additionally, toxic by-products are removed and secreted product is continuously recovered, avoiding the risk of product degradation [12]. The fresh nutrient supply and metabolites removal, combined with the retention of cells in the bioreactor, allows a high cell concentration to be achieved. This usually results in high product titers even when working at relatively high medium throughput rates, leading to productivities which have been reported to be 10-fold greater than in batch and fed-batch processes [13, 14]. Moreover, perfusion-based processes can produce large volumes of product from a size-limited bioreactor on a continuous basis for extended periods of time [5], reducing capital costs. Additionally, the self-conditioning ability of cells and the less reactor turnover observed in perfusion cultures contribute to reduced operating costs. The self-conditioning ability of cells results from the secretion of growth factors and other proteins by the cells and seems to increase with cell concentration [15], allowing the reduction or complete removal of expensive medium components (e.g. serum) throughout a perfusion cultivation. Less reactor turnover leads to a reduction in labor and energy costs [16].

Other advantages related to perfusion operation are [12]:

- reduced unproductive growth phase as a proportion of the total process time;
- more consistent product quality because conditions in the bioreactor are held stable;
- more extensive automation with improved process control.

From an economic point of view, perfusion cultures of animal cells should be operated at high perfusion rates [17]. However, the high cell concentrations achieved in such cases result in several technical constraints, such as oxygen transfer, CO_2 removal, medium formulation, and, especially, cell retention efficiency.

Several different separation devices have been used for retaining cells in the bioreactor during perfusion cultures. They are usually based on centrifugal action (centrifuges, hydrocyclones), gravitational settling, filtration (spin-filters, tangential flow filters, dynamic filters), ultrasonic and dielectrophoretic separation. Besides the suitability for large-scale operation [18], other prerequisites for separation devices to be adequate for perfusion of mammalian cells are [16]:

- the retention efficiency of cells within the bioreactor should be high;
- stable, long-term operations should be possible;
- the device should be cleanable, sterilizable and reusable;
- it should maintain high culture viability, not damaging the cells by, for instance, mechanical shear stress, and should not induce changes in cell metabolism.

Cell retention devices can be placed internally in the bioreactor or externally, connected to it through a recirculation loop. Although internal devices are claimed to allow simple and safer operation [19], external devices permit that operation and scale-up parameters are completely decoupled from bioreactor operation and design. They also enable aseptic replacement in case of failure during long-term operation, allowing cultivation to continue. For instance, Trocha et al. [20] showed an example of a hybridoma perfusion cultivation over 1300 h, where several cell concentration declines could be observed throughout the cultivation, corresponding to failures in the retention device. When this happened, they switched to a second spare device, in order to allow the culture to continue. This is just one of various examples found in the literature reporting the lack of reliability of cell retention devices. In spite of the great effort that has been made in this field over the last ten years, this matter seems still not properly solved. In this context, the advantages and disadvantages of the different available devices will be discussed here.

2 Centrifugation

There are basically two families of centrifuges, the sedimenting centrifuges and the filtering centrifuges. The former uses centrifugal force to move the particles radially either outwards or inwards through a liquid, depending on whether

they are heavier or lighter than the suspending liquid. The principle of separation of these centrifuges is, therefore, sedimentation in a centrifugal field and, as such, they will be seen in this item. The latter, also known as centrifugal filters, uses the centrifugal field to promote the necessary pressure to force the mother liquor through both the filter medium and the cake. Therefore, they are, in reality, filters.

Centrifuges can be very efficient when separating cells from culture media. Consequently, they can be used either in harvesting of mammalian cells [1,21–23] or, despite their mechanical complexity, as cell retention device in long-term perfusion systems (Table 3).

The degree of cell separation is an important parameter to be evaluated in perfusion systems. This can be done through the use of some concepts as cell separation efficiency, grade efficiency, and cut size. These concepts are applicable to any equipment whose performance remains constant if the operational conditions do not change. They are valid, therefore, for equipment such as sedimenting centrifuges, hydrocyclones, gravitational settlers, etc.

Eq. (1), known as Stokes' law, gives the terminal settling velocity of a spherical particle settling in the laminar region (Stokes region) under the influence of a gravitational or centrifugal field.

$$v_t = \frac{(\rho_s - \rho)\, b d^2}{18\eta} \tag{1}$$

where:

$b = g$ for the gravitational field,
$b = \omega^2 R$ for centrifugal fields.

Eq. (1) is valid for a particle settling without the interference of other particles, i.e., for diluted systems. The particle settling velocity decreases as particle concentration increases. This phenomenon is known as hindered settling. Several equations can be found in the literature to account for this phenomenon, but a simple method to calculate the hindered settling velocity is to use Eq. (1) replacing the liquid density and viscosity by the apparent density and viscosity of the suspension [24].

Miller and Phillips [25] measured the terminal velocities due to gravity of some mammalian cells settling in a gradient of fetal calf serum in phosphate buffered saline at 4°C. Based on their experimental results, they proposed Eq. (2), which is a simplification of Eq. (1):

$$v_t = \frac{r^2}{4} \tag{2}$$

where the terminal settling velocity v_t is given in mm h^{-1} and r is the cell radius in μm.

Since first proposed, Eq. (2) has been used in some works [26, 27] for calculating terminal velocities of mammalian cells and even suggested in books [28]. Eq. (1) reduces to Eq. (2), for instance, for a density difference ($\rho_s - \rho$) of 0.05 g cm^{-3} and a medium viscosity (η) of 1.56×10^{-3} Pa s (water viscosity at 4°C). Mammalian cells are usually cultivated at 37°C and the water viscosity at this

Table 3. Overview of reported perfusion processes employing centrifuges as cell retention device

Cell Line	Product	Reactor Volume (L)	Max. Perfusion Rate (d^{-1})	Cultivation Time (d)	Centrifuge Type	g-factor[a]	Feed Flow Rate[b] (L min^{-1})	Max. Viable Cell Conc. (10^6 mL^{-1})	Separation Efficiency (%)	Reference
Hybridoma	IgG	6.0	5.5	12	disc-stack	50	0.50 (C)	20	100	40–42
HeLa	–	21.5	3.0	15	disc-stack	50	0.72 (C)	10	100	40–42
HeLa	–	21.5	3.8	27	disc-stack	50	2.25 (C)	10	100	40
CHO	–	100.0	10.1[c]	16	disc-stack	400	1.17 (C)	>3	100 → 95	37
Hybridoma	IgM	1.3	0.5	18	centritech	18–49	0.04 (SC & I)	3–6	>99	44
Hybridoma	IgG	40	1.8	40	special[d]	50	0.2 (I)	10	100	38–39
Hybridoma	IgG	10	2.0	37	special[d]	63	n.a. (C)	12	n.a.	35
Hybridoma	IgG	3	2.1	27	special[d]	100	n.a. (I)	17	n.a.	34

n.a.: Information not available.
[a] g-factor = $\omega^2 R/g$.
[b] C: continuous operation, SC: semi-continuous, I: intermitent operation.
[c] Most of the supernatant was sent back to the reactor, in order to simulate the operation of a 1000 L reactor working at a 1 d^{-1} perfusion rate.
[d] Rotor with a non-conventional design, containing 4 layers of spiral settling zones.

temperature is 6.9×10^{-4} Pa s. For the same density difference, and considering that the culture medium viscosity in perfusion cultures at 37 °C is around 10 % higher than the water viscosity, it is possible to deduce from Eq. (1) that the factor in Eq. (2) would change from 4 to 2. Under these conditions, Eq. (2) would then give a terminal settling velocity around half of the correct value. Therefore, since viscosity is a strong function of temperature, the use of Eq. (2) should be avoided. Instead, Eq. (1) should be employed.

The main streams of a separator are usually three: the feed stream containing the cells to be separated, the underflow containing the separated cells, and the overflow containing the cells that the separator could not capture. The cell separation efficiency (or retention efficiency) E is defined by Eq. (3), and gives the fraction of cells recovered in the underflow.

$$E = \frac{Q_u X_u}{QX} \tag{3}$$

The fraction of fluid discharged in the underflow is called flow ratio R_f. Separators can operate with or without a fluid flow rate in the underflow. For instance, tubular centrifuges operate usually with $R_f = 0$, and scroll type centrifuges and hydrocyclones with $R_f > 0$. A flow ratio equal to R_f means that this fraction of feed fluid is leaving the separator through the underflow. Since the fluid carries solid particles with it, some particles will be discharged into the underflow not due to the centrifugal action of the separator but due to entrainment. In spite of some controversy regarding hydrocyclones [29–31], this bypass is normally assumed to be equal to the flow ratio [24, 32]. Therefore, R_f is the minimal efficiency at which a separator will operate even if no centrifugal action takes place. For the conditions usually found in mammalian cell cultures:

$$R_f \cong \frac{Q_u}{Q} \tag{4}$$

The reduced separation efficiency E' (Eq. 5), also called centrifugal efficiency, is used for separators with $R_f > 0$, and gives the separation efficiency taking into account only those particles that will be separated or not due to the centrifugal field intensity. Hence, E' does not consider the particles that are separated due to entrainment in the overflow stream.

$$E' = \frac{E - R_f}{1 - R_f} \tag{5}$$

Based on Eqs. (3), (4) and (5), and on a material balance on the separator:

$$E' = 1 - \frac{X_o}{X} \tag{6}$$

The same concepts on separation efficiency expressed by Eqs. (2) and (4) can be applied to a given size of cell, generating curves of efficiency as a function of cell size [33].

Mammalian cells may be affected by the relatively high shear stresses present in separation under centrifugal fields. Hamamoto et al. [34] found that exposing hybridoma cells to a centrifugal acceleration intensity of 100 *g* twice a day for 30 minutes did not affect the cell growth rate. However, accelerations of 500 g caused some depression on cell growth. Tokashiki et al. [35], also working with hybridoma cells, found no effect on either cell growth or MAb specific productivity for accelerations varying from 100 *g* to 500 *g* twice a day for 10 minutes. However, in a similar experiment using another hybridoma cell line, Tokashiki and Yokoyama [36] found a 50% decrease in the antibody production at 500 *g*, although no effect was observed at 200 *g*. The authors concluded, then, that the influence of centrifugal fields on cell proliferation and product formation is a function of the cell type. Nevertheless, higher stressing conditions have been imposed on cells, without noticeable effects on cell growth, viability or product formation [37].

Tokashiki et al. [35] showed that it was possible to use continuous centrifugation for cell retention in perfusion cultures. Their results for viable cell concentration and IgG specific productivity were equivalent to the results obtained with a centrifuge operating in a intermittent fashion or with a gravitational settler [34]. In another work, the same research group [38, 39] proposed a novel centrifuge with multiple settling zones to separate cells from culture medium. They were able to run a perfusion system for 40 days using the new centrifuge in an intermittent fashion. A disadvantage of this equipment is the necessity of introducing a liquid carrier (e.g. perfluorocarbon) to wash the settled cells from the centrifuge back to the reactor. This liquid carrier has to remain inside the reactor during the whole culture time.

Among the conventional industrial centrifuges, only the disc-stack type has been studied as an option of cell retention device for perfusion bioreactors. Jäger [40–42] used a continuous disc-stack centrifuge (Westfalia CFA-01) to conduct perfusion cultures of mammalian cells. When cultivating hybridoma cells in a 6 L reactor, the author used a 0.5 L min^{-1} feed flow rate and, to avoid cell settling in the pipes, he worked with a flow ratio of 95.4%. At these feed rates, cells were passing through the centrifuge every 12 min and the perfusion was kept for 6 days. Even under these extremely hard conditions, Jäger did not observe any significant effect on viability and only a slight effect on cell growth (population doubling time changed from 25.3 h in batch to 27.7 h in perfusion). Even better results were obtained when cultivating HeLa cells in a 21.5 L bioreactor. In this case, the viabilities were kept for most of the perfusion time (10 days) over 95% and the doubling time was slightly better when compared with the batch period (26.3 h *vs* 28.7 h). The feed flow rate in this experiment was 0.72 L min^{-1} and the flow ratio was 93.7%. A longer perfusion run (25 days) was then accomplished by the author [40] using higher feed flow rate (2.25 L min^{-1}) and flow ratio (97.5%). In this case, the author noticed that one of the 18 pouches that direct the separated cells to the centrifuge underflow was clogged.

Different results regarding clogging were obtained by Björling et al. [37] when using the same centrifuge as Jäger [40–42]. These authors evaluated the separation efficiency of CHO cells from the culture medium using rotor speeds

from 400 to 2000 rpm (22 *g* to 560 *g*) and feed flow rates from 0.4 to 4.2 L min^{-1}. Despite the high values of angular velocities and flow rates, no negative effects were detected on cell viability or growth rate. The authors used a 100 L reactor and, in order to simulate a larger reactor in perfusion, most of the centrifuge overflow were recycled together with the underflow back to the bioreactor. When simulating a 1000 L bioreactor (feed flow rate of 1.17 L min^{-1} and flow ratio of about 40%), the cell retention of 100% initially given by the centrifuge, running at 1700 rpm, could only be kept for about a week. The cell separation efficiency started to decrease reaching about 95% on the 15^{th} day. An inspection of the internal parts of the separator showed that cells had accumulated in the concentrate channels and between the separation discs. As Björling et al. [37] worked with the same underflow rate as Jäger in his first perfusion run (0.47 L min^{-1}), the reason for the difference in behavior could be the high stickiness of the CHO cells, as suggested by those authors. Another possible reason could be related to the higher centrifugal forces applied by Björling et al. [37] coupled with a higher underflow concentration (concentration factor of 2.5 against 1.03 – 1.07 used by Jäger). In any case, it appears that disc-stack centrifuges, depending on the application, may present limitations and thus cannot be recommended as a universally applicable cell retention device.

Shear stress is always present in centrifugal separations in a relatively high degree. The Centritech® centrifuge was developed aiming at shear stress minimization. The operational g-factor goes only up to 320 and, according to the manufacturer, the industrial machine can process up to 2800 L d^{-1}. It uses a sterile and flexible plastic bag that is placed in a rotor, and employs a "principle of the inverted comma" that requires no seals between rotating and non rotating parts. The feed enters at one top end of the plastic bag and the overflow exits at the other top end. The cell concentrated suspension is withdrawn intermittently through the underflow pipe situated at the bottom end of the plastic bag. It has been reported that viable cell concentrations of around 1.4×10^7 cells mL^{-1} could be achieved when cultivating CHO cells in a 50 L perfusion bioreactor [43]. In another work, the growth rates and monoclonal antibody production were compared to those obtained with a filtration-based perfusion system when operating the Centritech® centrifuge in a continuous and in an intermittent fashion [44]. The growth rates in the continuous centrifugation were comparable to those obtained with the filtration-based perfusion system, but the MAb concentration was 35% lower. When operating in an intermittent way (cell suspension circulating through the centrifuge twice a day, for 30 min each time, while fresh medium was fed continuously to be reactor), the MAb concentrations achieved were similar to those obtained with the filtration-based perfusion system. However, the viable-cell specific MAb productivity was 20 – 25% lower. This difference in productivity may be due to the rigid operational conditions established, since the authors could not optimize the perfusion rate. A disadvantage of the Centritech® is related to the necessity of an aseptic replacement of the plastic bag placed in the rotor at every 20 million revolutions, or 31 days of continuous operation at a rotational speed of 450 rpm [44].

3
Hydrocyclones

A hydrocyclone is a very simple equipment, as shown in Fig. 2. It consists of a conical section joined to a cylindrical portion, which is fitted with a tangential inlet and closed by an end plate with an axially mounted overflow pipe, also called vortex finder. The end of the cone terminates in a circular apex opening, called underflow orifice. Unlike centrifuges, which use the same separation principle (sedimentation in a centrifugal field), hydrocyclones have no moving parts and the vortex motion is performed by the fluid itself. The feed is introduced tangentially through the inlet duct into the upper part of the cylindrical section acquiring a strong swirling downward movement (Fig. 2). As the underflow orifice is usually not large enough to allow a complete discharge, only part of the feed liquid escapes through the underflow carrying the coarser (or denser) particles. The other part of the flow reverses its vertical direction and goes up in an eventually stronger vortex motion and out through the overflow pipe carrying the smaller (or lighter) particles.

Hydrocyclones can be easily designed to promote a desired separation [45], and their performance can be easily predicted [31]. It is worth mentioning that Eqs. (1) to (6) are also applicable to hydrocyclones.

In the recent years, the advance of computer power has allowed numerical solutions for the differential equations that describe fluid motion. The use of computational fluid dynamics (CFD) is beginning to give a better understanding of the strongly swirling turbulent flow inside hydrocyclones and, consequently, of their performance [46–50].

Hydrocyclones were originally designed to promote solid-liquid separations, but nowadays they are also used for solid-solid, liquid-liquid and gas-liquid separations. Possible new applications, such as cell separation, are being devel-

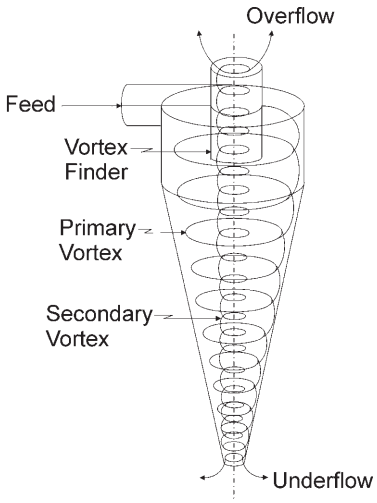

Fig. 2. Perspective view of a hydrocyclone showing its internal flow pattern

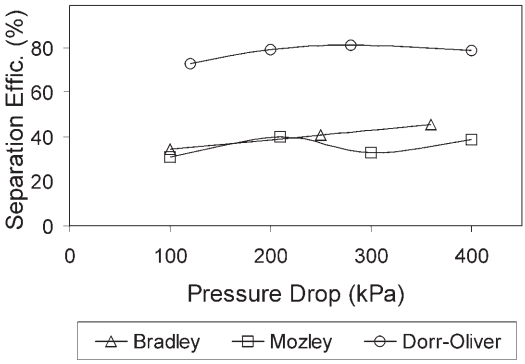

Fig. 3. Separation efficiency of HeLa cells when using a 10 mm Mozley hydrocyclone, a 10 mm Dorr-Oliver hydrocyclone and a 7 mm Bradley hydrocyclone [65]

oped and some works can be found in the literature. These works refer to separation of yeast either from fermented broths or from water suspensions [51–56], separation of yeast from filter aids [57, 58], separation of biological sludge in wastewater treatments [59–63] and, more recently, separation of mammalian cells [46, 64–66].

Lübberstedt [64] tested three different hydrocyclones for HeLa cell separation: a 7 mm Bradley [67], a 10 mm Mozley (Richard Mozley Ltd., Redruth, UK), and a 10 mm Dorr-Oliver (Dorr-Oliver GmbH, Wiesbaden, Germany) (the dimension quoted here is the diameter of the cylindrical part of each hydrocyclone). The best results were obtained with the Dorr-Oliver hydrocyclone (Fig. 3), which produced a cell separation efficiency of 81% when working at a pressure drop of 300 kPa and a flow rate of 2.8 L min^{-1}. When operating with two 10 mm Dorr-Oliver connected in series (the overflow of the first as feed for the second) at 200 kPa, the global efficiency of the arrangement was 94% [65]. These experimental values confirm the computational fluid dynamics (CFD) predictions that high levels of efficiencies for mammalian cells could be achieved with small diameter hydrocyclones [46].

Figure 4 shows the influence of pressure drop on the viability of HeLa cells in the underflow and overflow of three different hydrocyclones [66]. It can be seen that in the underflow of the three hydrocyclones the viability did not decrease with pressure drops up to 400 kPa, and in the overflow, it only started to decrease for pressure drops higher than 300 kPa. Therefore, in spite of the relatively high shear stresses generated inside hydrocyclones, the cells could resist up to a certain limit of pressure drop. This is probably due to the extremely low average residence time of the cells inside the tested hydrocyclones, which lies in the range of 0.03–0.1 seconds. As cell damage is a function of shear stress and time [68, 69], these low residence times could explain why the cells could resist to high shear rates. Furthermore, the residence time of most cells leaving the hydrocyclone through the overflow is greater than that of the cells leaving through the underflow. This could explain why the limiting pressure drop before cell damage starts is lower in the overflow. The small fluctuations in the

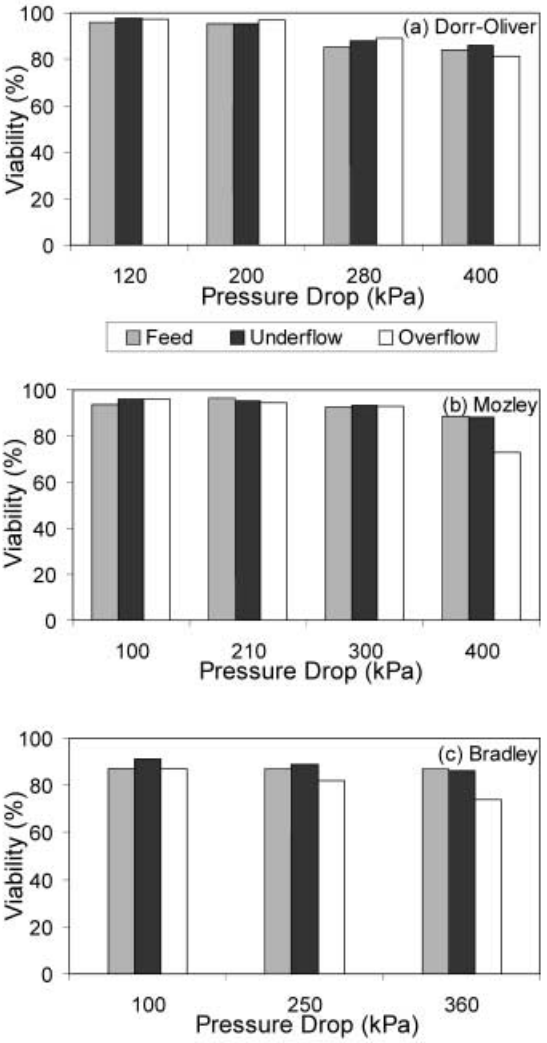

Fig. 4. Influence of pressure drop on cell viability in the underflow and overflow of the following hydrocyclones: Dorr-Oliver (a), Mozley (b) and Bradley (c) with diameters of 10 mm, 10 mm and 7 mm, respectively [66]

feed, overflow and underflow viabilities at lower pressure drops, seen in Fig. 4, are within the measurement inaccuracy. In all cases, the sum of viable cells in the overflow and the underflow corresponded to the number of viable cells in the feed.

The use of hydrocyclones for separating mammalian cells from the culture medium opens the possibility of using them to perform perfusion in bioreactors. As hydrocyclones have no moving parts, they are ideally suited for operation under aseptic conditions as required by the biotechnology industry.

Furthermore, for such application, they would require no maintenance, which would avoid additional risks of contamination and allow a continuous operation of the perfusion bioreactor for several months.

4 Gravitational Settling

As occurs in centrifugal fields, separation under gravity will only occur if there is a density difference between the cells and the liquid. Unfortunately, this difference is usually small when dealing with mammalian cells (around 5% of the liquid medium density). Apart from that, their sizes are relatively small. These two facts explain why mammalian cells attain very low terminal settling velocities when settling individually under the gravitational field (from 1 to 15 cm/h in a culture medium at 37°C). Consequently, the settler area must be large enough to avoid cell wash-out.

If a 100% separation efficiency for the viable cells in a vertical settler is desired, the settling velocity of the smallest viable cell present in the feed suspension must be larger than the spent medium upwards velocity. Under the limiting conditions:

$$A_{\min} = \frac{Q_o}{v_{t,\min}} \tag{7}$$

The terminal settling velocity $v_{t,\min}$ can be obtained by Eq. (1) and, in a perfusion system, the overflow rate Q_o is equal to the product between the specific perfusion rate D and the bioreactor volume V. Hence:

$$A_{\min} = \frac{DV}{v_{t,\min}} \tag{8}$$

In practice, an area three times larger than $A_{\min}$ is recommended. As Eq. (8) shows, when scaling up perfusion systems, the settling area is directly proportional to the reactor volume, for a constant specific perfusion rate.

For an existing settler with a known settling area, the theoretical minimum cell diameter to be separated is given by a combination of Eqs. (1) and (8):

$$d_c = \left[\frac{18\eta DV}{(\rho_s - \rho)gA}\right]^{1/2} \tag{9}$$

Eq. (9) assumes that the settler is an ideal separator and, consequently, the diameter d_c obtained would be the cut size, i. e., all cells with higher diameter would settle and all cells with smaller diameter would escape through the overflow. Therefore, to improve the settler separation efficiency, the diameter given by Eq. (9) should decrease. As this equation shows, for a given reactor-settler system, this could be achieved by decreasing viscosity or perfusion rate or increasing the cell density difference. Since the operational temperature is usually fixed at 37°C and the cell density difference is not an easy variable to be manipulated,

the easiest way to change settler performance is through changes in the perfusion rate.

Lamella settlers are gravity settlers that use a large number of inclined flat plates, closely packed, so that the distance between the plates is small. The gravitational action makes the cells move in the direction of the lower surface of the individual separating space between two plates. Once settled, the particles slide down in a layer towards the plate periphery and then into the sludge hopper. For the same required sedimentation area, lamella settlers are much more compact than vertical ones. Theoretically, their total sedimentation area is the sum of the horizontally projected areas of all plates. In practice, however, only 50 % of this total area is effective [137]. The main problem with inclined settlers is that the cells tend to adhere to the plates. Special coating of the plate surface and vibration of the whole lamella pack may alleviate this problem.

Vertical settlers have been used in several laboratory works as cell retention device for perfusion systems (Table 4). Tokashiki and Arai [70] used a column as culture vessel equipped with three vertically arranged settling zones, where each settling zone was an annulus between two concentric cylinders. The authors were able to keep perfusion for almost a month with viable cell concentration and IgG specific productivity comparable to those obtained in a culture vessel equipped with only one gravitational settling zone. Based on this comparison, they stated that vessels with multi-settling zones could be a promising way to overcome difficulties usually associated with the scale-up of gravitational settlers. In another work, the same authors [71] employed the same system but using perfluorocarbon as oxygen supplier to the cells. They found that, under the same specific perfusion rate, the viable cell concentration and IgG concentration in the supernatant were about twice as high as in the perfusion reactor using only one settling zone. The same group [72] scaled up a somewhat similar reactor with only one settling zone. They used reactors of 0.12, 4, 20, and 50 liters and could reach in all reactors viable cell concentrations higher than 10^7 cells mL^{-1} and IgG specific productivity around 4 – 5 pg $cell^{-1}$ d^{-1}. These results showed that it was possible to conduct high cell density cultures of mammalian cells in a relatively large reactor volume, using gravitational settlers as cell retention device.

Hülscher et al. [26] tested a perfusion system with a settling device known as Dortmund Settler consisting of a cylindrical and a conical part. The feed inlet pipe discharged the suspension into the settler at the end of the cylindrical part, while two outlets conveyed the overflow collected at the top of the cylindrical part out of the system and the underflow, concentrated in cells, back to the reactor. By cooling down the suspension entering the settler, they could not only reduce the cell metabolic activity but also induce a steady downward flow in the settler. With increasing perfusion rates, it was observed that the retention efficiency of viable cells was kept at 100 % up to 1.3 d^{-1}, starting to decrease for larger values, whereas the retention efficiencies of nonviable cells decreased continuously with increasing perfusion rates. Therefore, the settler could preferentially separate viable cells. For instance, at a 2.0 d^{-1} perfusion rate, the retention efficiencies of viable and nonviable cells were 94 % and 56 %, respectively.

Table 4. Overview of reported perfusion processes employing gravitational settlers as cell retention device.

Cell Line	Product	Reactor Volume (L)	Max. Perfusion Rate (d^{-1})	Operation Time (d)	Settler Type	Settler Details	Max. Viable Cell Conc. (10^6 mL^{-1})	Viable Cell Separ. Eff. (%)	Reference
Hybridoma	IgG	1.5	2.0	17	vertical & tangential	two settlers	13	88	27
Hybridoma	IgG	0.12 to 50	2.0 & 4.0	26 to 70	vertical	conc. cylinders	10 to 16	n.a.	72
Hybridoma	IgG	5.4	1.3	25	vertical	deep cone	6	100	26
Hybridoma	IgG	–	2.0	27	vertical	multiple zones	20	n.a.	71
Hybridoma	IgG	0.8–1.0	2.3	27	vertical	multiple zones	30	n.a.	70
CHO	–	1.5	1.4	21	inclined	flat, one channel	2.5 & 6	93 & 85	74–75
Hybridoma	–	5.4	1.0	34	inclined	lamellae	4	>90	79
Hybridoma	IgM	21.0	2.4	24	inclined	lamellae	5	95	78
Hybridoma	–	2.7	2.0	30	inclined	internal lamellae	6.5	n.a.	77
Hybridoma	MAb	1.8	1.0	30	inclined	mod. Erlenmeyer	10	98	76
Hybridoma	IgG	1.5	1.7	12	inclined	flat, one channel	10	100	73

n.a.: Information not available.

A two step sequential sedimentation was used by Wen et al. [27]. Their cell retention apparatus consisted of a vertical settler tank and a horizontal flat settler, both internally siliconized to avoid cell attachment. The vertical settler tank contained a baffle that divided the device in two zones, a circulation zone and a clarification zone. The feed inlet pipe discharged the suspension into the circulation zone and the overflow was collected through a pipe immersed in the clarification zone. The underflow was collected at the settler bottom part and could flow back to the reactor. The flat settler also had an independent feed inlet and overflow and underflow outlets. This flat settler was operated in a semi-continuous fashion, i.e., it was operated for several hours until an observable thin layer of cells formed in the settler bottom. The feed inlet was, then, closed and gas was injected to resuspend the cells, before sending them back to the reactor. During operation, both settlers were kept at room temperature, which was maintained under 15 °C. The global efficiency of viable cell separation was always higher than that of nonviable cells for the whole range of perfusion rates tested, e.g., at 2.0 d^{-1} the global efficiencies were 88 % and 47 % for viable and nonviable cells, respectively.

Some works employed inclined settlers, instead of vertical ones (Table 4). For instance, Batt et al. [73] used two external settlers with different sedimentation areas, both made from a rectangular glass tubing. To try to minimize adherence of settled cells, the internal surface of the settlers was siliconized. They employed the settlers, one at a time, at a constant angle of 30° from the vertical, keeping them at 37 °C during operation. As can be predicted by Eq. (9), they observed a better total cell retention when using the settler with the largest area coupled with the lowest perfusion rate. The authors also observed an improved selective removal of nonviable cells when using a higher perfusion rate. According to them, this occurred due to the associated increase in viable cell size with increasing perfusion rates. In another work of the same group [74, 75], they found that, from the settled cells, around 50 % of both viable and nonviable CHO cells were retained within the settler due to adhesion, when operating the settler at 37 °C with a flow ratio of 50 %. The adhesion degree decreased to around 25 % of the settled cells when the settler started to be vibrated and the feed suspension was cooled to 4 °C [75]. These adhered cells were recovered by bubbling the settler. They found that cells returning to the bioreactor through the settler underflow had an average residence time of the 1.46 h inside the cooled, vibrated settler. The authors also presented an interesting plot of cell size distribution as a function of viability [74], showing that the average CHO size decreased from 14.7 μm to 9.4 μm as the viability decreased from 98 % to 0 %, respectively.

Hansen et al. [76] used a siliconized modified 300 mL Erlenmeyer flask as an external settling device, with its undersize at 45° to the vertical. The flask was isolated to maintain the temperature at 37 °C. The low separation capacity of this adapted flask limited the perfusion rate to a maximum of 1.0 d^{-1} otherwise the cells would be washed out.

Knaack et al. [77] developed an ingenious reactor design that incorporates a conical lamella settler within a conical reactor vessel. Unfortunately, this new design presents a serious scale-up limitation, since the maximum perfusion rate attainable decreases hyperbolically with the reactor working volume. For

instance, depending on the reactor geometry, the maximum perfusion rate of 1.0 d^{-1} is achieved for reactor volumes between 10 L and 25 L, and for increasing volumes, the maximum perfusion rate tends asymptotically to 0.5 d^{-1}.

Thompson and Wilson [78] operated a 21-L air-lift perfusion reactor coupled to an external lamella settler. The sedimentation device bearing an angle of inclination of 30° to the vertical was maintained at 37°C. They found a reasonable agreement between the theoretical and experimental values of breakthrough for viable and nonviable cells in the harvest stream. As expected (see Eq. 8), the maximum perfusion rates increased with an increasing settling area.

The system used by Stevens et al. [79] consisted of an air-lift reactor with an external lamella settler. They did not need to pump the cell suspension through the settler, since free flow convection was achieved by cooling the cell suspension (20°C) before entering the sedimentation device. As also found by other authors, they could achieve selective retention of viable cells by varying the perfusion rate.

Compared to filtration and centrifugation, gravity settling avoids the problem of filter clogging and cell damage by high shear stresses [27]. Nevertheless, the long residence times required for separation by gravity sedimentation must be a matter of concern, since the settler interior is an unoxygenated and unmixed environment [18]. Apart from that, the scale-up of settlers able to cope with large scale bioreactors is still a problem, since the required area for vertical settlers is directly proportional to the reactor volume and more compact settlers, like the lamella ones, are prone to cell adhesion.

5 Spin-Filters

Himmelfarb et al. [80] introduced spin-filters as a cell retention device for high cell density perfusion cultivations of mammalian cells in suspension. Spin-filters are cylinders with a porous wall, which are placed inside stirred tank bioreactors, either mounted on the impeller shaft or driven by an independent motor (Fig. 5). Perfusate is pumped out from inside the spin-filter at the same

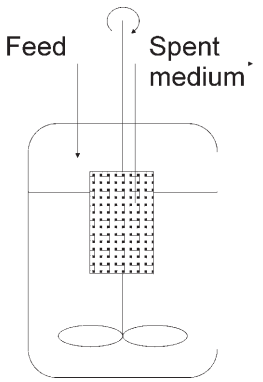

Fig. 5. Schematic view of a spin-filter mounted on the impeller shaft of a bioreactor. Alternatively, spin-filters can be driven by an independent motor

rate at which fresh medium is pumped into the bulk of the bioreactor, i.e. outside the spin-filter.

Since the pioneer work by Himmelfarb et al. [80], many studies have been published (Table 5) investigating the effects of rotation speed, perfusion rate, filter material and cell concentration on the performance of spin-filters in perfusion cultures, as given by their cell retention efficiency and their fouling characteristics. A minimum fouling and an optimum cell retention at high specific perfusion rates are important for efficient operation of a spin-filter based bioreactor. Furthermore, the performance of a spin-filter can be considered optimal if its design and operating conditions allow selective retention to occur, i.e. if debris and dead cells are removed from the bioreactor, while living cells are retained.

In a spin-filter based stirred bioreactor, there are various forces acting on both the liquid medium and the cell particles: gravity force, axial force due to impeller rotation, centrifugal force created by the spin-filter rotation, and radial force (drag) generated by the perfusion flux.

Yabannavar et al. [81] assumed that there is, additionally, a hydrodynamic lift force produced by the spinning motion of the filter, similar to the force observed on particles near a wall in a laminar flow field [82, 83]. The hydrodynamic lift force acts on small spherical particles in laminar flow, causing them to migrate away from the wall and, in the case of spin-filter based bioreactors, counteracting the drag force due to perfusion flux, which pushes the particles toward the filtration surface. In cross-flow filtration [84], it is commonly assumed that it is the balance of lift and drag force that determines if the cells are likely to hit the filter surface. Although this assumption has been frequently adopted for spin-filter systems, attention should be payed to the fact that, in spin-filters, the centrifugal force due to rotation may be non-negligible. In this case, it would be the balance of drag, centrifugal and lift forces that would determine if the cells are likely to hit the filter surface.

Favre and Thaler [85] proposed that fouling due to cell attachment may be determined by three sequential events: (a) cell-screen collision, the collision frequency being largely affected by hydrodynamic conditions and particle concentration; (b) cell adhesion, the adhesion strength depending mainly on cell line and screen material, and to a lesser extent on surface roughness and medium; and (c) cell removal, which essentially results from hydrodynamic conditions at the screen surface (i.e., in the boundary layer). According to Deo et al. [13], after cell attachment a further fouling stage occurs, which consists of cell growth, leading to the formation of a large cell mass on the screen surface. Thus, spin-filter rotation speed is an important factor concerning filter fouling, since it simultaneously influences the centrifugal and lift forces, determining cell/screen collision frequency, and also the shear rates at the screen surface, determining the removal of cells from the screen.

As discussed above, fouling of the filter screen is a major concern regarding efficient operation of the spin-filter, because ideally perfusion processes should reliably operate for longer periods of time. Since replacement of internal units is practically impossible, the spin-filter should be designed and operated to avoid clogging, preventing a premature termination of the culture [18]. Dif-

Table 5. Overview of reported perfusion processes employing spin-filters as cell retention device

Cell Line	Product	Reactor Volume (L)	Max. Perfusion Rate (d^{-1})	Cultivation Time (d)	Filter Material/ Pore Size	Rotation Speed (rpm)	Did fouling occur?	Max. Viable Cell Conc. (10^6 mL^{-1})	Separation Efficiency (%)	Ref.
Hybridoma	IgG	1.2	2.0	37	n.a., 75 µm	n.a.	no	15	n.a.	14
CHO	prothrombin	2 & 100	1.0	14	SS[a], 20 µm	35–150	n.a.	5	75–95	90
Hybridoma and myeloma	IgM and IgG	7 to 500	1.2	30	SS[a], 15 µm	80–220	n.a.	>10	n.a.	13
Hybridoma	n.a.	175	0.5	at least 8	SS[a], 25 µm	28	no	2.8	79–89	81
Hybridoma	IgG	1.5[b]	7[b]	7[b]	SS[a], 10 µm polyamide, 11 µm	3[b]	yes (SS[a]); no (polyamide)	1.2–1.6[b]	63–95	87
CHO	rscu-PA	10	4	31	ETFE[c], 127 µm	150	no	7.4	99	8
Human tumor cell	–	15	2.88	2 months	SS[a], 53 µm	80–120	no	10	95–99.9	86
Rat tumor cell	–	4 & 40	20 mL h^{-1} per 10^9 cells	<6	porcelain, 1 µm	200–300	eventual buildup of subcellular debris	30.8[d] (4 L) 13.6[d] (40 L)	n.a.	88
Mouse leukemia cell	–	n.a.	100 mL/h	10	SS[a] mesh covered by 3-µm polymeric membrane	300	n.a.	100[d]	n.a.	80

n.a.: Information not available.
[a] SS: stainless steel.
[b] Simulated perfusion experiments: recycle of filtrate without fresh medium addition.
[c] ETFE: ethylene-tetrafluoroethylene.
[d] Total cell concentration.

ferent strategies have been proposed in the literature to circumvent the problems of filter plugging. Avgerinos et al. [8] employed adherent cell lines growing on microcarriers to get aggregates (200–600 µm) that were far larger in size than the mesh opening employed (120 µm). By doing this, they were able to operate the filter for at least 31 days with no fouling problems. Varecka and Scheirer [86] used wire cages with 53 µm mesh opening and cells of approximately 20 µm size, and observed no sign of fouling for more than two months of continuous operation.

Esclade et al. [87] evaluated the influence of the screen material on fouling of spin-filters. They compared, under the same culture conditions, screens made out of stainless steel and polyamide with similar pore sizes (10 and 11 µm, respectively), similar screen surfaces and same porosity. After measuring the number of living and dead cells, and the protein and nucleic acids content in the deposits found on the screens after one week of recirculation experiments (recycle of perfusate without addition of fresh medium), they verified that the polyamide screen was superior to the stainless steel one, because it presented a low binding of proteins, nucleic acids and cells (either alive or dead). Scanning electron micrographs revealed that in the stainless steel screen nearly all the pores were filled with veils and cells, whereas in the polyamide screen the pores were practically free of cells and veils. They related this different behaviour to the different surface charge densities of both materials, metals being highly positively charged, polyamide being more neutral and cells rather negatively charged.

Analogous results concerning screen material were obtained by Avgerinos et al. [8]. In different experiments using stainless steel screens with various pore sizes (44–105 µm), the spin-filter became plugged after only 11 to 21 days of operation, with cells attached and growing on both sides of the mesh. Contrastingly, five perfusion cultivations up to 54 days in duration were carried out with a polymeric ethylene-tetrafluroethylene (ETFE) screen (120 µm pore size) without filter fouling. The authors concluded that the hydrophobic nature of the ETFE screen apparently minimized the attachment of cells to the screen and thus greatly extended the life of the spin-filter.

Beyond screen material and pore size, operating conditions have significant effects on filter clogging. Deo et al. [13] showed that fouling is heavily influenced by spin-filter rotation. They observed that the maximum perfusion rate achievable without clogging correlated with the square of the tangential velocity at the screen surface. Esclade et al. [87] observed that high perfusion rates increased screen clogging by increasing the drag towards the screen surface. They found in recirculation experiments (without fresh medium addition) that at a perfusion rate of 2 d^{-1} filter plugging just started after a viability decrease due to medium depletion occurred. Contrastingly, at a perfusion rate of 7 d^{-1} plugging took place instantaneously due to sucking of the cells onto the screen. Similar results had already been obtained by Tolbert et al. [88], who verified that at high medium withdrawal rates there was a buildup of subcellular debris in the range of the filter pore size, limiting the maximum perfusion rate and thus the maximum viable cell concentration attainable.

Fouling caused by increasing perfusion rates can be partially compensated by increasing the spin-filter rotation speed. However, according to Yabannavar

et al. [89], too high rotation speeds may increase cell leakage and, thus, there is an optimal intermediate rotation speed, which assures effective cell retention and unclogged filter operation.

Besides fouling, cell retention efficiency is another important factor regarding spin-filter performance. A poor retention capacity of a spin-filter leads to a low apparent growth rate of the cell culture due to cell leakage (Eq. 10).

$$\mu_{app} = \frac{1}{X}\frac{\mathrm{d}X}{\mathrm{d}t} \tag{10}$$

For a spin-filter based bioreactor, an overall cell balance as given by Eq. (11) can be applied [89]:

$$V\frac{\mathrm{d}X}{\mathrm{d}t} = (\mu V - \beta DV)X \tag{11}$$

where β, the cell passage factor, is the ratio between cell concentration in the perfusate and in the bioreactor, or $(1 - E)$, according to Eq. (6).

Based on Eqs. (10) and (11), it is possible to relate the apparent cell growth rate to the perfusion rate and the retention efficiency E (Eqs. 12 and 13):

$$\mu_{app} = \mu - \beta D \tag{12}$$

$$\mu_{app} = \mu - D(1-E) \tag{13}$$

Iding et al. [90] observed an apparent cell growth rate of 0.27 d^{-1} after perfusion started, as compared to $\mu = 0.65\ d^{-1}$ in the batch phase. Contrastingly, Avgerinos et al. [8] took advantage of the aggregating propensity of CHO cells, which formed clumps 200–600 µm in size, to operate with a high separation efficiency using a 120 µm pore-size filter. Under these conditions, the specific rate (0.026 d^{-1}) at which cells were lost through the screen was negligible in comparison to the apparent specific growth rate of the culture (0.26 d^{-1}).

Yabannavar et al. [89] employed Eq. (11) to calculate the maximum perfusion flow rate attainable before cell wash-out, which occurs when cell growth is compensated by cell passage through the spin-filter or, according to Eq. (12), when $\mu_{app} = 0$. Under these conditions:

$$D_{\max} = \frac{\mu}{\beta} \tag{14}$$

As a consequence, the perfusion bioreactor can only be operated up to a cell concentration supported by the perfusion rate $D_{\max}$. In this way, spin-filter retention efficiency determines the maximum attainable cell concentration in a given perfusion process.

Scale-up of spin-filters has been often studied in the recent years, and simple scale-up procedures have been proposed by Yabannavar et al. [81] and Deo et al. [13]. Yabannavar et al. [81] suggested a procedure based on keeping the ratio of permeation drag to lift force constant for the different production scales, in

order to avoid fouling. In cross-flow filtration [84], this ratio is defined as in Eq. (15):

$$r_{cf} = \frac{v_{permeation}}{\mathrm{Re}\, k^2 v_{tang}} \tag{15}$$

Yabannavar et al. [81] proposed a proportionality relationship valid for spin-filters based on an analogy to Eq. (15). They defined the Reynolds number based on the tangential velocity at the screen surface. Since in spin-filters the permeation velocity, or perfusion flux, is given by Eq. (16), and it can be assumed that the screen porosity ε will be maintained constant throughout the scale-up process, it is possible to write a proportionality relationship for the ratio from drag to lift force in spin-filters as given by Eq. (17).

$$J_p = \frac{DV}{\varepsilon A} \tag{16}$$

$$r_{sf} \propto \frac{DV}{A\ v_{tang}^2} \tag{17}$$

Eq. (18) can be obtained by expressing the variables in Eq. (17) in terms of geometric dimensions:

$$r_{sf} \propto \frac{d_{bioreactor}^2 h_{bioreactor}}{(d_{sf} h_{sf})\quad (d_{sf}^2 \omega^2)} \tag{18}$$

As bioreactor scale-up is usually accomplished by applying geometric similarity and assuming fixed aspect /ratios ($d_{sf}/d_{bioreactor}$, $h_{sf}/h_{bioreactor}$, $d_{bioreactor}/h_{bioreactor}$), Eq. (18) reduces to:

$$r_{sf} \propto \frac{1}{d_{sf} \omega^2} \tag{19}$$

or, in terms of bioreactor volume:

$$r_{sf} \propto \frac{1}{V^{1/3} \omega^2} \tag{20}$$

Yabannavar et al. [81] used Eqs. (19) and (20) for scale-up purposes. Based on successful operation conditions determined for an existing 12-L bioreactor, they calculated the spin-filter dimensions and operation conditions for an existing 175-L bioreactor. Experiments with the spin-filter designed for the large-scale bioreactor resulted in an absence of filter clogging with cell retention efficiency similar to the 12-L bioreactor. This was considered as an evidence that the suggested scale-up strategy is adequate.

Deo et al. [13] proposed an empirical model based on experimental results obtained with a small-scale spin-filter based bioreactor. They observed that the perfusion flux capacity, which was defined as the perfusion flux at which fouling begun to occur, was proportional to the inverse of the cell concentration and to the square of the tangential velocity at the screen surface (Eq. 21):

$$J_p \propto \frac{v_{tang}^2}{X} \tag{21}$$

Since the perfusion flux is given by Eq. (16) and the screen porosity can be assumed to be constant, the proportionality given in Eq. (22) is obtained.

$$D \propto \frac{A v_{tang}^2}{V X} \tag{22}$$

Eq. (22) shows that, at fixed tangential velocity and cell concentration, perfusion capacity increases proportionally with the *A/V* ratio. Alternatively, maintaining the tangential velocity and the cell concentration constant, an increasing bioreactor volume requires a proportional increase in the spin-filter area in order to maintain the perfusion rate *D* constant. Deo et al. [13] employed this strategy to scale-up a process to the 500-L scale on the basis of the operating conditions established in a 7-L bioreactor. They considered the strategy successful, since the scaled-up process showed the same temporal profiles of cell growth rate, maximum cell concentration and product level as in the small scale.

Although much progress has been made in the last decade regarding operation, design and scale-up of spin-filters, in most works found in the literature either fouling or retention problems (or both) were observed. A better comprehension of the fluid and particle dynamics involved in spin-filter perfusion would improve this situation. In this context, a valuable tool that could be used is computational fluid dynamics (CFD), which has been recently employed for the design and performance prediction of other cell separation devices [46,114].

6 Tangential Flow Filtration

In tangential flow filtration (TFF) systems, feed solution flows perpendicular to the permeation direction. The tangential flow generates high shear rates at the filter surface, contributing to avoid filter fouling and thus enabling a continuous operation and a high filtrate flux. TFF units usually consist of hollow fiber (HF) or flat plate (FP) membrane systems.

Since the early work by Radlett [91], many works have been published on the use of membrane-based TFF for both harvesting [1, 92, 93] and perfusion of mammalian cells (Table 6). According to these works, membrane-based TFF presents various advantages over other separation devices:

- process simplicity and easy adaptation to currently available stirred-tank bioreactors [94];
- high filtration capacity with complete cell retention, generating a particle-free harvest and thus facilitating further downstream processing [1];
- external operation, which enables aseptic filter replacement if fouling occurs, and represents no constraint to process scale-up, such as in the case of internal retention devices [95];
- low operating costs and ability to use the same process for a large amount of different products without great additional development work [92].

Table 6. Overview of reported perfusion processes employing tangential flow filtration units as cell retention device

Cell Line	Product	Reactor Volume (L)	Max. Perfusion Rate (d^{-1})	Cultivation Time (d)	Filter Material/ Pore Size	Filter configuration	Did fouling occur?	Max. Viable Cell Conc. (10^6 mL^{-1})	Reference
Mouse cancer cell	–	0.5	2.9	34	PVDF[a], 0.65 µm	FP	yes	30	97
Hybridoma	IgM	3.6	0.5	20 (2 µm), 40 (10 µm)	PC[b], 2 & 10 µm	FP	yes	4.35	99
Hybridoma	IgM	3.6	1.0	45	PC[b], 2 µm	FP	yes	6	102
Hybridoma	IgG	1.1	1.1	9	nylon, 0.2 µm	FP	no	28	95
Hybridoma	IgM	1.5	0.43 (FP[c]) 0.5 (HF[d])	22 (FP[c]) 48 (HF[d])	nylon, 0.2 µm (FP[c]) PS[e], 0.1 µm (HF[d])	FP[c] and HF[d]	n.a.	13 (FP[c]) 18 (HF[d])	103
Hybridoma	IgG	1.0	4.0	10 – 14	MCE[f], 0.2 µm	HF	eventually	8	94
Hybridoma	IgG	2 & 10	2.0	17.5	MCE[f], 0.2 µm	HF	no	2.1 – 5.5	98

n.a.: Information not available.
[a] PVDF: polyvinylidene fluoride.
[b] PC: polycarbonate.
[c] FP: flat plate system.
[d] HF: hollow fiber system.
[e] PS: polysulfone.
[f] MCE: mixed cellulose ester.

However, in spite of the cleaning action generated by the tangential flow, shear rates and thus feed flow rates are limited by the shear sensitivity of the cell line employed. Thus, fouling remains a major concern when developing a TFF-based perfusion process. Although different authors reported no significant cell damage during TFF processes with either FP or HF units [1, 92, 96], limitations in flow rates due to adverse shearing effects have been frequently reported.

Maiorella et al. [93] carried out tests with flat plate and hollow fiber units with various cell lines (NS-1 myeloma cells, three different hybridoma cell lines and SF-9 insect cells). They observed in all cases that cells were not damaged in laminar flow at average wall shear rates up to 3000 s^{-1}. However, cell damage started to occur beyond this shear level. Zhang et al. [94], using a hollow-fiber cartridge for a hybridoma perfusion culture, observed that shear damaging effects on cell growth occurred for a recirculation rate of 700 mL/min, which corresponded to a calculated maximum shear rate at the fiber walls of 1266 s^{-1}.

Because shear rates and feed flow rates are limited by the shear stability of cells, other strategies have been proposed to avoid fouling. Kawahara et al. [97] reduced the filtrate flux by increasing the membrane area, and adapted a washing line to their perfusion system. In order to wash accumulated cells and debris out of the system, a daily washing process was carried out at a flow rate 80 times higher than that used to pump the cell suspension. Even though, an increasing membrane clogging was observed from the 20^{th} day on and culture had to be terminated on the 30^{th} day.

Smith et al. [98] employed three different techniques to reduce fouling, and suggested that the third one was the most effective method to avoid blocking of the fibers:

- backflush on the HF cartridge shell side;
- increased recirculation rate through the fiber lumen;
- pulsing the feed, whereby care was required to prevent rupture of the fibers when using this technique.

Zhang et al. [94] also implemented different methods to reduce membrane blockage and to prolong cultivation time:

- membranes were coated with polyethylene glycol, which reduces protein adsorption and cell adhesion;
- periodical backflushing of the HF cartridge was carried out;
- a cell-bleeding line was used during backflushing to remove cell debris accumulated in the cartidge.

Combining these techniques, they carried out cultivations for 250–350 h, and were able to repeatedly use the same cartridge (four times at least) without measurable deterioration in filtration efficiency. However, when perfusion rate and cell concentration in the bioreactor increased, fouling eventually occurred. Van Reis et al. [92] provided backpressure on the filtrate line to control filtrate rates and so to avoid too high initial filtration rates, which can cause rapid fouling. De la Broise et al. [99] compared the filter performance using membranes of different pore sizes (2 and 10 µm). In both cases partial retention of the produced IgM was observed and membranes had to be changed every 5 days, the

fouling effects being more accentuated when using the 2 µm membranes. Even though, it was possible to carry out cultivations for about 30 days.

Maiorella et al. [93] observed that fouling behavior was dependent on cell size. For smaller cells or suspensions containing significant levels of debris, high flux rates could not be maintained without inducing high transmembrane-pressures. This behavior is in qualitative agreement with the hydrodynamic lift theory, since lift velocity is predicted to increase with particle diameter to the second [100] or third power [101].

Scale-up of TFF processes is usually done by arranging a large number of short devices in parallel. The individual filters should be kept relatively small in axial dimension, helping to avoid the excessive build-up of feed pressure resulting from the pumping of viscous slurries [96]. By arranging TFF membranes in parallel or in series, units can be scaled-up to process thousands of liters of cell culture fluid in a few hours [1].

Van Reis et al. [92] reported the scale-up of a HF system for the recovery of human tissue plasminogen activator (t-PA) produced by recombinant CHO cells from the 2.5-m^2 to the 180-m^2 scale. A robust and reproducible process was achieved by combining linear scale-up principles, control of fluid dynamic parameters and experimentally defined limits of product retention, which meant maintaining channel length, wall shear rate and flux constant.

Although the fouling problem seems not yet to be completely solved, the simple scale-up, combined with reproducibility of repeated TFF runs, membrane reusability, and suitability of a TFF system for different cell lines and culture media [1] make TFF an attractive choice for mammalian cell separation.

7 Dynamic Filtration

As discussed previously, minimization of filter clogging and fouling requires the generation of sufficient wall shear stress at the filter surface. However, cell lysis has to be avoided in mammalian cell cultivation, in order to allow high cell densities and viabilities to be obtained. Therefore, optimization of animal cell filtration requires careful adjustment of the wall shear stress at the whole membrane area [104]. Dynamic filtration is based on creating a relative motion between the membrane and its housing or between the membrane and a rotor, so that the shear rate produced by this relative motion is independent of feed flow rate [105]. Basically, there are dynamic filtration devices of two different geometries: vortex flow filters (VFF) and rotating disc filters (RDF). A third filtration device which takes advantage of the relative motion between membrane and cell suspension is the double membrane stirrer (DMS) developed by Büntemeyer et al. [106]. Although this is not considered a traditional dynamic filter, it will be briefly discussed in this item. An overview of reports that used dynamic filters for mammalian cell perfusion is given in Table 7.

VFF devices consist of a stationary cylinder, inside which a concentric cylinder rotates. The rotating movement of the inner surface of the annular gap creates a Taylor-Couette flow [16], generating Taylor vortices. The filter medium can

Table 7. Overview of reported perfusion processes employing dynamic filters as cell retention device

Cell Line	Product	Reactor Volume (L)	Max. Perfusion Rate (d^{-1})	Cultivation Time (d)	Filter configuration	Filter Material/ Pore Size/Surface area	Rotation Speed (rpm)	Separation efficiency (%)	Did fouling occur?	Max. Viable Cell Conc. (10^6 mL^{-1})	Reference
CHO, HEK 293, HeLa, mouse myeloma	t-PA, intracellular enzyme, MAb	3.0	2.0	32–60	VFF[a]	SS[b], 10 µm, 200 cm^2	500	> 95	no	20–30	16
Hybridoma	n.a.	n.a.	1.5	58	VFF[a]	SS[b], 10 µm, 300 cm^2	80–250	75–95	n.a.	10	107
Hybridoma	IgM	1.35	0.5	100	VFF[a]	hydrophilized PS[c], 0.8 µm, 200 & 400 cm^2	200–1200	100	partial retention of product	9	141
B-lymphocyte	MAb	1.2	1.3	62	DMS[d]	PP[e], 0.3 µm, 163 cm^2	n.a.	100	no	20	106

n.a.: Information not available.
[a] VFF: vortex flow filter.
[b] SS: stainless steel.
[c] PS: polysulfone.
[d] DMS: double membrane stirrer reactor.
[e] PP: polypropylene.

be mounted either on the rotating or, more commonly, on the stationary cylinder. The stable Taylor vortices generated induce mixing perpendicular to the membrane surface and reduce the extent of concentration polarization and fouling. The flow rate passing through the annulus can be kept low, because the fouling preventive action comes from the Taylor vortices and is thus not coupled to the feedstream flow [16]. VFF have also been called external or *ex-situ* spin-filters [20, 107].

RDF units consist of a rotating disc inside a stationary housing, the membranes being mounted either on the rotating disc [108, 109] or on the housing [104, 110]. Such rotating disc devices have been shown to be very effective not only for solute recovery from microbial suspensions [111, 112], but also for mammalian cell separation [104, 113]. Like in VFF, this concept permits the independent adjustment of wall shear stress, transmembrane pressure and residence time, allowing a straightforward optimization of the filtration process and the establishment of a controlled shear field. Therefore, it has also been called CSF – controlled shear filtration [104].

The core of double membrane stirrer perfusion bioreactors is a stirrer on which two microporous hollow fiber membranes are mounted, one of them being hydrophobic and used for bubble-free aeration, the second of them being hydrophilic and used for cell-free medium exchange [15]. This system has been reported to provide viable cell densities of 20 million cells per milliliter for more than two months [106]. Although Lehmann et al. [15] have described the scale-up of this system to the 20-L and 150-L scale, it has been most commonly employed at the bench-scale.

Rebsamen et al. [138, 139] were among the first to investigate the use of vortex flow filters for mammalian cell separation. They carried out experiments with suspensions of hybridoma and human breast carcinoma (SKBR-5) cells. For rotor angular velocities up to 500 rpm no viability decrease was observed. A concentration of SKBR-5 cells under sterile conditions with subsequent cultivation of the concentrated cells showed that the cells were able to grow normally after being subjected to vortex flow filtration. The authors suggested that the VFF could be employed as a long-operating-life cell retention device in perfusion cultures or, in a miniaturized version, as an on-line sampling device.

Hawrylik et al. [140] investigated the influence of rotor speed, retentate flow rate and system back pressure on the separation of U-937 human lymphoma cells expressing interleukin-4 (IL-4) on the cell surface, aiming at a reduction of shear damage to cells and a minimization of contaminating cellular proteins in the process stream. They verified that even under the gentlest conditions applied no evidence of clogging or buildup of differential pressure across the membrane occurred. Under these conditions, the cell surface IL-4 binding capacity was completely recovered and a minimal loss of cell viability was observed. These facts suggested that the cells remained intact during filtration. The authors concluded that VFF proved to be an efficient, low shear method for mammalian cell separation and medium harvesting.

Mercille et al. [141] compared TFF and VFF for the perfusion cultivation of a hybridoma cell line producing an IgM, either using serum-supplemented or protein-free medium, with and without the addition of DNAse. They observed

that the use of the VFF module allowed the maintenance of an optimal filtration efficiency for a much longer period than by using the TFF module. Similar overall growth and production kinetics were observed in both modules. However, they observed that the number of cell aggregates found at the outlet of the VFF module was considerably lower than the number found at the inlet, indicating that vortex flow in the filtration device led to some disaggregation of cell clumps found in the protein-free culture. A low product retention, which is an indication of low incidence of fouling, was found for the VFF. The addition of DNAse resulted in complete elimination of product retention in the VFF module, indicating that DNA fragments were partially responsible for membrane fouling. As suggestion for further efficiency improvements of the VFF, they proposed the use of new, hydrophilized membranes; the use of increased Pluronic F68 concentrations to allow higher rotation speeds to be applied; and a reduction in the amount of protein, DNA and lipid liberation from dead cells, possibly through genetic engineering targeted at reducing apoptosis.

Fraune et al. [107] and Trocha et al. [20] employed VFF devices containing stainless steel meshes of 10 and 20 µm mesh size, respectively. Fraune et al. [107] carried out a hybridoma cell perfusion cultivation for 1400 hours, and observed that at a rotation rate of 250 rpm a selective retention of viable cells occurred, the dead cells being washed out. Under these operating conditions, the cleaning effects at the filter surface were enhanced and the operation time of the VFF device was prolonged. The authors concluded that the external VFF provided a flexible easy-to-use perfusion system for mammalian cells, and that manipulating the operating conditions (rotation speed, perfusion rate, recirculation and filtrate flow rate) was an appropriate tool for enhancing the viability of the culture.

Trocha et al. [20] observed that relatively small shear rates (at 400 rpm) were sufficient to prevent the formation of a filter cake at the mesh/annulus interface, but that for higher rotation speeds (900 rpm) the centrifugal field in the interior of the rotating cylinder caused a filter cake to be formed onto the mesh/lumen interface. The authors suggested that this inner surface fouling was responsible for the high retention observed in filters with large pores at high rotation rates. Roth et al. [16] tested a VFF with a 10 µm stainless steel mesh for long-term (30–60 days) perfusion cultivations of different cell lines (HEK 293, HeLa, a mouse myeloma and two CHO cell lines). In all cases, retention efficiency was reported to be greater than 95%, no negative influence of the system on cell viability and protein expression level was verified, as well as no substantial cell lysis was observed by DNA measurement. Sterility was maintained over the duration of all experiments, and the measurement of transmembrane pressure indicated no problems of filter fouling or perforation. As in the work by Mercille et al. [141], the authors observed that cell clumps were disaggregated, so that the cell size distribution became much more monodisperse. Since in the case of aggregating cultures the exchange of nutrients and metabolites with the surrounding medium becomes restricted for cells which are not on the surface of the aggregates, Roth et al. [16] claimed that the VFF can be used to exert a selective pressure that modulates cell aggregate size, increasing cultivation efficiency. Since the authors could successfully use the VFF device for perfusion reactors

with working volumes ranging from 3 to 50 L at a perfusion rate of 2 d^{-1} by varying the recirculation and the filtrate flow rates, they concluded that the VFF was a reliable and versatile cell retention system for mammalian cell cultures in perfusion mode.

Kempken et al. [113] employed a rotating disc filter to harvest CHO cells, and observed that the filter could be operated at low transmembrane-pressure with high wall shear rates, leading to high filtrate flow rates, high product yields and minimum fouling. They concluded that their system offered a powerful alternative to conventional tangential flow filtration.

Vogel and Kroner [104] proposed a RDF where one side of the disc (the one facing the membrane) had a slightly conic shape. They carried out batch experiments simulating both perfusion and harvesting conditions. The results obtained under varying conditions showed that the cells presented a threshold level of shear stability, which depended on the frequency and exposure time to shear, as well as on cell status. By operating the RDF close to this threshold value, cell viability could be maintained, while concentration polarization and fouling could be efficiently minimized. Applying this concept, they attained steady state filtrate flux rates of about 60 L h^{-1} m^{-2} when simulating perfusion, and 290 L h^{-1} m^{-2} when using harvesting conditions with a 3-μm membrane. Flux rates at least 3-fold higher than with a conventional TFF device (thin channel module) could be obtained, with the benefit of enhanced cell viability. According to the authors, the system showed promising performance and could be comparatively easily scaled-up, so that the only disadvantages were the higher mechanical complexity and the lower membrane packing density in comparison to conventional TFF.

Castilho et al. [114] used a computational fluid dynamics (CFD) tool combined with an statistical design approach to optimize the rotor geometry and angular velocity of a RDF suited for mammalian cell separation. The strategy and tools employed in this work made it possible to determine an optimized filter geometry that minimizes problems of fouling by generating high shear forces on the membrane surface, while controlling the global maximal shear stress in the whole module at a given level in order not to damage the cells. The authors proposed the use of this filter combined with affinity membranes (Fig. 6) to allow the execution of an integrated, one-stage perfusion/purification process for the production of recombinant proteins from mammalian cells, which could result in a reduction of manufacturing costs.

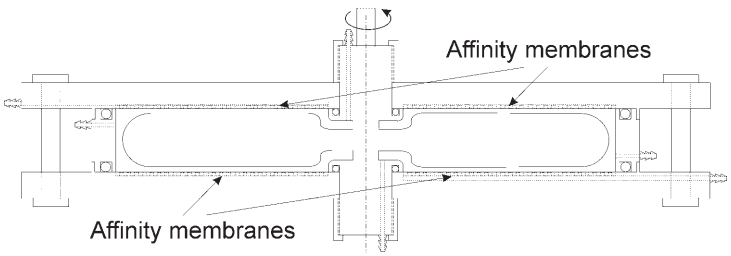

Fig. 6. Rotating disc filter designed using computational fluid dynamics [114]

Although perfusion cultures using RDF devices have not yet been reported, the results obtained in harvesting [113] and simulated perfusion experiments [104] indicate that it could be a promising cell retention device for suspended-cell perfusion processes.

8 Ultrasonic Separation

Ultrasonic separation of cells (and other particles) occurs due to acoustic forces generated in a plane standing-wave. These forces are a result of interactions between fluid and cells, and their magnitude depends on the difference in density and compressibility between the cells and the medium [115]. A plane standing-wave arises as a result of the interference between waves of equal wavelength and amplitude travelling in opposite directions. It is formed by parallel stationary node (zero velocity or pressure amplitude) and antinode planes (maximum velocity or pressure amplitude). The node planes are separated from each other by a half wavelength distance and the antinode planes lie equidistant between them (Fig. 7). Velocity nodes coincide with pressure antinodes and vice versa [116]. The ultrasonic forces first drive the cells towards the pressure nodes of the resonance field. The cells then migrate laterally within the nodes, due to inhomogeneities in the sound field, aggregating to form relatively large clumps. The retention efficiency of acoustic cell filtration devices is dependent on the magnitude of the acoustic forces developed inside the apparatus, and these forces are a function of the acoustic energy density distribution in the liquid. It has been suggested that this distribution is a function of the dimensions, imposed boundary conditions and

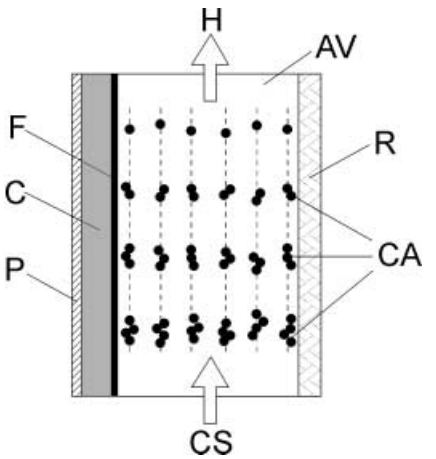

Fig. 7. Schematic view of an acoustic cell filter [127]. P: piezoceramic, C: carrier (glass), F: polysulfone foil, AV: active volume, R: reflector, CA: cell aggregates, CS: cell suspension, H: harvest (clarified fluid). The nodal planes (pressure nodes) of the standing acoustic field are schematically indicated by dashed lines

physical properties of the filter reflector and transducer [117]. A versatile method for experimental measurements of the acoustic forces acting upon single particles has been developed [116, 118], and the knowledge of the spatial distribution of the ultrasonic forces can lead to models for performance prediction.

Ultrasonic separators have been used for the separation of microorganisms [119–121] and animal cells [115, 122–124], and as cell retention devices in perfusion cultures (Table 8) [125–128]. The high amplitudes necessary to achieve cell separation produce a local increase in temperature, which poses a serious problem when dealing either with animal cells or with thermolabile products. Medium temperature increases of up to 1.3 °C min^{-1} have been reported [115]. This heating appears as a result of attenuation of the acoustic energy in the transducer, reflector, and cell suspension [115]. Thus, a temperature gradient is created in the fluid, which produces inhomogeneities in the acoustic properties of the resonator and, consequently, a decrease in its performance [123]. Doblhoff-Dier et al. [123] overcame this problem using a dual-chamber resonator composed of a separator chamber and a cooling chamber. The authors also observed that, for keeping a constant cell separation efficiency, it was necessary to increase the input power as the flow rates increased. This was also observed by Gröschl et al. [127], and can be explained as the required increase in the ultrasonic forces in order to compensate the increase in the drag forces acting on the cells.

Pui et al. [115], using a 75 mL resonance chamber, found that ultrasonic exposures up to 220 W L^{-1} had no influence on the viability and product formation, as also observed by Trampler et al. [128] and Ryll et al. [125]. Pui et al. [115] just observed a decrease in cell viability at a power level of 260 W L^{-1}, probably due to cavitation leading to cell disruption. They also found, as Kilburn et al. [124], that cell separation increased with acoustic treatment time and cell concentration, so that efficiencies over 97 % were achieved for cell concentrations between 10^6 and 10^7 cell mL^{-1}. However, Ryll et al. [125] found a sudden and sharp drop in the separation efficiency above a certain perfusion rate, which varied with the cell concentration. They explained this sudden drop in performance as a consequence of the accumulation of cell mass inside the separation chamber of the separator, with the consequent breakthrough of a large amount of cells. Gaida et al. [122] demonstrated that, through the control of operational parameters, such as flow rate and power input, it is possible to selectively remove nonviable cells and cell debris, while retaining up to 99 % of the viable cells within the reactor. They suggested 0.75 mm s^{-1} as a realistic operational average fluid velocity inside the separator, which had a 50 mL separation chamber and a 30 mL cooling chamber. Ultrasonic separators have been used so far only in small scale perfusion systems, since their scale-up has not yet been properly solved.

Table 8. Overview of reported perfusion processes employing ultrasonic separators as cell retention device

Cell Line	Product	Reactor Volume (L)	Max. Perfusion Rate (d^{-1})	Operation Time (d)	Resonator Volume (mL)	Max. Viable Cell Conc. (10^6 mL^{-1})	Separation Efficiency (%)	Reference
CHO	glycoprotein	1.5	3.0	up to 51	10	50	>95	125
Insect	protein	5.0	5.4	10	n.a.	33	100 → 20	126
Hybridoma	MAb	5.3	5.4 & 2.9	42 & 18	50	9 & 28	99.5	127
Hybridoma	IgG	1.0	3.2	30	6	23	>97	128

n.a.: Information not available.

9
Dielectrophoretic Separation

The movement of particles under the influence of an applied electric field can be due to electrophoresis or dielectrophoresis. The former is the movement of electrically charged particles in either direct current or low-frequency alternating current fields. The latter is the movement of particles in a nonuniform electric field and, unlike electrophoresis, it does not require a net charge on the particle to occur [129]. A particle (cell) immersed in an electrical field will become electrically polarized, i.e., an induced dipole moment is imposed on the particle [130]. For nonuniform electrical fields, the field on one region of the cell will be stronger than on other regions, leading to greater charge densities in specific areas of the cell relative to those charges of opposite sign aligned where the field is less intense (Fig. 8) [131]. As a result, the particle experiences a net translational force, which may direct it either towards or away from the high field regions [130]. This dielectrophoretic force is a function of the particle dielectric properties relative to that of the medium, and on the frequency and level of nonuniformity of the applied electrical field [132].

Although dielectrophoretic separation of cells have been used for separation of microrganisms [129–132], plant cells [129] and mammalian cells [133], only recently its application in perfusion systems has been cogitated [134–136]. Doscolis et al. [134] developed a microelectrode filter, which was applied in the dielectrophoretic separation of C174 myeloma cell suspensions. They found that the optimum frequency range for selective retention of viable cells was in the range 5–15 MHz. Moreover, they observed a maximum separation efficiency of 98% when working at 10 MHz with a flow rate of 0.5 mL min^{-1}, equivalent to a superficial velocity of 0.9 mm min-1 through the filter channels, whereas the separation efficiency was low, often below 15%, for nonviable cells

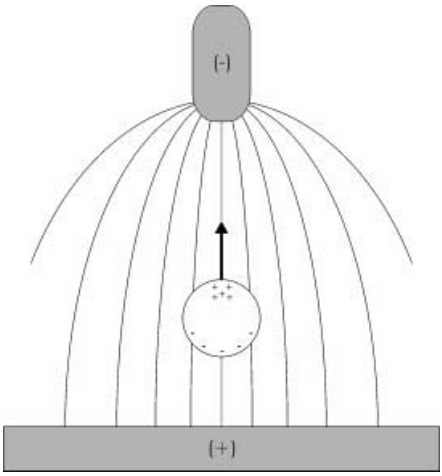

Fig. 8. Dielectrophoretic action on a particle in a non-uniform electric field, demonstrating direction of movement towards high field intensity regions [131]

regardless of the operating conditions. In another work [135, 136], the same research group used a 5 mL modified vial to simulate the conditions in the vicinity of the dielectrophoretic filter inside a bioreactor. When working with a hybridoma cell line, they noticed no adverse effect on viable cell concentration, viability, glucose uptake, lactate production, and monoclonal antibody production. No noticeable effect was also found when working with CHO cells. The authors then concluded that no negative effects should be expected during a perfusion culture using a dielectrophoretic separator as cell retention device. It should be pointed out that, to date, no actual perfusion culture has been performed using such a device. Furthermore, a problem that may arise when applying this device in perfusion bioreactors is the possible heating of the medium inside the filter channels.

10 Conclusions

In the recent years, much progress has been made regarding design, operation and scale-up of cell retention devices. Furthermore, mammalian cell separation has been achieved using new separators or new applications of established equipment, enlarging the range of available cell retention apparatuses. Since perfusion systems can be operated at relatively high medium throughput rates at substantially higher cell concentrations, resulting in higher productivities than those obtained in batch mode, the continuous improvement of such retention devices may lead to a shift in industrial processes from the still prevailing batch or fed-batch processes to perfusion-based strategies.

References

1. Berthold W, Kempken R (1994) Cytotechnology 15:229
2. Emery N, Gerin P (1998) Biofutur 184(dec):26
3. Griffiths JB (1992) J Biotechnol 22:21
4. Lubiniecki AS (1998) Cytotechnology 28:139
5. Yang JD, Angelillo Y, Chaudhry M, Goldenberg C, Goldenberg DM (2000) Biotechnol Bioeng 69:74
6. Birch JR, Arathoon R (1990) In: Lubiniecki AS (ed) Large-scale mammalian cell culture technology. Marcel Dekker, New York, p 251
7. Mercille S, Johnson M, Lanthier S, Kamen AA, Massie B (2000) Biotechnol Bioeng 67:435
8. Avgerinos GC, Drapeau D, Socolow JS, Mao J, Hsiao K, Broeze RJ (1990) BioTechnol 8:54
9. Griffiths JB (1990) In: Lubiniecki AS (ed) Large-scale mammalian cell culture technology. Marcel Dekker, New York, p 217
10. Kadouri A, Spier RE (1997) Cytotechnology 24:89
11. Burrows MT (1912) Anat Rec 6:141
12. Su WW (2000) In: Spier RE (ed) Encyclopedia of cell technology – Volume 1. John Wiley & Sons, New York, p 230
13. Deo YM, Mahadevan MD, Fuchs R (1996) Biotechnol Prog 12:57
14. Heine H, Biselli M, Wandrey C (1999) In: Bernard A, Griffiths B, Noé W, Wurm F (eds) Animal cell technology: products from cells, cells as products. Kluwer, Dordrecht, p 83
15. Lehmann J, Vorlop J, Büntemeyer H (1988) In: Spier RE, Griffiths JB (eds) Animal cell biotechnology, vol 3. Academic Press, London, p 221

16. Roth G, Smith CE, Schoofs GM, Montgomery TJ, Ayala JL, Horwitz JI (1997) Biopharm 10(oct):30
17. Zeng AP, Deckwer WD (1999) Biotechnol Prog 15:373
18. Woodside SM, Bowen BD, Piret JM (1998) Cytotechnology 28:163
19. Fenge C, Klein C, Heuer C, Siegel U, Fraune E (1993) Cytotechnology 11:233
20. Trocha M, von Rohr PR, Sümeghy Z (1997) In: Carrondo MJT (ed) Animal cell technology. Kluwer, Dordrecht, p 405
21. Tebe H, Lütkemeyer D, Gudermann F, Heidemann R, Lehmann J (1997) Cytotechnology 22:119
22. Tebe H, Gudermann F, Lütkemeyer D, Lehmann J (1996) In: Carrondo MJT, Griffiths B, Moreira JLP (eds) Animal cell technology: from vaccines to genetic medicine, Kluwer Academic Pub, Dordrecht, p 391
23. Kempken R, Preissmann A, Berthold W (1995) Biotech Bioeng 46:132
24. Heiskanen K (1993) Particle Classification. Chapman & Hall, London
25. Miller RG, Phillips RA (1969) J Cell Physiol 73:191
26. Hülscher M, Scheibler U, Onken U (1992) Biotechnol Bioeng 39:442
27. Wen Z-Y, Teng X-W, Chen F (2000) J Biotech 79:1
28. Freshney RY (1994) Culture of Animal Cells, 4th edn. Wiley, New York
29. Frachon M, Cilliers JJ (1999) Chem Eng J 73:53
30. Nageswararao K (2000) Chem Eng J 80:251
31. Coelho MAS, Medronho RA (2001) Chem Eng J (in press)
32. Svarovsky L (ed) (1990) Solid-Liquid Separation, 3rd edn. Butterworths, London
33. Medronho RA (2002) Solid-liquid separation. In: Mattiasson B, Hatti-Kaul R (eds) Isolation and purification of proteins. Marcel Dekker Inc, New York (in press)
34. Hamamoto K, Ishimaru K, Yokoyama S, Tokashiki M (1989) J Ferment Bioeng 67:190
35. Tokashiki M, Arai T, Hamamoto K, Ishimaru K (1990) Cytotechnology 3:239
36. Tokashiki M, Yokoyama S (1997) Bioreactor designed for animal cells. In: Hauser H, Wagner R (eds) Mammalian cell biotechnology in protein production. Walter de Gruyter, Berlin, p 279
37. Björling T, Dudel U, Fenge C (1995) In: Beuvery EC, Griffiths JB, Zeijlemaker WP (eds) Animall cell technology: developments towards the 21st century. Kluwer Academic Pub, Dordrecht, p 671
38. Yokoyama S, Takamatsu H, Hamamoto K, Motoki M, Arai T, Ishimaru K, Kimura M, Tanokura A, Ono S, Nagura K, Tokashiki M (1995). In: Beuvery EC, Griffiths JB, Zeijlemaker WP (eds) Animal cell technology: developments towards the 21st century. Kluwer Academic Pub, Dordrecht, p 917
39. Takamatsu H, Hamamoto K, Ishimaru K, Yokoyama S, Tokashiki M (1996) Appl Microbiol Biotechnol 45:454
40. Jäger V (1992) In: Kreysa G, Driesel AJ (eds) Microbial principles in bioprocesses: cell culture technology, downstream processing and recovery. DECHEMA, Frankfurt am Main, p 265
41. Jäger V (1992) In: Murakami H, Shirahata S, Tachibana H (eds) Animal cell technology: basic & applied aspects. Kluwer Academic Pub, Dordrecht, p 209
42. Jäger V (1992) In: Spier RE, Griffiths JB, MacDonald C. In Animal cell technology: developments, processes and products. Butterworth-Heinemann, Oxford, p 397
43. Apelman S (1992) In: Murakami H, Shirahata S, Tachibana H (eds) Animal cell technology: basic & applied aspects. Kluwer Academic Pub, Dordrecht, p 149
44. Johnson M, Lantier S, Massie B, Lefebvre G, Kamen AA (1996) Biotechnol Prog 12:855
45. Castilho LR, Medronho RA (2000) Miner Eng 13:183
46. Medronho RA, Schütze J, Deckwer W-D (2002) Braz J Chem Eng (in press)
47. He P, Salcudean M, Gartshore IS (1999) Chem Eng Res Des 77:429
48. Dai GQ, Li JM, Chen WM (1999) Chem Eng J 74:217
49. Averous J, Fuentes R (1997) Can Metall Quart 36:309
50. Devulapalli B, Rajamani RK (1996) In: Claxton D, Svarovsky L, Thew M (eds) Hydrocyclones '96. Mechanical Engineering Publications, London & Bury Saint Edmunds, p 83

51. Rickwood D, Onions J, Bendixen B, Smyth I (1992) In: Svarovsky L, Thew MT (eds) Hydrocyclones: Analysis and Applications. Kluwer Academic Pub, Dordrecht, p 109
52. Yuan H, Rickwood D, Smyth IC, Thew MT (1996) Bioseparation 6:159
53. Yuan H, Thew MT, Rickwood D (1996) In: Claxton D, Svarovsky L, Thew M (eds) Hydrocyclones '96. Mechanical Engineering Publications, London & Bury Saint Edmunds,p 135
54. Harrison STL, Davies GM, Scholtz NJ, Cilliers JJ (1994) In: Pyle DL (ed) Separations for Biotechnology 3. SCI, The Royal Society of Chemistry, Cambridge, p 214
55. Cilliers JJ, Harrison STL (1996) In: Claxton D, Svarovsky L, Thew M (eds) Hydrocyclones '96. Mechanical Engineering Publications, London & Bury Saint Edmunds, p 123
56. Cilliers JJ, Harrison STL (1997) Chem Eng J 65:21
57. Rickwood D, Freeman GJ, McKechnie M (1996) In: Claxton D, Svarovsky L, Thew M (eds) Hydrocyclones'96. Mechanical Engineering Publications, London & Bury Saint Edmunds, p161
58. Matta VM, Medronho RA (2000) Bioseparation 9:43
59. Thorwest I, Bohnet M (1992) Chem Ing Tech 64:1123
60. Ortega-Rivas E, Medina-Caballero HP (1996) Powder Hand Proc 8:355
61. Bednarsky S (1996) In: Claxton D, Svarovsky L, Thew M (eds) Hydrocyclones'96. Mechanical Engineering Publications, London & Bury Saint Edmunds, p 151
62. Marschall A (1997) Dr. rer. nat. Thesis, Technical University of Braunschweig
63. Müller M (2000) Dr.-Ing. Thesis, Technical University of Braunschweig
64. Lübberstedt M (2000) MSc Thesis, University of Applied Sciences of Berlin (TFH-Berlin)
65. Lübberstedt M, Medronho RA, Anspach FB, Deckwer W-D (2000) Chem Ing Tech 72:1089
66. Lübberstedt M, Medronho RA, Anspach FB, Deckwer W-D (2000) Proc Biotechnology 2000, vol 1, Dechema eV, Frankfurt am Main, p 460
67. Bradley D (1965) The Hydrocyclone. Pergamon Press, Oxford
68. Yim SS, Shamlou PA (2000) Adv Biochem Eng Biotechnol 67:83
69. Born C, Zhang Z, Al-Rubeai M, Thomas CR (1992) Biotechnol Bioeng 40:1004
70. Tokashiki M, Arai T (1989) Cytotechnology 2:5
71. Tokashiki M, Arai T (1991) In: Spier RE, Griffiths JB, Meignier B (eds) Production of biologicals from animal cells in culture, Butterworth-Heinemann, Oxford, p 467
72. Arai T, Yokoyama S, Tokashiki M (1993) In: Kaminogawa S, Ametani A, Hachimura S (eds) Animal cell technology: basic & applied aspects, Vol 5. Kluwer Academic Pub, Dordrecht, p 149
73. Batt BC, Davis RH, Kompala DS (1990) Biotechnol Prog 6:458
74. Searles JA, Todd P, Kompala DS (1994) Biotechnol Prog 10:198
75. Searles JA, Todd P, Kompala DS (1994) In: Spier RE, Griffiths JB, Berthold W (eds) Animal cell technology: products for today prospects for tomorrow, Butterworth-Heinemann, Oxford, p 240
76. Hansen HA, Damgaard B, Emborg C (1993) Cytotechnology 11:155
77. Knaack C, André G, Chavarie C (1994) In: Spier RE, Griffiths JB, Berthold W (eds) Animal cell technology: products for today prospects for tomorrow, Butterworth-Heinemann, Oxford, p 230
78. Thompson KJ, Wilson JS (1994) In: Spier RE, Griffiths JB, Berthold W (eds) Animal cell technology: products for today prospects for tomorrow, Butterworth-Heinemann, Oxford, p 227
79. Stevens J, Eickel S, Onken U (1994) In: Spier RE, Griffiths JB, Berthold W (eds) Animal cell technology: products for today prospects for tomorrow, Butterworth-Heinemann, Oxford, p 234
80. Himmelfarb P, Thayer PS, Martin HE (1969) Science 164:555
81. Yabannavar VM, Singh V, Connelly NV (1994) Biotechnol Bioeng 43:159
82. Segré G, Silberberg A (1961) Nature 189:209
83. Drew DA, Schonberg JA, Belfort G (1991) Chem Eng Sci 46:3219
84. Belfort G (1988) J Membr Sci 35:245
85. Favre E, Thaler T (1992) Cytotechnology 9:11

86. Varecka R, Scheirer W (1987) Develop Biol Standard 66:269
87. Esclade LRJ, Carrel S, Péringer P (1991) Biotechnol Bioeng 38:159
88. Tolbert WR, Feder J, Kimes RC (1981) In Vitro 17:885
89. Yabannavar VM, Singh V, Connelly NV (1992) Biotechnol Bioeng 40:925
90. Iding K, Lütkemeyer D, Fraune E, Gerlach K, Lehmann J (2000) Cytotechnology 34:141
91. Radlett PJ (1972) J Appl Chem Biotechnol 22:495
92. van Reis R, Leonard, LC, Hsu CC, Builder SE (1991) Biotechnol Bioeng 38:413
93. Maiorella B, Dorin G, Carion A, Harano D (1991) Biotechnol Bioeng 37:121
94. Zhang S, Handa-Corrigan A, Spier RE (1993) Biotechnol Bioeng 41:685
95. Velez D, Miller L, Macmillan JD (1989) Biotechnol Bioeng 33:938
96. Shiloach J, Kaufman JB, Kelly RM (1986) Biotechnol Prog 2:230
97. Kawahara H, Mitsuda S, Kumazawa E, Takeshita Y (1994) Cytotechnology 14:61
98. Smith CG, Guillaume JM, Greenfield PF, Randerson DH (1991) Bioproc Eng 6:213
99. de la Broise D, Noiseux M, Massie B, Lemieux R (1992) Biotechnol Bioeng 40:25
100. Eckstein EC, Bailey DG, Shapiro AH (1974) J Fluid Mech 79:191
101. Vasseur P, Cox RG (1976) J Fluid Mech 78:385
102. de la Broise D, Noiseux M, Lemieux R, Massie B (1991) Biotechnol Bioeng 38:781
103. Brennan AJ, Shevitz J, Macmillan JD (1987) Biotechnol Tech 1:169
104. Vogel JH, Kroner KH (1999) Biotechnol Bioeng 63:663
105. Bouzerar R, Jaffrin MY, Ding L, Paullier P (2000) AIChE J 46:257
106. Büntemeyer H, Bödeker BGD, Lehmann J (1987) In: Spier RE, Griffiths JB (eds) Modern approaches to animal cell technology. Butterworth, London, p 411
107. Fraune E, Meichsner S, Kamal MN (1997) In: Carrondo MJT (ed) Animal cell technology. Kluwer, Dordrecht, p 283
108. Engler J, Wiesner MR (2000) Wat Res 34:557
109. Frenander U, Jönsson AS (1996) Biotechnol Bioeng 52:397
110. Nuortila-Jokinen J, Nyström M (1996) J Membr Sci 119:99
111. Meyer F, Gehmlich I, Guthke R, Gorak A, Knorre WA (1998) Biotechnol Bioeng 59:189
112. Pessoa AP, Vitolo M (1998) Proc Biochem 33:39
113. Kempken R, Rechtsteiner H, Schäfer J, Katz U, Dick O, Weidemeier R, Sellick I (1997) In: Carrondo MJT (ed) Animal cell technology. Kluwer, Dordrecht, p 379
114. Castilho LR, Anspach FB, Deckwer WD (2000) Proc Biotechnology 2000, vol 4, Dechema eV, Frankfurt am Main, p 252
115. Pui PWS, Trampler F, Sonderhoff AS, Gröschl M, Kilburn DG, Piret JM (1995) Biotechnol Prog 11:146
116. Woodside, SM, Bowen BD, Piret JM (1997) In: Carrondo MJT, Griffiths B, Moreira JLP (eds) Animal cell technology: from vaccines to genetic medicine, Kluwer Academic Pub, Dordrecht, p 251
117. Woodside, SM, Piret JM, Gröschl M, Benes, E, Bowen BD (1998) AIChE J 44:1976
118. Woodside, SM, Bowen BD, Piret JM (1997) AIChE J 43:1727
119. Hawkes JJ, Limaye MS, Coakley WT (1997) J Appl Microbiol 82:39
120. Hawkes JJ, Coakley WT (1996) Enzyme Microb Tech 19:57
121. Coakley WT, Whitworth G, Grundy MA, Gould RK, Allman R (1994) Bioseparation 4:73
122. Gaida Th, Doblhoff-Dier O, Strutzenberger K, Katinger H (1996) Biotecnol Prog 12:73
123. Doblhoff-Dier O, Gaida Th, Katinger H (1994) Biotechnol Prog 10:428
124. Kilburn DG, Clarke DJ, Coakley WT, Bardsley DW (1989) Biotechnol Bioeng 34:559
125. Ryll T, Dutina G, Reyes A, Gunson J, Krummen L, Etcheverry T (2000) Biotechnol Bioeng 69:440
126. Zhang J, Collins A, Chen M, Knyazev I, Gentz R (1998) Biotechnol Bioeng 59:351
127. Gröschl M, Burger W, Handl B (1998) Acustica 84:815
128. Trampler F, Sonderhoff AS, Pui PWS, Kilburn DG, Piret JM (1994) Bio/Technol 12:281
129. Markx GH, Pethig R (1995) Biotechnol Bioeng 45:337
130. Markx GH, Talary MS, Pethig R (1994) J Biotechnol 32:29
131. Brown AP, Harrison AB, Betts WB, O'Neil JG (1997) Microbios 91:55
132. Markx GH, Dyda PA, Pethig R (1996) J Biotechnol 51:175

133. Huang Y, Wang X-B, Becker FF, Gascoyne PRC (1997) Biophys J 73:1118
134. Doscolis A, Kalogerakis N, Behie LA, Kaler KVIS (1997) Biotechnol Bioeng 54:239
135. Doscolis A, Kalogerakis N, Behie LA (1999) Cytotechnology 30:133
136. Kalogerakis N, Doscolis A, Behie LA (1998) In Merten OW, Perrin P, Griffiths B (eds) New developments and new applications in animal cell technology, Kluwer Academic Pub, Dordrecht, p 369
137. Svarovsky L (1985) Solid-liquid separation processes and technology. Elsevier Science Pub, Amsterdam
138. Rebsamen E, Goldinger W, Scheirer W, Merton OW, Palfi GE (1987) In: Spier RE, Griffiths JB (eds) Modern approaches to animal cell technology. Butterworth, London, p 548
139. Rebsamen E, Goldinger W, Scheirer W, Merton OW, Palfi GE (1987) Develop Biol Standard 66:273
140. Hawrylik SJ, Wasilko DJ, Pillar JS, Cheng JB, Lee SE (1994) Cytotechnology 15:253
141. Mercille S, Johnson M, Lemieux R, Massie B (1994) Biotechnol Bioeng 43:833

Received: April 2001

Fed-Batch Cultures of *Escherichia coli* Cells with Oxygen-Dependent *nar* Promoter Systems

Ho Nam Chang*, Se Jong Han[1], Seong-Chun Yim, Mu-ri Han[2], Jongwon Lee[3]

* Department of Chemical Engineering, KAIST, Taejon 305-701, Korea
E-mail: hnchang@mail.kaist.ac.kr
[1] Fine Chemical Research Institute, Samchully Pharmaceutical, Shiheung, Kyunggi 429-450, Korea
[2] R&D Center of Coreana Cosmetics, Cheonan, Chungnam 330-830, Korea
[3] Department of Biochemistry, School of Medicine, Catholic University of Daegu, Taegu 705-034, Korea

Dedicated to Prof. Dr. Wolf-Dieter Deckwer on the occasion of his 60th birthday

The recombinant proteins produced from *Escherichia coli* as a host cell need to be made at as low a cost as possible because of the end of the monopoly following expiry of the patent on early pharmaceutical proteins, and thus expanding applications to non-pharmaceutical large-scale products. We review in this article how the various promoters used in recombinant *E. coli* could affect its protein products, especially with emphasis on relatively new oxygen-dependent *nar* promoters for β-galactosidase production. Several studies carried out in the authors' laboratory show that the *nar* promoter does not require any chemicals except 1% nitrate and oxygen for protein production. And according to recent work with the modified strains it is possible to produce the enzyme (β-galactosidase) even without the nitrate ions at 45% of its total protein content when its cell density reached OD = 176.

Keywords. *Nar* promoter, Oxygen-dependent, Inducible promoter, Fed-batch, Recombinant

Advances in Biochemical Engineering/
Biotechnology, Vol. 74
Managing Editor: Th. Scheper

List of Abbreviations

DO Dissolved oxygen
OD_{600} Optical density at 600 nm

1 Introduction

The early stages of the genetic engineering era focused on the production of high-value products such as insulin, interferons, etc. Attention had to be paid to the bioreactor operation and downstream processing to meet regulatory standards. However, the progress of genetic engineering and bioprocessing techniques made it possible to diversify its products from high-value to medium- and low-value ones. Late participants in the recombinant DNA product markets always came up with new production technologies and, furthermore, expiration of patents forced manufacturers to lower the production cost of existing products already on the market. Optimization of recombinant protein production activities was focused on increasing cell densities and protein content in each cell to as high a level as possible.

Several excellent review articles have addressed this issue from molecular biology to high density cell cultures of *Escherichia coli* cells [1–4]. We will briefly review *E. coli* promoter system with emphasis on oxygen-dependent *VHb* and *nar* promoters and discuss fed-batch cultures of the *nar* promoter system requiring nitrates or no nitrates. These new systems will be compared with other existing promoter systems.

2 *E. coli* Promoters

A promoter to be used in *E. coli* should have certain characteristics to render it suitable for high-level production of recombinant protein. First, it must be strong, resulting in the accumulation of protein making up to 10–30% or more of the total cellular protein. Second, it should exhibit a minimal level of basal transcriptional activity. Third, promoters should be capable of induction in a simple and cost-effective manner.

2.1 Thermal and Chemical Promoters

The most widely used promoters for large-scale protein production are thermal or chemical inducible ones. Temperature-regulated promoters are based on the bacteriophage λ promoters P_L and P_R. These promoters are regulated by *cI* gene and induced by elevating culture temperature from approximately 30°C to about 40°C [5, 6]. General disadvantages of using temperature induction include induction of the heat-shock system, denaturation of overexpressed protein product, and expenditure of high energy [7, 8]. Induction of the *lac*, the *tac*, and the

phage T7 promoters are usually performed by addition of the lactose analog, isopropylthio-β-D-galactoside (IPTG). This is not very practical in large-scale production processes because IPTG is very expensive and furthermore the use of IPTG for the production of human therapeutic proteins is undesirable because of its toxicity [9]. Induction of the *trp* promoter is accomplished by starvation of tryptophan, a procedure that is well suited for large-scale cultures of recombinant *E. coli*. One disadvantage of *trp* promoter is that the best medium, including tryptophan for the growth, cannot be used for induction. Several other expression vectors can be modulated by simple cultivation parameters such as concentration of phosphate [10, 11] or oxygen [12 – 14]. Phosphate inducible systems are also of interest for large-scale processes, since the induction is easily accomplished by phosphate-limited growth conditions. The induction ratios of most phosphate promoters were reported to be more than 100-fold [15].

2.2 VHb Promoter

Promoters having an activity that can be modulated by varying the dissolved oxygen of the culture medium offer several favorable advantages for the design of vectors to be used in the industrial production of recombinant proteins [16]. Since ensuring adequate aeration in high-density cultures is a problem in any case in fermentors, the use of oxygen-regulated promoters provides an inexpensive means of controlling product synthesis. One of the oxygen-regulated promoters, *VHb* promoter from an obligate aerobe *Vitreoscilla*, was tested as an inducible promoter [17 – 20]. In a two-stage fed-batch fermentation Khosla et al. [19] overproduced β-galactosidase to levels approaching 10% of the soluble cellular proteins by growing recombinant *E. coli* to OD_{600} = 10 – 20 at a dissolved oxygen concentration of 20% for growth and then by reducing the oxygen concentration to below 5% air saturation for induction. An overall 30-fold increase in promoter activity and OD_{600} = 40 – 50 of cell density was achieved [19]. Buddenhagen et al. reported that oxygen-limited fermentation resulted in about a sixfold increase of recombinant α-amylase production in *E. coli* containing the *Vitreoscilla* hemoglobin gene [21].

2.3 The *nar* Promoter

Escherichia coli is a facultative bacterium which grows by a respiratory process under aerobic conditions or by a fermentative process under anaerobic conditions. Under aerobic conditions, oxygen serves primarily as a final electron acceptor in the electron transport chain. Reduction in oxygen supply can affect electron transport because the depletion of oxygen and substitutes of another terminal electron acceptor results in a smaller difference in the redox potential between the dehydrogenated couple and the final acceptor. In the absence of oxygen, the electron from the reduced carrier is transferred to other organic or inorganic compounds, thereby shortening the electron transport chain and resulting in a further reduction in ATP production [22]. When *E. coli* is grown

under anaerobic conditions, several genes not normally expressed under aerobic conditions are expressed [23]. The *nar* operon encoding nitrate reductase is one of them. Nitrate reductase plays an important role in the anaerobic energy metabolism of *E. coli* [24]. Nitrate reductase can utilize nitrate (NO_3^-) as an electron acceptor to convert it to nitrite (NO_2^-) in the absence of oxygen, changing the fermentative process to a respiratory process [25]. Therefore, the *nar* operon not normally expressed under aerobic conditions is maximally induced under anaerobic conditions in the presence of nitrate to use nitrate as an electron acceptor.

The *nar* operon (*narGHJI*) has been cloned and sequenced and the genetic basis of its regulation has been extensively characterized [26–28]. Regulation of expression of the *nar* operon is at the level of transcription and is dependent on three well-characterized transacting factors, FNR, NARL, and IHF (integration host factor) [29]. FNR is required for the transcription of the *nar* promoter under anaerobic conditions, while NARL and IHF mediate a dramatic stimulation of anaerobic transcription in the presence of nitrate. When growth conditions change from aerobic conditions to anaerobic conditions, the *nar* operon is partially induced by binding of the regulatory protein, FNR, to the *nar* promoter. Then it is maximally induced in the presence of nitrate by binding of another regulatory protein, NARL, to the *nar* promoter together with FNR [30]. IHF is a small, heterodimeric DNA-binding protein that is required for a number of different functions in *E. coli*, including DNA replication, chromosomal integration of λ-phage DNA, and regulation of expression of diverse genes and operons [31]. IHF is required along with NARL for the induction of transcription from the *nar* promoter by nitrate [29]. Zhang and DeMoss demonstrated that binding of IHF induces a sharp bend in the *narG* promoter, centered in the IHF binding site [32]. These results suggest that NARL binds at the upstream site and the FNR-RNA polymerase complex at the transcription start site [33]. Initiation of transcription of the *nar* operon increases when these three transacting proteins bind to the specific sites on the *nar* promoter, resulting in the expression of the structural genes, *narG*, *narH*, and *narI* [27, 34]. The *nar* promoter was cloned, and the *lacZ* gene was downstream to the *nar* promoter instead of the structural genes to make the study of the mechanism of the induction of the *nar* promoter easy [30].

3
Fed-Batch with *nar* Promoter System Requiring Nitrate

3.1
The *nar* Promoter as an Inducible Promoter

The characterization of the *nar* promoter in *E. coli* with the intact *nar* operon on the chromosome was carried out. Expression of β-galactosidase was maximal when the *nar* promoter was induced at $OD_{600} = 1.7$ under anaerobic conditions in the presence of 1% nitrate. At this optimal condition the induction ratio was approximately 250 and the specific β-galactosidase activity was approximately 7500 Miller units at $OD_{600} = 2.7$ [35]. In this study, we used plasmid

pXR8971 and *E. coli* strain Mv1190 that has the intact *nar* operon on the chromosome, which enables it to produce nitrate reductase. Lowering the cellular redox potential by nitrate reductase produced from chromosome can suppress further induction of the *nar* operon, resulting in the autoregulation of expression of nitrate reductase [36, 37].

Lee reported on the characterization of pMW616/ES2001 system [38]. The used strain, *E. coli* ES2001, was made by insertion of Tn*10* on *fnr* gene affecting expression of the *nar* promoter according to the dissolved oxygen level [28]. The plasmid, pMW616, has the modified *nar* promoter, by which several site-directed mutagenesis was performed [37]. The maximum specific β-galactosidase activity was obtained when *E. coli* was grown under aerobic conditions, and then the modified *nar* promoter was induced at $OD_{600} = 2.2$ under microaerobic conditions (DO = 1 – 2%). Under these conditions, the maximum specific β-galactosidase activity was 13,000 Miller units. However, the induction ratio was very low, approximately 2.

Another *nar* promoter system, pMW61/RK5265, was characterized by Lee et al. using flask and batch cultures [39]. The *E. coli* RK5265 has the mutant *nar* operon on the chromosome, the *narG* gene encoding one subunit of nitrate reductase was mutated, and thus the autoregulation of expression of nitrate reductase was eliminated [40]. The plasmid pMW61 having the *nar* promoter was constructed by introduction of *Kpn*I site into pSL8RB2, a derivative of pSL800 [37]. In batch experiments, it was found that induction of pMW61/RK5265 system was suppressed during the growth stage when *E. coli* was grown at high dissolved oxygen (DO) level (80%) in the presence of 1% nitrate. Then the *nar* promoter was fully induced when the culture was shifted to microaerobic conditions at $OD_{600} = 1.7$ by lowering the DO level to 1 – 2%. The maximum specific β-galactosidase activity expressed from the reporter *lacZ* gene was 36,000 Miller units, equivalent to approximately 35% of the total cellular proteins at $OD_{600} = 3.2$, and the induction ratio was approximately 300.

3.2 Fed-Batch Culture of pMW61/RK5265

As mentioned in the previous section, so far three different *nar* promoter systems (pXR8971/Mv1190, pMW616/ES2001, and pMW61/RK5265) were characterized using batch cultures. Of these systems, pMW61/RK5265 provided the most promising properties as a new inducible promoter system (Table 1). Therefore we carried out fed-batch culture of the pMW61/RK5265 system to investigate the feasibility of utilizing the *nar* promoter system for the industrial-

Table 1. Comparison of different *nar* promoter systems

System	Induction OD_{600}	Max units	Induction ratio	Reference
pXR8971/Mv1190	1.7	7,500	250	35
pMW616/ES2001	2.2	13,000	2	38
pMW61/RK5265	1.7	36,000	300	39

scale fermentation to produce recombinant proteins. Fed-batch cultures were performed in a 2.5-l jar fermentor at 37 °C using modified R medium. Dissolved oxygen level was adjusted by changing the stirring speed and the air supply [41].

As the growth state of cells may affect induction of the *nar* promoter, the effect of cell density on the expression of β-galactosidase was investigated. First, cells were grown to different cell densities (OD_{600} = 17, 35, 78, respectively) at high DO level (80%) before the *nar* promoter was induced by lowering the DO level to 1–2%. In the first attempt of induction, the *nar* promoter was induced after cells were grown at high DO level (80%) simply by lowering the DO levels to 1–2%, and the DO levels were kept at this low level continuously throughout the whole induction period (Table 2, row A). Under these induction conditions, however, the acetic acid concentration increased continuously to 37 g/l, and the cells stopped growing at an OD_{600} lower than 100 [41]. In an attempt to avoid accumulation of acetic acid, alternating aerobic and microaerobic conditions were applied until the cell density became high enough (OD_{600} > 80) so that acetic acid concentration did not have any significant effect on the growth of the cells by the end of the operation. When this operating strategy was adopted, the final acetic acid concentration became only 7 g/l, and the cell density reached OD_{600} = 160 [41]. When the *nar* promoter was induced too early (Table 2, row C) or too late (Table 2, row D), the maximal specific β-galactosidase activities were less than 30,000 Miller units. However, when the *nar* promoter was induced by lowering the DO level at OD_{600} = 35 after 15 h of cultivation, the maximum specific β-galactosidase activity reached 40,000 Miller units (Table 2, row B). As the specific β-galactosidase activity just before induction was 1000 Miller units, the induction ratio was 40 [41].

The maximum specific β-galactosidase activities were also strongly dependent on the DO levels before and after induction. Maintenance of high DO levels before induction and low DO levels during the induction period was important to maximize the expression of β-galactosidase (Table 2, rows C, E, F, and G).

In the absence of nitrate, the maximum specific β-galactosidase activity became only 4000 Miller units (Table 2, row H). Therefore, addition of nitrate into the growth medium before induction is necessary to maximize the expression of β-galactosidase.

Table 2. Results of fed-batch cultures of pMW61/RK5265 system

No.	Induction OD_{600}	DO before induction	DO after induction	NO_3^-	Max. units
A	35	80%	1–2%	1%	23,000
B	17	80%	Microaerobic/aerobic	1%	25,000
C	35	80%	Microaerobic/aerobic	1%	40,000
D	78	80%	Microaerobic/aerobic	1%	26,000
E	35	50%	Microaerobic/aerobic	1%	26,000
F	35	20%	Microaerobic/aerobic	1%	25,000
G	35	80%	10%	1%	11,000
H	35	80%	Microaerobic/aerobic	0%	4,000

4
Fed-Batch with *nar* Promoter System Requiring No Nitrate

Although wild type *nar* promoter system, pMW61/RK5265, has promising properties to be used as an inducible promoter, it has one disadvantage: addition of nitrate as an inducer in addition to low DO level is necessary for the maximal induction, which not only increases induction cost but also causes water contamination after discharge of waste culture medium. We characterized several different combinations of the *nar* promoter (pMW61, pMW618), mutations on the chromosome of host *E. coli* strains (*narL*$^-$, *narG*$^-$), and host *E. coli* strains (MC4100, JM107, W3110) to find the best *nar* promoter system which can be used as an oxygen-dependent inducible system even without addition of nitrate. Plasmid pMW618, a derivative of pMW61, was made by site-directed mutagenesis on the −10 and −35 regions of the wild type *nar* promoter to eliminate dependence of the *nar* promoter on nitrate [37].

4.1
Characterization of the *nar* Promoter System with Various Combinations of Plasmids and Mutant Host E. coli Strains

Cells were grown in a jar fermentor in LB medium at high DO level (DO > 80%), and then the *nar* promoter was induced by keeping the DO level low (DO = 1–2%) after cell density reached OD_{600} = 1.5. Table 3 shows the maximum specific β-galactosidase activities and induction ratios of the *E. coli* strain RK5265(*narG*$^-$), RK5278(*narL*$^-$), and RK5278*narG*$^-$(*narL*$^-$*narG*$^-$) having plasmid pMW61 or pMW618. This table shows that very low expression levels were obtained in cases of pMW61/RK5278 and pMW61/RK5278*narG*$^-$. The *E. coli* strain RK5278 was constructed by mutating the *narL* gene on the chromosome of MC4100 strain; thus NARL, one of the regulatory proteins of *nar* operon, could not be synthesized in this strain. Because NARL could not be produced in this strain, the *nar* promoter was only induced by FNR, another regulatory protein. In case of pMW618/RK5265, the maximum specific β-galactosidase activity was 35,000 Miller units, but the induction ratio was very low because the expression levels before induction were high. In the previous study it has already been shown that pMW61/RK5265(*narG*$^-$) cannot be used as an oxygen-

Table 3. Effect of combination of plasmids and mutant host *E. coli* on the induction of the *nar* promoters in batch cultures

System	Description	Max units	Induction ratio
pMW61/RK5265	*narG*$^-$	20,000	260
pMW618/RK5265	*narG*$^-$	34,000	23
pMW61/RK5278	*narL*$^-$	3,600	260
pMW618/RK5278	*narL*$^-$	29,000	112
pMW61/RK5278*narG*$^-$	*narL*$^-$*narG*$^-$	2,600	213
pMW618/RK5278*narG*$^-$	*narL*$^-$*narG*$^-$	15,000	78

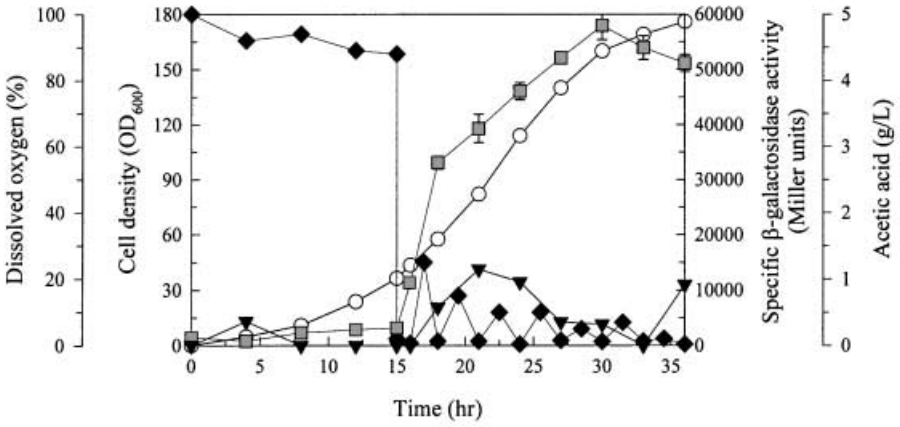

Fig. 1. Fed batch fermentation of E. coli W3110*narL*⁻ harboring plasmid pMW618. Cells were grown in a jar fermentor in modified R medium at high DO level (DO > 80 %) for 3.5 h before the feeding began. When cell density reached OD_{600} = 35, the *nar* promoter was induced by lowering DO level to 1 – 2 % with alternating microaerobic and aerobic conditions. OD_{600} *open circles*, DO level *filled diamonds*, the specific β-galactosidase activity *filled squares*, and acetic acid concentration *filled triangles* were measured. *Error bars* represent the standard deviation of at least three samples taken from a single run

dependent inducible promoter in the absence of nitrate because the expression level of β-galactosidase was low (Table 2, row H). From this study, it was concluded that pMW618/*narL*⁻ mutant was the best combination for the induction of the *nar* promoter in the absence of nitrate. This conclusion was supported when the *E. coli* W3110 was used [43]. Therefore, pMW618 and *narL*⁻ mutant were used as a plasmid and *E. coli* host, respectively, for further characterization.

4.2
Strain Effect on the Induction of the *nar* Promoter in Fed-Batch Cultures

The *E. coli* strains RK5278 (*narL*⁻), JM107*narL*⁻, and W3110*narL*⁻ harboring plasmid pMW618 were cultivated at the optimal conditions obtained in the previous study for the pMW61/RK5265 (Table 4, rows A, B, and C). Host *E. coli* strains have strong effects on the induction of the modified *nar* promoter. Of the three *E. coli* strains, the pMW618/W3110*narL*⁻ system had the highest expression level of β-galactosidase (58,000 Miller units) and the highest cell density (OD_{600} of 176) (Fig. 1). Therefore, W3110*narL*⁻ was chosen as the strain for the further studies.

4.3
Effects of Cell Density, DO Level, and Nitrate on the pMW618/W3110*narL*⁻ System in Fed-Batch Cultures

Of three cases of different cell densities (OD_{600} = 18, 35, 80) at the induction time, the highest value of specific β-galactosidase activity was obtained when

Table 4. Results of fed-batch cultures of pMW618/*narL*⁻ mutant system

No.	Strain	Induction OD_{600}	DO before induction	DO after induction	NO_3^-	Max. units
A	RK5278	35	80%	Microaerobic/aerobic	0%	8,000
B	JM107*narL*⁻	35	80%	Microaerobic/aerobic	0%	52,000
C	W3110*narL*⁻	35	80%	Microaerobic/aerobic	0%	58,000
D	W3110*narL*	18	80%	Microaerobic/aerobic	0%	54,000
E	W3110*narL*	80	80%	Microaerobic/aerobic	0%	51,000
F	W3110*narL*	35	50%	Microaerobic/aerobic	0%	47,000
G	W3110*narL*	35	80%	10%	0%	30,000
H	W3110*narL*	35	80%	Microaerobic/aerobic	1%	28,000

the *nar* promoter was induced at OD_{600} = 35 (Table 4, rows C, D, and E). It was also necessary to grow cells at as high a DO level as possible for maximal expression and to keep DO level low during induction period for the *nar* promoter to be fully induced (Table 4, rows C, F, and G). In case of pMW618/W3110*narL*–, the addition of nitrate resulted in negative effect on the expression of β-galactosidase (Table 4, row H).

5 Comparison with Other Promoter Systems

Rinas and her associates at GBF, Germany compared the production of human basic fibroblast growth factor (bFGF) using *E. coli* TG1 [44]. The cells with thermal induction promoter resulted in a final protein titer of 4.88 g/l with a cell mass of 61 g/l and 80 mg bFGF/g cell, and those with IPTG yielded 1.09 g protein/l with a cell mass of 135 g/l and 8.1 mg bFGF/g cell. Insulin fusion protein was produced in a final concentration of 4.5 g/l using *E. coli* with thermal promoter [45]. This corresponds to concentrations of insulin B-chain, 800 mg/l and A-chain, 600 mg/l, respectively. Interferon α (IFN-α) was produced in a concentration of around 4 g/l with a total biomass of 40 g/l containing 93 mg/g cell [46]. For β-galactosidase using tac promoter, Labes et al. [47] reported 11,000 Miller units/g cell with the induction at an OD of 0.2 – 0.6. The maximum specific activity of the enzyme in the present study was 58,000 Miller units/g cell at an OD of 176, which amounts to approximately 45 % of total cellular protein. Lee JW and associates characterized the *nar* promoter system from metabolic engineering viewpoint [48].

The *hmp* gene isolated from *Bacillus subtilis* can be induced to produce β-galactosidase under anaerobic conditions. The cells are grown in the presence of nitrate to OD_{600} = 0.2 at high DO level (80 %), and then induced by lowering the DO level to 1 – 2 %. The maximum specific β-galactosidase activity increased to the maximal value of 1750 Miller units at OD_{600} = 2.5 [49].

6 Conclusion

First, the objective of this study is to maximize overall concentration of a desired protein per reactor volume basis, which can be accomplished by increasing specific productivity of a single cell as well as a total biomass in a unit volume of the fermentor. For this purpose we alternated microaerobic and aerobic conditions to recombinant *Escherichia coli* cells.

Second, the cells were grown under aerobic conditions (DO > 80%) in the presence of nitrate to $OD_{600} = 35$, and then the *nar* promoter was induced by lowering the DO level to 1–2% with alternating microaerobic and aerobic conditions. Under the optimal operating conditions for fed-batch culture of the pMW61/RK5265 system, the highest specific β-galactosidase activity was 40,000 Miller units equivalent to approximately 35% of the total cellular proteins. This was also higher than that obtained from batch experiments, 33,000 Miller units. In addition, 40-fold more β-galactosidase per volume basis can be obtained by using fed-batch culture than that obtained by batch culture.

Third, one modified *nar* promoter (pMW618), whose expression is known to be independent of nitrate, was tested in different *E. coli* strains having *narL* mutation to make pMW618 more independent of nitrate. One combination, pMW618/W3110*narL*$^-$, had excellent properties to be used as an inducible promoter. The maximum specific β-galactosidase activity became 58,000 Miller units, equivalent to approximately 45% of total cellular proteins.

Finally, the *nar* promoter studied here has some important advantages as an inducible promoter in *E. coli*. First, its induction is easy and cheap, requiring only growth of cells under aerobic conditions and reduction of DO levels to induce. Second, no addition of any inducing agents is necessary. Third, promoter can be functional in any phase of growth. This study demonstrated that this simple induction strategy could be easily applied to fed-batch cultivation. Based on these results, it was concluded that the *nar* promoter provided a convenient and effective high-level expression system under condition of industrial-scale fermentation.

References

1. Georgiou G (1988) AIChE J 34:1233
2. Makrides SC (1996) Microbiol Rev 60:512
3. Lee SY (1996) Trends Biotechnol 14:98
4. Hannig G, Makrides SC (1998) Trends Biotechnol 16:54
5. Han SJ, Chang HN, Chang YK, Rhim SL (1996) J Microbiol Biotechnol 6:451
6. Strandberg L, Enfors S-O (1991) Biotechnol Lett 13:609
7. Hockney RC (1994) Trends Biotechnol 12:456
8. Remaut E, Stanssens P, Fiers W (1981) Gene 15:81
9. Figge J, Wright C, Collins CJ, Roberts TM, Livingston DM (1988) Cell 52:713
10. Carter P, Kelley RF, Rodrigues ML, Snedecor B, Covarrubias M, Velligan MD, Wong WLT, Rowland AM, Kotts CE, Carver ME, Yang M, Bourell JH, Shepard HM, Henner D (1992) Bio/Technology 10:163
11. Kasahara M, Makino K, Amemura M, Nakata A, Shinagawa H (1991) J Bacteriol 173:549
12. Khosla C, Bailey JE (1988) Nature 331:633

13. Chatfield SN, Charles IG, Makoff AJ, Oxer MD, Dougan G, Pickard D, Slater D, Fairweather NF (1992) Bio/Technology 10:888
14. Sawers G (1993) Mol Microbiol 10:737
15. Wanner BL (1996) Phosphorus assimilation and control of the phosphate regulation. In: Neidhardt FC, Curtiss R III, Ingraham JL, Lin ECC, Low KB, Magasanik B, Reznikoff WS, Riley M, Schaechter M, Umbarger HE (eds) *Escherichia coli* and *Salmonella*: cellular and molecular biology. ASM Press, Washington, DC, p 1357
16. Sawers G, Jarsch M (1996) Appl Microbiol Biotechnol 46:1
17. Hughes DE, Curtis JE, Khosla C, Bailey JE (1989) Biotechniques 7:1026
18. Khosla C, Bailey JE (1989) J Bacteriol 171:5995
19. Khosla C, Curtis JE, Bydalek P, Swartz JR, Bailey JE (1990) Bio/Technology 8:554
20. Khosla C, Curtis JE, DeModena J, Rinas U, Bailey JE (1990) Bio/Technology 8:849
21. Buddenhagen RE, Webster DA, Stark BC (1996) Biotechnol Lett 18:695
22. Ko Y-F, Bentley WE, Weigand WA (1993) Biotechnol Bioeng 42:843
23. Iuchi S, Lin ECC (1991) Cell 66:5
24. Stewart V (1988) Microbiol Rev 52:190
25. Gottschalk G (1986) Bacterial metabolism, 2nd edn. Springer, Berlin Heidelberg New York
26. Blasco F, Iobbi C, Giordano G, Chippaux M, Bonnefoy V (1989) Mol Gen Genet 218:249
27. Li SF, DeMoss JA (1987) J Bacteriol 169:4614
28. Sodergren EJ, DeMoss JA (1988) J Bacteriol 170:1721
29. Stewart V (1993) Mol Microbiol 9:425
30. Li SF, DeMoss JA (1988) J Biol Chem 263:13,700
31. Goodman SD, Nash HA (1989) Nature 343:251
32. Zhang X, DeMoss JA (1996) J Bacteriol 178:3971
33. DeMoss JA (1996) BPERC International Symposium '96. Taejon, Korea
34. Li SF, Rabi T, DeMoss JA (1985) J Bacteriol 164:25
35. Lee J, Cho M, Hong E-K, Kim K-S, Lee J (1996) Biotechnol Lett 18:129
36. Bonnefoy V, Pascal M-C, Ratouchniak J, Chippaux M (1986) Mol Gen Genet 204:180
37. Walker MS, DeMoss JA (1992) J Bacteriol 174:1119
38. Lee J (1996) Korean J Biotechnol Bioeng 11:431
39. Lee J, Cho MH, Lee J (1996) Biotechnol Bioeng 52:572
40. Stewart V, MacGregor CH (1982) J Bacteriol 151:788
41. Han SJ, Chang HN, Lee J (1998) Biotechnol Bioeng 59:400
42. Riesenberg D, Schulz V, Knorre WA, Pohl H-D, Korz D, Sanders EA, Rob A, Deckwer W-D (1991) J Biotechnol 20:17
43. Han SJ, Chang HN, DeMoss JA, Suh EJ, Lee J (2000) Biotechnol Bioeng 68:115
44. Seeger A, Schneppe B, McCarthy JFG, Deckwer W-D, Rians U (1995) Enzyme Microbiol Tech 17:947
45. Schmidt M, Babu KR, Khanna N, Marten S, Rinas U (1999), J Biotechnol 68:71
46. Babu KR, Swaminathan S, Marten S, Khanna N, Rinas U (2000) Appl Microbiol Biotechnol 53:655
47. Labes M, Puhler A, Simon R (1990) Gene 89:37
48. Han SJ, Chang HN, Lee JW (2001) Biotechnol Bioeng 72:573
49. Han MR (2000) KAIST MS Thesis, Taejon, Korea

Received: May 2001

Production of Core and Virus-Like Particles with Baculovirus Infected Insect Cells

Luis Maranga[1], Pedro E. Cruz[1,2], John G. Aunins[1,3], Manuel J. T. Carrondo[1,*,4]

[1] Instituto de Biologia Experimental e Tecnológica/Instituto de Tecnologia Química e Biológica IBET/ITQB, Apartado 12, P-2781-901 Oeiras, Portugal
E-mail: mjtc@itqb.unl.pt
[2] ECBio, Ltd, Taguspark, Núcleo Central, 332, P-2780-920 Porto Salvo, Portugal
[3] Fermentation and Cell Culture, Vaccine Bioprocess R&D, Merck Research Laboratories, Merck & Co., Inc., West Point, Pennsylvania, USA
[4] Laboratório de Engenharia Bioquímica, Faculdade de Ciências e Tecnologia, Universidade Nova de Lisboa, P- 2825-114 Monte da Caparica, Portugal

Dedicated to Prof. Dr. Wolf-Dieter Deckwer on the occasion of his 60th birthday

In this paper the fundamental aspects of process development for the production of core and virus-like particles with baculovirus infected insect cells are reviewed. The issues addressed include: particle formation and monomer composition, chemical and physical conditions for optimal cell growth, baculovirus replication and product expression, multiplicity of infection strategy, and scale-up of the process. Study of the differences in the metabolic requirements of infected and non-infected cells is necessary for high cell density processes. In the bioreactor, the specific oxygen uptake rate (OURsp) plays a central role in process scale-up, leading to the specification of the bioreactor operational parameters. Shear stress can also be an important variable for bioreactor operation due to its influence on cell growth and product expression.

The determination of the critical variables in process development is discussed, showing the relevance of the mathematical models that have been developed for the insect cells/baculovirus system in process implementation and control.

Keywords. Virus-like particles, Baculovirus, Insect cells, Process development, Mathematical models

* To whom all correspondence should be addressed at IBET.

Advances in Biochemical Engineering/
Biotechnology, Vol. 74
Managing Editor: Th. Scheper

List of Abbreviations and Symbols

AcMNPV	*Autographa californica* Multicapsid Nuclear Polyhedrosis Virus
BEVS	Baculovirus Expression Vector System
BTV	Bluetongue Virus
CCI	Cell Concentration at Infection
CLPs	Core-like Particles
CPV	Canine Parvovirus
Di	Impeller Diameter
DO	Dissolved Oxygen
ECV	Extracellular Virus
HBV	Hepatitis B Virus
HCV	Hepatitis C Virus
IBDV	Infectious Bursal Disease Virus
Km	Monod saturation constant
MOI	Multiplicity Of Infection
MVM	Minute Virus of Mice
NS	Non-Structural Protein
OB	Occlusion Bodies
OUR	Oxygen Uptake Rate
OURsp	Specific Oxygen Uptake Rate
PF-68	Pluronic F-68
PPV	Porcine Parvovirus
SEAP	Secreted Alkaline Phosphatase
Sf	*Spodoptera frugiperda*
TOI	Time Of Infection
VLPs	Virus-like Particles
VP	Viral Protein
α	infection efficiency factor of Licari and Bailey Model
Δt	time step (min)
ΔV_1	virus bound during step 1 (pfu/ml)

C	cell density (cells/ml)
k_a	attachment rate constant (ml/cells.min)
MOI(t)	multiplicity of infection at time t (pfu/cells)
P(t)	cumulative probability that cells are infected
p(t, j)	probability that cells are infected by j viruses
t	time (min)
V_{ex}	extracellular virus concentration (pfu/ml)

1 Introduction

Baculovirus infected insect cells have emerged as a powerful technology for heterologous protein production in the last two decades. Several different types of proteins have been expressed with this system, ranging from therapeutics like tPA [1], enzymes (*e.g.* human Fucosyltransferase III) [2] and viral structural proteins [3–5]. The Baculovirus Expression Vector System (BEVS), due to its high productivity and ability to achieve rapid implementation, has been widely used for the production of proteins for structural and other studies, since reasonably large amounts are needed for crystallography, screening, etc.

The *Baculoviridae* are a family of large enveloped DNA viruses that are characterised by rod-shaped nucleocapsids and relatively large double stranded DNA genomes. *Autographa californica* Multicapsid Nuclear Polyhedrosis Virus (AcMNPV) is the baculovirus most currently used as vector for protein production with insect cells. Several reviews are available describing baculovirus structure and its molecular biology [6–8].

Viral structural proteins expressed by baculovirus infected insect cells assemble into multimeric structures that resemble viral core-like particles and virus-like particles (CLPs and VLPs, respectively). This presentation has brought the attention of researchers for the potential use of these structures as safe immunological reagents for virus or antibody detection in enzyme immuno assays, as vaccines, and more recently, as gene delivering systems for gene therapy [9].

The industrial application of CLPs and VLPs is in the development phase. This can be expected since the baculovirus-insect cells system has become one of the most popular systems for heterologous protein and CLP/VLP production at laboratory scale. After defining the appropriate particle composition for the viruses of interest, research is now addressing the engineering issues in this system (Scheme 1).

In this paper the fundamental aspects concerning the production of CLPs and VLPs with baculovirus infected insect cells are reviewed. It is not the goal of this communication to review all the aspects of insect cell culture technology, since this would be a task impossible to achieve in a single chapter. The interested reader should refer to the references. This review is structured in four parts:

1. CLP and VLP Composition.
In this part the issues relating to CLP/VLP composition are discussed. This includes the ratios between protein monomers, infection strategy for particle

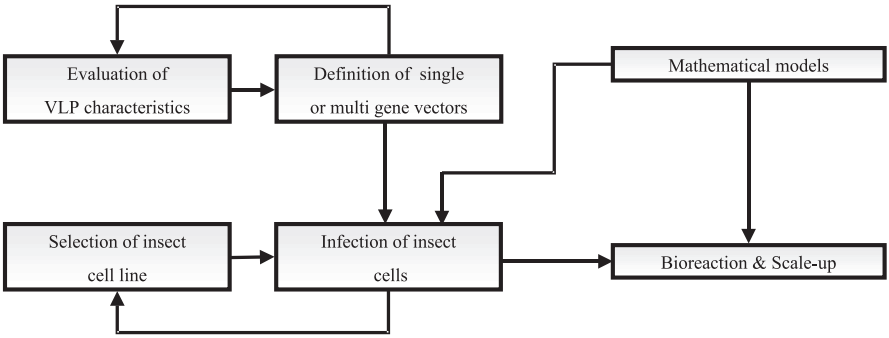

Scheme 1. Process development flowchart for VLP production

composition control, implications of particle composition in terms of proteins and particle localisation, antigenicity, and particle stability.

2. Cell Growth and Productivity.
In this part we deal with the major chemical and physical factors affecting insect cell growth, baculovirus replication and product expression. The issues addressed are: cell line selection for product expression, baculovirus-cell interactions and impact of differences in metabolic requirements of infected and non-infected cells in overall productivity.

3. Bioreactor Operation and Scale-up.
In this part the determination of critical variables for bioreactor operation and scale-up are reviewed. Special focus is put on the specific oxygen uptake rate (OURsp) and its influence upon the specification of bioreactor operational parameters. Shear stress can also be an important variable for process design and its importance in cell growth and product expression is discussed.

4. Mathematical Models
In this part the application of mathematical models to CLP and VLP production with baculovirus infected insect cell cultures is discussed. Special emphasis on model evaluation is made along with the definition of directions in future process development research with this system.

2
CLP and VLP Composition

VLPs offer several advantages as antigens or immunogens. First, compared to individual proteins or peptides, VLPs present conformational epitopes more similarly to native particles, so that antibody reactivity or immune system response is more relevant. Second, many of the viruses for which antigenic/immunogenic VLPs have been developed replicate poorly or not at all in tissue culture (e.g., HBV, B19 parvovirus, Norwalk calcivirus and human papillomavirus), thus precluding natural virus as an antigen/immunogen. Third, because VLPs

are theoretically non-infectious, inactivation is not required and this may be advantageous where epitopes can be modified unfavorably by inactivating treatments [10]. Balancing these advantages is the theoretical disadvantage of glycosylation infidelity for insect cells vs. humans cells, although subtleties of glycosylation structure have not generally been demonstrated to affect antigenicity or immunogenicity of inactivated viral vaccines.

For the production of CLPs and VLPs with baculovirus infected insect cells the specific proteins that are required for particle formation should be chosen at an early step. The specific particle composition, along with the expression of other non-structural (NS) proteins often has a great impact on particle stability [11] or on particle localisation [12], i.e. – cell-associated or secreted to the supernatant.

Antigenicity is the light that should guide researchers in the field of CLP and VLP production as vaccines and antigens. Although immunogenicity is the invaluable measure of how a vaccine antigen performs, it can be held hostage to the vagaries of vaccinology. Antigenicity measured via antibody reactivity is often a good surrogate marker for whether the BEVS production system is correctly expressing and assembling the CLP/VLP in the absence of good immunogenicity data. Several questions must be answered in order to ensure maximum antigenicity. The first issue that is usually addressed is the use of single vs. dual (or multiple) gene vectors; this is relevant in the cases where more than one different protein monomer is incorporated into the CLP or VLP. The different strategies have different outcomes depending on the particle of interest. This issue is discussed in the following pages with the representative examples of Bluetongue virus core-like particles and human Parvovirus B19 virus-like particles.

Taking into account process integration, i.e. – cultivation and product purification, particle localisation is an important issue. Strategies to produce a secreted particle, either by manipulation of its composition or by co-expression of NS protein(s) will be also discussed, since this can lead to an easier purification process and to a decrease in product losses due to intracellular proteolysis. The production of Rotavirus-like particles and Bluetongue virus-like particles production will be used as examples to illustrate this point.

2.1 Single vs. Dual-Gene Baculovirus Vectors

Different approaches have been reported in the literature regarding the number of genes cloned in the same baculovirus. Pioneering work has been done at Prof. Polly Roy's laboratory at Oxford University for Bluetongue virus (BTV) CLP and VLP production, where these authors generated BTV-CLP and BTV-VLP of different types and monomer compositions [4, 13–16].

Bluetongue virus, the prototype virus of the *Orbivirus* genus in the Reoviridae family, is an non-enveloped virus with seven structural proteins (VP1–VP7) [12]. The outer capsid consists of two proteins, VP2 and VP5. The core exhibits icosahedral symmetry and is composed of five proteins, two major (VP3 and VP7) and three minor (VP1, VP4 and VP6) classified according to

abundance [12]. The production of BTV CLP with a dual-gene vector expressing both major proteins of the virus core, VP3 and VP7 has been reported [13]. The VP3 to VP7 ratio obtained in the particles was 2:15 which is similar to the native BTV core [13]. Furthermore when the total protein expression was analysed for VP3 and VP7, the ratio achieved with the dual vector was also 2:15 [17] but only at a low multiplicity of infection (MOI). This result shows that in this system at high MOI particle composition does not change when an excess of one capsid component is present, suggesting an 'equilibrium' assembly stoichiometry.

In the case of parvovirus B19 the serologically immunodominant epitopes are localised in VP1 and in the VP1–VP2 connecting regions. However, the expression of VP2 alone of Parvovirus B19 is sufficient for capsid assembly [18–19], and this has also been obtained with the sole expression of VP2 of the closely related Porcine Parvovirus (PPV) [20], Canine Parvovirus (CPV) [3] and Minute Virus of Mice (MVM) [21]. In these cases the VP2 capsids obtained are highly immunogenic, even providing cross-species protection in one instance [22]. This would tend to suggest that the VP1 component of parvovirus VLPs is less relevant for immunogenicity. Like the above BTV case, a dual-gene vector was used by Brown *et al.* to produce VLPs of human parvovirus B19 [19]. The mass ratio of VP1 to VP2 obtained in the VLP, 4:96, was similar to the native parvovirus B19. The volumetric productivities for the major capsid proteins VP1 and VP2 were 13 and 33 mg/l, respectively, a ratio of ca. 1:3 unlike the native capsid composition. Interestingly, despite native-like composition, the VLP capsids obtained with the dual vector did not induce an immune response [23].

However, by employing two single-gene vectors and manipulating MOI's and MOI ratios [18], non-native-like capsids consisting of ≥25% of VP1 protein could be produced efficiently. These VLPs consistently induced a vigorous B19 virus neutralising antibody response [23]. It was found that an MOI ratio equal to unity led to a 35% final capsid composition in VP1 protein for individual MOI's higher than three [18]. Increasing the MOI of the VP1 vector, but maintaining the MOI of the VP2 vector led to a VP1 protein content of 50% [18]. This was considered the maximum amount of VP1 that would be possible to incorporate in the VLP since VP1 alone does not assemble to form capsids [18]. The above result does not rule out a structural peculiarity of the native-like 4:96 composition particles which may have precluded good antigen presentation; despite proper monomer ratios, imperfect capsid architecture could have occurred.

Contrary to the case of the parvovirus B19, the general rule is normally to obtain a capsid with a monomer ratio similar to the native virus core or capsid. However if it is intended to incorporate a large number of different viral proteins in the capsid or, at least, to express a large number of proteins, it is generally better to use a dual or even an higher-order vector to ensure that the capsids obtained are native-like.

2.2 Influence of the Expressed Proteins in Particle Localisation

The selection of the monomers to incorporate in the capsid should consider other items along with antigenicity, such as product release by the cells [15, 24]. Product secretion can have a large impact on overall particle production since baculovirus-infected insect cells often exhibit proteolytic activity, which is mainly intracellular at early times post-infection [25]. The appearance of proteases often coincides with p10 and polyhedrin-driven late protein production [26].

In Rotavirus-like particle production, incorporation of the outer capsid VP7 protein leads to high levels of double-layered (VP6/VP7) [15] and triple layered (VP2/VP6/VP7) [24] particles in the supernatant of infected cultures. Although the VP7 was efficiently incorporated in the triple layered rotavirus-like particle, due to the use of three single-gene vectors, two types of capsid were obtained. In the supernatant, almost all capsids were triple layered, i.e. with VP2/VP6/VP7; the capsids found in the cell cytoplasm were only double layered, i.e. VP2/VP6, although the expression level of VP7 was stoichiometrically high enough to allow that all the capsids could have been triple layered [24]. Although the VP7 protein is also secreted to the supernatant when it is expressed alone [15] or in co-infections [24], free VP7 in the supernatant is believed not to be incorporated in the VLPs and to be degraded over time [24]. These results may suggest that VP7 levels must be at a local critical concentration higher than was present in order to obtain uniformly triple-shelled VLP's. Alternatively, it could suggest that another factor other than VP7 concentration, for example a transport process, disallows complete conversion of components into triple-layered particles, much like the heterogeneity of glycosylation of recombinant proteins. In natural rotavirus cultivations in vitro, it is often observed that a mixture of particles is obtained. In a natural infection, rotavirus acquires its outer shell via budding through the endoplasmic reticulum membrane, and the mature triple-shelled particle egresses from the cell via lysis. The intracellular double-shelled particles may indicate that the VLP localisation and assembly pathway mimics the natural pathway in some respects.

Another issue that can be important in VLP capsid formation is the expression of key NS proteins or genomic sequences along with the expression of the viral structural proteins. One example exists in the Hepatitis C virus-like particle (HCV-VLP) formation [11], where capsid assembly requires inclusion of a 5′ untranslated region in the BEV in order to achieve assembly of core protein, E1 and E2 proteins that would not assemble otherwise [11]. Although particle assembly was obtained, specific HCV RNA encapsidation was also observed [11], which is expected since the core protein is known to bind the HCV genome for encapsidation [27]. The requirement to include encapsidation coding regions for assembly for certain VLP systems poses a general concern for their use in vaccination since the presence of genetic material may cause product safety issues in the clinic should expression occur from encapsidated RNA transcripts. Interestingly, in recombinantly-expressed HCV systems there are hints that glycosylation status of E2 can determine antigenicity [28]; here intracellular vs.

secreted localisation could conceivably have significant effects on VLP immunogenicity for this particular virus.

In another example of chaperone use, in BTV – VLP production, when NS3/NS3A proteins are expressed, several important conclusions can be drawn. To obtain budding of VLPs, expression of the NS proteins is essential. However, assembly only occurs if the VLP contains the full complement of proteins on both capsid shells, i. e. VP3 + VP7 in the core and VP2 + VP5 in the outer shell. In contrast, if only the core proteins are expressed, i. e. VP3 and VP7, then the self-assembled CLPs neither bud out from the cell nor even interact with cell cytoskeleton [12]. However, it has been shown that the presence of NS3/NS3A is required for the budding and subsequent release of VLPs from infected cells, although VLP assembly occurs in its absence.

2.3 Multi-Gene Baculovirus Vectors and Chimeric Particle Production

Until now we have addressed only combinations of single-gene vectors or the use of just one dual-gene vector. However, if the intention is to produce a complex VLP with both core and capsid proteins, the use of higher-order vectors or at least the use of combinations of dual vectors is recommended. For the production of BTV VLPs composed of the core proteins VP3 and VP7, and the outer shell proteins VP2 and VP5, two different strategies have been used with two different combinations of dual-gene vectors. One of these strategies includes one vector encoding both core proteins VP3 and VP7, and the other encoding outer shell proteins VP2 and VP5. The particles thus obtained were not always double shelled and the double shelled VLPs had highly variable VP2 to VP5 ratios [14]. Note that the outer shell proteins are not able to form capsids composed of VP2 and VP5. This drawback was overcome by co-infection with two dual-gene vectors, but now with one vector encoding VP3 and VP5, and the other encoding VP2 and VP7 [29]. With this strategy the VLP production was maximised and the CLP formation avoided [29]. However, the expression of the four proteins (VP2, VP3, VP5 and VP7) in a four-gene vector has led to the formation of only double-shelled particles [30], this being further improved by the use of five-gene vectors that give rise to protein ratios in the VLPs which are highly stable and very similar to the native ones [31]. With the use of a four-gene vector the possibility of some of the cells not being co-infected by both vectors has been overcome. Further examples exist with dual-gene vectors including the production of HIV-1 VLPs [32], and a three-gene vector example exists for the production of Infectious Bursal Disease Virus (IBDV) VLPs [33].

To conclude, an issue that is bringing great attention in recent years, the production of chimeric virus-like particles should be briefly analysed. These chimeric VLPs are potentially valid systems for broader vaccine production, i.e. against a large number of different serotypes [34]; in addition they can result in safe combination vaccines between closely related viruses [35], can be able to carry multiple foreign epitopes [36 – 39], or even, with the incorporation of tags (e. g. polyhistidine), allow easy single-step product recovery [40, 41].

3
Insect Cell Culture/Baculovirus Technology

Insect cell physiology has been extensively studied and excellent reviews are already available [42–44]. In this part, key aspects of insect cells/baculovirus technology are discussed, the issues addressed being: insect cell line selection, with emphasis on cell productivity, baculovirus-cell interactions and, to finalise, a short note on the metabolic differences between infected and non-infected cells.

3.1
Insect Cell Lines

Continuous insect cell lines were first established in culture over three decades ago when Grace [45] succeed in growing cells from female *Antherea eucalypti* moth ovaries. Since Grace's first report on four cell lines, over 400 lines have been established from more than 100 insect species representing every economically important insect order [46, 47].

Among the insect orders, tissues from *Lepidoptera* have attracted the most attention because of their historical importance as agricultural pests [48]. Insect cell lines have been established from a variety of tissues, mostly from undifferentiated ovarian or embryonic [49]. The undifferentiated nature of the embryonic tissue has made possible the establishment of continuous insect cell-lines from diploid tissues [49].

Cells derived from the ovary of the fall army worm *Spodoptera frugiperda* are the most common used cell lines for heterologous protein production with a baculovirus vector (see Table 1), but some authors have reported the use of a different cell line for VLP production, *Trichoplusia ni* HighFive™ cells (Invitrogen, San Diego, US) [24, 41, 50].

Table 1. CLPs and VLPs produced with baculovirus-infected insect cells for candidate vaccines

Virus	Cell line	References
B19 parvovirus	Sf9	[23]
Bluetongue virus	Sf9, Sf21	[4]
Epizootic hemorrhagic disease	Sf9	[35]
Hepatitis B	Sf9	[109]
Hepatitis C	Sf9	[11]
HIV	Sf9	[32]
Infectious bursal disease	Sf9, HighFive	[33, 41]
Norwalk virus	Sf9	[110]
Papillomavirus	Sf9	[111]
Parvovirus minute virus of mice	Sf9	[21]
Polyomavirus	Sf9	[112]
Porcine parvovirus	Sf9, Sf21	[20, 98]
Rotavirus	Sf9, HighFive	[15, 24]
SV40	Sf9	[113]

Spodoptera frugiperda IPLB-Sf21-AE cell line, simply named Sf21, was originally established by Vaughn et al. in 1977. Sf9 is a clone derived from Sf21 by the same authors [51].

Although Sf9 and Sf21 cells are from the same cell line there are some differences between them regarding maximum growth rate, productivity and susceptibility to baculovirus infection (authors' unpublished observations). Nevertheless, the use of Sf9 or Sf21 by most researchers is essentially dependent on historical precedent in their own labs.

Sf9 and Sf21 cells can grow either as adherent or as suspension cultures, are easily adapted to most of the common serum free insect cell culture media [52], and it is most often possible to obtain culture titers of viral structural proteins higher than 30 mg/l [20].

It has been reported that *Trichoplusia ni* cell lines such as HighFive™ have a superior capacity for heterologous protein production than Sf9 cells. For example, HighFive™ optimal per-cell expression levels of recombinant β-galactosidase (β-gal) [53], soluble tissue factor [54] and secreted alkaline phosphatase (SEAP) [55] were found to be 7-fold, 28-fold and 20-fold higher, respectively, than the levels obtained with Sf9 cells. Furthermore, the same has been observed for viral structural protein production since the per-cell productivity of Rotavirus-like particles [24] and Infectious Bursal Disease virus-like particles [41] was 5-fold higher with HighFive™ cells than with Sf9 cells. However, for a comparative assessment of protein productivity among different insect cell lines the work must be done not only in laboratory systems but in scalable bioreactors [56]. Most of the reports do not account for the much higher cell density that is achievable with Sf9 and Sf21 cells that, in the end, lead to a higher volumetric productivity.

Another issue that could have impact on cell line selection is its intrinsic capacity for post-translational modifications of the virus-like particle and/or release of virus-like particles. For example, retrovirus assembly involves a series of events in which a large number of proteins must be targeted to a specific point on the plasma membrane where immature viruses bud from the cell. When expressed with a recombinant baculovirus/insect cell system with Sf9 cells the immature particles bud out from the cell and the product is extracellular [57]; in contrast, when HighFive™ cells were used for expression, they appear to have a defect in the release of the immature capsids [50]. These factors should also be evaluated when making decisions in selecting a given cell line. In addition, other factors such as the lower protein degradation in the supernatant of HighFive™ cultures [24], or the higher susceptibility of HighFive™ cells to shear stress, which could be the cause of its tendency to grow poorly in suspension [56] compared to Sf9 cells, must be used as key information in cell line selection.

3.2 Infection of Insect Cells with Baculovirus

Baculovirus gene expression and replication has been described as a sequence of four phases: immediate early, delayed-early, late and very late. Most of the de-

veloped vectors have been cloned with the genes of interest under the control of the two very late promoters, polyhedrin and p10. These two strong promoters are extremely efficient and their combined proteins can account for up to 50% of the total cell protein mass in the terminal stages of infection [8].

Although early promoters have recently gained new attention, especially for complex glycosylated proteins to promote proper assembly, e.g. – rotavirus VP7, since at that time after infection the glycosylation and secretion pathway is still fully operational, most researchers still cloned their genes of interest under the control of the very late promoters, due to higher protein productivity obtained. Virus growth in culture can conceptually be broken-down into a series of events: delivery of virus to the cell, attachment to the cell, penetration into the cytoplasm, un-coating of the genome, and delivery of the nucleic acid to the site of transcription, transcription and translation of the genome in one or more cycles of expression, replication of the genome, final production of virion components, virion assembly, and egress from the cell [58]. If the virus is a vector for particle production other steps need to be considered e.g.: transcription of the codifying gene(s), protein synthesis, virus-like particle assembling and, in some cases, virus-like particle budding from the cell.

In Section 2, factors that could lead to particle assembly and secretion into the supernatant were discussed. At this point a deeper analysis of the factors affecting cell infection will be made. Optimisation of the production process should take into account virus-cell interactions, and more specifically viral attachment and internalisation into the cell. The impact of chemical modifications of the medium in baculovirus attachment-internalisation has not been carefully studied. It is widely known for example, that serum increases the "infectivity" of baculovirus. These reviewers have had one case where we were only able to succeed in infecting Sf9 cells adapted to growth in serum-free media [52], with a baculovirus produced by Sf9 cells (not adapted to grow in serum-free media), after adding serum to the culture (authors' unpublished observations). However, since serum is not desirable for use in industrial production, its utilisation should be avoided as much as possible.

Baculovirus attachment to insect cells, as with all virus-cell attachment, is receptor-mediated [59], and the putative receptor is a glycoprotein; however, there is no evidence of the direct involvement of oligosaccharides in attachment [60]. Wickham *et al.* have suggested that non-specific binding could have a great impact on overall virus infection rate, and the use of serum could, in some way, minimise this non-specific binding, by a blocking/saturation effect [59]. This hypothesis is currently being evaluated at our lab.

Further to this it has been shown that the post-attachment steps are fast events and therefore overall infection rate is actually controlled by the rate of attachment [61].

3.3
Metabolism of Infected and Non-Infected Insect Cells

Like any other animal cell line, insect cells have a great number of nutrient requirements for cell growth *in vitro*. These include: a carbon source such as glu-

cose or fructose, amino acids, vitamins and inorganic salts, and serum and related compounds. Medium design has been a well covered issue in insect cell cultivation and today a range of good serum-free media for insect cell growth are available for use with the majority of the relevant insect cell lines. These include: SF900 II (Gibco, Glasgow, UK), Excell 401 and 405 (JRH Biosciences, Sussex, UK) and HyQ-SFX Insect (HyClone, Logan, US).

The range of carbohydrate utilisation differs between different insect cell lines. Glucose, fructose and maltose can be used individually as carbon sources in Sf9 cell cultures [42].

Bedard et al. found that glucose was growth limiting and was the most important single source of organic carbon for the cells in all cultures, although there is no clear correlation between the final cell density and the initial glucose concentration in the medium (4–24 mM) [62]. Cells utilised fructose and maltose but not sucrose. α-Ketoglutarate and malate contributed significantly to the carbon budget of cells. Lactate generally did not accumulate during growth, except under oxygen limitation. During aerobic culture it is consumed.

Most of the amino acids are consumed by insect cells, with the exception of alanine which is produced; however, it has been reported that alanine overflow metabolism is energetically wasteful as it is with mammalian cells [63]. The alanine production by insect cells has been interpreted as a strategy to avoid the accumulation of toxic ammonia produced from amino acid catabolism [64].

Optimal conditions for insect cell growth have been extensively studied, but for product expression with a baculovirus infected insect cell the focus should be on the difference in the metabolic requirements of infected vs. uninfected cells, which has been observed to differ after infection. The alanine specific production rate decreases almost four-fold, while phenylalanine specific consumption rate increase 11-fold and glutamine specific consumption decrease [65]. Both an increase [66] and a decrease [67] in glucose consumption rates of insect cells after infection have been reported. This reflects some differences in the media and vectors that were used; however, it is normal to expect a higher metabolic burden after infection due to the increase in protein expression rates caused by the infection. This creates a concern about the impact of nutrient limitations on the productivity of the system.

Several different strategies to overcome nutrient depletion have been used, such as extra nutrient addition to the culture medium prior to infection [68] and partial to complete medium refeeding prior to infection [17].

It has been reported that specific oxygen uptake rate (OURsp) increases transiently after baculovirus infection (reviewed by Agathos [56]). This increase can vary between 7 and 100 %. In the production of HIV-CLPs, Cruz et al. reported a 100 % increase in OURsp of Sf9 cells after baculovirus infection [69] although no increase was detected in PPV-VLP production (authors' unpublished results).

General rules are not easy to infer from the existing literature, especially concerning particle production, since most of the literature reports deal only with genetic requirements for particle formation and have not investigated the effect of nutrient levels on particle productivity. Also, in most of the cases the process was not intended for industrial application, and the use of serum containing medium at laboratory scale is still ubiquitous.

4
Bioreactor Operation and Scale-Up

Volumetric productivity is a good performance index in what concerns the optimization of bioreactor operation. It can be used in process improvement at a defined scale and also for process scale-up, since it is a dimensionless variable. Therefore bioreactor operation and scale-up for CLP and VLP production will be addressed as the identification of the operational conditions that result in the best volumetric productivity.

Bioreactor operation and scale-up are not completely independent processes and should be assessed as different aspects of the same problem. Bioreactor operation must then consider process scale-up not only as the next step but also, as in the classic scale-down method, as a starting point. This means that bioreaction design should be done in scalable systems. A scalable system has to be inherently simple and reliable in operation and control, for easy validation and control in a production facility [56].

The bioreactor operation mode is normally defined at the outset of process configuration. Insect cells have been cultured in almost all known cultivation modes: batch [10], repeated-batch [70], perfusion [71–74], fed-batch [75, 76], semi-continuous [77, 78] and continuous [79]. In spite of this multitude of different strategies, the batch or, eventually, fed-batch mode is normally preferred due to the lytic infection cycle of the baculovirus.

The operational conditions and culture parameters that have a higher impact on bioreaction are: temperature, medium pH, dissolved oxygen (DO), aeration rate and mode, agitation rate and mode, cell density, cell viability, growth stage, MOI, time post-infection for harvesting, and medium ingredients and time of feeding [56]. These are not independent variables and optimization around them should be performed in an integrated fashion.

As indicated earlier, insect cells have been cultured either as attached or suspension cultures. For scale-up purposes, systems where cells grow attached to surfaces are less suitable because of the fundamental limitation in surface area upon further increase in reactor volume (surface-to-volume ratio decreases as volume increases) unless microcarriers are utilised, which increases complexity and cost. In contrast, suspension systems are easily scalable and therefore their use is widespread since insect cells, like Sf9, have already been well adapted to suspension systems.

Along with the bioreactor operation mode, bioreactor type is also an important aspect of process development. Two types of suspension bioreactors have been mostly used in insect cell cultivation: the stirred tank [77] and the air-lift bioreactor [80]. Although air-lift bioreactors are simpler in design and construction than stirred tank reactors, leading to reduced capital and maintenance costs (no shaft bearings, seals or drive mechanisms to service) [56], the stirred tank reactor system is widely available in the industry, is suitable for multipurpose use, and experience in design and understanding of the scale-up principles for stirred tanks exists, thus rendering it the most used option currently.

4.1
Effect of Cultivation Temperature and Medium pH

Insect cells have an optimal cultivation temperature of 27 – 28 °C. However, for protein production this temperature may not always be the most adequate.

Reuveny et al. [81] suggested that lowering the incubation temperature from 27 °C to 25 °C may alleviate eventual oxygen limitations without compromising the maximum cell yield. The expression level of the recombinant proteins at 27°C was similar to that obtained at 22 °C and 25 °C but lower protein yields were obtained at 30 °C. An increase in temperature from 22 °C to 27 °C led to earlier production of the proteins and to an increase in the proportion of the product released by the cells [81].

Besides the currently used constant temperature mode it has been reported that temperature oscillation can enhance cell viability of Sf9 insect cells and baculovirus production of occlusion bodies (OB) and extracellular virus (ECV) compared with constant temperature in stationary culture and suspension culture, with the optimal oscillation range at 24 – 28 °C [82]. As a curiosity Pham et al. found that, by raising the infection temperature to 30 °C, they more than doubled the protein productivity of human interleukin-2 (IL-2), in insect larvae, *Trichoplusia ni* [83].

The cultivation temperature has also a great impact on specific glycosylation of human secreted alkaline phosphatase (SEAP), since by lowering the temperature from 28 °C to 24 °C or even 20 °C, a twofold increase in oligosaccharides containing terminal $\alpha(1,3)$-mannose residues was observed; this could result in more complete glycosylation of recombinant proteins in the BTI Tn5B1-4 cell line, because more structures with the potential for further processing would be produced [84].

The effect of temperature in the production of Parvovirus B19 VLPs was assessed by Tsao et al. [18]. They showed that at 25 °C the production of Parvovirus B19 capsid protein at harvest was significantly higher than those at 27 °C and 29 °C. The reduction in the specific yield at higher temperatures correlated well with higher concentrations of lactate accumulated in the medium. It is known that insect cells only produce lactate under O_2 limitation, and they cannot direct all the pyruvate to the TCA cycle. In this last case the oxygen limitation was alleviated without compromising the maximum cell yield by lowering the incubation temperature, as suggested by Reuveny et al. [81]. Since higher lactate concentrations have been shown to be detrimental to the specific productivity of Parvovirus B19 capsids [18], at a lower incubation temperature the slowest growth rate of the cells does not lead to a toxic accumulation of lactate, and the final outcome is a higher product yield.

Incubation temperature and medium pH are also important regarding proteolytic activity of baculovirus infected insect cell cultures. Cruz et al. [25] have shown that the highest proteolytic activity was obtained at the normal culture conditions, 27 °C and pH 6.5. This could then be considered a drawback when the production of protease sensitive particles like HIV-CLPs and HIV-VLPs is envisaged [5]. The pH of Sf9 cells has been reported to reach a minimum of 5.9 in serum-free media under uncontrolled pH conditions in stirred tank reactors

[66]. It has been reported that insect cells have a strong internal buffering capacity [85]; however, there are indications that medium pH must be optimised for growth and production phases and should be kept under tight control in bioreactors, especially in high-density large scale cultivations [56].

4.2 Cell Density and Culture Feeding

An important consequence of the increase in OURsp after baculovirus infection is that cells can not be infected at the highest cell density achievable without oxygen limitation. Consequently, the cultures are often infected at a lower cell density in order to obtain effective infections without a decrease in the cell specific productivity. Nevertheless, complex feeding strategies have been used and the maximum cell density that has been reported in fed-batch mode is 52×10^6 cells/ml [86]. Although this cell density is more than 5-fold higher than the cell density obtained without feeding [69], effective infections were only obtained at 14×10^6 cells/ml and a decrease of almost 50% in specific productivity was obtained with cultures infected at 17×10^6 cells/ml [86]. Therefore, cell density at infection is highly important for bioreaction design. Although a great number of reports have dealt with the effect of the cell density at infection [65, 87] the lower productivity obtained at higher cell densities is due to some nutrient limitation that was already affecting cell status rather than a direct effect of the cell density by itself.

A couple of feeding strategies have been developed to increase the volumetric productivity of the system [75, 76, 86, 88, 89]. However some of these strategies are unwieldy for industrial application, in particular if large bioreactor volumes need to be managed and replaced under sterility conditions, involving cell retention. For instance in BTV CLP production Zheng et al. [17] diluted the cells two-fold in fresh medium before cell infection; this implies large volume management if intended to be used at large scale. Feeding strategies with concentrated nutrient cocktails are preferred since from a process development point of view, this strategy simplifies large-scale protein production because it allows operations of growth and infection of high cell density without requiring an intermediate step of cell liquid-separation for medium replacement.

4.3 Dissolved Oxygen

There have been misconceptions among some researchers regarding the influence of the dissolved oxygen tension (DO) in baculovirus infection and product expression, as often no distinction is made between dissolved oxygen tension and oxygen limitations in mass transfer. The analysis of the effects of DO levels can only be studied effectively in bioreactors with controlled DO levels [56].

Overall influence of DO levels in product expression and insect cell growth was reviewed by Agathos [56]. Generally there are indications that Sf9 cells show similar growth characteristics at 10 to 70% air saturation. This has been confirmed more recently by Cruz et al. [69] for Sf9 cells in DO levels in the

range 10–50% of air saturation. These results are in good correlation with Palomares and Ramirez [90], who showed that growth rate appears to have Monod type kinetics with a Km in the range of 10% air saturation.

Nevertheless, DO levels seem to be more important for product expression than for cell growth and the effect seems to be product specific. Cruz et al. [69] studying the influence of DO levels in HIV-VLPs production have analysed product titer and quality at DO levels of 10, 25 and 50%, with quality defined as the percentage of high molecular weight particles in the final product; they concluded that the best quality was obtained at a DO of 10%, but the best titer was obtained at 25% DO level. Conversely, Hu and Bentley studying IBVD [33] have obtained the best titer at 50 to 80% DO level, and a lower yield at 25%; the same group has reported for the expression of epoxide hydrolase that the best DO level was 25% [89]. Thus, the operational DO conditions should be optimised for each product.

4.4 Oxygen Transfer, Shear Stress and Scale-Up

The influence of oxygen limitations at the inception of infection on product expression has been extensively reported [5, 65, 81, 84, 87–91]. Interestingly all have reached the same conclusion that by increasing the oxygen transfer rate the productivity is increased, suggesting the culture was limited by oxygen transfer before changing the operational parameters (or eventually by CO_2 stripping from the culture).

In a general way the increase in the OUR of the culture is compensated for by varying (sequentially) the agitation rate, the aeration rate and the oxygen partial pressure in the gas inlet [69]. However, insect cells are far more fragile than microorganisms and their susceptibility to high shear stress imposes limitations on the maximum oxygen transfer rate that can be attained. Nevertheless, the work of Kunas and Papoutsakis [92] has shown that it is not turbulent fluid flow which is responsible for the cell injury at agitation rates normally shown to affect cell viability in culture; it is the combined effect of stirring, sparging and bubble entrapment by vortex formation that leads to cell death. This issue is far more evident at small bioreactor scales since vortex formation occurs at relatively low agitation rates. For example in 2 litre bioreactors with two Rushton turbines (standard geometry) 300 rpm is enough to create a vortex, and this stirring rate already affects cell growth [69].

Murhammer and Goochee [93, 94] have confirmed the beneficial effect of Pluronic F-68 addition to insect cell cultures and its protective effect upon bubble damage. The use of PF-68 is today ubiquitous in bioprocess development involving insect cell culture technology, although it may conceivably interfere with VLP formation in some instances. For a more detailed study of the effect of bubble in cell damage mechanisms and the mechanism of protection of PF-68 see the review by Chalmers and the references cited therein [95].

Cruz et al. [69] have optimised bioreactor operational conditions for HIV-VLPs production using the concept of minimising local shear stress, i.e., they assumed that all the energy liberated by the stirring turbine was dissipated

in a cube of dimensions of D_i^3 (with D_i being the impeller diameter) [96, 97]. They have shown for clone Sf9 that although shear stress conditions greater than 1 N m^{-2} did not affect cell viability, it was already affecting cell growth rate, baculovirus infection and product expression. This concept was also applied to scale-up the production of PPV-VLPs [98] from 2 to 25 litre. Here Sf21 cells were used for PPV-VLPs production; however, this clone seems not to be affected by shear stress values up to 2 N m^{-2}, and was only limited by foam formation at the highest stirring rates, which is in agreement with the reported observations of Kunas and Papoutsakis [92].

4.5 Multiplicity of Infection (MOI)

The use of high vs. low MOI's has been preferred for two main reasons: easier harvest time definition and elimination of the 'passage effect' from the baculovirus inoculum. The so-called passage effect results in a decrease with time (passage number) of the fraction of virus that carries the recombinant gene [3]. This phenomenon is similar to that observed in wild-type AcMNPV in highly passaged baculovirus that generates few polyhedra phenotypes [99]. Nevertheless, at large scale, the use of low MOI is recommended since it avoids an additional viral expansion step. The normal baculovirus titre that can be expected from an optimised infection is in the order of $1-5 \times 10^8$ pfu/ml. Therefore a volume between 1 and 5 litres is necessary to infect a 25 litre bioreactor at a cell concentration at infection (CCI) of 4×10^6 cells/ml (MOI = 5); this represents an inoculum of 4 to 20 % of final bioreactor volume. If high MOI's are used, it is necessary to optimise the production of baculovirus inoculum, and to continuously produce new stocks, due to the large consumption and to the loss of the virus expression efficiency caused by DI particles. As a result, this will lead to the increase of the production cost, and to the decrease of the process performance, since large volumes of waste medium are added to the bioreaction vessel.

Wong et al. [100] reported that very low multiplicities of infection could be used with the model β-Galactosidase baculovirus/insect cell system. They proposed the Cell Yield Concept stating that choosing the appropriate TOI (time of infection) it is possible to achieve the optimal cell yield for whatever MOI is chosen.

Initial reports proposed that very low MOI's are only useful when used to produce simple protein products that are insensitive to proteolysis, and even then, it is difficult to predict the extent of post-infection cell growth under such conditions [101]. Nevertheless, product stability may not be an issue of concern, using low multiplicities of infection, since the productivity after the secondary infection is much higher [100]. Recently, when producing Bluetongue CLPs Zheng et al. [17] have shown that it is possible to use very low MOI's (0.0001 – 0.001) and still achieve specific and volumetric yields similar to those obtained using high MOI's. However, to achieve this a lot of experiments were necessary in order to define the best (MOI, CCI) pair(s) that led to the optimal productivity. Wong and co-workers [100] have also reported some failures in infections using low MOI's.

Cruz and co-workers have used MOI's of 2 to 5 for the production of HIV-VLPs and HIV-CLPs [69]. They found that, for their system, the peak volumetric particle titre did not coincide with maximum particle quality, due to the increase of proteolytic activity in the supernatant, which is coincident with cell lysis. Nevertheless, that issue was surpassed by correct integration with downstream processing, where low weight particles were removed by gel filtration chromatography [32].

Contrary to the previous case, using strategies with low MOI's, cell infection will not be synchronised and the cell population will be distributed over different cell status and different specific infection times (τ_I) [102], leading to a non-obvious definition of the optimal harvest time, extension of cell lysis and the increase in the proteolytic activity is not easy to predict and account. Although this could be considered a drawback in low MOI strategies, it is possible to control the extension of proteolysis [33, 83] by the addition of protease inhibitors.

Due to the complexity of insect cell/baculovirus interactions and the possibility of using low MOI's, which, in turn, increase the complexity of the process since several different population types coexist simultaneously in the bioreactor vessel, the development of mathematical models as tools for describing the system dynamics is extremely useful.

5
Mathematical Models

A substantial number of models have been proposed for the insect cells/BEVS system ranging from empirical approaches [103], through unstructured [102, 104], structured and mechanistic [60, 61] to a recent kinetic and statistical-thermodynamic model [105].

For process development purposes it is useful to consider two steps in the infection process. First the binding and post-attachment steps (internalisation, endosomal fusion, lysosomal routing, and gene deliver to the nucleus) and secondly the expressing phase of the baculovirus components and production of the product of interest.

5.1
Binding and Infection

Baculovirus binding to insect cells is receptor-mediated [60]. From the work of Dee and Shuler it seems that the post-attachment steps occur much faster than attachment and thus the limiting step is the rate of attachment [61]. Another interesting result from the Dee and Shuler report that could have a great impact on bioreaction operational parameter specification is the observation that even in attached cultures, i.e. with baculovirus transport limited by diffusion, the rate of the diffusion of the baculovirus is 10-fold higher than the rate of attachment. This suggests that the overall rate of infection is, in suspension systems like in stirred tank reactors, independent

of the stirring rate. This also implies that when the process is scaled-up to a large scale, keeping the shear stress constant, the overall infection rate should be the same independent of the higher turbulence regime at the larger scale [98].

From the Dee and Shuler model the virus depletion rate function can be defined as [106]:

$$\frac{dVex}{dt} = -k_a .C.Vex \tag{1}$$

Where C is the cell concentration (cells/ml), V_{ex} is concentration of free virus in suspension (pfu/ml) and k_a is the attachment constant (ml/cells h^{-1}).

To know the binding kinetics is also important in MOI-TOI specification, in particular at low MOI's, for different cell lines. *T. ni* cells like HighFive™ have a constant of attachment almost 10-fold higher than *S. frugiperda* cells such as Sf9 [60].

Considering equal time steps (Δt) Dee and Shuler propose that the amount of virus bound during the first time step could be approximated by:

$$\Delta V_1 = k_a C_1 V_0 \Delta t \tag{2}$$

Where C_1 is the cell concentration after time step 1.

In the Licari and Bailey Model [102] and also in the latest Hu and Bentley Model [105] it is proposed that the infection process be described by the Poisson distribution with mean and variance equal to α.MOI. The α-value has been proposed to be dependent on the physical system and a value of $\alpha = 0.04$ was proposed for static systems [102]. For agitated systems suspension cultures Hu and Bentley proposed a value of $\alpha = 0.08$ because they state that agitation systems enable higher efficiency of contact between viruses and cells [105]. This is not absolutely true, at least the true reason is not the higher mixing level but the fact that in static cultures, less cell surface is exposed to the virus, since to the cells are attached to a surface. This gives an overall constant of attachment 3-4 fold lower than in suspension systems [61].

Licari and Bailey used the Poisson distribution in the following form:

$$p(t, j) = \frac{e^{-\alpha.MOI(t)} \times (\alpha.MOI(t))^j}{j!} \tag{3}$$

p (t, j) is the probability at time t that a cell could be infected by j viruses, t is the time (h), j is the number of viruses infecting one cell, α is the empirical factor and MOI(t) is the Multiplicity of Infection at time t.

The sum of all possible combinations of the number of viruses that could be infecting one cell is given by:

$$P(t) = \sum_{j=1}^{\infty} p(t, j) = 1 - e^{-\alpha.MOI(t)} \tag{4}$$

Dee and Shuler [106] applied the same Poisson distribution but with a mean and variance equal to:

$$\lambda = \frac{\Delta V_1}{C_1} = \frac{k_a C_1 V_0 \Delta t}{C_1} = k_a C_0 MOI_0 \Delta t \tag{5}$$

Where MOI_0 represents the multiplicity of infection at time 0. Comparing the Licari and Bailey parameter α with the Dee and Shuler expression means that:

$$\alpha = k_a C_0 \Delta t \tag{6}$$

If we take the value of $k_a = 0.44 \times 10^{-9}$ (ml/cells min) proposed by Wickham et al. [60] for static cultures with $C_0 = 1.5 \times 10^6$ cells/ml (mid-exponential curve of Licari and Bailey data [102]) and a time step $\Delta t = 1$ h = 60 min, the computed value of α is 0.04, in agreement with Licari and Bailey [102].

Also if we apply the same concept, to the data available for suspension cultures, with $k_a = 1.3 \times 10^{-9}$ (ml/cells min), proposed by Dee and Shuler [61], with $C_0 = 1.0 \times 10^6$ cells/ml (early-exponential curve of Hu and Bentley data [33]) and a time step $\Delta t = 1$ h = 60 min, the computed value of α is 0.08.

Nevertheless, the parameter with real physical meaning is k_a and not α, since k_a is a real constant that has been measured, contrary to the case of the empirical parameter α. Licari and Bailey have used an assumption that the α value will remain constant for all initial infections since the physical system and the volume used are the same [102]. This is likely not to be the case since as can be seen by the expression above, the α value is dependent upon cell concentration. Also in the Hu and Bentley Model they propose that α will remain constant over time [105].

Secondary infection is an issue that is dealt with only in the Dee and Shuler Model [61] and Hu and Bentley Model [105]. Since today there is not sufficient knowledge regarding the number of viruses that are really infecting a single cell, the linear approach taken by Hu and Bentley [105] for cell "infectivity" status is an approach as good as any other. However, Hu and Bentley assume that all viruses initially infecting cells are effective (not degraded), while all viruses that secondarily infect the already-infected cells are defective and degraded after entering the cells; these authors claim that approximates the formulation of Dee and Shuler [61] in a mathematically tractable form. Although mathematically this appears equivalent it is not obvious that this assumption correlates well with the effect of the number of viruses infecting a single cell has on its specific productivity. As suggested by Power and Nielsen [107] since these measurements can not be validated, the model that arises with this kind of formalism becomes a sophisticated fitting machine.

5.2 Production of VLPs

All models developed dealt with product expression by a sub-division of cellular events and a more or less linear relationship between product expression rates and infected cell concentrations. Although this is a simplification, since the

expression occurs in a transient mode, the models in general fit the data with good correlation.

The Hu and Bentley model is the only one that tries to describe VLP production and assembling in baculovirus infected insect cells [105]. Nevertheless, regarding VLP assembly, the formalism presented is completely theoretical and based on the assembly pathway of icosahedral viruses. From a process development point of view, this model does not generate enough output to make it applicable to bioreaction operational parameters definition. However, it can be used as the basis for a more structured approach to the VLP assembling process in baculovirus infected insect cells.

The application of mathematical modelling to baculovirus infection and virus-like particle production was also successfully done to Parvovirus B19 virus-like particle production with two different baculovirus at low MOI's [18]. But in this model the same concepts proposed in the Licari and Bailey Model was applied, i.e. baculovirus infection follows Poisson distribution with mean and variance equal to α.MOI, but with co-infection with two single-vectors, each one encoding a specific viral protein.

However, as important as the Hu and Bentley Model is the stepwise approach to process optimisation that Hu and Bentley have reported [33]. The focus on quantitative analysis of protease degradation of the product over time, along with the similar approach followed by Cruz et al. [25], also indicate new directions to follow in mathematical modelling regarding product expression optimisation.

Mathematically modelling of VLP production by baculovirus infected insect cells is not a closed chapter of research, and probably never will be, at least until complete structured models have been developed, taking into account intracellular pools.

James Bailey has said, talking about the inextricable coupling between a model and its intended application (citing Casti) that "Basically the point of making models is to be able to bring a measure of order to our experience and observations, as well as to make specific predictions about certain aspects of the world we experience" [108]. So models are not an end in themselves but should be looked more as tools to think and calculate logically about what components and interactions are important in a complex system. Mathematical models can also be justifiable to minimize the experimental effort, predict system behaviour and identify new research avenues [10].

6 Conclusion

The production of VLPs with baculovirus infected insect cells is entering the phase of industrial application. Due to the complexity of the system a multitude of vector strategies have been developed, ranging from single to fifth-level baculovirus vectors, along with combinations between them.

Bioreaction optimisation involves assessment of good oxygen transfer conditions and evaluation of shear stress influence on cell growth and productivity.

Scalability of the systems is a must and the use of low MOI strategies is obligatory if the goal is the industrial application. Complex feeding strategies must be avoided since they impose high risks, and costs, to the overall process.

Better mathematical models providing a better understanding of the basic events are still needed, incorporating the attachment steps, the intracellular events, and product expression, assembling and degradation.

Acknowledgement. The authors acknowledge and appreciate the financial support received from the European Commission (BIO4-CT98-0215) and from Fundação para a Ciência e Tecnologia – Portugal (PRAXIS XXI/BD/16136/98).

References

1. Wu SC, Jarvis DL, Dale BE, Liao JC (1994) Biotechnol Prog 10:55
2. Morais VA, Serpa J, Palma AS, Costa T, Maranga L, Costa J (2001) Biochem J 353:719
3. Casal JI (1996) Cytotechnology 20:261
4. Roy P (1990) FEMS Microbiol Immunol 2:223
5. Cruz PE, Peixoto CC, Moreira JL, Carrondo MJT (1998) J Chem Technol Biotechnol 72: 149
6. Blissard GW (1996) Cytotechnology 20:73
7. O'Reilly DR, Miller LK (1989) Baculovirus expression vectors, a laboratory manual. WH Freeman and Co., New York
8. King LA, Possee RD (1992) The Baculovirus Expression System: a laboratory guide. Chapman Hall, London
9. Touze A, Coursaget P (1998) Nucleic Acids Res 26:1317
10. Cruz PE (1999) PhD Thesis – Optimization of the Production of Complex Bioproducts, PhD Thesis, ITQB-UNL
11. Baumert TF, Ito S, Wong DT, Liang TJ (1998) J Virol 72:3827
12. Hyatt AD, Zhao Y, Roy P (1993) Virology 193:592
13. French TJ, Roy P (1990) J Virol 64:1530
14. French TJ, Marshall JJ, Roy P (1990) J Virol 64:5695
15. Sabara M, Parker M, Aha P, Cosco C, Gibbons E, Parsons S, Babiuk LA (1991) J Virol 65: 6994
16. Roy P (1992) Vet Microbiol 33:155
17. Zheng YZ, Greenfield PF, Reid S (1999) Biotechnol Bioeng 65:600
18. Tsao EI, Mason MR, Cacciuttolo MA, Bowen SH, Folena-Wasserman G (1996) Biotechnol Bioeng 49:130
19. Brown CS, Van Lent JW, Vlak JM, Spaan WJ (1991) J Virol 65:2702
20. Martinez C, Dalsgaard K, Lopez de Turiso JA, Cortes E, Vela C, Casal JI (1992) Vaccine 10: 684
21. Hernando E, Llamas-Saiz AL, Foces-Foces C, McKenna R, Portman IAgbandje-McKenna M, Almendral JM (2000) Virology 267:299
22. Langeveld JP, Kamstrup S, Uttenthal A, Strandbygaard B, Vela C, Dalsgaard K, Beekman NJ, Meloen RH, Casal JI (1995) Vaccine 13:1033
23. Bansal GP, Hatfield JA, Dunn FE, Kramer AA, Brady F, Riggin CH, Collett MS, Yoshimoto K, Kajigaya S, Young NS (1993) Journal of Infectious Diseases 167:1034
24. Jiang B, Barniak V, Smith RP, Sharma R, Corsaro B, Hu B, Madore HP (1998) Biotechnol Bioeng 60:369
25. Cruz PE, Martins PC, Alves PM, Peixoto CC, Santos H, Moreira JL, Carrondo MJ (1999) Biotechnol Bioeng 65:133
26. Naggie S, Bentley WE (1998) Biotechnol Prog 14:227
27. Fan Z, Yang QR, Twu JS, Sherker AH (1999) J Med Virol 59: 131

28. Heile JM, Fong YL, Rosa D, Berger K, Saletti G, Campagnoli S, Bensi G, Capo S, Coates S, Crawford K, Dong C, Wininger M, Baker G, Cousens L, Chien D, Ng P, Archangel P, Grandi G, Houghton M, Abrignani S (2000) J Virol 74:6885
29. Roy P, Bishop DH, LeBlois H, Erasmus BJ (1994) Vaccine 12:805
30. Belyaev AS, Roy P (1993) Nucleic Acids Res 21:1219
31. Belyaev AS, Hails RS, Roy P (1995) Gene 156:229
32. Cruz PE, Peixoto CC, Devos K, Moreira JL, Saman E, Carrondo MJT (2000) Enzyme Microb Technol 26:61
33. Hu YC, Bentley WE (1999) Biotechnol Prog 15:1065
34. Loudon PT, Hirasawa T, Oldfield S, Murphy M, Roy P (1991) Virology 182:793
35. Le Blois H, Fayard B, Urakawa T, Roy P (1991) J Virol 65:4821
36. Belyaev AS, Roy P (1992) Virology 190:840
37. Sedlik C, Sarraseca J, Rueda P, Leclerc C, Casal I (1995) J Gen Virol 76 (Pt 9):2361
38. Sedlik C, Saron M, Sarraseca J, Casal I, Leclerc C (1997) Proc Natl Acad Sci USA 94: 7503
39. Rueda P, Martinez-Torrecuadrada JL, Sarraseca J, Sedlik C, del Barrio M, Hurtado A, Leclerc C, Casal JI (1999) Vaccine 18:325
40. Hu YC, Bentley WE, Edwards GH, Vakharia VN (1999) Biotechnol Bioeng 63:721
41. Wang MY, Kuo YY, Lee MS, Doong SR, Ho JY, Lee LH (2000) Biotechnol Bioeng 67:104
42. Bhatia R, Jesionowski G, Ferrance J, Ataai MM (1996) Cytotechnology 20:33
43. Schmid G (1996) Cytotechnology 20:43
44. Schlaeger E-J (1996) Cytotechnology 20:57
45. Grace TDC (1962) Nature 195:788
46. Hink WF (1976) Invertebrate Tissue Culture Research Applications. Academic Press, New York p 319
47. Hink WF, Hall RL (1989) In: Mitsuhashi J (ed) Invertebrate Cell System Applications, vol II. CRC Press, Inc., Boca Raton, FL, p 269
48. Baines D (1996) Cytotechnology 20:13
49. Agathos SN, Jeong YH, Venkat K (1990) Ann N Y Acad Sci 589:372
50. Parker SD, Hunter E (2000) J Virol 74:784
51. Vaughn JL, Goodwin RH, Tompkins GJ, McCawley P (1977) In Vitro 13:213
52. Cruz PE, Moreira JL, M. J. T. C (1997) Biotechnology Techniques 11:117
53. Wickham TJ, Davis T, Granados RR, Shuler ML, Wood HA (1992) Biotechnol Prog 8:391
54. Wickham TJ, Nemerow GR (1993) Biotechnol Prog 9:25
55. Davis TR, Wickham TJ, McKenna KA, Granados RR, Shuler ML, Wood HA (1993) In Vitro Cell Dev Biol Anim 29A:388
56. Agathos SN (1996) Cytotechnology 20:173
57. Gheysen D, Jacobs E, de Foresta F, Thiriart C, Francotte M, Thines D, De Wilde M (1989) Cell 59:103
58. Aunins JG (2000) In: Spier RE, Editor in Chief, The Encyclopedia of Cell Technology. Wiley, New York, p 1182
59. Wickham TJ, Granados RR, Wood HA, Hammer DA, Shuler ML (1990) Biophys J 58:1501
60. Wickham TJ, Shuler ML, Hammer DA, Granados RR, Wood HA (1992) J Gen Virol 73: 3185
61. Dee KU, Shuler ML (1997) Biotechnol Bioeng 54:468
62. Bedard C, Tom R, Kamen A (1993) Biotechnol Prog 9:615
63. Ohman L, Ljunggren J, Haggstrom L (1995) Appl Microbiol Biotechnol 43:1006
64. Ferrance JP, Goel A, Ataai MM (1993) Biotechnol Bioeng 42:697
65. Wong TK, Nielsen LK, Greenfield PF, Reid S (1994) Cytotechnology 15:157
66. Hensler WT, Agathos SN (1994) Cytotechnology 15:177
67. Rhiel M, Mitchell-Logean CM, Murhammer DW (1997) Biotechnol Bioeng 55:909
68. Bedard C, Kamen A, Tom R, Massie B (1994) Cytotechnology 15:129
69. Cruz PE, Cunha A, Peixoto CC, Clemente J, Moreira JL, Carrondo MJ (1998) Biotechnol Bioeng 60:408
70. Kloppinger M, Fertig G, Fraune E, Miltenburger HG (1990) Cytotechnology 4:271

71. Caron AW, Tom RL, Kamen AA, Massie B (1994) Biotechnol Bioeng 43:881
72. Deutschmann SM, Jager V (1994) Enzyme Microb Technol 16:506
73. Fertig G, Rahn HP, Angermann A, Kloppinger M, Miltenburger HG (1993) Cytotechnology 11:67
74. Jäger V (1996) Cytotechnology 20:191
75. Chan LC, Greenfield PF, Reid S (1998) Biotechnol Bioeng 59:178
76. Nguyen B, Jarnagin K, Williams S, Chan H, Barnett J (1993) Journal Biotechnol 31:205
77. van Lier FL, van den End EJ, de Gooijer CD, Vlak JM, Tramper J (1990) Appl Microbiol Biotechnol 33:43
78. Piergiovani PR, Dutt K (1993) Biotechnology Techniques 7:765
79. Wang MY, Bentley WE (1994) Appl Microbiol Biotechnol 41:317
80. Maiorella B, Inlow D, Shauger A, Harano D (1988) Bio/Technology 6:1406
81. Reuveny S, Kim YJ, Kemp CW, Shiloach J (1993) Appl Microbiol Biotechnol 38:619
82. Hong-Liang S, Zuo-Hu L (1998) Appl Environ Microbiol 64:2237
83. Pham MQ, Naggie S, Wier M, Cha HJ, Bentley WE (1999) Biotechnol Bioeng 62:175
84. Donaldson M, Wood HA, Kulakosky PC, Shuler ML (1999) Biotechnol Bioeng 63:255
85. Medina M, Domingo E, López-Rivas A, Zuidema D, Vlak JM, Belsham GJ (1995) Cytotechnology 17:21
86. Elias CB, Zeiser A, Bedard C, Kamen AA (2000) Biotechnol Bioeng 68:381
87. Scott RI, Blanchard JH, Ferguson CH (1992) Enzyme Microb Technol 14:798
88. Konz JO, King J, Cooney CL (1998) Biotechnol Prog 14:393
89. Wang MY, Kwong S, Bentley WE (1993) Biotechnol Prog 9:355
90. Palomares LA, Ramirez OT (1996) Cytotechnology 22:225
91. Taticek RA, Shuler ML (1997) Biotechnol Bioeng 54:142
92. Michaels JD, Mallik AK, Papoutsakis ET (1996) Biotechnol Bioeng 51:399
93. Murhammer DW, Goochee CF (1988) Bio/Technology 6:1411
94. Murhammer DW, Goochee CF (1990) Biotechnol Prog 6:391
95. Chalmers JJ (1996) Cytotechnology 20:163
96. Tatterson GB (1991) Fluid mixing and gas dispersion in agitated tanks. MacGraw-Hill, Inc., New York
97. Tramper J, Vlak JM, Gooijer CDd (1996) Cytotechnology 20:221
98. Maranga L, Cunha A, Clemente J, Carrondo MJT (2000) Conference Proceedings of Biotechnology 2000 – The World Congress in Biotechnology. Dechema, Berlin, p 392
99. Krell PJ (1996) Cytotechnology 20:125
100. Wong KTK, Peter CH, Greenfield PF, Reid S, Nielsen LK (1996) Biotechnol Bioeng 49:659
101. Radford KM, Cavegn C, Bertrand M, Bernard AR, Reid S, Greenfield PF (1997) Cytotechnology 24:73
102. Licari P, Bailey JE (1992) Biotechnol Bioeng 39:432
103. Wu S, Dale BS, Liao JC (1993) Biotechnol Bioeng 41:104
104. Power J, Greenfield PF, Nielsen L, Reid S (1992) Cytotechnology 9:149
105. Hu Y-C, Bentley WE (2000) Chem Eng Sci 55:3991
106. Dee KU, Shuler ML (1997) Biotechnol Prog 13:14
107. Power JF, Nielsen LK (1996) Cytotechnology 20: 209
108. Bailey JE (1998) Biotechnol Prog 14:8
109. Lanford RE, Luckow V, Kennedy RC, Dreesman GR, Notvall L, Summers MD (1989) J Virol 63:1549
110. White LJ, Hardy ME, Estes MK (1997) J Virol 71:8066
111. Kirnbauer R, Booy F, Cheng N, Lowy DR, Schiller JT (1992) Proc Natl Acad Sci USA 89: 12180
112. Montross L, Watkins S, Moreland RB, Mamon H, Caspar DL, Garcea RL (1991) J Virol 65: 4991
113. Kosukegawa A, Arisaka F, Takayama M, Yajima H, Kaidow A, Handa H (1996) Biochim Biophys Acta 1290:37

Received: May 2001

Integrated Approach To Explore the Potential of Marine Microorganisms for the Production of Bioactive Metabolites

Irene Wagner-Döbler[1], Winfried Beil[2], Siegmund Lang[3,*], Marinus Meiners[4], Hartmut Laatsch[5]

[1] Gesellschaft für Biotechnologische Forschung, Mascheroder Weg 1, 38124 Braunschweig, Germany
E-mail: iwd@gbf.de
[2] Institut für Allgemeine Pharmakologie, Medizinische Hochschule Hannover, Konstanty-Gutschow-Strasse 8, 30625 Hannover, Germany
E-mail: beil.winfried@mh.hannover.de
[3] Institut für Biochemie und Biotechnologie, TU Braunschweig, Spielmannstrasse 7, 38106 Braunschweig, Germany
E-mail: s.lang@tu-bs.de
[4] Fachbereich Naturwissenschaftliche Technik, Fachhochschule Ostfriesland, Constantiaplatz 4, 26726 Emden, Germany
E-mail: meiners@nt-newton.fho-emden.de
[5] Institut für Organische Chemie, Universität Göttingen, Tammannstrasse 2, 37077 Göttingen, Germany
E-mail: hlaatsc@gwdg.de

Dedicated to Prof. Dr. Wolf-Dieter Deckwer on the occasion of his 60th birthday

During the last 10 years marine organisms have provided a large number of new natural products. Interesting compounds have mainly been derived from macroorganisms such as sponges, ascidians, corals and bryozoans. The number of secondary metabolites from marine microorganisms is smaller, but rapidly increasing. Because of the enormous difficulties involved in harvesting products from marine animals, and the fact that some of the bioactive compounds are produced by associated bacteria, the advantages of sustainable production of bioactive metabolites by bacteria or fungi, under the protection of natural resources, seem to be very attractive for the future. This review describes current progress in the isolation and identification of novel marine microorganisms, the discovery of new secondary metabolites, the biotechnological approaches to overproduce them, as well as the evaluation and characterization of their bioactivity.

Keywords. New bacteria from the North Sea, Secondary metabolites, Bioactivity, Biotechnological production, Structure elucidation, Phylogenetic screening

* To whom all correspondence should be addressed.

Advances in Biochemical Engineering/ Biotechnology, Vol. 74
Managing Editor: Th. Scheper

1 Introduction

1.1 Marine Bacteria as Sources of New Bioactive Compounds

The search for bioactive compounds is presently reaching a new dimension – with such diverse approaches as genomics, proteomics, bioinformatics, combinatorial biosynthesis, combinatorial chemistry, targeted drug development, directed evolution of key enzymes, phage display libraries, automation and high throughput screening [1–4]. What role can traditional natural product screening play in today's drug development approaches [5], and what in particular

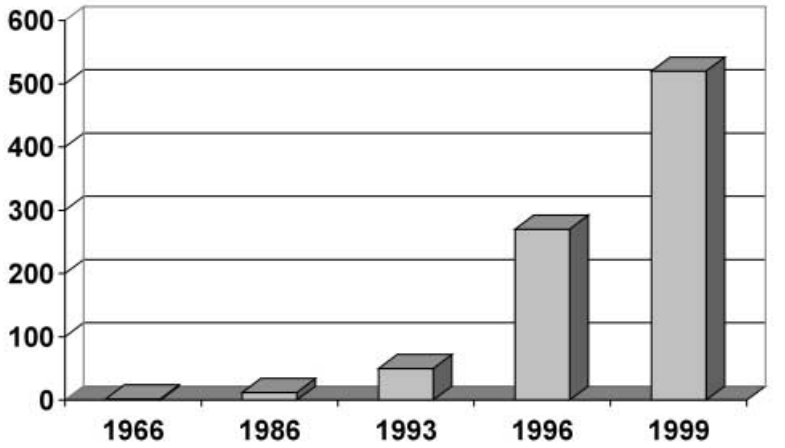

Fig. 1. Total number of metabolites from marine microorganisms (1966–1999)

can be expected from marine microorganisms [6, 7] as sources of novel compounds?

Marine organisms have provided a seemingly endless parade of novel structures. New carbon skeletons were described with a frequency that exceeded all expectations. Several structural features are uniquely or predominantly marine (reviewed by Faulkner since 1986 [8–10]). Thus, ample raw material was provided for combinatorial chemistry, synthetic chemistry, and biocatalysis [11]. The most striking change in the direction of marine natural product chemistry since 1993 was reflected in the sudden increase in reports of new metabolites from marine microorganisms (Fig. 1): Whereas less than ten compounds had been known 20 years ago [12], the number of structures has exponentially grown since then. Although a total number of around 400 compounds is still small in comparison with more than 15,000 structures from terrestrial microorganisms, new compounds are presently almost exclusively found in marine organisms (W Fenical, personal communication).

A number of invertebrate phyla is restricted to the marine environment, with no or few representatives in aquatic and terrestrial habitats, e.g., the Ascidia, Porifera, Coelenterata and Bryozoa. Consequently, from these organisms, a whole range of new chemical structures has been discovered that are not found in terrestrial organisms. However, in many cases, it is not yet clear whether the bioactive compound is produced by the invertebrate, by endosymbiontic or epiobiotic bacteria, or in a cooperative way by both. There is increasing evidence for an important role of the bacterial endosymbionts in the bryostatin-producing bryozoon *Bugula neritina* [13, 14] or for metabolite production in demospongiae [15].

1.2 The Phylogenetic Tree and the Production of Bioactive Compounds

What are marine bacteria? Defining them as bacteria with an absolute requirement for sodium chloride is not a practical solution, because many marine isolates may tolerate quite a wide range of salinities, prompting speculation that they are in fact terrestrial organisms that have been swamped into the oceans from rivers, estuaries and sewage outfalls. Pragmatically, marine microorganisms are therefore defined as bacteria that have been isolated from marine sources on marine media [16].

However, one has to bear in mind that the microbial ecology of marine habitats has been revolutionized by cultivation-independent analyses based on 16S rRNA. It is now well documented that only a fraction of the marine microbial diversity has been cultivated, presumably far less than 1% [17], no more than the "tip of the iceberg" [18]. Clone libraries of marine bacterioplankton 16S rRNA genes are dominated by a few phylotypes that have not been cultivated to date, and which are distributed globally [19, 20]. It can therefore be concluded that the "true" marine microorganisms are in most cases presently not known.

Within the operationally defined "marine bacteria", i.e., bacteria isolated from marine samples on marine media, bioactive compounds have been reported from *Pseudoalteromonas*, *Cytophaga*, *Alteromonas*, *Micrococcus*, *Bacillus*, *Acinetobacter*, *Agrobacterium* and *Pseudomonas* or from unidentified bacteria (Fig. 2).

Cultivated marine bacteria are scattered throughout the phylogenetic tree of the domain Bacteria. However, at lower phylogenetic levels, clusters of marine bacteria have been found which are distinct from those of terrestrial origin. One example is the so-called α3-subgroup of the α-Proteobacteria subclass of the division Proteobacteria, the *Roseobacter* clade [20]. A marine group of *Actinobacteria* [21] has been described, which has, to date, however not been cultivated.

Presently, there are three microbial phylogenetic hot spots known for the production of secondary metabolites:

1. The Streptomycetes, a group of filamentous Gram-positive bacteria (Actinomycetes) that are the work horses of natural product isolation [22];
2. the Myxobacteria, motile bacteria with a complex life cycle which form a distinct cluster within the δ-subclass of the Proteobacteria and have shown to be a rich source of novel structures and biological activities [23, 24];
3. the Cyanobacteria, the former bluegreen algae, photosynthetic bacteria which are distributed globally and produce extremely potent toxins (e.g., [25–27]).

In addition, the antibiotics and other bacteriocins were originally detected in lactic acid bacteria, but were later also found in other Gram-positive microorganisms [28]. Lactic acid bacteria are a group of non-spore-forming, anaerobic fermentative bacteria within the Gram-positives with low GC content.

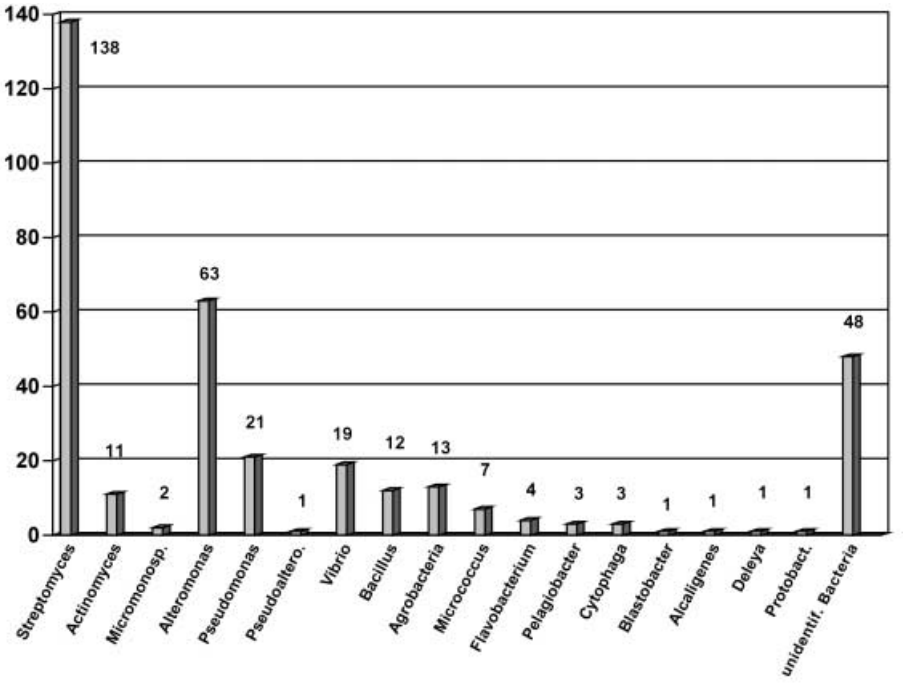

Fig. 2. Number of secondary metabolites isolated especially from marine bacteria until 1999

1.3 Research Network Marine Biotechnology in Lower Saxony

Within the network Marine Biotechnology in Lower Saxony [29] an integrated approach between research groups in microbiology, natural product chemistry, biotechnology, and medicine is underway to systematically explore the metabolic capabilities of North Sea bacteria for the production of bioactive compounds with respect to their phylogenetic position.

Cultivated marine bacteria are notorious for their slow growth and their preference for low nutrient media. Extract yields are therefore often small, resulting in problems with detection limits for natural product chemists. Moreover, it is known that growth media and growth conditions have a profound effect on the production of secondary metabolites and may be different for different strains [30]. It is our working hypothesis that interesting activities that are only expressed under specific conditions, and structures present in low concentrations, may not be detected during conventional mass screening of marine bacteria.

The tools of molecular biology and the phylogenetic framework which is now available as 16S rDNA sequence alignments allow a complementary strategy to be pursued. It is based on a phylogenetic screening of marine isolates and the in-depth investigation of selected phylogenetic groups in order to identify a new hot spot for the production of bioactive compounds.

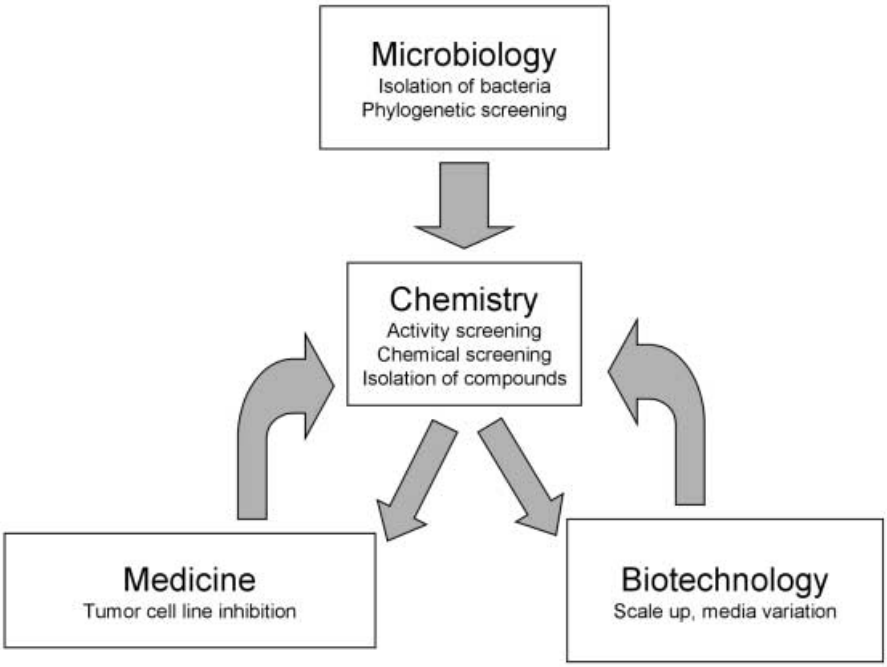

Fig. 3. Integrated approach to explore the metabolic capabilities of North Sea bacteria for the production of bioactive compounds

Isolates from interesting phylogenetic groups (Microbiology) are screened for their biological activity and chemical diversity (Natural Product Chemistry, Medicine). Selected isolates are then cultivated on a large scale and under a variety of cultivation conditions (Biotechnology). Interesting compounds are isolated and their structures are elucidated (Natural Product Chemistry). The concept is shown schematically in Fig. 3.

2
Molecular Tools for Phylogenetic Screening of the Marine Microbial Diversity and First Results on an Indigenous Group of Marine Microorganisms

2.1
Isolation of Marine Bacteria

Cultivation and isolation of bacteria are in some respects more similar to an art than to a scientific method, since there is a strong element of subjectivity involved. Many diverse parameters influence the result of cultivation experiments, including the precise source of the sample (it is probably almost impossible to extract identical samples from nature), the pre-treatment of the sample (storage, cooling, transport, mixing, sieving, filtering, etc.), the enrichment pro-

cedure, if any, and last, but not least, the media and incubation conditions used to cultivate the bacteria. Given the huge diversity of bacteria present in any natural sample and their ability to quickly grow under the right conditions, it is not surprising that totally different subsets of bacteria can be cultivated from a given sample by different cultivators or cultivation methods.

One of our strategies was to isolate marine bacteria which are abundant in the pelagial of the North Sea using "natural" conditions which do not select for the fastest growing strains. We used an unfiltered North Sea water sample obtained with a Ruttner-Schöpfer. The sample was processed within an hour after taking it. No enrichment was performed, but individual colonies were obtained by serially diluting the sample and spread-plating appropriate dilutions on agar plates containing a variety of marine media. Plates were incubated at room temperature for up to 4 weeks. The growth of eukaryotes and protozoan grazing were prevented by the addition of the antibiotic cycloheximide. The isolated bacteria were compared to the total community structure of the sample determined by the small subunit rDNA approach. Such combined approaches have been shown to be successful in retrieving numerically abundant bacteria from anoxic rice paddy soil [31] or oil reservoirs [32].

Other cultivation strategies which were followed were the enrichment of picoplankton bacteria under a wide range of nutrient and incubation conditions [33], and isolation of biofilm bacteria that had grown in situ on artificial surfaces.

2.2 Phylogenetic Screening of Marine Bacteria

Classification of isolates into the main taxa is usually performed using ribosomal probes, either by dot blot hybridization of extracted DNA or by whole cell hybridization using fluorescent probes [34]. However, since we processed a large number of isolates (approx. 900 strains), a polymerase chain reaction (PCR) approach based on crude DNA extracts of individual colonies was a faster and more versatile method. A so-called signature PCR was developed, which is based on amplification of 16S rDNA fragments of taxon-specific lengths using a mix of 16S rDNA targeted primers (Fig. 4) [33]. While hybridization with ribosomal probes requires several hybridization steps with a suite of probes, the signature PCR approach used here allows the diagnosis of the phylogenetic affiliation of a strain with one PCR reaction, since multiple primers are used simultaneously. If the result is ambiguous, it can be clarified using a second PCR reaction with a second set of primers. Moreover, the level of resolution of the signature PCR can be tailored to the phylogenetic groups under investigation, e.g., by including specific primers for uncultivated marine clones or groups of ecological interest (*Verrucomicrobia*, *Planktomycetes*, phototrophic α-*Proteobacteria*).

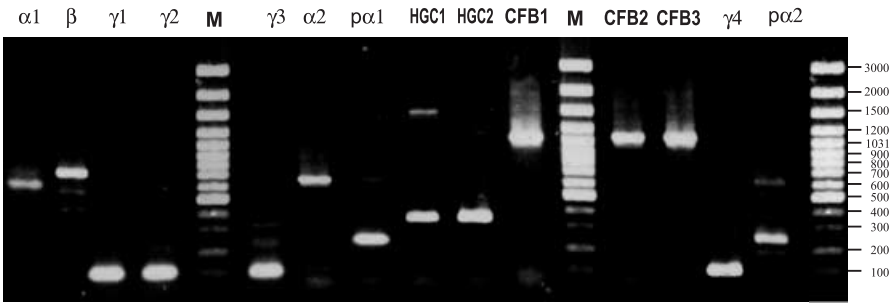

Fig. 4. Phylogenetic fingerprints of reference organisms obtained by signature PCR (SIG-PCR). An oligo primer mixture of nine taxon-specific 16S rDNA targeted primers yielded PCR products with taxon-specific lengths. α1 *Sphingomonas* sp. Hel9, α2 *Sphingomonas* sp. Hel42, pα1 *Erythrobacter* sp. Hel2, pα2 *Sulfitobacter* sp. Hel77, β *Burkholderia* sp. Hel3, γ1 *Halomonas aquamarina* Hel4, γ2 *Pseudoalteromonas carrageenovora* Hel5, γ3 *Pseudomonas sp*. Hel7, γ4 *Vibrio sp*. Hel11, CFB1 *Cytophaga hutchinsonii* (DSM 1761), CFB2 *Weeksella virosa* (LMG 8349), CFB3 *Cytophaga* sp. Hel21, HGC1 coryneform strain Hel1, HGC2 coryneform strain Hel12. The approx. lengths of the expected PCR products are as follows: 650 bp for α-Proteobacteria, 700 bp for β-Proteobacteria, 100 bp for γ-Proteobacteria, 1000 for CFB, 350 for high GC Gram-positives

2.3 Screening of Genetic Diversity – Genomic Fingerprints

Production of secondary metabolites is usually a strain-specific trait. Thus, typing of the isolated bacteria with a high resolution is necessary to assess the genetic diversity of the strains within a given phylogenetic group. The resolution limit of rRNA-targeted methods is not high enough for this purpose, since strains of the same species have the same 16S rRNA sequence. Even different species may sometimes have nearly identical 16S rDNA sequences. Using the variability in length and sequence in the region between the 16S and 23S rRNA operon, the so-called interspacer region polymorphism is a possibility, since this is a very stable but species- to strain-specific trait. However, an even higher resolution is obtained by genomic fingerprint methods. Here, we used a RAPD (random amplified polymorphic DNA) technique with arbitrary primers.

Figure 5 presents genomic fingerprints of 36 α-*Proteobacteria* isolates that had been enriched from a North Sea picoplankton sample. Only four of the bands (lanes 11 and 12, lanes 33 and 34) showed identical patterns. Thus, there were 32 different α-*Proteobacteria* strains present. The data show that a large diversity of bacteria can be enriched from a North Sea picoplankton sample, using a range of incubation and nutrient amendment conditions. The large diversity of the cultivated picoplankton isolates screened may be expected to house numerous phylogenetically and physiologically interesting microorganisms for future investigations [33].

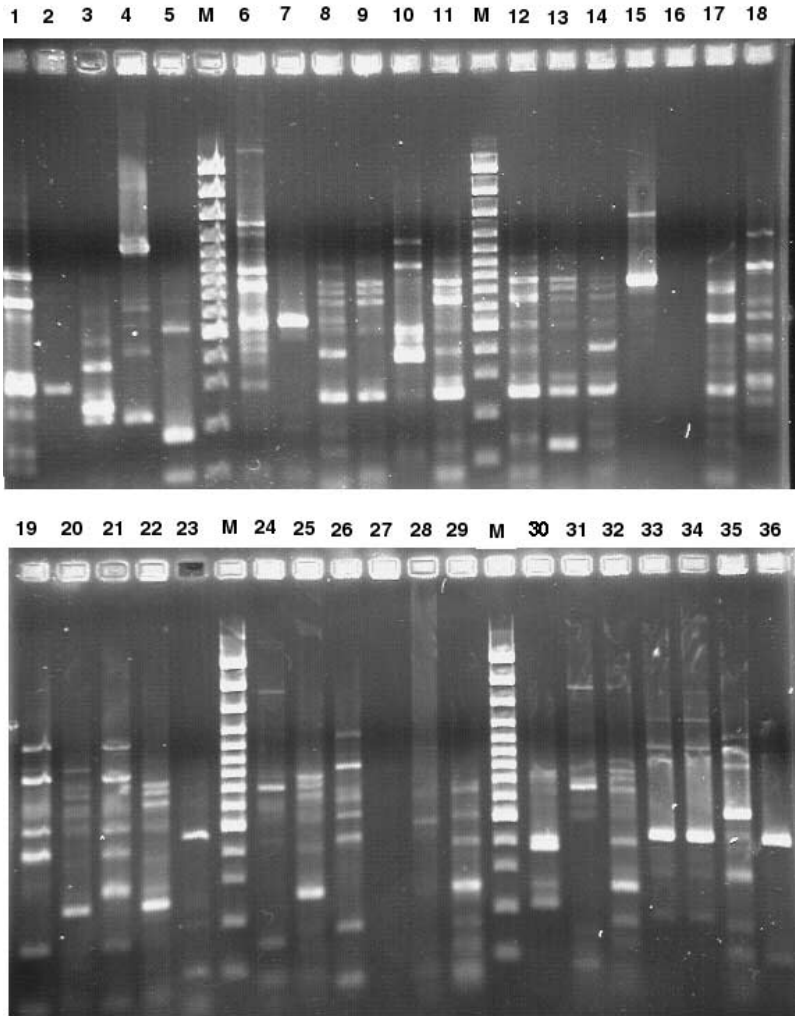

Fig. 5. Genetic diversity of marine picoplankton bacteria from the α-subclass of the Proteobacteria. Determination by random amplified polymorphic DNA (RAPD) fingerprinting of colonies from marine Cytophaga medium (lanes 2–32) and from Hg medium (lanes 33–35). Identical strains are present in lanes 33 and 34 and in lanes 11 and 12, while all other lanes represent different isolates

2.4 The Marine *Roseobacter* Clade of the *Proteobacteria*

One of the largest collections of published environmental small subunit rRNA gene clones from any source is that from marine prokaryotic plankton [20]. This dataset currently includes more than 600 identified bacterial clones. A comprehensive analysis of these sequences has shown that identical sequences falling into similar clades are recovered from geographically and ecologically

diverse regions of the oceans and thus represent global constituents of marine bacterioplankton communities. *Proteobacteria* from the α-subclass represent the largest group of bacterial clone types recovered from marine bacterioplankton and fall into three clusters:

1. The SAR116 cluster, whose cultivated members belong to the α1-subclass of the *Proteobacteria* but have a similarity of less than 90%.
2. The SAR11 cluster with no cultivated counterparts.
3. The *Roseobacter* clade in the α3-subclass of the *Proteobacteria*.

While cultivated microorganisms are not known for any of the two other clades, and indeed for none of the other marine bacterioplankton clades (with some notable exceptions, e.g., the detection of clones of *Pseudomonas putida*), the *Roseobacter* clade is the exception to the rule. Cloned sequences and cultivated organisms form a mixed phylogenetic assemblage and are closely related. Cloned *Roseobacter* sequences have been recovered from the oligotrophic Sargasso Sea, the Eastern Atlantic coast of the USA, the highly productive Oregon coast, and in shallow, enclosed lagoons off the Atlantic and Mediterranean coasts of France. Thus, the *Roseobacter* clade contains globally distributed members of bacterioplankton communities both in the oligotrophic open ocean and in marine coastal environments.

Cultivated members of the *Roseobacter* clade are almost exclusively found in marine or hypersaline habitats and have an absolute requirement for sodium chloride for growth. Their physiological characteristics are diverse. Two genera, *Erythrobacter* and *Roseobacter*, belong to the obligate aerobic phototrophic bacteria which possess bacteriochlorophyll *a* [35] and are capable of aerobic photosynthesis. However, bacteriochlorophyll synthesis only occurs in the dark and is completely inhibited even by low light intensities. Thus, photoautotrophic growth is not possible for these bacteria, only a transient enhancement of growth.

Representatives of the *Roseobacter* clade use thiosulfate as an electron donor, but are unable to grow autotrophically. By contrast, they are chemolitoheterotrophs, i.e., heterotrophic growth is enhanced by reduction of thiosulfate. Some strains can grow on diverse aromatic carbon sources [36] including lignin [37]. *Roseobacter* strains are also able to grow on dimethyl sulfopropionate (DMSP) [38, 39] that is produced by algal blooms at certain seasons in the Atlantic ocean. Consequently, *Roseobacter* strains comprised >20% of the 16S rDNA sampled during the bloom. Recently, *Roseovarius tolerans* was described [40], a budding bacterium isolated from a hypersaline lake in Antarctica. The production of bacteriochlorophyll *a* was apparently genetically remarkably variable in these isolates. A bacteriochlorophyll *a* producing new isolate was even obtained from a deep-sea hydrothermal vent [41]. Other members of the *Roseobacter* clade are entirely non-photosynthetic, e.g., *Sulfitobacter pontiacus* [42–44], *Marinosulfonomonas methylotropha* [45], *Antarctobacter heliothermus* [46], *Octadecabacter* [47], *Sagittula* [37], and *Ruegeria atlantica* [48].

A striking feature of the *Roseobacter* clade is that many isolates are symbionts of marine organisms, e.g., algae, diatoms, dinoflagellates, or have been obtained from surfaces of marine macrophytes. For example, gall inhabitants of

the marine algae *Prionis lanceolata* were closely related to *Roseobacter* [49]. Organisms belonging to the *Roseobacter* subgroup are ubiquitous and rapid colonizers of surfaces in coastal environments [50], and have been found in the accessory nidamental glands of *Sepia officinalis* [51], on the scallop *Pecten maximus* [52, 53], and on the seagrass *Halophila stipulacea* [54]. The dinoflagellate *Prorocentrum lima* is known to produce diarrhetic shellfish poisons. However, it is not yet clear if the dinoflagellates themselves or the *Roseobacter* strains associated with them produce the toxins [55, 56].

The *Roseobacter* clade thus comprises an ecologically interesting phylogenetic group of marine microorganisms that are distributed globally in coastal and open ocean marine bacterioplankton as judged from culture independent analyses. Cultivated isolates and bacteria known from environmental rDNA sequences form a mixed clade with high similarities between both. The *Roseobacter* clade thus forms the exception to the rule, being both abundant in the environment and readily cultivable. The isolates studied to date exhibit several physiological features which can be interpreted as adaptations to the marine environment, e.g., an absolute requirement for sodium chloride and the presence of an oxygenic photosynthesis apparatus, whose occurrence is however variable and which yields only additional energy. *Roseobacter* clade bacteria are able to use a wide spectrum of carbon sources, including aromatic compounds. Additional energy is gained by using oxidized sulfur compounds as electron acceptors, which are important components of the marine sulfur cycle

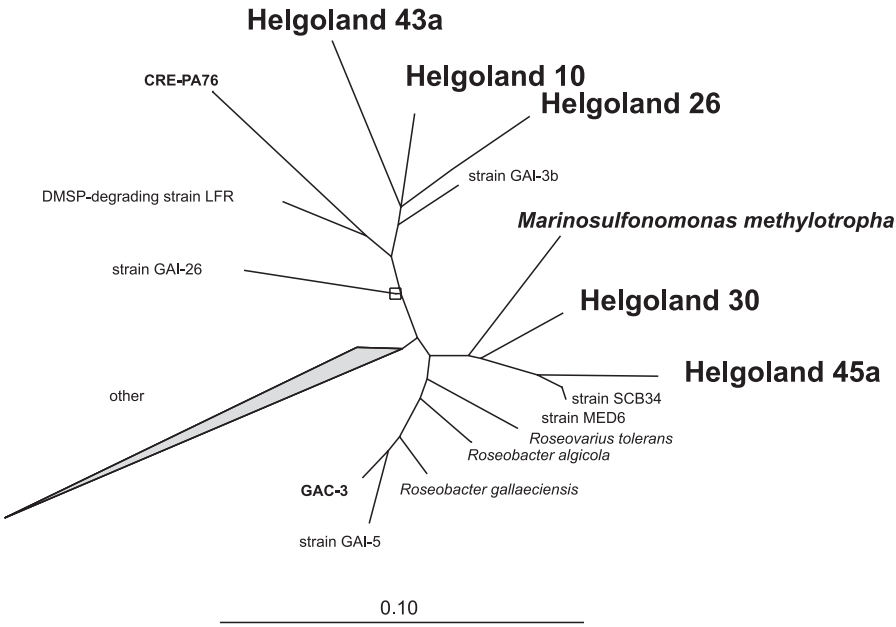

Fig. 6. Phylogenetic tree of the *Roseobacter* clade and the new strains Hel10, Hel26, Hel43 and Hel45

and in some cases coupled to algal blooms. Symbiotic relationships with marine organisms are frequently observed and may point to specific chemical defense mechanisms of these bacteria.

When screening 75 isolates from a water sample taken at a depth of 10 m about 2 km off the coast of Helgoland for phototrophic α3-subclass *Proteobacteria* (the *Roseobacter* clade) using the signature PCR approach, approx. 10 strains were found. From approx. 400 picoplankton isolates, 78 phototrophic α-Proteobacteria (*Roseobacter* clade), and in biofilms, 20 have been found. Several of those were characterized in depth and belong to new species and a new genus (Fig. 6). Descriptions of these new organisms are presently underway. The *Roseobacter* clade will also be investigated for its ability to produce bioactive compounds, since these organisms are phylogenetically unique, clearly marine, readily colonize surfaces and have co-evolved with marine invertebrates in close symbiotic relationships.

3
Screening for Novel Products and New Capabilities

A search for bioactive compounds in nature is a multistep procedure which begins with the selection of suitable sources. Biological, chemical or physical interactions of metabolites with test systems are then qualitatively or quantitatively evaluated [57]: This is the so-called screening which results in arrays of "interesting" or "less-interesting" cultures in the case of microorganisms. Whereas industrial high-throughput systems (100,000 samples and more per year) mostly use highly selective target-oriented test systems, screening systems with lower selectivity are advisable for the manual primary screening: This is dictated mainly by the low hit rate of industrial test systems which is close to 1:10,000 and requires high sample numbers. It is obvious that with capacities of less than 1000 strains per year at universities the success rate would be disappointingly low.

For a first orientation, crude extracts are investigated using the agar diffusion or serial dilution test to evaluate antibacterial, antifungal or – using microalgae – phytotoxic activity. Brine shrimp toxicity has a strong correlation with cytotoxicity and is therefore a good indicator for potential anticancer activity. Strongly positive hits have to be screened further in detail using cancer cell lines or target-oriented systems.

Thirty percent of 500 marine *Streptomyces* strains showed interesting properties in some respect. From 100 selected strains more than 50 new compounds were isolated in a previous project. Their structural diversity, however, was similar to that from terrestrial sources.

In parallel to the biological screening, a search for chemical and physical properties is widely used: This so-called *chemical* screening takes into account that only an unknown fraction of the total metabolite spectrum shows bioactivity in a given test system, but other potential drugs do not respond.

A mass-spectrometric screening for molecular ions using electrospray ionization techniques or matrix-assisted laser desorption/ionization time-of-

flight (MALDI-TOF) needs only microgram amounts and has been used successfully even with intact bacteria from slant agar cultures [58]. However, if a whole array of tests is to be served, much higher amounts of extracts are needed: Experience shows that in most cases bacteria produce secondary metabolites with yields of only 1 mg per liter of culture broth or less.

In chemical screening in its simplest version, extracts are evaluated by thin layer chromatography (TLC) using chloroform/methanol for development, and unspecific spray reagents like anisaldehyde, Ehrlich's reagent, or iodine vapor for detection. Combinations of high-performance liquid chromatography (HPLC) and ultraviolet (UV), nuclear magnetic resonance (NMR) or mass spectroscopy have a much higher resolution and may allow the dereplication of known compounds or even structure determinations. HPLC/UV or HPLC/MS combinations are widespread and are powerful tools in combination with databases.

Chemical and biological screening complement each other very well: The sensitivity of biological methods is much higher than that of chemical analyses and can detect even trace amounts, whereas the chemical screening targets new structures even if they are not obviously bioactive.

4 Strategies for Identifying Anticancer Compounds

During the past five decades of research in anticancer drug discovery about 100 products have been provided for the clinical treatment of malignancy. Important progress has been made in the chemotherapeutic management of hematologic malignancies. On the other hand, more than 50% of patients with tissue tumors either fail to respond or will relapse from the initial response and die from their metastatic disease. In particular, the status of the p53 gene that is mutated in a high percentage of human cancers (particularly lung, breast, colorectal, prostate, gastric and brain tumors) is an important determinant of the efficacy of chemotherapeutic agents [59]. In response to chemotherapeutic agents p53 protein levels rise and produce cell-cycle arrest and apoptosis [60]. Thus, the absence of p53 expression leads to an increase in cellular resistance to these agents. Other mechanisms of drug resistance include enhanced drug metabolism, altered drug accumulation, mutation of topoisomerase 2 and the presence of P-glycoprotein. Hence, the discovery of new cancer therapeutic agents remains critically important.

Marine organisms represent a largely unexplored source of unique toxic chemicals. These toxins are produced by the organisms as defense weapons against their predators. Several potent compounds demonstrating antitumor activity in vitro and in vivo have been isolated from marine organisms, e.g., the bryostatins (from *Bugula neritina*), dolastin 10 (from *Dolabella auricularia*) and halichondrine B (from *Halichondria okadai*) [61].

4.1
Anticancer Drug Development

The steps in the development of anticancer drugs from (marine) organisms are schematically shown in Fig. 7. The most important step in the selection process is initial mass screening. The screening methods can either be simple, such as tumor cell line or enzymatic (e.g., topoisomerase inhibition, microtubule assembly/dissassembly) tests, or more complex, such as an animal tumor in vivo.

4.1.1
In Vitro Tests

Current efforts favor tumor cell line tests, conducted by the National Cancer Institute (NCI) drug development program [62]. In the current NCI anticancer screen, each compound is tested against 60 human tumor cell lines derived from several cancer types (lung, colon, melanoma, kidney, breast, ovary, brain, leukemia). The tumor cells are seeded on 96-well microtiter plates and pre-incubated for 24 h. The test agents are then added to the wells (five 10-fold dilutions; 0.01 – 100 μmol/l) and are incubated for 48 h with the tumor cell lines. At the termination of the assay, the cells are fixed in situ with trichloroacetic acid (TCA), washed and dried. Sulforhodamine B (SRB), a dye that binds to the basic amino

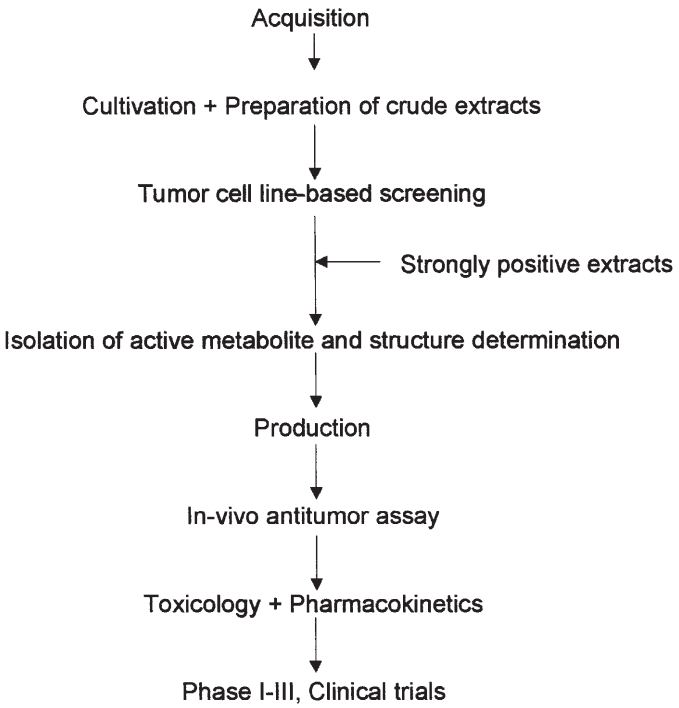

Fig. 7. Steps in cancer drug development from marine organisms

acids, is added. The cells are washed again and the remaining dye which is a function of the remaining adherent cell mass is solubilized and measured spectrophotometrically [63]. From these data the response parameters GI50 (drug concentration causing 50% growth inhibition), TGI (drug concentration causing 100% growth inhibition) and LC_{50} (drug concentration causing 50% reduction of the cell mass present before adding the test agents) are calculated. The individual response of each cell line to the test agent is then compared with a computer program (COMPARE) using a simple algorithm for aligning and contrasting the pattern of the test compound with those of known anticancer drugs. A similar pattern of cellular responsiveness implies a common intracellular target or mechanism of action. Active compounds are then selected for further testing for the following criteria: (i) potency, (ii) cell-type specificity, (iii) unique structure, and (iv) unique mechanism of action. An agent selected for further studies is then subjected to pharmacological studies in animals (pharmacodynamics, pharmacokinetics, toxicology).

4.1.2
In Vivo Antitumor Tests

Compounds selected from the cell line screen are tested in nude mice bearing the tumor cell line which is most sensitive in the in vitro screen. The tumor cell line is introduced subcutaneously or intraperitoneally in a minimal-stage xenograft model for initial testing. The test compound is administered continuously by osmotic mini-pumps or repeated intravenous injection and is initiated on the day of tumor injection. Agents that show significant tumor growth inhibition are then selected for further in vivo evaluation against more advanced stage tumors. Failure of in vivo efficacy for an agent should prompt additional studies to determine whether there is a pharmacokinetic explanation for loss of activity.

4.1.3
Preclinical Pharmacokinetics

Pharmacokinetic studies (absorption, bioavailability, distribution and excretion) in different animal species (e.g., mice, rat and dog) are of fundamental importance for the interpretation of animal pharmacology and toxicology data and the extrapolation of these data to humans. One goal of phase I clinical trials is to determine the maximally tolerated dose (MTD) of a new cytotoxic drug. The dose-limiting toxicity is a function of drug exposure, as measured by the area under the drug concentration versus time curve (AUC). Therefore, animals and humans are predicted to experience toxicity when the AUC of the drug is quite similar. With this assumption a simple method for escalating the dose in phase I clinical trials can be used. The steps are: (i) determine the LD_{10} in the mouse and the AUC of the drug at LD_{10}; (ii) start human testing with one-tenth of the mouse-equivalent LD_{10} dose and determine the AUC of the drug; (iii) compare the AUC at the starting dose with the target AUC (the AUC in mouse at LD_{10}) and increase the dose based on this ratio [64].

4.1.4
Preclinical Toxicology

The vast majority of anticancer drugs are cytotoxic compounds which have significant side-effects and a very small therapeutic index. The objective of preclinical toxicologic studies is to find a safe initial dose for clinical phase I studies and to define the qualitative and quantitative organ toxicities. The current toxicological investigations involve a two-step procedure. First, the acute toxicity in mice and rat is determined. The endpoint is the determination of the LD_{10} value, the dose that causes lethality in approximately 10% of the animals. The major objective of the subsequent second phase is to give qualitative and quantitative characterization of the organ-specific toxicities which can be observed at doses slightly higher than the highest nontoxic dose in acute toxicity. At best, these evaluations can establish data for a safe starting dose for human trials and predict organ toxicity.

4.2
The Screening of Extracts from North Sea Microorganisms

Several groups in the Marine Biotechnology Network of Lower Saxony are studying the cultivation of novel organisms isolated from the North Sea. Crude extracts of these organisms are used to determine antibacterial, antifungal, phytotoxic and cytotoxic activity. In our screening for cytotoxic activity we use routinely three tumor cell lines (HM02 cells derived from human gastric adenocarcinoma; HepG2 cells derived from a human hepatoblastoma; and MCF7 cells derived from human breast carcinoma). In addition we test the extracts in Huh 7 cells (hepatocellular carcinoma), a cell line which expresses p53 with increased half-life as a result of a point mutation at codon 220 [65]. This cell line is insensitive to vinblastine (Fig. 8) and other anticancer drugs such as cisplatin and methotrexate [66], and therefore provides the potential to identify new agents with specific activity against p53-negative tumor cell populations.

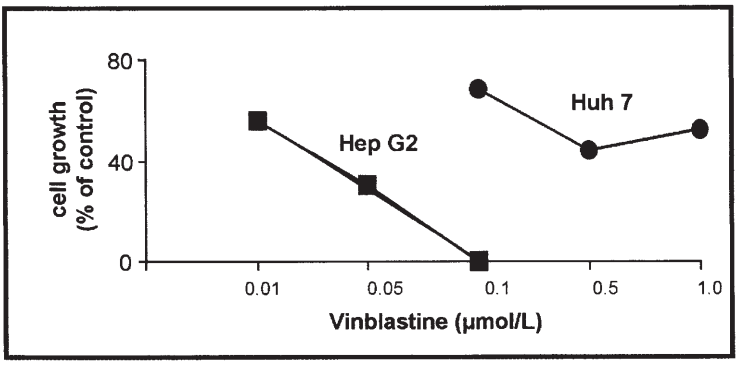

Fig. 8. Effect of vinblastine in hepatoma cells carrying wild-type p53 (HepG2) or in hepatoma cells with mutated p53 (Huh 7). Cells were incubated for 48 h with indicated concentrations of vinblastine

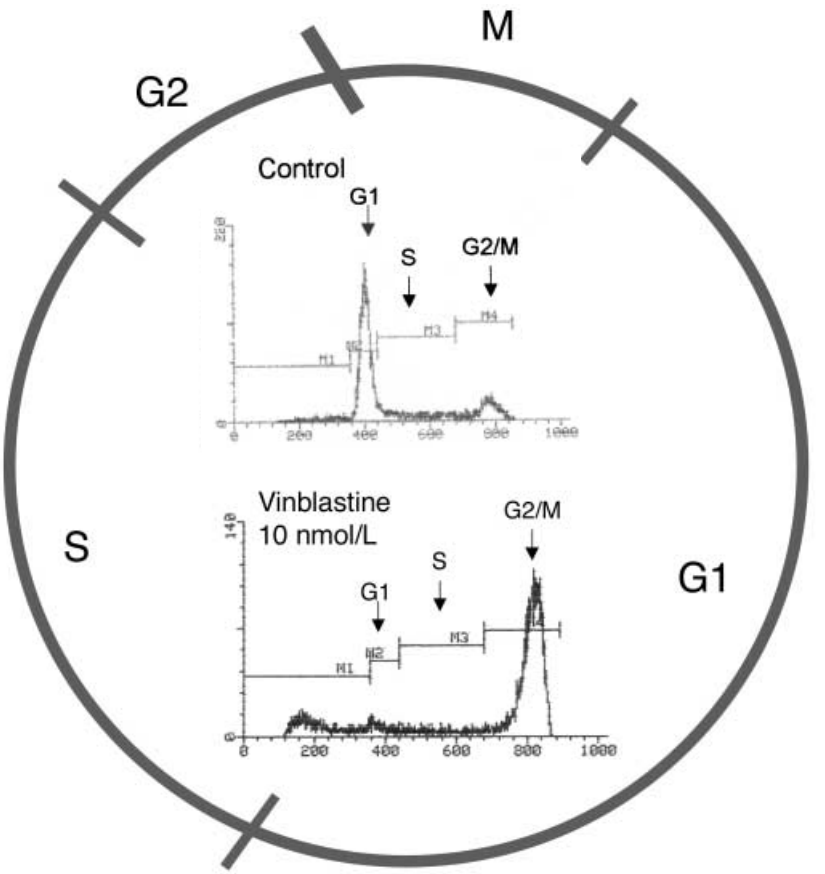

Fig. 9. The cell cycle. *M* mitosis; *G1+S+G2* interphase, i.e., the period between cell division. During G1 (G for gap) the cellular genome is in the diploid state. This is followed by the S-phase (S for synthesis) during which the DNA is replicated, and finally G2. *Insert* Cell-cycle analysis of HM02 cells cultured with and without vinblastine. Cell-cycle distribution was determined by staining DNA with propidium iodide, and the number of cells in different phases of the cell cycle was measured with a FACStar flow cytometer. Vinblastine, which disrupts the formation of microtubules, causes cell-cycle arrest in the G2/M-phase

We have examined approximately 1000 extracts over the past two years. Fifteen extracts (e.g., from the bacteria Hel3, Hel25, Hel37, Hel38 and strain Hel115aa) were highly active with GI50 values < 1 µg/ml. To obtain information on the mechanism of action, highly active compounds (and extracts) are subjected to cell-cycle analysis. Continuously dividing tumor cells go from one mitosis (M) to the next, passing through G1-, S- (DNA synthesis phase) and G2-phases. Phase-specific anticancer drugs alter the cell cycle in a specific manner. Vinblastine, which disrupts the formation of microtubles, causes cell arrest in the G2/M-phase (Fig. 9). The antimetabolite 5-fluorouracil (5-FU), which alters RNA processing, inhibits DNA elongation and alters DNA stability, causes cell cycle arrest in the S-phase and induces apoptosis.

Thus, cell-cycle analysis can be used as a first indicator to identify the mechanism of action of a new compound (or extract). Using this strategy we were able to define rapidly the intracellular targets of ratjadone. This compound was isolated in 1994 by Höfle et al. from *Sorangium cellulosum* collected as a soil sample at Cala Ratjada (Mallorca, Spain) [67]. In an initial biological evaluation it was found that ratjadone exhibits high cytotoxicity in the mouse cell line L929 and the HeLa cell line KB 3.1 [67]. In our cell lines ratjadone inhibited cell growth with GI50-values ranging from 0.38 (HM02 cells) to 1.1 ng/ml (MCF7 cells). In contrast, Huh 7 cells were remarkably insensitive to ratjadone. Cell-cycle analysis revealed prominent G1 arrest, which was accompanied by a dramatic decrease in the S-phase. The G1 arrest was associated with elevation of p21 protein. This protein is an inhibitor of the cyclin E/cyclin dependent kinase 2 complex, involved in the control of the G1/S transit in eukaryotes. These results suggest that ratjadone inhibits tumor cell growth via G1 arrest in association with p21 induction.

5
Biotechnological Studies To Overproduce Metabolites by Marine Microorganisms

5.1
Overview of Biochemical Engineering Approaches

To date, the technical approaches used to cultivate marine bacteria and fungi have reached different standards. For example, marine barophiles or hyperthermophiles require high pressure (40–80 MPa) or high temperatures (70–110°C), raising a number of engineering challenges for bioreactor operation. These include vessels/equipment that are resistant to extreme conditions, maintenance of high temperature and reduction of evaporative loss of liquid media containing high salt concentrations. For instance, in the case of hyperthermophiles, several bioreactor configurations, such as gas lift bubble columns, continuously stirred tank reactors, three-phase fluidized beds and an oscillary-baffled reactor, have been tested [68–70]. Products of interest from the above microorganisms are thermostable enzymes. To date, the most familiar commercial application for such an enzyme is the use of Taq DNA polymerase, from *Thermus aquaticus* (not a marine microorganism), in the polymerase chain reaction. Fortunately, these "thermozymes" can now be produced by recombinant DNA technology.

As for the cultivation of other types of marine microorganisms, e.g., those with a specific potential for the production of biologically active metabolites, predominantly small-scale experiments (shake flasks) have been described. Alternatively, artificial seawater or 25:50:75:90% natural seawater has served as a basis for nutrient media. The concentrations of carbon and nitrogen sources reached up to 2% (w/w): starch, glucose, molasses, glycerol, soybean oil, yeast extract, malt extract, beef extract, peptone, cornsteep liquor and NZ-amine. In the absence of artificial or natural seawater, high concentrations of

$Na^+/Mg^{2+}/Cl^-$ ions were used instead. Temperatures in the range 20–28 °C and a pH value of 7.5 were favored. Jensen and Fenical [71] recommended replacing the above traditional nutrient components by natural C and N sources, polysaccharides and proteins from marine eukaryotic systems.

Compared to the number of publications on the structural analyses of marine microbial metabolites, those on quantitative biochemical engineering studies are negligible in the literature. There are only the following exceptions: The time courses of pH, biomass and bioactive product concentration were reported for three different *Micromonospora* species, isolated from a soft coral, a sponge and from seawater, respectively. Using 250-ml cultures in Erlenmeyer flasks, thiocoraline (depsipeptide), the macrolide IB-96212 and the tetrocarcin antibiotics arisostatins A and B were produced [72–77]. Both the depsipeptide and the macrolide were extracted (organic solvent) from the biomass; the tetrocarcin antibiotics were extracted from the supernatant. For cultivation on a larger scale and under more controlled conditions in bioreactors, the parameters of interest are summarized in Table 1. In most cases, for primary separation of all products, an extraction with organic solvents, such as chloroform/methanol or ethyl acetate, was the method of choice. Using this method, bioxalomycin and exophilin were isolated from the supernatant, agrochelin and the glucosylmannosyl glycerolipid from the cells and the lipodepsipeptides/po-

Table 1. Literature data on bioreactor cultivations of marine bacteria and fungi with respect to some important bioprocess conditions and metabolites

Strain; cultivation conditions	Product	Yield (mg/l)	Ref(s)
Streptomyces sp. (from sediment sample); 300 l, tap water, glucose, 28 °C, 200 rpm, 0.67 v/vm, 50 h	Bioxalomycins	10[a]	[78]
Exophiala pisciphila (from *Mycale adherens*); 15 l, potato/glucose, pH 7[b], 25 °C, 0 rpm, 0.67 v/vm, 10 d	Exophilin A	2	[79]
Hypoxylon oceanicum (from mangrove wood); 300 l, glycerol/soy peptone, pH 7[b], 22/28 °C, 250 rpm, 1 v/vm, 6–8 d	Lipodepsipeptide Polylactones	400 50	[80–82]
Agrobacterium sp. (from *Ecteinascidia turbinata*); 50 l, instant ocean salts, glucose, pH 7.2[b], 28 °C, 350 rpm, 0.67 v/vm, 30 h	Agrochelin	5	[83]
Microbacterium sp. (from *Halichondria panicea*); 40 l, artificial seawater salts, glucose, pH 7.5, 30 °C, 800 rpm, 0.4 v/vm, 27 h	Glucosylmannosyl glycerolipid	200	[84]

[a] Relative units.
[b] Initial value.

lylactones from the whole broth. When the bacteria do not form pellets or mycelia, we have applied successfully the solvent-free floating bed extraction technique using adsorber resins.

Some recent results on marine biochemical engineering were presented at the International Marine Biotechnology Conference (IMBC) 2000 in Townsville, Australia (29.09.–04.10.2000) dealing with the cultivation of microalgae and the development of photobioreactors [85, 86]. Low concentrations of biomass and metabolites are regarded as a bottle-neck in the elucidation of structures in marine microbial biotechnology, which can, however, be regarded as minor problems compared with the major problem of the marine microorganisms that have so far proved elusive in terms of cultivation [87].

5.2 Cultivation of North Sea Bacteria

In the North Sea project, the results from primary screening for biological activity or new compounds guide the selection of strains for upscaling and finally isolation and structural elucidation. Since even modern methods for structure determination and an initial biomedical evaluation require 10 mg of every compound or more, a scale-up fermentation is necessary. With the aid of biotechnical methods, fermentation conditions have to be optimized to achieve maximum yield of metabolites, to increase the genetic stability of the producer or to improve other parameters.

After reproduction of 100-ml flask experiments under the aspects of growth and metabolite spectra (TLC), from the end of 1999 the cultivation experiments were transferred to a 50-l scale in glass or stainless steel bioreactors. Preliminary results on nutrient components (mainly 10 g/l tryptone and 5 g/l yeast extract in 50% artificial seawater), pH (7–7.5) and temperature (30°C) were strictly considered. The bioreactor design, aeration and agitation were chosen depending on the individual strain requirement: 200–300 rpm, 0.1–0.3 v/vm. The higher aeration rates recommended in the literature (Table 1) have proved unnecessary until now. Additionally pO_2, qO_2 and qCO_2 were determined/calculated on-line, whereas optical density or biomass and natural products concentration (crude organic extract) were determined off-line. For downstream processing, cells and supernatant were separated by centrifugation (16,000 rpm) and extracted separately with ethyl acetate/acetone (cells, after freeze-drying) or ethyl acetate (supernatant). To date, many fermentations of new bacteria with a high potential to produce bioactive metabolites have been carried out. Depending on the strain the cultivation time has been in the range 24–72 h. The yield of crude organic material reached 150 mg/l at maximum. These experiments provided material for high-performance chromatography and subsequent structural elucidation and studies on bioactivity.

For strain Hel45 (*Roseobacter* sp.), some of the details regarding a 40-l cultivation, using a Rushton disc turbine for agitation, are presented in Fig. 10. Following the steps of the primary downstream processing, in total 70 mg/l of crude products were isolated from the cells and the supernatant [88]. More recently, by varying the carbon and nitrogen sources, the pattern of TLC spots

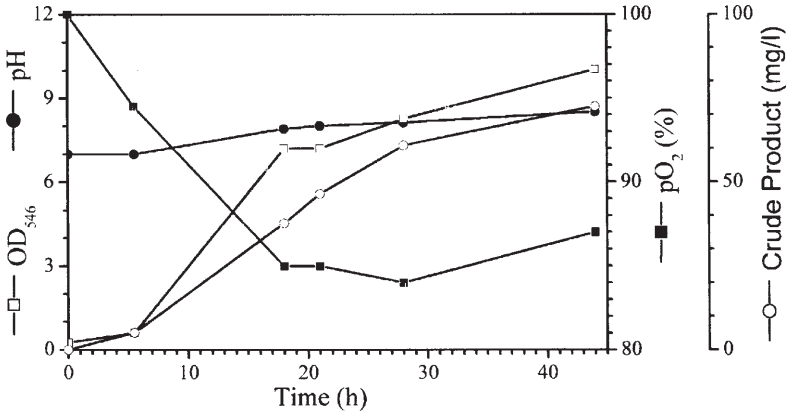

Fig. 10. Growth and metabolite production of the marine strain Hel45. OD_{546} Optical density at 546 nm; pO_2 oxygen partial pressure

showed another composition and additionally new TLC spots were visible. The constituent of one of them was identified as indole-3-carboxylic acid thiomethyl ester (**23**), a compound that has not been described as a natural product previously.

Except for providing chemists and pharmacists with material, further tasks of the biotechnology groups are as follows: (1) The product-oriented improvement of basic microbial cultivation, including the variation of nutrients (genetic algorithms), the quantitative estimation of single metabolites (HPLC) and the precursor-directed biosynthesis, (2) studies on the induction of special pathways for secondary metabolites, (3) studies on the mode of fermentation (batch, fed-batch, continuous culture), the aeration and agitation rates, as well as (4) the biocatalytical modification of naturally produced metabolites.

Because degraded components of dead organic matter are widely distributed in the sea, marine microorganisms mostly live in an environment of highly diluted nutrients. Following this observation, a minimal supply may be more important for marine microorganisms than for their terrestrial counterparts. A minimal medium was defined based on artificial seawater containing glucose as carbon and energy source, ammonia as nitrogen source, phosphate and trace elements. First results with a number of marine bacteria indicated that the addition of selected amino acids and vitamins increased their growth rate significantly [89]. For example, the growth of Hel42 is strongly enhanced by addition of vitamin B12 and two amino acids. All other strains tested needed at least two amino acids.

6
Chemical Structures

6.1
Dereplication

The isolation and structural determination of natural products is a time-consuming and expensive process, even using modern methods. It is most important therefore to recognize and exclude known compounds at the earliest possible stage, a process which is called *dereplication*.

For this task, easily accessible properties of mixtures or pure metabolites are compared with literature data. This may be the biological activity spectrum against a variety of test organisms. Widely used also is the comparison of UV [90] or MS data and HPLC retention times with appropriate reference data collections, a method which needs only minimal amounts and affords reliable results. Finally, there are databases where substructures, NMR or UV data and a variety of other molecular descriptors can be searched using computers [91]. The most comprehensive data collection of natural compounds is the Dictionary of Natural Products (DNP) [92], which compiles metabolites from all natural sources, also from plants. More appropriate for dereplication of microbial products, however, is our own data collection (AntiBase [93]) that allows rapid identification using combined structural features and spectroscopic data, tools that are not available in the DNP.

A yellow, strongly blue fluorescent metabolite from a marine streptomycete gave a very unusual proton NMR spectrum with only three heteroatom-bound methyl signals in the region of $\delta = 3.5 - 3.9$; C-Me, CH_2 or CH signals were not visible. A search for compounds with three or more hetero-methyl groups gave 1120 hits (out of 25,000 entries), and, on subtraction of all compounds with C-Me, CH_2 or CH groups, only four entries remained. Two had to be removed because of symmetry reasons. The experimental data matched those of 2-methylfervenulone (**1**), a structure which is difficult to solve on the basis of NMR data alone.

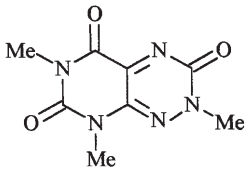

2-Methyl fervenulone (**1**)

In the case of new compounds a database search is also helpful, because novel skeletons are rare and usually related compounds are already known which are easily revealed by a database search, thus identifying at least the compound class.

6.2 Structural Elucidation and Results

The only method for structural elucidation that is also applicable to mixtures is mass spectrometry, mainly when electrospray ionization (ESI) is used and precursor ions are investigated. Not all types of compounds, however, are accessible by this method, and, due to insufficient charge stabilization, compounds like labilomycin are not visible in the ESI spectra of crude extracts. As pure compounds are needed for further biological testing anyway, mixtures have to be separated before analysis.

The purification of bacterial constituents usually starts in a very conventional way with an extraction step of the crude broth at neutral or slightly acidic pH. Mycelium-forming organisms are separated by filtration, and the cell mass and the filtrate are extracted separately. For the liquid phase, adsorber resins allow high recovery rates of metabolites and low process costs due to repeated use of the resins. If liquid-liquid extraction has to be applied, medium or highly polar solvents are favored. Ethyl acetate is the solvent of choice, and only in few cases is butanol superior. To extract the moist cell material, ethyl acetate, acetone or dichloromethane/methanol can be used.

In the crude extracts, triglycerides, long-chain acids, hydrocarbons and some other nonpolar compounds dominate which require different separation techniques. The majority of these compounds are removed from the methanolic solution by cyclohexane extraction. Antibiotic activity is seldom found in the lipophilic phase; however, using modern gas chromatography/mass spectrometry (GC/MS) methods and cellular tests for cytotoxicity, we have found now strong cytotoxicity in some cases and a wide range of unexpected compounds: Whereas isoprenoids are common constituents of fungi [94], it was not known that bacteria also contain a rich variety of low-molecular terpenes, among them calarene (**2**), eudesmole (**3**) and many others [95].

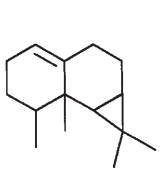

Calarene (**2**)

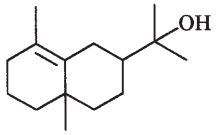

Eudesmole (**3**)

For the final purification, a sequence of normal phase chromatography, size exclusion chromatography, reversed-phase (RP)-HPLC and other techniques are used. There are no general rules as to how to proceed but, due to the high capacity and low irreversible absorption of Sephadex, size exclusion should be used in the very beginning, whilst HPLC is better employed for the final purification steps.

Gram-negative *Pseudomonads* and *Bacilli* from terrestrial sources do not produce many secondary metabolites. This seems to be similar in the sea; however, some of the compounds found there have extraordinary structures. The

antibiotic and cytotoxic pentabromopseudiline (**4**) was the first marine bacterial metabolite to be reported. It was isolated from a bacterium first assigned as *Pseudomonas bromoutilis* (later re-assigned to the genus *Alteromonas*) [96]. Related strains producing the same antibiotic have subsequently been repeatedly isolated from seawater samples.

A closer inspection of *A. luteoviolaceus* by different groups provided a further variety of highly active metabolites, tetrabromopyrrole, hexabromo-2,2′-bipyrrole, tetrabromobiphenol, several simple phenols including 4-hydroxybenzaldehyde and *n*-propyl-4-hydroxybenzoate, violacein (**5**) and related pigments, and the extremely strong siderophore alterobactin [97].

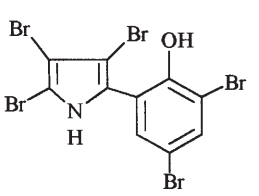

Pentabromopseudiline (**4**)

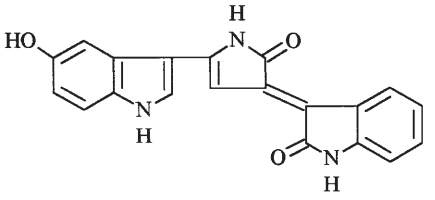

Violacein (**5**)

Other outstanding structures from marine *Alteromonads* are thiomarinol [98] (**6**) and the related holothines, or the bromoalterochromides (**7**) [99]. The latter are yellow chromopeptides due to their polyene chain; however, simple peptides (e.g. the leupeptins) have also been described.

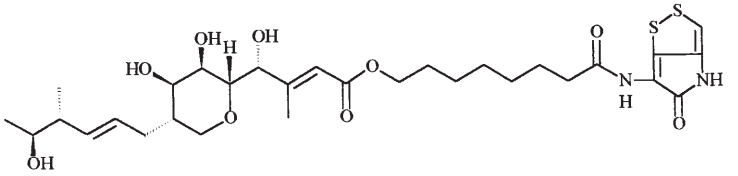

Thiomarinol (**6**)

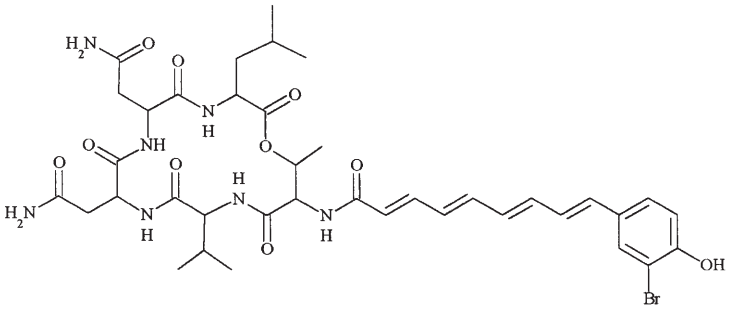

Bromoalterochromide A (**7**)

Diketopiperazines are rather abundant in marine bacteria. In spite of their simple structures, some are reported to have herbicidal [100] (**8**, **9**), chitinase

inhibitory [101] (**10**), phytotoxic and antifungal [102] (**11**) activity. A weak cytotoxicity [103] was reported for cyclo(D-Pro, L-Tyr) (**12**).

From the North Sea strain Bio39 we have isolated the α,β-unsaturated diketopiperazine **13**. The same metabolite has been isolated very recently from a *Penicillium* sp. [104]; however, the NMR data are different. Compounds of this type [105] (**14, 15**) show pronounced antitumor activity; however, compound **13** is inactive. Only restricted information is available for similar structures, as these compounds have not been reported often.

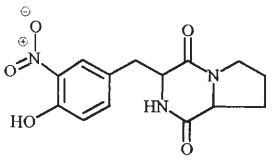

Pyriculamide (**8**)

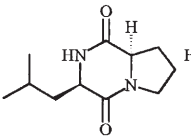

Maculosin 6 (**9**)

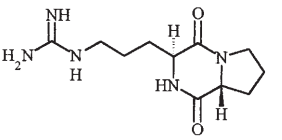

cyclo(L-Arg,D-Pro) (**10**)

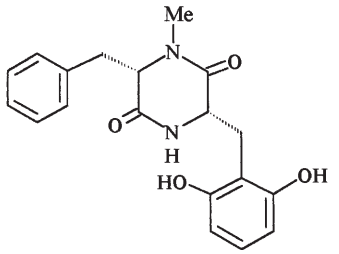

Mactanamide (**11**)

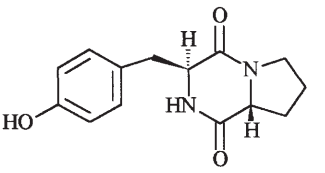

cyclo(D-Pro,L-Tyr) (**12**)

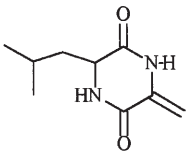

13

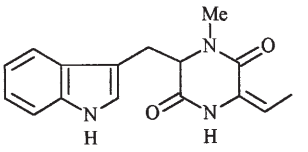

TDD (**14**)

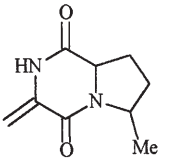

SF-2771 (**15**)

In the case of diketopiperazine **13** and related compounds, dehydrogenation of the preceding diketopiperazine occurs in the side chain. A shift of the double bond into the central ring and dehydration may result in the formation of substituted pyrazines. Simple pyrazines are known as signaling compounds from animals. The pyrazines **16** and **17** have also been isolated from marine Streptomycetes [106]. GC/MS investigations of bacterial flavor components [95] indicate that these and others are very wide-spread.

More complex pyrazines, however, are rare, and again a decreasing oxygen content of the aromatic system seems to indicate an origin from diketopiperazines (**18** [107], **19** [108]). We have now isolated another fully deoxygenated new

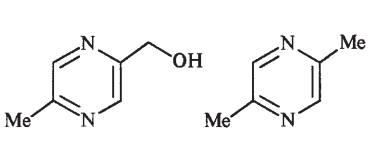

16 17

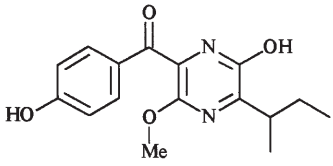

Septorin (**18**)

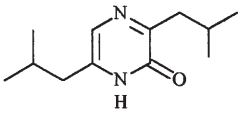

Flavacol (**19**)

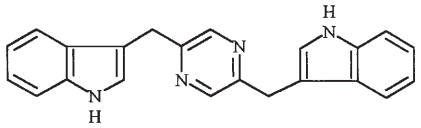

20

pyrazine **20** from a strain AM13,1 which belongs to the Cytophaga/Flexibacteria cluster.

Whereas simple indole derivatives are rare in marine Streptomycetes, they are rather common amongst the North Sea bacteria so far investigated. The extracts of strain Hel 45 that contain the diketopiperazines cyclo(Phe, Pro) and cyclo(Tyr, Pro), however, are dominated by large amounts of unsubstituted indole, the known dimer 3-(3,3′-diindolyl)propane-1,2-diol [109] (**21**) and various other, still unidentified, indole derivatives.

The indole **22** was previously isolated from the sponge *Dysidea etheria* [110] and has now been obtained from the Antarctic ice bacterium ARK 13-2-437. The lipid phase of Hel45 delivered additionally *N*-(2-hydroxyethyl)-11-octadecenamide and the new natural products 17-methyl-16-octadecenoic acid [95] and indole-3-carboxylic acid thiomethyl ester (**23**).

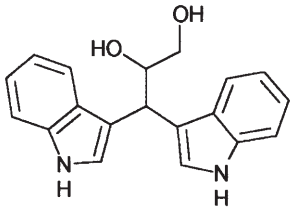

21

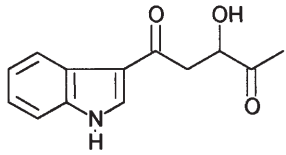

22

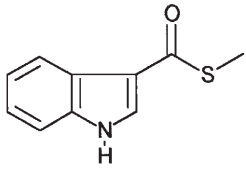

23

AM13,1, a microorganism from the Cytophaga/Flexibaterium cluster, is one of the few 'talented' strains amongst the North sea bacteria so far investigated: In addition to the indole **20**, the culture yielded phenylethyl acetate, indole-3-carboxylic acid, indolyl-3-acetic acid, uracil, anthranilic acid (**24**) and the new compounds *i*-valeryl-β-phenylethylamide (**27**) and N^{β}-*i*-valeryltryptamine (**28**). Very unexpected, however, was the isolation of yellow tryptanthrin (**26**) which is probably responsible for the broad but moderate antibiotic activity. The antifungal and antimicrobial pigment **26** is a biocondensation product of anthranilic acid (**24**) and isatin (**25**) that was isolated originally from the pathogenic yeast *Candida lipolytica*; however, it has also been found in plants [*Couroupita guianensis* (Lecythidaceae), *Isatis indigotica*]; an occurrence in bacteria has not yet been reported.

The yellow color of the AM13,1 colonies is due to their content of compound **26**. In most other cases, yellow cultures owe their color to the carotenoid zeaxanthin (Hel21) or one of the many vitamin K derivatives (e.g., menaquinone MK6 in Hel21).

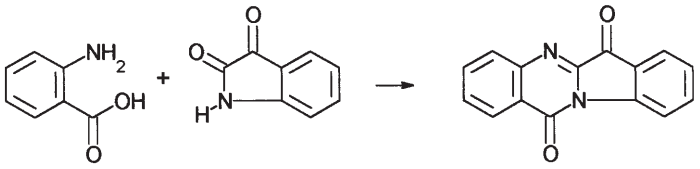

Anthranilic acid (**24**) Isatin (**25**) Tryptanthrin (**26**)

The activity of extracts against microalgae has led to the isolation of a large group of simple phenylethyl amides and various indolylethyl amides (e.g., **27**, **28**). We have obtained some of these compounds also from limnic bacteria, and, although their activity is low, it seems plausible that they play a role in the competition of bacteria with microalgae for free surfaces, perhaps on seaweed or other sessile organisms.

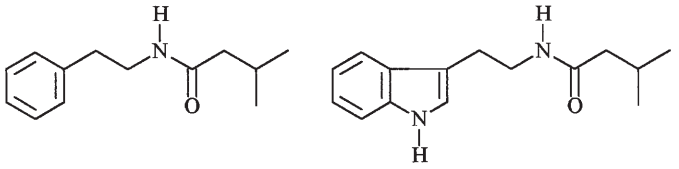

27 **28**

Polyhydroxybutyric acid (PHB) is a bacterial biopolymer which has gained much interest because of its potential use as a biodegradable plastic material. This compound is produced by various terrestrial bacteria and serves as an energy reservoir. PHB is usually highly polymeric (10,000 monomer units) and is stored in the bacteria as an insoluble material in inclusion bodies that are visible with an electron microscope [111]. Although PHB has been inten-

sively investigated, it was not known that also very low oligomers (OHB) occur. We were able now to isolate an OHB mixture **29** with n = 8 – 20 from the marine bacterium *Alteromonas distincta* strain Hel69, and from marine streptomycetes. Whether inclusion bodies are also present in Hel69 has still to be explored.

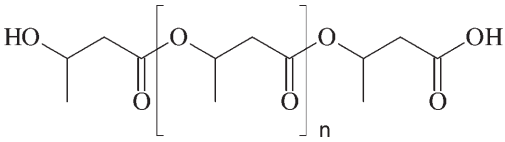

Oligohydroxybutyric acid (OHB; n = 8 – 20) (**29**)

7 Concluding Remarks

Culture-independent investigations of marine communities have provided a wealth of information on the phylogenetic positions and, in some instances, also on enzymes and pathways of uncultivated marine microorganisms. Clone libraries of amplified 16S rDNA fragments from marine habitats are dominated by sequences which have no match in cultivated bacteria. Judging from the extent of sequence differences observed, entirely new subdomains (*Crenarchaeota*), divisions (termed "candidate divisions") and genera, and an almost unlimited amount of species of Bacteria and Archaea, have thus been detected and represent a completely untapped source of new metabolic diversity awaiting successful cultivation attempts [112] and culture-independent characterization using tools of molecular biology [113 – 116].

The search for new chemical metabolites in marine microorganisms is a multistep procedure which starts with the selection of suitable sources and cultivation. Screening of crude extracts of North Sea bacteria using the agar diffusion method and a variety of test organisms has yielded inhibition zones of 15 – 25 mm diameter, whilst highly active strains gave inhibition diameters of up to 50 mm. Tests with brine shrimps and human cell lines in screens for antitumor activity have given surprisingly often positive results on the nanogram scale (Hel3, Hel38, 115a). In addition, high leishmaniacidal or antimalarial activities [117] in the range of a few μg crude extract per ml were found (Hel12, Hel38, GW135a), and it is certainly advisable therefore to extend the number and character of the test models. A p53 negative cell line, e. g., should be included in the initial screening process to provide the potential for identifying new agents with activity against p53-negative tumor cell populations.

Strong biological activities are obviously widespread amongst bacteria from the North Sea (Fig. 11). For the ongoing isolation and structural determination of the active constituents, conventional methods are suitable, but very low yields and genetic instabilities are causing time-consuming technical problems and have dictated long investigation times. We are confident, however, that marine bacteria are rewarding targets, and the strong bioactivities are an encouraging signal.

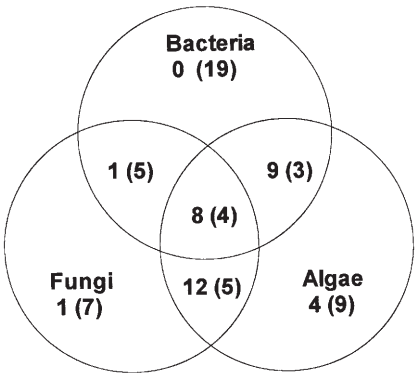

Fig. 11. Activity pattern of extracts from bacteria from the North Sea. Among 188 tested strains, 35 (19%) showed high and 52 (28%) moderate activity (values in *brackets*), 35 (19%) of them with selective and 17 (9%) with multiple activity (values in *overlapping areas*)

Acknowledgement. The authors would like to thank their co-workers for excellent experimental studies and the Government of Lower Saxony (Hanover, Germany) and the VW foundation for generous financial support.

References

1. Page MJ, Amess B, Rohlff C, Stubberfield C, Parekh R (1999) Drug Discovery Today 4:55
2. Searls DB (2000) Drug Discovery Today 5:135
3. Hutchinson CR (1998) Curr Opin Microbiol 1:319
4. Thorpe DS (2000) Comb Chem High Throughput Screening 3:421
5. Strohl WR (2000) Drug Discovery Today 5:39
6. Moore BS (1999) Nat Prod Rep 16:653
7. Pietra F (1997) Nat Prod Rep 14:453
8. Faulkner DJ (2000) Nat Prod Rep 17:1
9. Faulkner DJ (2000) Nat Prod Rep 17:7
10. Faulkner DJ (2000) Antonie Van Leeuwenhoek 77:135
11. Buckland BC, Robinson DK, Chartrain M (2000) Metab Eng 2:42
12. Fenical W (1993) Chem Rev 93:1673
13. Davidson SK, Haygood MG (1999) Biol Bull 196:273
14. Haygood MG, Davidson SK (1997) Appl Environ Microbiol 63:4612
15. Bewley CA, Faulkner DJ (1998) Angew Chem 110:2280
16. Faulkner DJ (1999) Nat Prod Rep 16:155
17. Amann RI, Ludwig W, Schleifer KH (1995) Microbiol Rev 59:143
18. DeLong EF (1997) Trends Biotechnol 15:203
19. Mullins TD, Britschgi TB, Krest RL, Giovannoni SJ (1995) Limnol Oceanogr 40:148
20. Rappe MS, Vergin K, Giovannoni SJ (2000) FEMS Microbiol Ecol 33:219
21. Rappe MS, Gordon DA, Vergin KL, Giovannoni SJ (1999) System Appl Microbiol 22:106
22. Hodgson DA (2000) Adv Microb Physiol 42:47
23. Dawid W (2000) FEMS Microbiol Rev 24:403
24. Reichenbach H (1986) Microbiol Sci 3:268
25. Baslow MH (1971) Ann Rev Pharmacol 11:447
26. Nassar MM (2000) J Egypt Soc Parasitol 30:631
27. Pereira P, Onodera H, Andrinolo D, Franca S, Araujo F, Lagos N, Oshima Y (2000) Toxicon 38:1689

28. van Kraaij C, de Vos WM, Siezen RJ, Kuipers OP (1999) Nat Prod Rep 16:575
29. <url>http://www.gwdg.de/~ucoc/zeeck/hom3.htm</url>
30. Chen G, Wang GY, Li X, Waters B, Davies J (2000) J Antibiot 53:1145
31. Hengstmann U, Chin KJ, Janssen PH, Liesack W (1999) Appl Environ Microbiol 65: 5050
32. Orphan VJ, Taylor LT, Hafenbradl D, DeLong EF (2000) Appl Environ Microbiol 66:700
33. Uphoff H, Felske A, Wagner-Dobler I (2001) FEMS Microbiol Ecol, in press
34. Ravenschlag K, Sahm K, Pernthaler J, Amann R (1999) Appl Environ Microbiol 65: 3982
35. Yurkov VV, Beatty JT (1998) Microbiol Mol Biol Rev 62:695
36. Buchan A, Collier LS, Neidle EL, Moran MA (2000) Appl Environ Microbiol 66:4662
37. Gonzalez JM, Mayer F, Moran MA, Hodson RE, Whitman WB (1997) Int J Syst Bacteriol 47:773
38. Gonzalez JM, Keine RP, Moran MA (1999) Appl Environ Microbiol 65:3810
39. Ledyard KM, DeLong EF, Dacey JWH (1993) Arch Microbiol 160:312
40. Labrenz M, Collins MD, Lawson PA, Tindall BJ, Schumann P, Hirsch P (1999) Int J Syst Bacteriol 49:137
41. Yurkov VV, Beatty JT (1998) Appl Environ Microbiol 64:337
42. Labrenz M, Tindall BJ, Lawson PA, Collins MD, Schumann P, Hirsch P (2000) Int J Syst Evolut Microbiol 50:303
43. Pukall R, Buntefuss D, Fruhling A, Rohde M, Kroppenstedt RM, Burghardt J, Lebaron P, Bernard L, Stackebrandt E (1999) Int J Syst Bacteriol 49 Pt 2:513–9:513
44. Sorokin DY (1995) Microbiology 64:295
45. Holmes AJ, Kelly DP, Baker SC, Thompson AS, DeMarco P, Kenna EM, Murrell JC (1997) Arch Microbiol 167:46
46. Labrenz M, Collins MD, Lawson PA, Tindall BJ, Braker G, Hirsch P (1998) Int J Syst Bacteriol 48:1363
47. Gosink JJ, Herwig RP, Staley JT (1997) Syst Appl Microbiol 20:356
48. Uchino Y, Hirata A, Yokota A, Sugiyama J (1998) J Gen Appl Microbiol 44:201
49. Ashen JB, Goff LJ (1996) J Phycology 32:286
50. Dang HY, Lovell CR (2000) Appl Environ Microbiol 66:467
51. Grigioni S, Boucher-Rodoni R, Demarta A, Tonolla M, Peduzzi R (2000) Mar Biol 136: 217
52. Ruiz-Ponte C, Cilia V, Lambert C, Nicolas JL (1998) Int J Syst Bacteriol 48:537
53. Ruiz-Ponte C, Samain JF, Sanchez JL, Nicolas JL (1999) Mar Biotechnol 1:52
54. Weidner S, Arnold W, Stackebrandt E, Puhler A (2000) Microbial Ecol 39:22
55. Prokic I, Brummer F, Brigge T, Gortz HD, Gerdts G, Schutt C, Elbrachter M, Muller WEG (1998) Protist 149:347
56. Lafay B, Ruimy R, Detraubenberg CR, Breittmayer V, Gauthier MJ, Christen R (1995) Int J Syst Bacteriol 45:290
57. Omura S (1992) The search for bioactive compounds from microorganisms, 1st edn. Springer, Berlin Heidelberg New York
58. (a) Erhard M, von Doehren H, Jungblut PR (1998) BIOspektrum 4:42; (b) Leenders F, Stein TH, Kablitz B, Franke P, Vater J (1999) Rapid Commun Mass Spectrom 13:943
59. Lowe SW, Ruley HE, Jacks T, Housman DE (1993) Cell 74:957
60. Fisher DE (1994) Cell 78:539
61. Grabley S, Thiericke R (eds) (1999) Drug discovery from nature. Springer, Berlin Heidelberg New York
62. Grever MR, Schepartz SA, Chabner BA (1992) Semin Oncol 19:622
63. Skehan P, Storeng R, Scudiero D, Monks A, McMahon J, Vistica D, Warren JT, Bokesch H, Kenney S, Boyd MR (1990) JNCI 82:1107
64. Wooley PV, Schein PS (1979) Clinical pharmacology and phase I design. In: DeVita VT, Busch H (eds) Methods in cancer research, Vol XVII. Academic Press, New York, p 177
65. Hsu IC, Tokiwa T, Bennett W, Metcalf RA, Welsh JA, Sun T, Harris CC (1993) Carcinogenesis 14:987

66. Müller M, Strand S, Hug H, Heinemann EM, Walczak H, Hofmann WJ, Stremmel W, Krammer PH, Galle PR (1997) J Clin Invest 99:403
67. Gerth K, Schummer D, Höfle G, Irschik H, Reichenbach H (1995) J Antibiot 48:973
68. Kato C, Li L, Nogi Y, Nakamura Y, Tamaoka J, Horikoshi K (1998) Appl Environ Microbiol 64:1510
69. Wirsen CO, Molyneaux SJ (1999) Appl Environ Microbiol 65:5314
70. Bustard MT, Burgess JG, Meeyoo V, Wright PC (2000) J Chem Technol Biotechnol 75:1095
71. Jensen PR, Fenical W (1996) J Ind Microbiol 17:346
72. Romero F, Espliego F, Pérez Baz, De Quesada TG, Grávalos D, De La Calle F, Fernández-Puentes JL (1997) J Antibiot 50:734
73. Pérez Baz J, Canedo LM, Fernández Puentes JL, Silva Elipe MV (1997) J Antibiot 50:738
74. Fernández-Chimeno RI, Canedo L, Espliego F, Grávalos D, De La Calle F, Fernández-Puentes JL, Romero F (2000) J Antibiot 53:474
75. Canedo LM, Fernández Puentes JL, Pérez Baz, Huang X-H, Rinehart KL (2000) J Antibiot 53:479
76. Furumai T, Takagi K, Igarashi Y, Saito N, Oki T (2000) J Antibiot 53:227
77. Igarashi Y, Takagi K, Kan Y, Fujii K, Harada K-I, Furumai T, Oki T (2000) J Antibiot 53:233
78. Bernan VS, Montenegro DA, Korshalla JD, Maiese WM, Steinberg DA, Greenstein M (1994) J Antibiot 47:1417
79. Doshida J, Hasegawa H, Onuki H, Shimidzu N (1996) J Antibiot 49:1105
80. Abbanat D, Leighton M, Maiese W, Jones EBG, Pearce C, Greenstein M (1998) J Antibiot 51:296
81. Schlingmann G, Milne L, Williams DR, Carter GT (1998) J Antibiot 51:303
82. Albaugh D, Albert G, Bradford P, Cotter V, Froyd J, Gaughran J, Kirsch, DR, Lai M, Rehnig A, Sieverding E, Silverman S (1998) J Antibiot 51:317
83. Acebal C, Canedo LM, Fernández Puentes JL, Pérez Baz J, Romero F, De La Calle F, Garcia Grávalos MD, Rodriguez P (1999) J Antibiot 52:983
84. Wicke C, Hüners M, Wray V, Nimtz M, Bilitewski U, Lang S (2000) J Nat Prod 63:621
85. Wijffels HR (2000) Strategy to scale-up closed photobioreactors for cultivation of microalgae. In: Abstracts of the International Marine Biotechnology Conference, Townsville, Australia, September 29–October 4, p 197
86. Boronitzka MA (2000) Optimization of culture conditions in a large-scale tubular photobioreactor. In: Abstracts of the International Marine Biotechnology Conference, Townsville, Australia, September 29–October 4, p 18
87. Webster NS, Watts J, Russell TH (2000) Microbial diversity and bacterial symbiosis in the Great Barrier Reef sponge, *Phopaloeides odorabile*. In: Abstracts of the International Marine Biotechnology Conference, Townsville, Australia, September 29–October 4, p 193
88. Weser U, Müller M (2000) private communication, Braunschweig, Germany
89. Heidorn T (2000) PhD. thesis, in preparation, Fachhochschule Ostfriesland, Emden, Germany
90. Fiedler HP (1993) Nat Prod Lett 2:119
91. Bukingham J, Thompson S (1997) Dictionary of natural products and other information sources for natural products scientists. In: Phytochemical diversity – a source of new industrial products, Royal Society of Chemistry, London, pp 53–67
92. (2001) Dictionary of Natural Products on CD-ROM, Chapman and Hall/CRC Press
93. Laatsch H (1994 and annual updates) AntiBase, A database for rapid structural determination of microbial natural products, Chemical Concepts, Weinheim, Germany
94. Breheret S, Talou T, Rapior S, Bessière JM (1997) J Agric Food Chem 45:831
95. Schulz S (2001) private communication, Braunschweig, Germany
96. Burkholder PR, Pfister RM, Leitz FH (1966) Appl Microbiol 14:649
97. Reid RT, Live DH, Faulkner DJ, Butler A (1993) Nature 366:455
98. Shiozawa H, Kagasaki T, Kimoshita T, Haruyama H, Domon H, Utsui Y, Kodama K, Takahashi S (1993) J Antibiot 46:1834
99. Speitling M (1998) PhD thesis, University of Göttingen, Germany

100. (a) Sviridov SI, Ermolinskii BS (1990) Khim Prir Soedin 811; CA 115:45749; (b) Huang Q, Tezuka Y, Hatanaka Y, Kikuchi T, Nishi A, Tubaki K (1995) Chem Pharm Bull 43:1035
101. Izumida H, Imamura N, Sano H (1996) J Antibiot 49:76
102. Lorenz P, Jensen PR, Fenical W (1998) Nat Prod Lett 12:55
103. Barrow CJ (1994) J Nat Prod 57:471
104. Kwon OS, Park SH, Yun BS, Pyun YR, Kim CJ (2000) J Antibiot 53:954
105. (a) Kakinuma K, Rinehardt EL Jr (1974) J Antibiot 27:733; (b) Japanese Patent (1995) 95165761; CA 123:254695u
106. Balk W (1995) PhD thesis, University of Göttingen, Germany
107. Devys M, Barbier M, Kollmann A, Bousquet JF (1982) Tetrahedron Lett 23:5409
108. Sasaki M, Kikuchi T, Asao Y, Yokosuka T (1967) Nippon Nogei Kagaku Kaishi 41:154
109. Porter JK, Bacon CW, Robbins JD, Himmelsbach DS, Higman HC (1977) J Agric Food Chem 25:88
110. Cardellina JK II, Nigh D, VanWagenen BC (1986) J Nat Prod 49:1065
111. Pieper-Fürst U, Madkour MH, Mayer F, Steinbüchel A (1995) J Bacteriol 177:2513
112. Vives-Rego J, Lebaron P, Nebe-von Caron G (2000) FEMS Microbiol Rev 24:429
113. Rondon MR, August PR, Bettermann AD, Brady SF, Grossman TH, Liles MR, Loiacono KA, Lynch BA, MacNeil IA, Minor C, Tiong CL, Gilman M, Osburne MS, Clardy J, Handelsman J, Goodman RM (2000) Appl Environ Microbiol 66:2541
114. Schleper C, DeLong EF, Preston CM, Feldman RA, Wu KY, Swanson RV (1998) J Bacteriol 180:5003
115. Schleper C, Swanson RV, Mathur EJ, DeLong EF (1997) J Bacteriol 179:7803
116. Vergin KL, Urbach E, Stein JL, DeLong EF, Lanoil BD, Giovannoni SJ (1998) Appl Environ Microbiol 64:3075
117. Kayser O (2001) private communication, Berlin, Germany

Received: May 2001

Bulk Chemicals from Biotechnology: The Case of 1,3-Propanediol Production and the New Trends

An-Ping Zeng, Hanno Biebl

Biochemical Engineering Division, GBF – German Research Centre for Biotechnology, Mascheroder Weg 1, 38124 Braunschweig, Germany
E-mail: aze@gbf.de

Dedicated to Prof. Dr. Wolf-Dieter Deckwer on the occasion of his 60th birthday

The need for a sustainable resource supply, the rapid advances in plant biotechnology and microbial genetics and the strategic shift of major chemical companies into the area of life sciences are some of the driving forces for renewed interest in producing bulk chemicals from renewable resources by biological processes. The microbial production of 1,3-propanediol as briefly reviewed in this article and compared with the competing chemical processes demonstrates the promise and constraints of bioprocesses for bulk chemicals. The new concept of biorefinery and biocommodity engineering and future research needs in this area are also outlined.

Keywords. Bulk chemicals, Renewable resources, 1,3-Propanediol, Metabolic engineering, Biocommodity engineering

Advances in Biochemical Engineering/ Biotechnology, Vol. 74
Managing Editor: Th. Scheper

Abbreviations

ATP	adenosine triphosphate
DHA (*dha*)	dihydroxyacetone
dhaB	gene for the enzyme glycerol dehydratase
DHAK	dihydroxyacetone kinase
DHAP	dihydroxyacetone phosphate
dhaT	gene for the enzyme 1,3-propanediol oxidoreductase
GA-3-P	glycerinaldehyde-3-phosphate
GDH	glycerol dehydrogenase
GDHt	glycerol dehydratase
G-3-P	glycerol-3-phosphate
GPD	glycerolphosphate dehydrogenase
GPP1/2	gene for glycerol-3-phosphatase
3-HPA	3-hydroxypropionaldehyde
NAD	nicotinamide adenine dinucleotide (oxidized)
$NADH_2$	nicotinamide adenine dinucleotide (reduced)
1,3-PD	1,3-propanediol
PDOR	1,3-propanediol oxidoreductase
PDH	pyruvate dehydrogenase
PEP	phosphoenolpyruvate
PFL	pyruvate formate lyase
PK	pyruvate kinase
PTT	polytrimethylene terephthalate
TCA	tricarboxylic acid

1 Introduction

Bulk chemicals are referred to as basic or technical chemicals such as ethylene, propylene, methanol and acetone that are either directly used or further processed for the production of large-volume and value-added products in the chemical industry. These chemicals usually have production volumes in the range of 1 – 100 million tons per year and selling prices less than 2000 US$/t. At present, almost all the important technical chemicals except for ethanol are produced via the petrochemical route, although biotechnology has the potential to produce many of these chemicals directly or indirectly from renewable materials [1 – 3]. As pointed out by Deckwer et al. [1], biotechnology has so far established a firm position only in producing fine or specialty chemicals such as amino acids, organic acids, vitamins, antibiotics and other pharmaceuticals. Compared with the bulk petrochemicals, the bulk fermentation products have generally much lower production volumes (less than 1 million tons per year) but higher selling prices. Although these fermentation products achieve an impressive annual sale of more than 10 billion US$ and thus represent no more a niche market, the majority of them find their outlets in the food and feed market and are almost totally absent from technical applications like solvents, polymers and plastics. It seems that this situation is about to change.

Driving forces for the anticipated change come from many directions. The finite nature of the world's petroleum resources and abundant supply of biomass have been widely recognized and attracted significant interest in biological production of chemical feedstocks and fuels. Recent strong fluctuations in the price of crude oil have prompted several large oil importing nations to seriously seek alternatives to relieve their dependency on oil imports. In a recent report of the US National Research Council (NRC) "Biobased Industrial Products: Priorities for Research and Commercialization" the importance and benefits of producing feedstocks and liquid fuels from renewable materials have been summarized as follows [4, 5]:

- Use of currently unexplored productivity in agriculture and forestry;
- Favorable impact on global climate and environment;
- Decreased dependence on foreign resources and diminishing supplies of oils;
- Higher political and economical security; and
- Functionally superior, value-added products.

However, the ecological challenge and political intention alone cannot create the desired change. Economic restraints, i. e., cost competitiveness, are the reality in this area. Significant recent achievements in molecular plant genetics, transgenic crop breeding and genetic manipulation of cellular metabolism are the major scientific driving forces that are making plant-based production routes more and more technically attractive and economically competitive [2, 6 – 11]. Novel process engineering concepts are also under development to overcome some of the major economic constraints [7, 8].

For a long time, the chemical industry considered biotechnology as an expensive high-tech tool that was not appropriate for bulk chemical synthesis on a large scale. This perception is undergoing a gradual change as reflected by several current development projects of major chemical companies to produce bulk chemicals via biotechnological routes. These emerging commodity chemicals include 1,3-propanediol [12, 13], lactic acid [2, 14] and succinic acid [2, 15]. In fact, today's largest fermentation product, bioethanol, although subsidized, is proof of the bulk manufacturing potential of biotechnology [16, 17]. More than 13 million tons/year of fuel grade ethanol is supplied to a non-food market segment. The second largest fermentation products are citric acid and monosodium glutamate. Their worldwide production volumes are approaching 1 million ton/year, respectively, and resemble thus the manufacturing output of some petrochemical bulk products.

In this article, recent progress in the microbial production of 1,3-propanediol (1,3-PD) is reviewed. This special case is used to illustrate the promise and some of the critical constraints of biological processes as compared to the chemical processes. General trends and research needs in the utilization of renewable resources are briefly discussed.

2
The Case of 1,3-Propanediol Production

2.1
1,3-Propanediol and its Applications: from a Fine to a Bulk Chemical

As a bifunctional organic molecule 1,3-PD has several promising properties for many synthetic reactions, particularly as a monomer for polycondensations to produce polyesters, polyethers and polyurethanes. However, in the past, its high production cost strongly restricted its uses. For a long time it only found niche applications such as as a solvent and for the production of dioxanes and specialty polymers that have small market volumes [18]. This situation began to change in 1995 – 1996 when two leading chemical companies, Shell and Dupont, announced their commercialization of a new 1,3-PD-based polyester, polytrimethylene terephthalate, termed PTT (Shell) or 3GT (Dupont). This copolyester is a condensation product of 1,3-PD and terephthalic acid. I has excellent properties such as good resilience, stain resistance, low static generation, etc., and is particularly suitable for fiber and textile applications [19, 20]. It is also a very promising engineering plastic that has the potential to replace the traditional polyethylene terephthalate (PET) and polybutylene terephthalate (PBT). PTT can be produced in an environmentally friendly way and at a price very competitive to that of PET and PBT. According to Shell, PTT can be offered at a price near 1 US$/kg. The price of PET fluctuates between 0.9 and 1.8 US$/kg, PBT between 1.1 and 1.9 US$/kg.

Because of this new application 1,3-PD has evolved from a fine to a bulk polymer in only a few years. The production volume in the year 2000 was estimated to be around 70 000 – 80 000 t/a. According to a projection of the consulting company CONDUX (USA), the production volume of PTT will increase up to a level of 1 Mio. t/a in a few years.

1,3-PD also has a number of other interesting applications in addition to that of a polymer constituent. It can give improved properties for solvents (increased flexibility in blending ester quats and other additives), adhesives, laminates, resins (low intrinsic viscosity, less solvent for coating), detergents (preventing phase separation and loss of enzyme activity), and cosmetics (long-lasting but not sticky moisturizing effect). It can even be used to produce biocides for industrial disinfection and treatment of industrial circulation water [21], and freshness-keeping agents for cut flowers [22]. In a recent patent it was also discussed as a component of animal feed [23].

2.2
Chemical Processes for 1,3-Propanediol

Until recently, 1,3-PD was regarded as not easily chemically amenable due to the relatively low selectivity in the existing processes. Increasing demand has now led to new patents that are both practiced on a considerable scale.

The process of Degussa, now owned by Dupont, uses the conventional preparation method starting from acrolein which is obtained by catalytic oxidation

of propylene [24]. Acrolein is hydrated at moderate temperature and pressure to 3-hydroxypropionaldehyde which, in a second reaction, is hydrogenated to 1,3-PD over a rubidium catalyst under high pressure (90 bar) [25, 26].

The process of Shell starts from ethylene oxide, which is prepared by oxidation of ethylene. Ethylene oxide is transformed with synthesis gas in a hydroformylation process to 3-hydroxypropanal as well, but for this reaction very high pressure (150 bar) is required [27]. The aldehyde is extracted from the organic phase with water and subjected to hydrogenation using nickel as a catalyst, again under high pressure.

In the first process the yield does not exceed 65% of the starting compound due to simultaneous formation of 1,2-propanediol, while, in the second, a yield of 80% is obtained. Adding the fact that the market price of ethylene oxide is lower than acrolein, the Shell process can be regarded as economically more favorable. This is reflected in the much higher production volume reported for the production of 1,3-PD from ethylene oxide, which amounted to 45,000 t/a in 1999 as opposed to 9000 t/a from acrolein. The relatively high production costs with the acrolein process have probably induced the Dupont Company to invest in research efforts to further develop the biological process (see below).

2.3 Microbial Formation of 1,3-Propanediol

For almost 120 years a bacterial fermentation has been known in which glycerol is converted to 1,3-PD, but only very recently, since 1990, has its biotechnological significance been recognized, and more directed research initiated [12, 13, 28]. There has been some economic interest in this reaction as glycerol has been a surplus product at times. It is released from fat cleavage to further manufacture the fatty acids and is also a by-product in biodiesel production from rape-seed oil. In addition, glycerol is also a minor by-product in ethanol fermentation and its recovery from this process has recently been discussed [29]. Its concentration can be increased by cultural measures or strain development [30]. Unpurified glycerol, in particular from biodiesel plants, has been shown to be an excellent fermentation substrate for 1,3-PD production [31–33].

The metabolic reactions involved in the glycerol fermentation are diverse (Fig. 1), but, in principle, the glycerol fermentation can be divided into two pathway branches. In the reductive branch, glycerol is first dehydrated to 3-hydroxypropionaldehyde that is then reduced to 1,3-PD under the consumption of reducing power ($NADH_2$). The reducing power is generated in the oxidative metabolism of glycerol that makes use of the major glycolysis reactions and results in the formation of by-products.

The yield of 1,3-PD depends on the combination and stoichiometry of the reductive and oxidative pathways. It has been shown that the combination of 1,3-PD generation with acetic acid as the sole by-product of the oxidative pathway results in the maximum yield of 1,3-PD [34, 35]. For this combination, the fermentation equations can be written as:

$$CH_2OH–CHOH–CH_2OH + H_2O \rightarrow CH_3COOH + CO_2 + H_2 + 4\,[H]$$

$$2\,CH_2OH–CHOH–CH_2OH + 4\,[H] \rightarrow 2\,CH_2OH–CH_2–CH_2OH + 2H_2O$$

$$3\,CH_2OH–CHOH-CH_2OH \rightarrow CH_3COOH + CO_2 + H_2 + 2\,\mathbf{CH_2OH–CH_2–CH_2OH} + H_2O$$

The yield of 1,3-PD for this reaction is 67 % (mol/mol). If biomass formation is considered the theoretical maximal yield reduces to 64 %. In the actual fermentation a number of other by-products are formed, i. e., ethanol, lactic acid, succinic acid, and 2,3-butanediol, by the enterobacteria *Klebsiella pneumoniae*, *Citrobacter freundii and Enterobacter agglomerans*, butyric acid by *Clostridium butyricum*, and butanol by *Clostridium pasteurianum* (Fig. 1). All these by-products are associated with a loss in 1,3-PD relative to acetic acid, in particular ethanol and butanol, which do not contribute to the $NADH_2$ pool at all.

2.4 Optimization of Glycerol Bioconversion

There are numerous ways to optimize the microbial production of 1,3-PD from glycerol, and remarkable progress has already been achieved. Main concerns for optimization are: (1) preventing undesired by-product formation to achieve

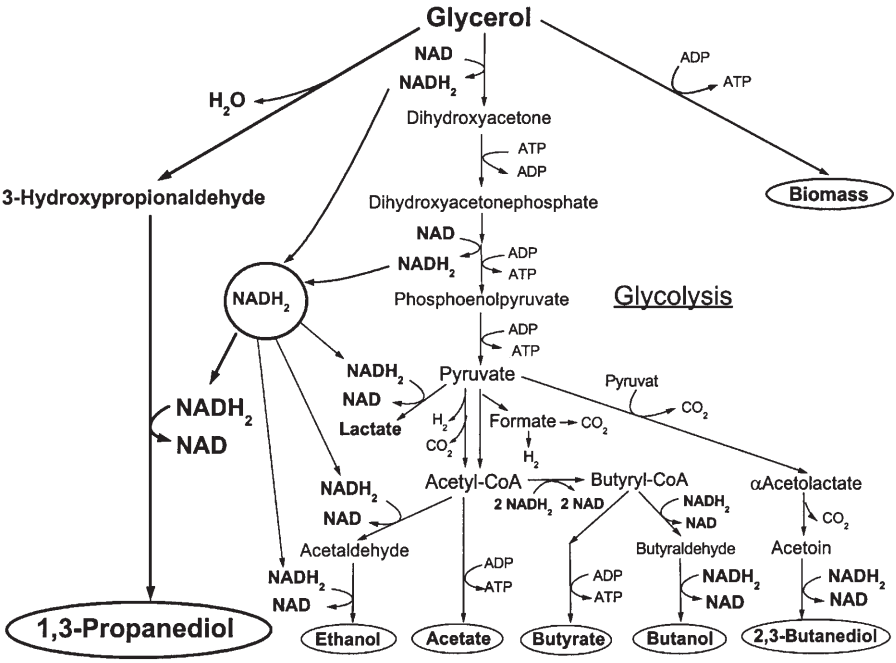

Fig. 1. Metabolic pathways of glycerol metabolism

high product yield; (2) increasing tolerance for 1,3-PD to achieve higher final product concentration; and (3) increasing the productivity of the bioreactor.

By-product control has been elaborated chiefly for *K. pneumoniae*. It has been shown in continuous cultures that production of ethanol is restricted to conditions of limitation by glycerol [34]. If the bacteria are limited by other nutrients or by inhibition through the fermentation products, ethanol is almost completely suppressed [36–38]. However, under conditions of high glycerol excess and severe product inhibition, other by-products, in particular lactic acid and 2,3-butanediol, appear in the medium diminishing the propanediol yield [38, 39]. This is particularly the case in the late phase of batch cultures grown with high concentrations of glycerol. A pH distinctively lower than 6.5 considerably stimulates production of 2,3-butanediol [40]. Butyrate formation in *Clostridium butyricum* was also found to decrease under substrate excess, but also seems to be dependent on the growth rate [38].

In addition to the liquid products the hydrogen gas released from pyruvate cleavage to acetyl-CoA (Fig. 1) is also significant for the 1,3-PD yield [34, 35]. Its formation can be varied. In *C. butyricum* the reducing equivalents from this reaction are transferred to ferredoxin and may be further transferred to NAD by the NAD:ferredoxin oxidoreductase instead of being released as molecular hydrogen, thus contributing to additional 1,3-PD formation. The enzyme is particularly active under substrate excess conditions [41]. *K. pneumoniae* has the same capability but uses another mechanism. As shown by Menzel et al. [42], *K. pneumoniae* can simultaneously use the two enzymes pyruvate dehydrogenase and pyruvate:formate lyase for anaerobic cleavage of pyruvate in the glycerol fermentation, the former particularly under substrate-sufficient conditions. Pyruvate dehydrogenase generates $NADH_2$ from pyruvate cleavage instead of forming formate with pyruvate formate lyase, leading to an increased yield of 1,3-PD (0.72 mol/mol glycerol). The yield can be increased up to 0.88 mol/mol if acetyl-CoA from pyruvate cleavage is channeled into the tricarboxylic acid (TCA) cycle for reducing power and adenosine triphosphate (ATP) generation. Enzymatic assay showed that a part of the TCA cycle reaction is active in the anaerobic glycerol fermentation. The effect of oxygen on glycerol fermentation is not known. It has recently been shown that a microaerobic production of 1,3-PD from glycerol is possible (unpublished results).

Product inhibition in the glycerol fermentation has been studied in several investigations [12, 38, 43–45]. The strongest inhibitor seems to be 3-hydroxypropionaldehyde. This compound is normally an intracellular intermediate that does not accumulate. However, under conditions of high glycerol excess, it may be excreted into the medium. Whereas *K. pneumoniae* is able to reduce the accumulated 3-hydroxypropanal further to 1,3-PD, *Enterobacter agglomerans* is killed by the aldehyde as soon as a concentration of 2.2 g/l has been reached [44]. *C. butyricum* excretes only very small amounts of 3-hydroxypropanal [46]. 1,3-PD is the least toxic product in the glycerol fermentation, but nevertheless determines the achievable final concentration. A final concentration of propanediol around 60–70 g/l is usually achieved with wild-type strains. More than 85 g/l 1,3-PD can be produced with these microorganisms in special fed-batch fermentations (unpublished results). With externally added 1,3-PD,

Cameron et al. [12] showed that recombinant *E. coli* can tolerate more than 100 g/l. The strain itself however produced little propanediol. In a recent study, Colin et al. [45] showed that *C. butyricum* can tolerate up to 83.7 g/l propanediol when it is added externally. These values may represent the maximum achievable product concentration with wild-type strains.

Improvement of 1,3-PD tolerance beyond these limitations may be achieved by conventional and directed mutagenesis, but only limited work has been done in this direction. Abbad-Andaloussi et al. [47] increased the propanediol production of *C. butyricum* by chemical mutagenesis. This mutant was also strongly reduced in hydrogen formation and resulted in a final propanediol concentration of 70 g/l.

With regard to process optimization, almost all of the existing culture techniques, including batch culture, fed-batch culture [31, 48, 49], chemostat and two stage chemostat [33, 49], have been practiced and evaluated up to now. By continuous cultures with immobilization [50, 51] or cell retention [52], the productivity, but not the final 1,3-PD concentration, could be substantially increased. Taking advantage of the higher end-product concentration of the batch culture and the benefits of permanent slight glycerol excess, the most efficient cultivation method appears to be a fed-batch variant which uses automatic pH correction by alkali addition for growth-adapted glycerol supply. Using this method a 1,3-PD concentration of 70.4 g/l for product-tolerant mutants of C. *butyricum* [48] and 70–78 g/l for *K. pneumoniae* [53] have been reached, the productivity being in the range 1.5–3.0 g/l/h. Best values for continuous cultures are 35–48 g/l for *K. pneumoniae* as well as for *C. butyricum* [33, 39], whereby the productivity was higher in *K. pneumoniae.*

Some time ago, the group of Bothast made some efforts in using the intermediate of 1,3-PD formation, 3-hydroxypropionaldehyde (3-HPA) [54], which was suggested as the basis for acrylic acid production. It was obtained by converting glycerol in the presence of a semicarbazide in a concentration up to 46 g/l using resting cells of *K. pneumoniae*. The method appears to be rather tedious. However, an enzymatic conversion of glycerol, in particular with non-B_{12}-dependent glycerol dehydratase, deserves further development. 3-HPA could be converted to 1,3-PD by chemical catalysis [25, 26, 55] or using isolated 1,3-PD oxidoreductase in an enzymatic step. The theoretical yield of the enzymatic process is 1 mol PD/mol glycerol.

2.5
Metabolic Flux Analysis and Pathway Design

Further success in increasing yield and concentration of 1,3-PD is expected from the application of metabolic engineering and recombinant DNA technology, especially with respect to extending the substrate spectrum to use cheaper and abundant substrates such as glucose and starch [12, 13].

A prerequisite for a successful genetic modification of the producing strains is a thorough understanding of the distribution and regulation of the metabolic fluxes and the identification of limiting steps (Fig. 2). Ahrens et al. [56] and Menzel et al. [57] studied the in vivo and in vitro activities of the key enzymes

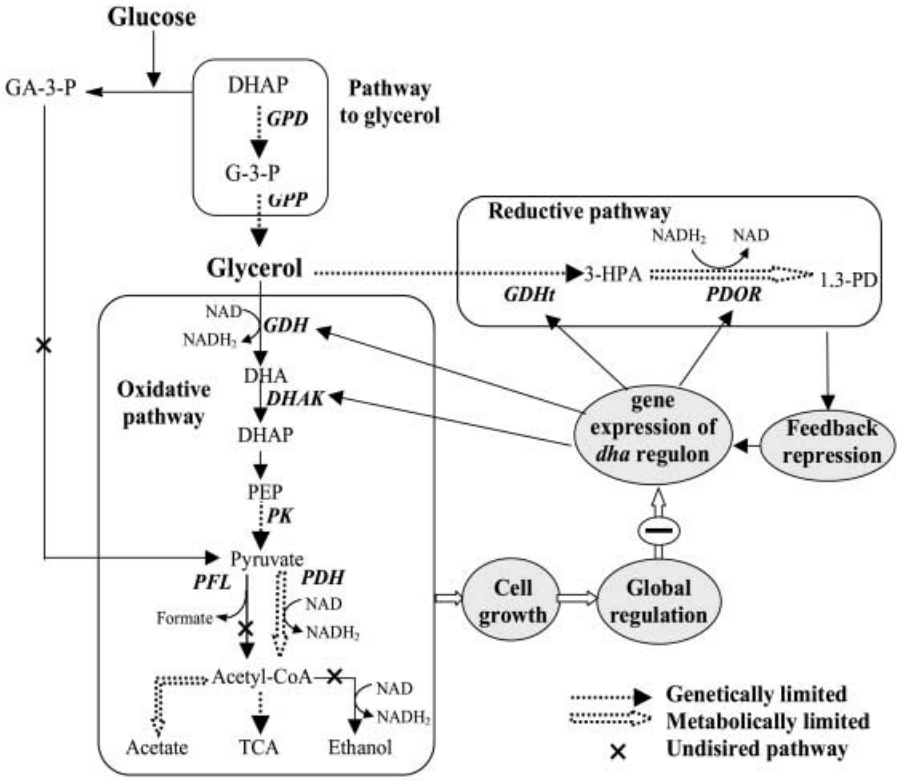

Fig. 2. Multiple targets for metabolic engineering of 1,3-PD production

involved in the glycerol fermentation of *K. pneumoniae*. By comparing the in vivo and in vitro activities of these enzymes, metabolic flux bottlenecks due to limited enzyme synthesis can be identified. With *K. pneumoniae* it was found that mainly the synthesis of glycerol dehydratase and pyruvate kinase limits the metabolism of the reductive and oxidative pathways, respectively, especially under substrate excess conditions. Measurements of enzyme activity suggested that glycerol dehydratase is also the limiting step of 1,3-propanediol production by *C. butyricum* [58].

Recently, the metabolic fluxes in the glycerol metabolism by *K. pneumoniae* and *C. butyricum* were estimated based on experimental data and the respective reaction networks of these microorganisms [59, 60]. The investigations showed that, although the enzymes for pyruvate metabolism are present in excess, the metabolic fluxes through these enzymes are tightly controlled. The cleavage of pyruvate thus represents a limiting step at the metabolic level. It severely limits the generation of reducing power and may also impair cell growth.

In all bacteria able to ferment glycerol to 1,3-PD the genes encoding for the four enzymes specific for glycerol fermentation are expressed in common in the so-called *dha* regulon (*dha* from dihydroxyacetone, the first intermediate in the

oxidative metabolic branch) (Fig. 2). The genes of the two enzymes of the reductive branch, the B_{12}-dependent glycerol dehydratase (GDHt) and the 1,3-propanediol oxidoreductase (PDOR), have been cloned and sequenced for *K. pneumoniae* [61–63], *Citrobacter freundii* [64, 65], and *Clostridium pasteurianum* [66, 67]. Experiments to express or overexpress these genes in *E. coli* have been successful, but the 1,3-PD concentrations obtained with these constructs could originally not be raised above 9 g/l [68]. However, in a recent patent publication issued to Dupont and Genencor [69] (see below), a final concentration of 129 g/l obtained with transformed *E. coli* was reported.

An approach to directly improve the glycerol fermentation of *K. pneumoniae* by genetic engineering was undertaken in our laboratory [70]. By construction of plasmids containing the genes for glycerol dehydratase and 1,3-propanediol oxidoreductase and inserting them into the wild-type strain, a many-fold overexpression for the two enzyme activities was obtained. However, in batch as well as in continuous culture, the engineered strain was unable to produce more 1,3-PD than the wild-type strain. In addition to a possible instability of the plasmid a strong feedback repression of gene expression of the *dha* regulon by the final product (1,3-PD or other metabolites) was suggested and analyzed by model simulation [59]. Model analysis of experimental data also indicated the involvement of global regulation, the exact nature of which is not known.

An unprecedented effort to establish a profitable biotechnological production of 1,3-PD has been implemented in a cooperative research project of Genencor and Dupont. The results obtained up to now have been put down in eight voluminous patents. The project is principally aimed at extending the substrate spectrum to fermentable carbohydrates which, in particular glucose or starch hydrolysates, are available at 3 to 5 times lower prices than glycerol in the USA. All conceivable alternatives have been examined and claimed as invention. As carbohydrates are not fermented by naturally occurring organisms, gene recombinations from at least two organisms are required, one that converts glucose to glycerol and one that ferments the glycerol to 1,3-PD (Fig. 2). Cocultures or consecutive cultures of wild-type glycerol producers, mainly yeasts, and glycerol fermenters are hampered by a number of circumstances, predominantly by relatively slow conversion of the yeast cultures and the competitive inhibition of the glycerol fermenters by glucose and possibly by other products of the yeast culture [71, 72].

Three concepts for appropriate recombinants are possible and have been followed in the DuPont project. First, the genes required for glycerol formation are transformed into a 1,3-PD producer such as *K. pneumoniae* or *C. freundii*. These genes encode for two enzymes operating in yeasts, the glyceraldehydephosphate dehydrogenase (GPD) and the glycerol phosphatase (GPP) of which two isoenzymes are necessary (Fig. 2). (The dehydrogenase is more or less contained in all organisms for lipid synthesis; however, as has been shown, not in sufficient quantity.) Second, the genes of the two enzymes required for 1,3-PD production, *dhaB* and *dhaT*, are inserted in glycerol-producing yeasts. Eventually, all five genes can be transformed into an organism that forms neither glycerol nor propanediol but exhibits favorable growth properties and gene expression conditions such as *E. coli*. Best results were reported for recombinants con-

structed according to the first and second concepts. *K. pneumoniae* transformed with the three yeast genes produced up to 11 g 1,3-PD per liter, while the inverse construct, yeast cells with inserted 1,3-PD genes, provided only traces of the diol [73]. Recently, Genencor and Dupont described a new approach to genetically modify the 1,3-PD pathway. By expressing a non-specific alcohol dehydratase instead of *dhaT* for the conversion of 3-HPA a final 1,3-PD concentration of 129 g/l was reported [69]. The exact nature of the non-specific alcohol dehydratase was not known.

2.6 Comparison of Chemical and Biological Processes

In general, for the production of bulk chemicals such as 1,3-PD by chemical routes, the raw materials (natural gas, naphtha) have to be first broken down into small molecules like C_1-C_4 (CO, H_2, olefins) by cracking and endothermic fission processes at relatively high temperatures. The desired products are then catalytically synthesized from these small molecule compounds, often at high pressures and/or by oxidation with oxygen. Materials with high oxygen contents such as glucose and glycerol are recalcitrant for chemical processing into bulk chemicals but are excellent substrates for biological processing. In terms of the composition and structure, fermentation products are much closer to their starting materials than the petrochemicals to their corresponding raw materials. This structural similarity of raw materials and products and the inherent high efficiency of microorganisms make it possible to carry out bioprocesses with generally high selectivity and under environmentally benign operational conditions.

Despite the obvious advantages of a biological production of commodities it is generally expressed that this production mode is not at all economically competitive with a chemical synthetic process. In a recent thesis issued at the University of Braunschweig, Germany, a cost assessment of all stages of the fermentative 1,3-PD production from glycerol was performed [74]. The study considered fed-batch and continuous cultivations for the fermentation, a multistage evaporation device for the removal of the process water, and two rectification columns with eight plates for separation and purification of the propanediol. The results were compared with the corresponding data of the two chemical processes described and to those of the Genencor/DuPont project for production from glucose using engineered organisms. Consistent with several previous cost estimations [28], the outcome of these calculations is that 1,3-PD production by fermentation, if compared at high production volumes (e.g., 65,000 t/a), can be run at comparable costs to chemical syntheses (Fig. 3). It is worth mentioning that, if the cost comparisons are made on the basis of market prices of raw materials (e.g. average US market prices of 1998), for all processes the biological processes can even be run at lower costs. In-plant prices for the raw materials can largely determine the economy of the process. Shell and Degussa are two major producers of ethylene oxide and acrolein, respectively, and this may have determined their choice of production process for 1,3-PD. In addition, the large price fluctuation of some of the raw materials should be kept

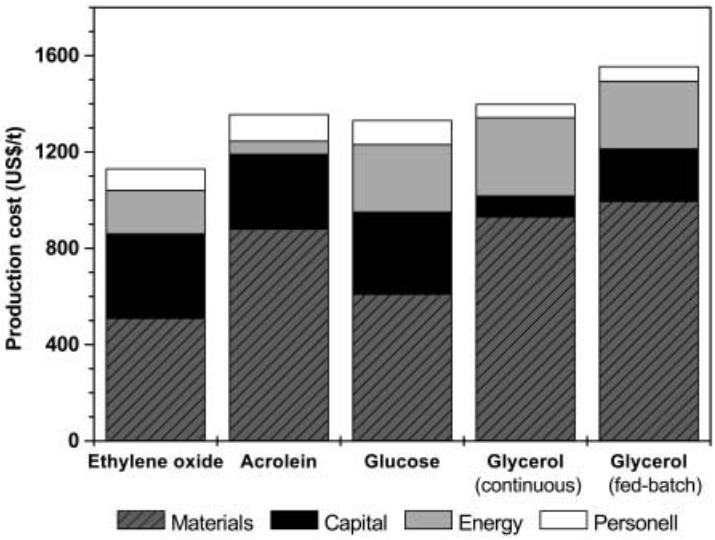

Fig. 3. Cost comparison of different routes to 1,3-propanediol [74]. Production costs for the chemical processes and glucose route are based on estimations from ChemSystems. Estimations for the glycerol processes are based on US market prices of raw materials in 1998 and a production scale of 65,000 t/a. The energy costs for the glucose process are assumed to be the same as the fed-batch glycerol process

in mind. The results as depicted in Fig. 3 are nevertheless useful for understanding the cost structure of chemical and biological processes for bulk chemicals. In all these processes, raw materials have the major part in the total costs: 40 % – 60 %. Energy costs make up a significant part in the cost of biological processes due to downstream processing.

Fermentation from glucose turned out to be indeed more favorable than from glycerol with unmodified organisms because of the lower raw material costs; however, the difference is not that high, especially compared to the continuous glycerol fermentation. The reason for the relatively high capital costs of the glucose process as estimated by ChemSystems is not known. Since glucose is two to four times cheaper than glycerol on the US market, a much stronger reduction for the raw materials would be expected for the glucose process. The still relatively high raw material costs for the glucose route may be due to the relatively low yield of 1,3-PD from glucose so far achieved. A maximum yield of about 0.29 g PD/g glucose can be obtained for a two-step process in which glucose is first converted into glycerol (maximum yield ca. 0.5 g/g) and glycerol is then converted into 1,3-PD in a second step (maximum yield ca. 0.58 g/g). Cameron et al. [12] recently estimated the theoretical maximal yield of 1,3-PD from glucose by linear optimization of the bioreaction network of genetically modified microorganisms. For anaerobic culture a maximum yield of 0.42 g/g was estimated. If glucose conversion is carried out under aerobic conditions and no other by-products except CO_2 and H_2O are formed, a maximum yield as high as 0.6 g/g could be estimated. If these product yields could be experimen-

tally achieved or approximated the advantage of producing 1,3-PD from glucose would be more significant. In general, the chances of a biotechnological production of 1,3-PD appear to be good, even if the original glycerol process is maintained. In the cost study mentioned above, the by-products of the fermentation were treated as waste. If these were recovered, too, the costs could be further reduced (see below).

3
General Constraints and New Concepts for Bulk Chemicals from Biotechnology

3.1
General Constraints and Possible Solutions

The example of 1,3-PD production as outlined above demonstrates some of the potentials and limitations of production of bulk chemicals from bioprocesses. The potentials and limitations of biological production of chemicals have also been discussed in several excellent reviews [7, 75, 76]. The relatively high costs of the raw materials are one of the major limitations. For most of the chemicals from biological routes the raw material costs are above 50% of the total costs. Two basic strategies have been used to overcome this problem: (1) to increase the conversion yield, and (2) to use cheaper or waste materials. Both of these strategies can be implemented either by a process approach or by a genetic approach. On the process level optimal strains and cultivation conditions are normally sought by trial-and-error. For a new product or process this approach can often give an immediate improvement at the beginning. The extent of the improvement is however limited by the stoichiometry of the metabolic pathways and by the inherent metabolism regulation of the producing microorganisms. A genetic approach (metabolic engineering) can principally lead to a more profound improvement by altering the stoichiometry or the fluxes of the metabolic pathways, as demonstrated for the production of several amino acids. With respect to the use of cheaper or waste materials, genetic manipulation of the pathway is sometimes the only possibility, as in the case of producing 1,3-PD from glucose or technical substrates other than glycerol and in the case of producing ethanol from hemicellulosic materials.

The second major limitation of bioprocesses is the low reaction rate and reactor productivity, primarily because bioprocesses are carried out at physiological temperature, atmospheric pressure and mostly in batch or fed-batch operation mode. A process approach can have a significant effect on volumetric production rates by increasing cell density in the bioreactor and by developing a continuous process. This is mostly achieved by continuous cultivation with cell recycling or with immobilized cells, as demonstrated for the microbial production of 1,3-PD [51, 52]. Continuous culture has successfully been used in the industrial production of bioethanol. A genetic approach can be used to increase the productivity by overexpressing the key or limiting enzymes of product formation. An alteration to the multiple limiting steps or regulatory features of en-

zyme synthesis and activities is often required for this purpose (Fig. 2). This is a difficult and challenging task of metabolic engineering for metabolite production.

The third major limitation of bioprocesses is the quite low product concentration compared with chemical processes, resulting in high downstream processing costs. This is mainly caused by product inhibition of cell growth and biosynthesis. Physiological improvements in cell growth and product formation only have a limited impact on this aspect. Chemical or directed mutagenesis may provide better chances for improvement. Unfortunately, the molecular mechanisms of product inhibition are not well understood.

Another problem with fermentation products is often the limited outlet. The primary fermentation products such as alcohols require chemical transformations to convert them into species acceptable by the chemical industry as intermediates. This can normally occur through dehydration reactions [77]. For example, ethanol may need to be dehydrated into ethylene, isopropanol into propylene and n-butanol into n-butylene. These reactions are reversed petrochemical reactions and normally lead to products that have a lower selling price than the starting materials under the present structure of the chemical industry. For this reason, bioethanol is still used unchanged as an oxygenated gasoline additive.

3.2
The Concept of Biorefinery and Biocommodity Engineering

The overall goal of the strategies mentioned above is to optimize the formation of a single main product and suppress the by-products. It is questionable if this is the technically most feasible and economically reasonable strategy. It is worth mentioning that the petrochemical processes work with a different principle. In a typical oil refinery (Fig. 4), numerous important basic chemicals, i.e., paraffin, olefins and aromatic compounds, are simultaneously and efficiently produced from the same raw material (crude oil). The amounts or yields of these bulk chemicals can be varied by adjusting the process configuration or operating conditions in the different processing units such as reforming, steamcracking or high-temperature pyrolysis depending on the market demand and/or source and quality of the crude oil. In such a way, flexibility is achieved in the spectrum of products. A systemic analysis and simulation of process configurations and operating conditions further enables an efficient and almost complete utilization of the raw material. Apart from the large scale this might be one of the most important features of petrochemical processes that make them economically more competitive than biological processes for the production of bulk chemicals.

The success of petrochemical processes may provide some lessons for developing bioprocesses for chemical production. In fact, microorganisms have adopted a similar strategy as oil refineries in their evolution of the metabolism of substrates. As shown in Fig. 5, the metabolism of glucose can lead to the formation of a large number of organic compounds through different microorganisms using several processing “blocks” or “units” such as glycolysis, anaerobic

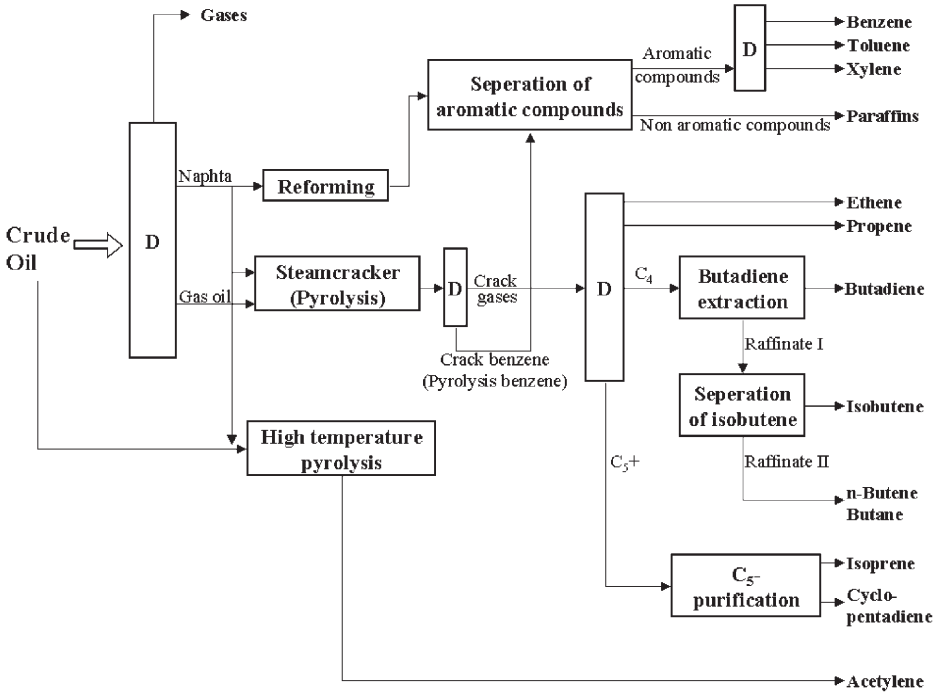

Fig. 4. Simplified diagram of a typical oil refinery (modified after [79])

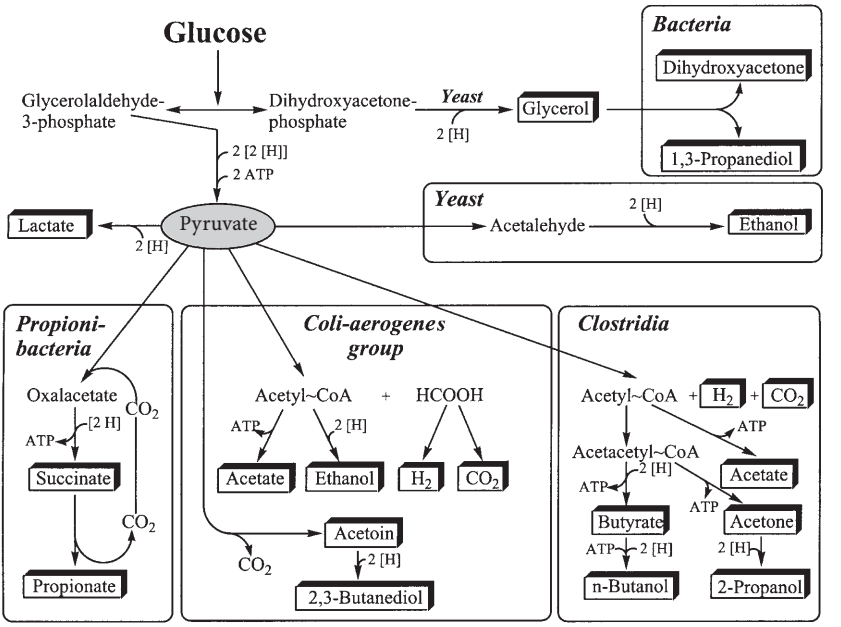

Fig. 5. Possible products from glucose fermentation in different microorganisms (modified after [80])

and aerobic metabolism of pyruvate. In real fermentation processes one can hardly achieve the formation of only a single metabolite. For reasons of energy generation or balance of reducing equivalents, microorganisms normally produce coupled products. As in the anaerobic fermentation of glycerol, several so-called by-products, such as acetate, ethanol, lactate, butyrate and 2,3-butanediol, can be produced additionally to the desired main product (1,3-PD) in varied amounts depending on the microorganisms and fermentation conditions (Fig. 1). In some "optimized" fermentation runs (for example with ca. 80 g/l propanediol), acetate, ethanol or lactate at concentrations as high as 15 – 20 g/l can be produced. In the estimation of production costs for microbial 1,3-PD as mentioned in Sect. 2.6, these by-products were not taken into account. If the glycerol fermentation were to be optimized towards the formation of multiple products and an efficient separation process for these products were available the benefits of such a multi-product approach could be significant. Assuming that 80 g/l lactate or other useful products were produced in addition to 80 g/l 1,3-PD in the same fermentation process and that a similar thermal process were applied for product separation, a simple calculation would indicate reductions of both substrate and downstream processing costs by nearly 50%.

The recent announcement of the company High Plains Corporation (US) to recover glycerol from ethanol fermentation broth is a good example to illustrate the benefits of such a practice [29]. Glycerol is a by-product of ethanol fermentation at a typical yield of about 60 g glycerol/l ethanol produced and can be increased to 120 g/l ethanol simply by changing the fermentation conditions without reduction in the ethanol yield. Normally, glycerol remains in the distillation stillage of the thermal ethanol separation process. Glycerol-rich stillage is then dried to yield an animal feed. According to the High Plains Corp. glycerol can be recovered from the ethanol fermentation broth by a novel filtration process at costs below 0.3 – 0.4 US$/kg glycerol (99.7 % pure), which is well below the production cost of glycerol from the soap and oleochemistry industries and/or from chemical synthesis via the epichlorohydrin route. If all bioethanol plants were implemented with the glycerol recovery step about 600 000 t/a glycerol could be produced. This is very close to the present world production volume of glycerol (800 000 – 900 000 t/a) [78] and would have a significant economical impact.

In fact, the multi-product approach may be a necessary step toward a competitive production of biobased industrial products [7]. As pointed out by Palsson et al. [77] and partly evidenced in Fig. 4 (oil refinery), the chemical industry is highly interactive, mainly through co-product production. Large-scale introduction of a single chemical compound can cause substantial imbalances and result in a higher price penalty for the new chemical. For example, propylene, the second largest organic bulk chemical in terms of production volume, is presently mainly produced as a co-product of ethylene production in oil refineries. To replace petroleum ethylene by dehydration of bioethanol, one has to select an alternative, less economical route to ethylene with more propylene as co-product. This constraint on ethylene production results in a higher price penalty for bioethanol as a chemical intermediate than if it only had to compete with ethylene production. A possible relief for this situation is to offer biomass-

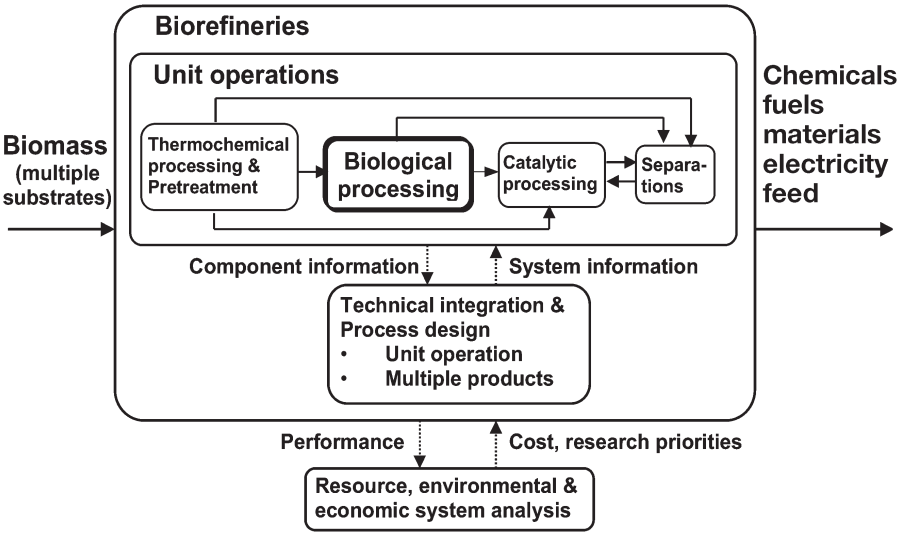

Fig. 6. The concept of "biorefinery" or "biocommodity engineering" (modified after [7])

derived propylene (i.e., through dehydration of isopropanol) in appropriate proportions to ethylene within the production schema of a so-called "biorefinery" or "biocommodity engineering" (Fig. 6).

The concept "biorefinery" is discussed in the US National Research Council Report "Biobased Industrial Products" [4] and by Lynd et al. [7] in much detail. The basic idea is the processing of multiple renewable resources and the production of multiple products in a production complex. Another characteristic of biorefinery is the integration of thermal, chemical, biological and/or catalytical processes for an efficient and optimal processing and utilization of the raw materials. Technological, ecological and economic analysis and system design should be implemented to ensure an overall optimization of raw material conversion and product formation in a similar way as for oil refineries.

The feedstock for biorefinery may include wood, other lignocellulosic biomass, vegetable crops, starch-producing crops, and oil seeds. Current feedstock for bioprocesses is mainly based on starch-derived carbohydrates. In the long term, the utilization of all three fractions of lignocellulosic biomass, i.e., the lignin (15–30%), the cellulose (35–50%) and the hemicellulose (20–40%), is desirable and necessary to reach the scale and the raw material costs competitive with oil refineries. This requires a combined use of thermal, chemical, mechanical and/or biological processes for a cost-effective pretreatment of the raw materials and their subsequent conversion. Despite the efforts and impressive progress in the past, cost-effective and environmentally benign technologies for the pretreatment and conversion of lignocellulosic biomass do not generally exist. Biological processing plays a particularly important role in relieving some of these technical barriers. In general, biological processes involved in the utilization of renewable biomass can be divided into microbial and enzymatic sys-

tems. Several specific research needs and priorities have been identified in these two respective areas which can be further divided into process-related or fundamental issues [4, 7]. On the process level these include:

- fermentation of xylose and other non-glucose sugars;
- combining the biological and chemical operations of sugar production, fermentation, and product recovery in fewer vessels and use of fewer microorganisms to reduce capital costs and product inhibition, thereby increasing rates, yields and selectivity;
- improving bioreactor design for heat, momentum and mass transfer for viscous, non-Newtonian fermentation broths and solid-liquid broths;
- improving large-scale production of industrially useful enzymes; and
- enhancing and developing rational control of enzyme performance in organic solvents.

The development and improvement of biological processes will depend on continuing research to elucidate fundamental biological principles. Future fundamental work on microbial systems related to bio-refinery should include:

- identification of physiological and genetic changes that enable use of multiple substrates;
- analysis of metabolic pathways and their regulation for a more predictable and efficient metabolic engineering to increase microorganisms' selectivity and productivity;
- identification of microorganisms that can convert xylose and other non-sugar components into useful chemicals and of organisms that can use ethanol or other oxygenated intermediates as a substrate to produce target chemicals;
- basic research on biochemical and genetic mechanisms of product inhibition and tolerance; and
- basic research on cultures containing multiple microorganisms for sequenced use of substrates or production of multiple products in single or multi-step processes.

Basic research areas related to enzymatic processing of renewable materials include:

- exploring catalysis by enzymes from thermophiles and other extremophiles;
- broadening the substrate specificity of enzymes by means of site-directed mutagenesis or protein-design; and
- identifying enzymes that can produce products for important biobased markets such as enzymes that can convert ethanol and other oxygenated intermediates into useful chemicals.

The integrated processing of renewable materials can lead to the generation of a wide range of products. Some examples of known and potential biorefinery products are [4]:

- fermentation feedstocks and food products (starch, dextrose, sucrose, cellulose, hemicellulose, molasses, oil, etc.);

- non-food industrial products (loose fill packing material, paper sizes, textiles sizes, adhesives);
- chemical intermediates and solvents (organic acids, alcohols, ketones, diols);
- fuels (ethanol and other alcohols, biodiesel);
- industrial enzymes; and
- biodegradable plastic resins.

It is believed that such a diversity of substrates and products of biorefinery will greatly improve the economical competitiveness of producing chemicals from biotechnology.

4 Outlook and Conclusions

It is generally recognized that bulk chemicals from biotechnology show great promise in relieving the dependence of modern industry and society on a diminishing and fragile supply of fossil feedstocks and in improving the industrial impact on global climate and environment. In some specific cases, such as the production of 1,3-PD, biological processes are in principle in a position to compete with the chemical routes. In general, however, there are still several technical barriers against and economical challenges to the realization of a biobased production of bulk chemicals, notably reflected by the high raw material and downstream processing costs, low reaction rate and limited substrate spectrum. The strategy applied in the past to develop and optimize bioprocesses for a single main product seems to lead to these unfavorable characteristics for a large-scale production of bulk chemicals from biotechnology. The new concept of biorefinery, namely the integrated processing of multiple substrates and production of multiple products in one facility, may represent a promising direction. Realizing the promises of biorefinery requires the close collaboration of chemical engineers, process engineers and scientists from fundamental biology and microbiology. With such an integrated technical strategy and strong driving forces from government organizations, industry and the scientific community, the US National Research Council has recently projected the following targets for a biobased production: 10% of the liquid fuels and 50% of the organic chemicals and materials to be produced from renewable biomass by 2020; by 2090 almost the complete organic chemical industry should be switched to a biobased production. This may be regarded as a "second wave" of biotechnology applied to fields other than health care [7]. While the first half of the 20th century had witnessed a transition of chemical raw material basis from coal to oil and natural gas, the first half of the 21st century may experience a gradual replacement of the petroleum resources by renewable biomass. To achieve this, efforts and innovations from biochemical engineering and biotechnology are desperately needed. In this connection, we would like to quote Deckwer et al. [1]: "if we want to see significant contributions from biotechnology to the chemical marketplace we have to start now".

References

1. Deckwer W-D, Diekmann H, Wilke D (1995) FEMS Microbiol Rev 16:79
2. Wilke D (1999) Appl Microbial Biotechnol 52:135
3. Demain AL (2000) Biotechnol Adv 18:499
4. Committee on Biobased Industrial Products, Board on Biology, Commission on Life Sciences, National Research Council (2000) Biobased industrial products: priorities for research and commercialization. National Academy Press, Washington, DC
5. Thayer A (2000) Chem Eng News May 29:40
6. McCoy M (1998) Chem Eng News June 22:13
7. Lynd LR, Wyman CE, Gerngross TU (1999) Biotechnol Prog 15:777
8. Dale BE (1999) Biotechnol Prog 15:775
9. Louwrier A (1998) Biotechnol Appl Biochem 27:1
10. Ingram LO, Aldrich HC, Borges ACC, Causey TB, Martinez A, Morales F, Saleh A, Underwood SA, Yomano LP, York SW, Zaldivar J, Zhou S (1999) Biotechnol Prog 15:855
11. Bothast RJ, Nichols NN, Dien BS (1999) Biotechnol Prog 15:867
12. Cameron DC, Altaras NE, Hoffman ML, Shaw AJ (1998) Biotechnol Prog 14:116
13. Biebl H, Menzel K, Zeng AP, Deckwer WD (1999) Appl Microbiol Biotechnol 52:289
14. Tullo A (2000) Chem Eng News January 17:13
15. Zeikus JG, Jain MK, Elankovan P (1999) Appl Microbiol Biotechnol 51:545
16. Wheals AE, Basso LC, Alves DMG, Amorim HV (1999) TIBTECH 17:482
17. Sheehan J, Himmel M (1999) Biotechnol Prog 15:817
18. Sullivan CJ (1993) Propanediol. In: Ullmann's encyclopedia of industrial chemistry, vol A22. VCH, Weinheim
19. Chuah HH, Brown HS, Dalton PA (1995) Int Fiber J Oct 1995
20. Greene RN (1990) US Patent 4,937,314
21. Matsumoto S (1999) Japanese Patent 11130604A
22. Watanabe T (1992) Japanese Patent 4360802A
23. Kaesler B, Müschen H, Streicher H, Samson W (1998) WO9842205A1
24. Brossmer C, Arntz D (2000) US Patent 6,140,543
25. Arntz D, Haas T, Müller A, Wiegand N (1991) Chem-Ung-Tech 63:733
26. Arntz D, Wiegand N (1991) Eur Patent 412337
27. Lam KT, Powell JP, Wieder PR (1997) WO 97/16250
28. Deckwer WD (1995) FEMS Microbial Rev 16:143
29. McCoy M (2000) Chem Eng News February 14:28
30. Remize F, Roustan JL, Sablayrolles JM, Barre P, Dequin S (1999) Appl Environ Microbiol 65:143
31. Günzel B, Yonsel S, Deckwer W-D (1991) Appl Microbiol Biotechnol 36:289
32. Petitdemange E, Dürr C, Abbad-Andaloussi S, Raval G (1995) J Ind Microbiol 15:498
33. Papanikolaou S, Ruiz-Sanchez P, Pariset B, Blanchard F, Fick M (2000) J Biotechnol 77:191
34. Zeng A-P, Biebl H, Schlieker H, Deckwer W-D (1993) Enzyme Microb Technol 15:771
35. Zeng A-P (1996) Bioproc Eng 14:169
36. Streekstra H, Teixera de Mattos MJ, Neijssel OM, Tempest DW (1987) Arch Microbiol 147:268
37. Tag C (1990) PhD thesis, University of Oldenburg, Germany
38. Zeng A-P, Ross A, Biebl H, Tag C, Günzel B, Deckwer W-D (1994) Biotechnol Bioeng 44:902
39. Menzel K, Zeng A-P, Deckwer W-D (1997) Enzyme Microbiol Technol 20:82
40. Biebl H, Zeng A-P, Menzel K, Deckwer WD (1998) Appl Microbiol Biotechnol 50:24
41. Solomon BO, Zeng A-P, Biebl H, Ejiofor AO, Posten C, Deckwer WD (1994) Appl Microbiol Biotechnol 42:222
42. Menzel K, Zeng A-P, Deckwer W-D (1997) J Biotechnol 56:135
43. Biebl H (1991) Appl Microbiol Biotechnol 35:701
44. Barbarito F, Grivel JP, Soucaille P, Bories A (1996) Appl Environ Microbiol 62:1448
45. Colin T, Bories A, Moulin G (2000) Appl Microbiol Biotechnol 54:201

46. Jung K (2001) PhD thesis, Technical University of Braunschweig, Germany
47. Abbad-Andaloussi S, Maginot-Dürr AJ, Petitdemange E, Petitdemange H (1995) Appl Environ Microbiol 61:4413
48. Reimann A, Biebl H (1996) Biotechnol Lett 18:827
49. Boenigk R, Bowien S, Gottschalk G (1993) Appl Microbiol Biotechnol 38:453
50. Pflugmacher U, Gottschalk G (1994) Appl Microbiol Biotechnol 41:313
51. Wittlich P, Schlieker M, Willke T, Vorlop K-D (2000) In: Vorlop K-D, Warwel S, Puls J, Krüger A (eds) Bioconversion nachwachsender Rohstoffe. Landwirtschaftsverlag, Münster, Germany
52. Reimann A, Biebl H, Deckwer W-D (1998) Appl Microbiol Biotechnol 49:359
53. Hartlep (2000) MSc thesis, Technical University of Braunschweig, Germany
54. Vancauwenberge JE, Slininger PJ, Bothast RJ (1990) Appl Environ Microbiol 56:329
55. Powell JB, Pledger WR, Matzakos AN, Weider PR, Arhancet JP (1998) US Patent 5,786,524
56. Ahrens K, Menzel K, Zeng A-P, Deckwer W-D (1998) Biotechnol Bioeng 59:544
57. Menzel K, Ahrens K, Zeng A-P, Deckwer W-D (1998) Biotechnol Bioeng 60:617
58. Abbad-Andaloussi S, Guedon E, Spiesser E, Petitdemange H (1996a) Lett Appl Microbiol 22:311
59. Zeng A (2000) Habilitationsschrift, Technical University of Braunschweig, Germany
60. Jung K (2001) PhD thesis, Technical University of Braunschweig, Germany
61. Tong I-T, Cameron DC (1992) Appl Biochem Biotechnol 34/35:149
62. Tobimatsu T, Azuma M, Matsubara H, Zkatori H, Niida T, Nishimoto K, Satoh H, Hayashi R, Toraya T (1996) J Biol Chem 271:22352
63. Nagarajan V, Nakamura CE (1996) WO 96/35795
64. Daniel R, Boenigk R, Gottschalk G (1995) J Bacteriol 177:2151
65. Seyfried M, Daniel R, Gottschalk G (1996) J Bacteriol 178:5793
66. Luers F, Seyfried M, Daniel R, Gottschalk G (1997) FEMS Microbiol Lett 154:337
67. Macis L, Daniel R, Gottschalk G (1998) FEMS Microbiol Lett 164:21
68. Daniel R, Gottschalk G (1992) FEMS Microbiol Lett 100:281
69. Emptage M, Haynie SL, Laffend LA, Pucci J, Whited GM (2001) WO 01/12833
70. Menzel K (1999) PhD thesis, Technical University of Braunschweig, Germany
71. Haynie SL, Wagner LW (1996) WO 35799
72. Hußmann W (2001) MSc thesis, Technical University Berlin, Germany
73. Gatenby AA, Haynie SL, Nagarajan V, Nair RV, Nakamura CE, Payne MS, Picataggio SK, Dias-Torres M (1998) WO 98/21339
74. Grothe E (2000) PhD thesis, Technical University of Braunschweig, Germany
75. Bailey JE (1995) FEMS Microbiol Rev 16:271
76. Wilke D (1995) FEMS Microbiol Rev 16:89
77. Palsson BO, Fathi-Afschar S, Rudd DF, Lightfoot EN (1981) Science 213, 513
78. Claude S, Heming M, Hill K (2000) In: Stelter W et al (eds) Proceedings of CTVO-Net Conference Chemical-technical utilization of vegetable oils. pp 129 – 146
79. Onken U, Behr A (1996) Chemische Prozeßkunde. Thieme, Stuttgart
80. Schlegel HG (1985) Allgemeine Mikrobiologie, 6th edn. Thieme, Stuttgart

Received: April 2001